11.2.12 Tip-Over of Vertical Concrete Cask

Tip-over of the vertical concrete cask (concrete cask) is a non-mechanistic, hypothetical accident condition that presents a bounding case for evaluation. There are no design basis accidents that result in the tip-over of the cask.

Functionally, the cask does not suffer significant adverse consequences due to this event. The concrete cask, canister, and basket maintain design basis shielding, geometry control of contents, and contents confinement performance requirements.

Results of the evaluation show that supplemental shielding will be necessary, following the tip-over and until the cask can be righted, because the bottom ends of the concrete cask and the canister have significantly less shielding than the sides and tops of these components.

The cask is provided in the Standard and the Advanced configurations, with the Advanced concrete cask having a higher loaded canister weight. The canister used for the Standard and Advanced configurations are generally identical, except for the bottom plate thickness (Standard = 1.75 inch, Advanced = 2.0 inch); however, the Standard basket is a fuel tube and disk design, while the Advanced basket is a tabbed and slotted plate design. The canister and Standard basket together are referred to as the Standard canister configuration. Similarly, the canister and Advanced basket together are referred to as the Advanced canister configuration. The Standard and Advanced concrete casks are similar, but the Advanced concrete cask incorporates T-shaped channel weldments on the inside face of the concrete cask liner to support the canister during a tipover event. The evaluation of the Standard configurations is provided in Sections 11.2.12.3 and 11.2.12.4. The evaluation of the Advanced configuration is provided in Sections 11.2.12.5 and 11.2.12.6. The validation of the LS-DYNA program used in the evaluation is provided in Section 11.2.12.7.

11.2.12.1 Cause of Concrete Cask Tip-Over

A tip-over of the cask is possible in an earthquake that significantly exceeds the design basis described in Section 11.2.8. No other events related to design bases are expected to result in a tip-over of the cask.

11.2.12.2 Detection of Concrete Cask Tip-Over

The tipped-over configuration of the concrete cask will be obvious during site inspection following the initiating event.

11.2.12.3 Analysis of the Standard Concrete Cask Tip-Over

For a tip-over event to occur, the center of gravity of the Standard concrete cask and loaded canister must be displaced beyond its outer radius, i.e., the point of rotation. When the center of gravity passes beyond the point of rotation, the potential energy of the cask and canister is converted to kinetic energy as the cask and canister rotate toward a horizontal orientation on the concrete ISFSI pad (concrete pad). The subsequent motion of the cask is governed by the structural characteristics of the concrete cask, the concrete pad and the underlying soil. The parameters of the concrete pad and foundation for the Standard configuration are:

Concrete thickness	36 inches maximum
Pad subsoil thickness	10 feet minimum
Specified concrete compressive strength	$\leq$ 4,000 psi at 28 days
Concrete dry density (ρ)	$125 \leq \rho \leq 145$ lbs/ft^3
Soil in place density (ρ)	$100 \leq \rho \leq 145$ lbs/ft^3
Soil Modulus of Elasticity	$\leq$ 60,000 psi (PWR) or $\leq$ 30,000 psi (BWR)

11.2.12.3.1 Analysis of Standard Cask Tip-Over for PWR Configurations

The concrete pad in the model corresponds to a pad 30-feet by 30-feet square and 3-feet thick, supporting one concrete cask in the center of the pad. The soil under the concrete pad is considered to be 35-feet by 35-feet square and 10-feet thick.

The concrete is represented as a homogeneous isotropic material. The concrete cask (outer shell) and the pad are modeled as material Type Number 16 in LS-DYNA. The values for concrete pad and soil properties provided below are typical values for the input to the LS-DYNA model:

Compressive Strength ($f_c^{'}$)	= 4,000 psi	
Density (ρ_c)	= 125 pcf	
Poisson's Ratio (ν_c)	= 0.22	(NUREG/CR-6608 [38])
Modulus of Elasticity (E_c)	$= 33\ \rho_c^{1.5}\ \sqrt{f_c^{'}}$ = 2.917E6 psi	(ACI 318-95)
Bulk Modulus (K_c)	$= \frac{E_c}{3(1-2\nu_c)}$ = 1.736E6 psi	(Blevins [19])

The finite element model includes a half section of the concrete cask, the concrete pad and soil subgrade because of symmetry, as shown:

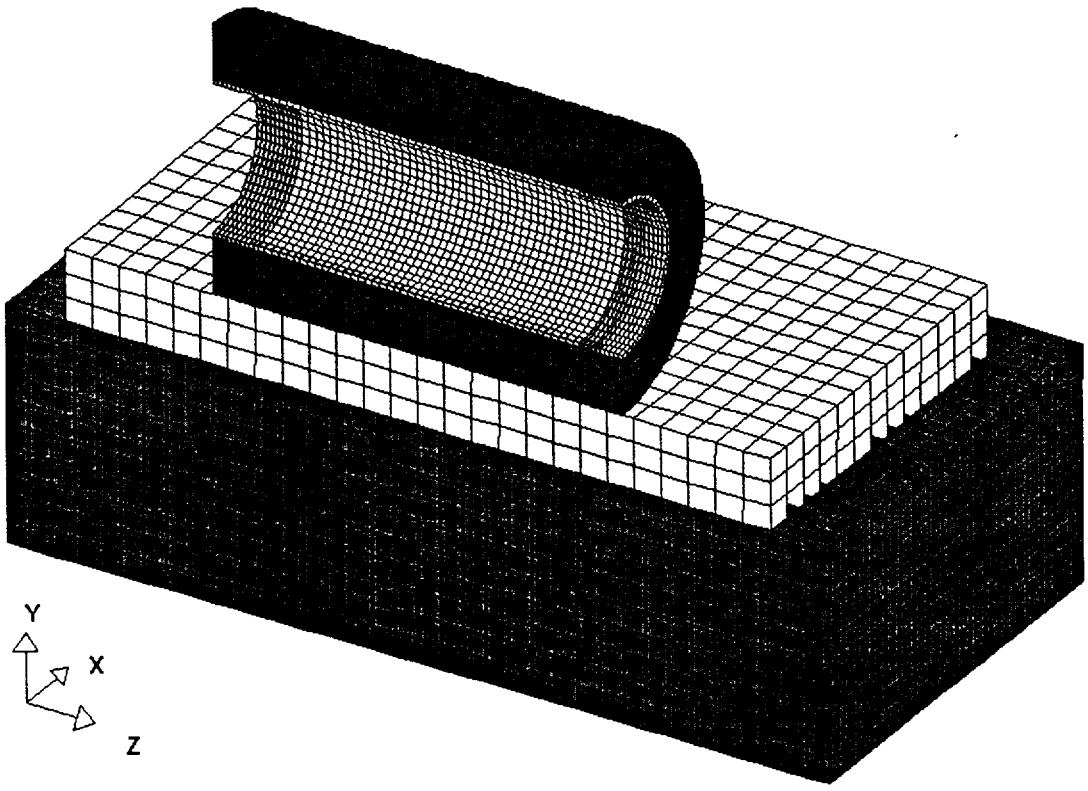

The material properties used in the model for the soil below the concrete pad are:

Density	= 120 pcf	
Poisson's Ratio (ν_s)	= 0.45	(NUREG/CR-6608)
Modulus of Elasticity	= 60,000 psi	

The Standard concrete cask steel liner has the properties:

Density	= 0.284 lbs/in^3
Poisson's ratio	= 0.31
Modulus of elasticity	= 2.9E7 psi

To account for the weight of the shield plug, the loaded Standard canister, and the Standard concrete cask pedestal, effective densities are used for the elements in the first row of the steel liner in the model adjacent to the impact plane of symmetry. These densities represent the regions (6° in the circumferential direction) of the steel liner subjected to the weight of the shield plug, the loaded canister and the pedestal, during the side impact (tip-over) condition. The contact angle (6°) is determined based on the Standard canister/basket analysis for the tip-over condition (Section 11.2.12.4).

Boundary and Initial Conditions for the Standard PWR Concrete Cask

A friction coefficient of 0.25 is used at the interface between the steel liner and the concrete shell, between the concrete cask and the pad, and between the pad and the soil. For all the embedded faces (three side surfaces and the bottom surface) of the soil in the model, the displacements in the direction normal to the surface are restrained. The symmetry boundary conditions are applied for all nodes at the plane of symmetry.

The initial condition corresponds to the concrete cask in a horizontal position with an initial vertical velocity into the concrete pad. The pad and soil are initially at rest.

The distribution of initial velocity of the Standard concrete cask is simulated by applying an angular velocity (ω) to the entire cask. The point of rotation is taken to be the lower edge of the base of the concrete cask. The angular velocity value is computed by considering energy conservation at the cask "center of gravity over corner" tip condition versus the side impact condition.

From energy conservation:

$$mgh = \frac{I\omega^2}{2}$$

where:

mg = total weight of the loaded Standard concrete cask
= 292,401 lbs (PWR Class 1)
= 303,317 lbs (PWR Class 2)
= 308,432 lbs (PWR Class 3)

h = height change of the Standard concrete cask center of gravity

$$(L_{CG}) = \sqrt{R^2 + \left(\frac{L_{CG}}{2}\right)^2} - R$$

= 59.11 inches (PWR Class 1)
= 62.80 inches (PWR Class 2)
= 66.16 inches (PWR Class 3)

where:

L_{CG} = location of the center of gravity above the pad for the Standard concrete cask
= 107.39 inches (PWR Class 1)
= 111.73 inches (PWR Class 2)
= 115.65 inches (PWR Class 3)

R = radius of the concrete cask = 68 inches

I = total mass moment of inertia of the Standard concrete cask about the point of rotation
= 7,779,111 lbs-sec^2-inch (PWR Class 1)
= 8,610,059 lbs-sec^2-inch (PWR Class 2)
= 9,264,863 lbs-sec^2-inch (PWR Class 3)

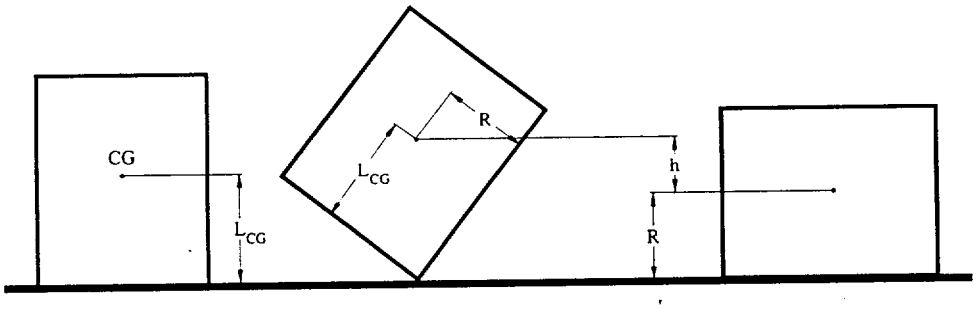

The mass moment of inertia for the concrete shell and the steel liner is calculated using the formula for a hollow right circular cylinder (Blevins).

$$I=\frac{m}{12}(3R_1^2+3R_2^2+4L^2)+md^2$$

where:

m = mass (lbs-sec^2/in)
R_1 and R_2 = the outer and inner radius of the cylinder (inch)
L = height of the cylinder (inch)
d = distance between the center of gravity and the point of rotation (inch)

For the mass of the shield plug, loaded canister and the pedestal, the formula for the moment of inertia for a solid cylinder is used:

$$I=\frac{m}{12}(3R^2+4L^2)+md^2$$

where:

m = mass of the cylinder (lbs-sec^2/in)
R = radius of the cylinder (inch)
L = height of the cylinder (inch)
d = distance between the two pivot axes (inch)

The angular velocity is given by $\omega=\sqrt{\frac{2mgh}{I}}$

= 1.493 radians/sec (PWR Class 1)
= 1.488 radians/sec (PWR Class 2)
= 1.484 radians/sec (PWR Class 3)

Filter Frequency for the Standard PWR Concrete Cask

The accelerations are evaluated at the inner surface of the cask liner, which physically corresponds to the interface of the liner and the loaded canister nearest the plane of impact. Following the methodology contained in NUREG/CR-6608 [38], the Butterworth filter is applied to the nodal accelerations. The filter frequency is based on the fundamental mode of the cask.

The fundamental natural frequency of a beam in transverse vibration due to flexure only is given by Blevins as:

$$f = \frac{\lambda^2}{2\pi}\sqrt{\frac{EI}{\rho AL^4}}$$

where:

$\lambda = 3.92660231$ for a pin-free beam

The frequencies of the concrete (f_c) and the steel liner (f_s) are computed as:

Area of concrete cask = $\pi\ \{(68)^2 - (39.75)^2\} = 9562.8\ in^2$

Moment of inertia of concrete cask = $\frac{\pi}{4}\{(68)^4 - (39.75)^4\} = 14{,}832{,}070\ in^4$

$f_c = 805819\ \frac{\lambda^2}{L^2}$

= 284 Hz (PWR Class 1)
= 261 Hz (PWR Class 2)
= 244 Hz (PWR Class 3)

Area of steel liner = $\pi\ \{(39.75)^2 - (37.25)^2\} = 604.8\ in^2$

Moment of inertia of steel liner = $\frac{\pi}{4}\{(39.75)^4 - (37.25)^4\} = 448{,}673\ in^4$

$f_s = 861068\ \frac{\lambda^2}{L^2}$

= 303 Hz (PWR Class 1)
= 279 Hz (PWR Class 2)
= 260 Hz (PWR Class 3)

Since the concrete cask is short compared to its diameter, the contribution of the flexibility due to shear is also incorporated. This is accomplished by using Dunkerley's formula (Blevins). The system frequency is:

$$\frac{1}{f^2} = \frac{1}{f_c^2} + \frac{1}{f_s^2}$$

Thus, the system frequencies are 207 Hz (PWR Class 1), 191 Hz (PWR Class 2), and 178 Hz (PWR Class 3). A cut-off frequency of 210 Hz (PWR Class 1), 190 Hz (PWR Class 2), and 180 Hz (PWR Class 3) is conservatively applied to filter the analysis results and measure the peak accelerations.

Results of the Transient Analysis for the Standard PWR Concrete Cask

The accelerations at key locations of the Standard concrete cask liner, which are required in the evaluation of the loaded canister/basket model (Section 11.2.12.4) are:

	Position Measured from the Bottom of the Concrete Cask (inches)			Acceleration (g)		
Location on Component	PWR Class 1	PWR Class 2	PWR Class 3	PWR Class 1	PWR Class 2	PWR Class 3
Top support disk	176.7	185.2	196.3	29.1	35.4	34.3
Top of the canister structural lid	197.9	207.0	214.6	31.8	35.1	36.9

11.2.12.3.2 Analysis of Standard Cask Tip-Over for BWR Configurations

The BWR finite element model is similar to that for the PWR configuration. The concrete pad in this model corresponds to a pad 30-feet by 30-feet and 3-feet thick, supporting one concrete cask in the center of the pad. The soil under the concrete pad is considered to be 35-feet by 35-feet in area and 10-feet thick. The material properties used in this model for the soil below the concrete pad are the same as those for the PWR model, except the modulus of elasticity of the soil is 30,000 psi.

The finite element model includes a half section of the Standard concrete cask, the concrete pad and soil subgrade, as shown:

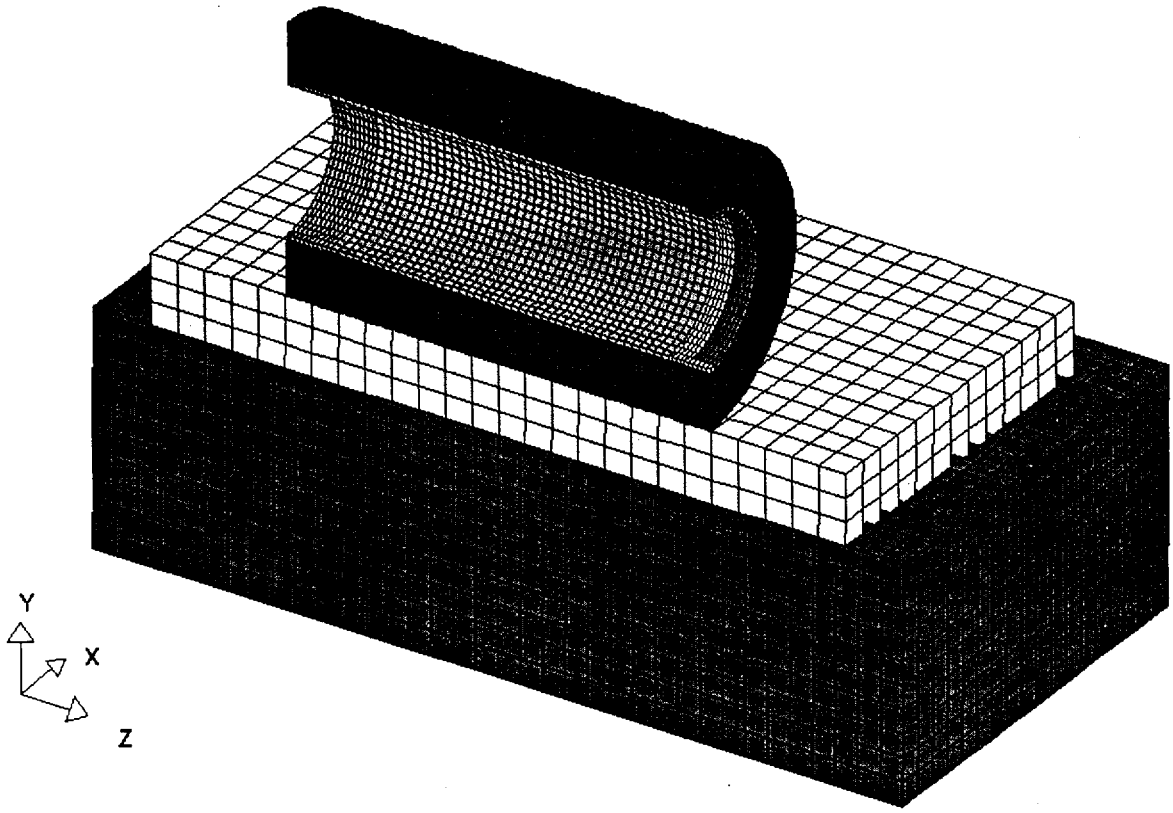

Boundary and Initial Conditions for the Standard BWR Concrete Cask

The initial velocity for the BWR fuel configurations is calculated in the same fashion as for the PWR fuel configurations, but using the following data:

mg = total weight of the loaded Standard concrete cask
= 307,087 lbs (BWR Class 4)
= 312,210 lbs (BWR Class 5)

h = height change of the Standard concrete cask center of gravity

$$(L_{CG}) = \sqrt{R^2 + \left(\frac{L_{CG}}{2}\right)^2} - R$$

= 63.26 inches (BWR Class 4)
= 65.54 inches (BWR Class 5)

where:

L_{CG} = location of the center of gravity above the pad for the concrete cask
= 112.27 inches (BWR Class 4)
= 114.93 inches (BWR Class 5)

I = total mass moment of inertia of the concrete cask about the point of rotation
= 8,785,335 lbs-sec^2-inch (BWR Class 4)
= 9,243,624 lbs-sec^2-inch (BWR Class 5)

The angular velocity is given by $\omega = \sqrt{\frac{2mgh}{I}}$

= 1.487 radians/sec (BWR Class 4)
= 1.488 radians/sec (BWR Class 5)

Filter Frequency for the Standard BWR Concrete Cask

The filter frequency for the BWR fuel configuration is calculated in the same fashion as for the PWR fuel configuration, but using the following data:

$$f_c = 805819 \frac{\lambda^2}{L^2}$$

= 257 Hz (BWR Class 4)
= 247 Hz (BWR Class 5)

$$f_s = 861{,}068 \frac{\lambda^2}{L^2}$$

= 275 Hz (BWR Class 4)
= 263 Hz (BWR Class 5)

Thus, the system frequencies are 188 Hz (BWR Class 4), and 180 Hz (BWR Class 5). A cut-off frequency of 190 Hz (BWR Class 4), and 180 Hz (BWR Class 5) is conservatively applied to filter the analysis results and measure the peak accelerations.

Results of the Transient Analysis for the Standard BWR Concrete Cask

The accelerations at key locations of the concrete cask liner, which are required in the evaluation of the loaded Standard canister/basket model (Section 11.2.12.4) are:

Location on Component	Position Measured from the bottom of the Concrete Cask (inches)		Acceleration (g)	
	BWR-4	BWR-5	BWR-4	BWR-5
Top support disk	178.7	182.9	24.4	25.3
Top of the canister structural lid	208.4	213.2	27.9	29.1

11.2.12.3.3 Validation of the Analysis Methodology

Tip-over tests of a steel billet onto a concrete pad were conducted and reported in NUREG/CR-6608. The purpose of the tests was to provide data, against which, analysis methodology could be validated. Using the geometry described in the benchmark along with the modeling methodology, these analyses were re-performed using the LS-DYNA program.

Using the filter frequency reported in the NUREG/CR-6608 benchmark, the following results are obtained:

Nodes / Gauge Location	Maximum Experiment (g)	NAC Analysis (g)
16115 / A1	237.5	237.1
17265 / A5	231.5	229.4

11.2.12.4 Analysis of the Standard Canister and Basket for the Cask Tip-Over Event

The Standard canister and basket structural evaluations are performed for the canister and fuel basket support disks for tip-over accident conditions for both PWR and BWR fuel configurations. ANSYS finite element models are used to evaluate this side impact loading condition.

Comparison of maximum stress results to the allowable stress intensities shows that the canister and support disks are structurally adequate for the concrete cask tip-over condition and satisfies the stress criteria in accordance with the ASME Code, Section III, Division I, Subsection NB and NG, respectively.

The structural response of the Standard PWR and BWR canisters and fuel baskets to the tip-over condition is evaluated using ANSYS three-dimensional finite element models consisting of the top portion of the canister, the top five fuel basket support disks, and the fuel basket top weldment disk. The PWR with Fuel Class 1 configuration is used to evaluate the PWR canister and fuel basket, and the BWR with Fuel Class 4 configuration is used to evaluate the BWR canister and fuel basket. These two representative configurations are chosen because they bound the maximum load-per-support disk for the respective fuel configurations. For each fuel configuration analyzed, the structural analyses are performed for various fuel basket drop orientations in order to ensure that the maximum primary membrane (P_m) and primary membrane plus primary bending ($P_m + P_b$) stresses are evaluated. For the PWR fuel configuration, fuel basket drop orientations of 0°, 18.22°, 26.28°, and 45° are evaluated (see Figure 11.2.12.4.1-1). For the BWR fuel configuration, fuel basket drop orientations of 0°, 31.82°, 49.46°, 77.92°, and 90° are evaluated (see Figure 11.2.12.4.2-1).

11.2.12.4.1 Analysis of the Standard Canister and Basket for PWR Configurations

Four three-dimensional models of the Standard PWR canister and fuel basket are evaluated for side loading conditions that conservatively simulate a tip-over event while inside the concrete cask. In each model, a different fuel basket drop orientation is used. Three-dimensional half-symmetry models are used for the basket orientation of 0° and 45°, since half-symmetry is applicable based on the support disk geometry and the drop orientation. Three-dimensional full-models are used for the basket drop orientations of 18.22° and 26.28°. Representative figures for the models are presented in this section (three-dimensional full-model with a basket orientation of 18.22°).

Model Description of the Standard PWR Canister and Fuel Basket

The finite element model used to evaluate the Standard PWR canister and fuel basket for the tip-over event is presented in Figure 11.2.12.4.1-2 through Figure 11.2.12.4.1-5. The figures presented are for the PWR canister and fuel basket model with a fuel basket drop orientation of 18.22° and are representative of the models for all drop orientations analyzed. Only half of the canister is shown in the figures to present the view of the fuel basket.

The canister shell, shield lid, and structural lids are constructed of SOLID45 elements, which have three degrees-of-freedom (UX, UY, and UZ) per node (see Figure 11.2.12.4.1-3). The interaction of the shield lid and structural lid with the canister shell (below the lid welds) is modeled using CONTAC52 elements with a gap size based on nominal dimensions. The interaction of the bottom edge of the shield lid with the support ring is modeled using COMBIN40 gap elements with a gap size of 1×10^{-8} inch. The interaction of the shield and structural lids is modeled using COMBIN40 gap elements with a conservative gap size of 0.08 inch, based on the flatness tolerance of the two lids. The interaction of the canister shell with the inner surface of the concrete cask is modeled using CONTAC52 elements with an initial gap size equal to the difference in the nominal radial dimensions of the outer surface of the canister and the inner surface of the concrete cask. A gap stiffness of 1×10^{6} lbs/inch is assigned to all CONTAC52 and COMBIN40 elements.

The top five support disks and top weldment disk of the Standard basket are modeled using SHELL63 elements, which have six degrees-of-freedom per node (UX, UY, UZ, ROTX, ROTY, and ROTZ). For the top (first) and fifth support disk, a refined mesh density is used (see Figure 11.2.12.4.1-4). The remaining support disks and the top weldment disk incorporate a course mesh density to account for the load applied to the canister shell. For the fine-meshed support disks, the tie-rod holes are modeled. CONTAC52 elements are included in the slits at the tie-rod holes. The interaction between the fuel basket support disks and top weldment disk and the canister shell is modeled using CONTAC52 elements with an initial gap size based on the nominal radial difference between the disks and canister shell. A gap stiffness of 1×10^{6} lbs/inch is assigned to all CONTAC52 elements.

The lower boundary of the canister shell (near the 5th support disk) is restrained in the axial (Y) direction. For the half-symmetry models (0° and 45° basket drop orientations), symmetry boundary conditions are applied at the plane of symmetry of the model. Since gap elements are used to represent the contact between the canister shell and the inner surface of the concrete cask, the nodes

corresponding to the concrete cask are fixed in all degrees of freedom (UX, UY and UZ). In addition, the axial (UY) and in-plane rotational degrees of freedom (ROTX and ROTZ) of the basket nodes are fixed since there is no out-of-plane loading for the support disk for a side impact condition.

Loading of the Standard configuration model includes an internal pressure of 15 psig (design pressure for normal condition of storage) applied to the inner surfaces of the canister, pressure loads applied to the support disk slots, and the inertial loads. The pressure load applied to the support disk slots represents the weight of the fuel assemblies, fuel tubes, and aluminum heat transfer disks multiplied by the appropriate acceleration (see Figure 11.2.12.4.1-5). For the inertial loads, a maximum acceleration of 40g is conservatively applied to the entire model in the X-direction (see Figure 11.2.12.4.1-2) to simulate the side impact during the cask tip-over event.

As shown in Section 11.2.12.3.1, the maximum acceleration of the concrete cask steel liner at the locations of the top support disk and the top of the canister structural lid during the tip-over event is determined to be 34.3g and 36.9g, respectively. To determine the effect of the rapid application of the inertia loading for the support disk, a dynamic load factor (DLF) is computed using the mode shapes of a loaded support disk. The mode shapes corresponding to the in-plane motions of the disk are extracted using ANSYS. However, only the dominant modes with respect to modal mass participation factors are used in computing the DLF. The dominant resonance frequencies and corresponding modal mass participation factors from the finite element modal analyses of the PWR support disk are:

Frequency (Hz)	% Modal Mass Participation Factor
109.7	85.8
370.1	2.7
371.1	7.2

The mode shapes for these frequencies are shown in Figures 11.2.12.4.1-8 through 11.2.12.4.1-10. The displacement depicted in these figures is highly exaggerated by the ANSYS program in order to illustrate the modal shape. The stresses associated with the actual displacement are shown in Tables 11.2.12.4.1-4 through 11.2.12.4.1-8.

Using the acceleration time history of the concrete cask steel liner at the top support disk location developed from Section 11.2.12.3.1, the DLF is computed to be 1.10. Applying the DLF to the 34.3g results in a peak acceleration of 37.7g for the top support disk. The DLFs for the canister lids

are considered to be unity since the lids have significant in-plane stiffness and are considered to be rigid (the structural lid is 3 inch thick and shield lid is 7 inch thick). Therefore, applying 40g to the entire canister/basket model is conservative.

A uniform temperature of 75°F is applied to the model to determine material properties during solution. During post processing for the support disk, temperature distribution with a maximum temperature of 700°F (at the center) and a minimum temperature of 400°F (at the outer edge) are conservatively used to determine the allowable stresses. A constant temperature of 500°F is used for the canister to determine the allowable stresses. These temperatures are the bounding temperatures for the normal, off-normal and accident conditions of storage.

Analysis Results for the Standard Configuration Canister

The sectional stresses at 13 axial locations of the canister are obtained for each angular division of the model (a total of 80 angular locations for the full-models and 41 angular locations for the half-symmetry models). The locations for the stress sections are shown in Figure 11.2.12.4.1-6.

The stress evaluation for the canister is performed in accordance with the ASME Code, Section III, Subsection NB, by comparing the linearized sectional stresses against the allowable stresses. Allowable stresses are conservatively taken at a temperature of 500°F, except that 300°F and 250°F are used for the shield lid weld (Section 10) and the structural lid weld (Section 11). The calculated maximum temperatures for the shield lid and structural lid are 212°F and 202°F, respectively (Table 4.4.3.1-1). The allowable stresses for accident conditions are taken from Subsection NB as shown below. S_m and S_u are 14.8 ksi and 57.8 ksi, respectively, for Type 304L stainless steel (canister shell and structural lid). S_m and S_u are 17.5 ksi and 63.5 ksi, respectively, for Type 304 stainless steel (shield lid).

Stress Category	Accident (Level D) Allowable Stress
P_m	Lesser of 0.7 S_u or 2.4 S_m
P_m+P_b	Lesser of 1.0 S_u or 3.6 S_m

The primary membrane and primary membrane plus bending stresses for the Standard PWR configuration for a 45° basket drop orientation are summarized in Table 11.2.12.4.1-1 and Table 11.2.12.4.1-2, respectively. The stress results for the canister are similar for all four basket drop orientation evaluations. The 45° basket orientation results are presented because this drop orientation results in the minimum margins of safety in the canister.

During the tip-over accident, the canister shell at the structural and shield lids is subjected to the inertial loads of the lids, which results in highly localized bearing stresses (Sections 7 through 9 at angular locations of approximately ± 4.5 degrees from the impact location). This stress is predominant because the weights of the structural and shield lids are transferred to the canister shell near these section locations. According to ASME Code Section III, Appendix F, bearing stresses need not be evaluated for Level D service (accident) conditions. Therefore, the stresses are not presented for the lid-bearing regions of the canister shell (Sections 7 through 9) in Tables 11.2.12.4.1-1 and 11.2.12.4.1-2. The stresses at the structural lid/canister shell weld region (Section 11) are determined by averaging the stresses over the impact region where the weld is in compression in the radial direction ($\sigma_x \leq 0.0$ psi). In accordance with ISG 4, Revision 1, a 0.8 weld reduction factor is applied to the allowable stresses for the structural lid / canister shell weld. Use of the 0.8 factor is valid because the ultimate tensile strength of the weld material exceeds the base metal strength.

The stress evaluation results for the tip-over accident condition show that the minimum margin of safety in the Standard canister for the PWR configuration is +0.13 for P_m stresses (Section 10). For P_m+P_b stresses, the margin of safety at is +0.23 (Section 10).

Analysis Results for the Standard Basket Support Disks

To evaluate the most critical regions of the support disk, a series of cross sections are considered. To aid in the identification of these sections, Figure 11.2.12.4.1-7 shows the locations on a support disk for the full-models. Table 11.2.12.4.1-3 lists the cross sections versus Point 1 and Point 2, which spans the cross-section of the ligament in the plane of the support disk. Note that a local coordinate system (x and y parallel to the support disk ligaments) is used for the stress evaluation.

The stress evaluation for the support disk is performed according to ASME Code, Section III, Subsection NG. According to this subsection, linearized sectional stresses are to be compared against the allowable stresses. The allowable stresses for tip-over accident conditions are taken from Subsection NG as shown below, at the temperature of the section. The temperature distribution of the disk is determined by a thermal conduction solution for a single disk with the maximum temperature of 700°F specified at the center and the minimum temperature of 400°F specified at the outer edge as boundary conditions.

Stress Category	Accident (Level D) Allowable Stresses
P_m	Lesser of 0.7 S_u or 2.4 S_m
P_m+P_b	Lesser of 1.0 S_u or 3.6 S_m

The shield lid and structural lid provide additional stiffness to the upper portion of the canister shell, which limits the shell and support disk deformations. Therefore, the maximum $P_m + P_b$ stress, and the minimum margin of safety, occur in the 5th support disk (from the top of the basket), where the stiffness effect of the shield and structural lids is not present.

The stress evaluation results for the 5th support disk for the tip-over condition are summarized in Table 11.2.12.4.1-4 for the four basket drop orientations evaluated. As shown in Table 11.2.12.4.1-4, the 26.28° drop orientation case generates the minimum margin of safety in the support disk; therefore, the P_m and $P_m + P_b$ stress intensities for the 26.28° basket drop orientation case are presented in Tables 11.2.12.4.1-6 and 11.2.12.4.1-7, respectively. These tables list stress results with the 30 lowest margins of safety for the 5th support disk. The highest P_m stress occurs at Section 18, with a margin of safety of +0.97 (See Table 11.2.12.4.1-6 for stresses and Figure 11.2.12.4.1-7 for section locations). The highest P_m+P_b stress occurs at Section 61, with a margin of safety of +0.05 (see Table 11.2.12.4.1-7 for stresses and Figure 11.2.12.4.1-7 for section locations).

Standard Basket Support Disk Buckling Evaluation

For the tip-over accident, the support disks experience in-plane loads. The in-plane loads apply compressive forces and in-plane bending moments on the support disk. Buckling of the support disk is evaluated in accordance with the methods and acceptance criteria of NUREG/CR-6322 [39]. Because the ASME Code identifies 17-4PH disk material as ferritic steel, the formulas for non-austenitic steel are used.

The buckling evaluation of the support disk ligaments is based on the Interaction Equations 31 and 32 in NUREG/CR-6322. These two equations adopt the "Limit Analysis Design" approach. Other equations applicable to the calculations are noted as they are applied. The maximum forces and moments for the tip-over accident are based on the finite element analysis stress results.

Symbols and Units

P = applied axial compressive load, kip
M = applied bending moment, kip-inch
P_a = allowable axial compressive load, kip
P_{cr} = critical axial compression load, kip
P_e = Euler buckling loads, kip

P_y = average yield load, equal to profile area times specified minimum yield stress, kips (for normal operating condition)

C_c = column slenderness ratio separating elastic and inelastic buckling

C_m = coefficient applied to bending term in interaction equation

M_m = critical moment that can be resisted by a plastically designed member in the absence of axial load, kip-in.

M_p = plastic moment, kip-in.

F_a = axial compressive stress permitted in the absence of bending moment, ksi

F_e = Euler stress for a prismatic member divided by factor of safety, ksi

k = ratio of effective column length to actual unsupported length

l = unsupported length of member, in.

r = radius of gyration, in.

S_y = yield stress, ksi

A = cross sectional area of member, in^2

Z_x = plastic section modulus, in^3

λ = allowable reduction factor, dimensionless

From NUREG/CR-6322, the following equations are used to evaluate the support disk:

$$\frac{P}{P_{cr}} + \frac{C_m M}{M_m\left[1 - \frac{P}{P_e}\right]} \le 1.0 \qquad \text{(Equation 31)}$$

$$\frac{P}{P_y} + \frac{M}{1.18\,M_p} \le 1.0 \qquad \text{(Equation 32)}$$

where:

$$P_{cr} = 1.7 \times A \times F_a$$

$$F_a = \frac{P_a}{A} \quad \text{for } P_a = P_y\left[\frac{1 - \frac{\lambda^2}{4}}{1.11 + 0.5\lambda + 0.17\lambda^2 - 0.28\lambda^3}\right]$$

and $\lambda = \frac{1}{\pi}\left(\frac{kl}{r}\right)\sqrt{\frac{S_y}{E}}$ (accident conditions)

$$Pe = 1.92 \times A \times Fe$$

$$F_e = \frac{\pi^2 \cdot E}{1.3\left(\frac{k \cdot l}{r}\right)^2}$$ (Level D–Accident)

$$P_y = S_y \times A$$

C_m = 0.85 for members with joint translation (sideways)

$$M_p = S_y \times Z_x$$

$$M_m = M_p \cdot \left(1.07 - \frac{\left(\frac{l}{r}\right) \cdot \sqrt{S_y}}{3160}\right) \leq M_p$$

Buckling evaluation is performed in all sections in the disk ligaments defined in Figure 11.2.12.4.1-7. Using the cross-sectional stresses calculated at each section located in the ligament for each loading condition, the maximum corresponding compressive force (P) and bending moment (M) are determined as:

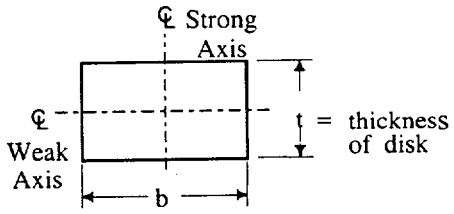

$$P = \sigma_m A$$

$$M = \sigma_b S$$

where, σ_m is the membrane stress, σ_b is the bending stress, A is the area (b × t), and S is the section modulus ($tb^2/6$). Note that the strong axis bending is considered in the buckling evaluation since the disk is only subjected to in-plane load during the tip-over event.

To determine the margin of safety:

$$P_1 = P/P_{cr} \qquad M_1 = \frac{C_m M}{(1 - P/P_e) M_m} \qquad (P_1 + M_1 \leq 1)$$

and

$$P_2 = P/P_y \qquad M_2 = \frac{M}{1.18\, M_p} \qquad (P_1 + M_1 \leq 1)$$

The margins of safety are:

$$MS1 = \frac{1}{P_1 + M_1} - 1$$

and

$$MS2 = \frac{1}{P_2 + M_2} - 1$$

The support disk buckling evaluation results for the 5th support disk (the 5th support disk experiences the highest stresses) for the tip-over impact condition are summarized in Table 11.2.12.4.1-5 for the four basket drop orientations evaluated. As shown in Table 11.2.12.4.1-5, the 26.28° case generates the minimum margin of safety for buckling; therefore, the results of the buckling analysis for the 26.28° basket drop orientation case are presented in Table 11.2.12.4.1-8. This table presents the 30 minimum margins of safety for this drop orientation. As the tables demonstrate, the support disks meet the requirements of NUREG/CR-6322.

Standard Basket Fuel Tube Analysis

The fuel tube provides structural support and a mounting location for BORAL neutron poison plates. The fuel tube does not provide structural support for the fuel assembly. To ensure that the fuel tube remains functional during a tip-over accident, a structural evaluation of the tube is performed for a side impact assuming a deceleration of 60g. This g-load bounds the maximum g-load (40g) calculated to occur for the PWR basket in a vertical concrete cask tip-over event.

In the tip-over event, the stainless steel support disks in the fuel basket support the fuel tube. The fuel basket support disks, which support the full length of the fuel tube, are spaced 4.42-inches apart (which is less than one half of the fuel tube width of 8.8 inch). Considering the fuel tube subjected to a maximum PWR fuel assembly weight of 1,602 pounds with a 60g load factor and the 30 support locations provided by the basket support disks, the fuel tube shear stress is calculated as:

Shear load = (60g)(1,602)/30 = 3,204 lbs
Area = (0.048)(8.8)(2) = 0.845 in^2
Shear Stress = 3,204/0.845 = 3,792 psi

The yield strength of the tube material, Type 304 stainless steel, is 17,300 psi at 750°F. Conservatively, using the allowable shear stress as one-half the yield strength of the tube material (8,650 psi) results in a large positive margin of safety. Conservative evaluation of the tube loading resulting from its own mass during a side-impact shows that the tube structure maintains position and function.

The load transfer of the weight of the fuel assembly to the fuel basket support disk in the side impact is through direct bearing and compression of the distributed load of the fuel assembly through the fuel tube to the support disk web. Two load conditions are considered in the fuel tube evaluation. The first considers the fuel assembly load as a distributed pressure on the inside surface of the fuel tube. The second postulates that the fuel assembly grid is located at the center of the span between the support disks and produces a localized distributed load over the effective area of the grid.

Two different ANSYS finite element models of the tube are developed for these two load conditions since the fuel tube structural performance for either load is nonlinear. As shown below, the first model represents a fuel tube section with a length of three spans, i.e., the model is supported at four locations by support disks. The model conservatively considers the fuel tube wall thickness of 0.048 inch as the only material subjected to a distributed pressure load representative of the fuel assembly deceleration of 60g. Fuel assembly stiffness is not considered in the development of the imposed pressure load on the fuel tube.

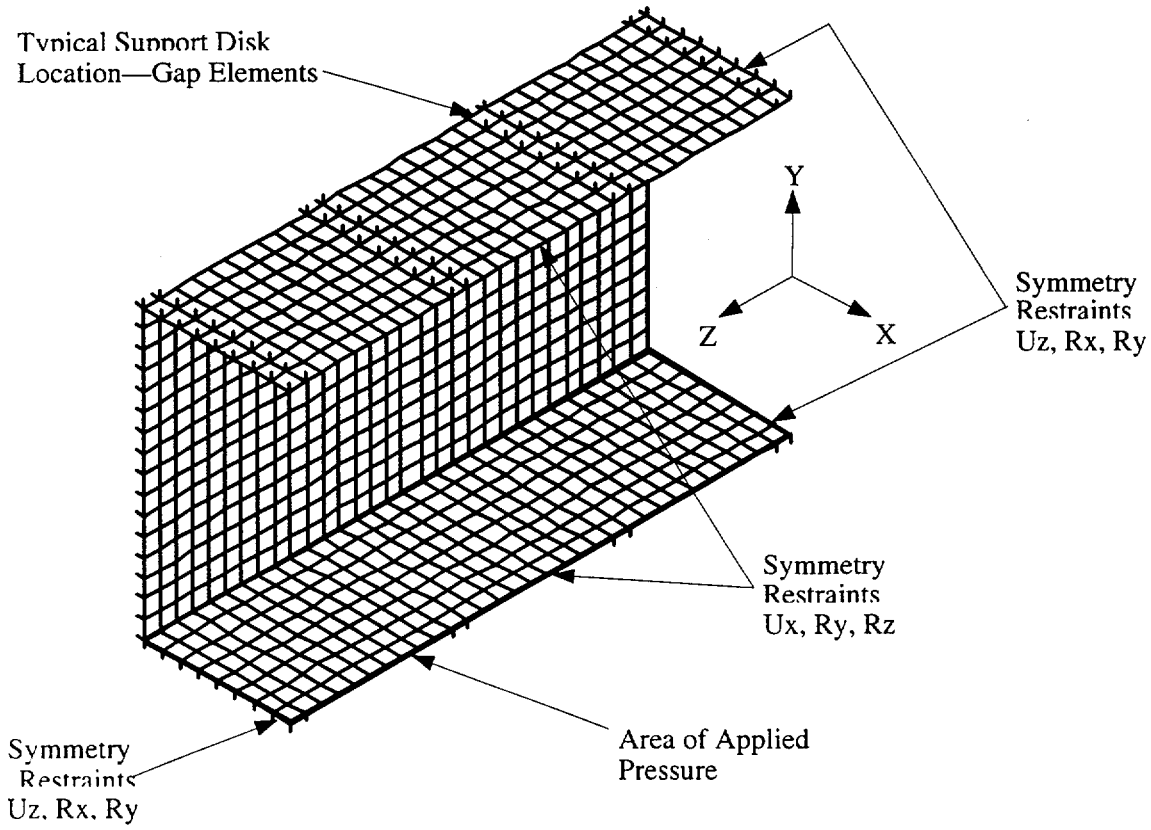

The tube is modeled with the ANSYS plastic, quadrilateral shell element (SHELL43). The support disks are represented by gap elements (CONTAC52). The outer nodes of the gap elements are fully restrained in all three translational directions. Edge restraints were applied to the model to represent symmetry boundary conditions. The effective load on the fuel tube due to the 60g deceleration of the fuel assembly is applied as a pressure to the inside area of the fuel tube.

The finite element analysis results show that the maximum stress in the tube is 23.8 ksi, which is local to the sections of the tube resting on the support disks. At 750°F the ultimate strength for Type 304 stainless steel is 63.1 ksi. The margin of safety is:

$$MS = \frac{63.1}{23.8} - 1 = +1.65$$

The analysis shows that the maximum total strain is 0.026 inch/inch. Defining the acceptable elastic-plastic response of the stainless steel as one half of the material failure strain of 0.40 in./in. at 750°F [42], the resulting margin of safety is:

$$MS = \frac{0.40/2}{0.026} - 1 = +\text{large}$$

Similarly, the margin of safety for elastic-plastic stress becomes

$$MS = \frac{63.1 - 17.3}{23.8 - 17.3} - 1 = 6.05$$

where the yield strength of Type 304 stainless steel is 17.3 ksi at 750°F.

The second finite element model is used to evaluate the load condition with the fuel assembly grid located at the center of the span between two support disks. The fuel tube is subjected to a localized distributed load over the effective area of the grid. As shown below, the model is a quarter-symmetry periodic section of the fuel tube. As in the finite element model used for the distributed pressure case, this model conservatively considers a fuel tube wall thickness of 0.048 inch. The BORAL plate (0.075 inch) and stainless steel cover plate (0.018 inch) are conservatively not included in the model. The tube wall is modeled with ANSYS SHELL43 elements. The support disks are modeled with CONTAC52 elements.

Based on the Lawrence Livermore evaluation of the fuel rods for a side impact (UCID-21246), the fuel rods and fuel assemblies maintain their structural integrity during the side impact resulting from a cask tip-over accident and the displacement of the fuel tube is limited. The maximum displacement of the fuel tube section between the support disks will not exceed the "thickness" of the grid spacer, which is the distance between the outer surface of the grid and the outer surface of the fuel rod array. When the displacement of the fuel tube reaches the "thickness" of the grid spacer, the fuel rods will be in contact with the inner surface of the fuel tube and the weight of the fuel rods will be transferred through the tube wall to the support disks. Therefore, a bounding load condition for this model is simulated by applying a constant displacement of 0.08 inch in the negative Y direction to the nodes corresponding to the grid location in the model. Note that 0.08 inch displacement bounds all PWR fuel assemblies. It is assumed that the fuel assembly grid spacer is rigid and therefore a constant displacement is conservatively applied.

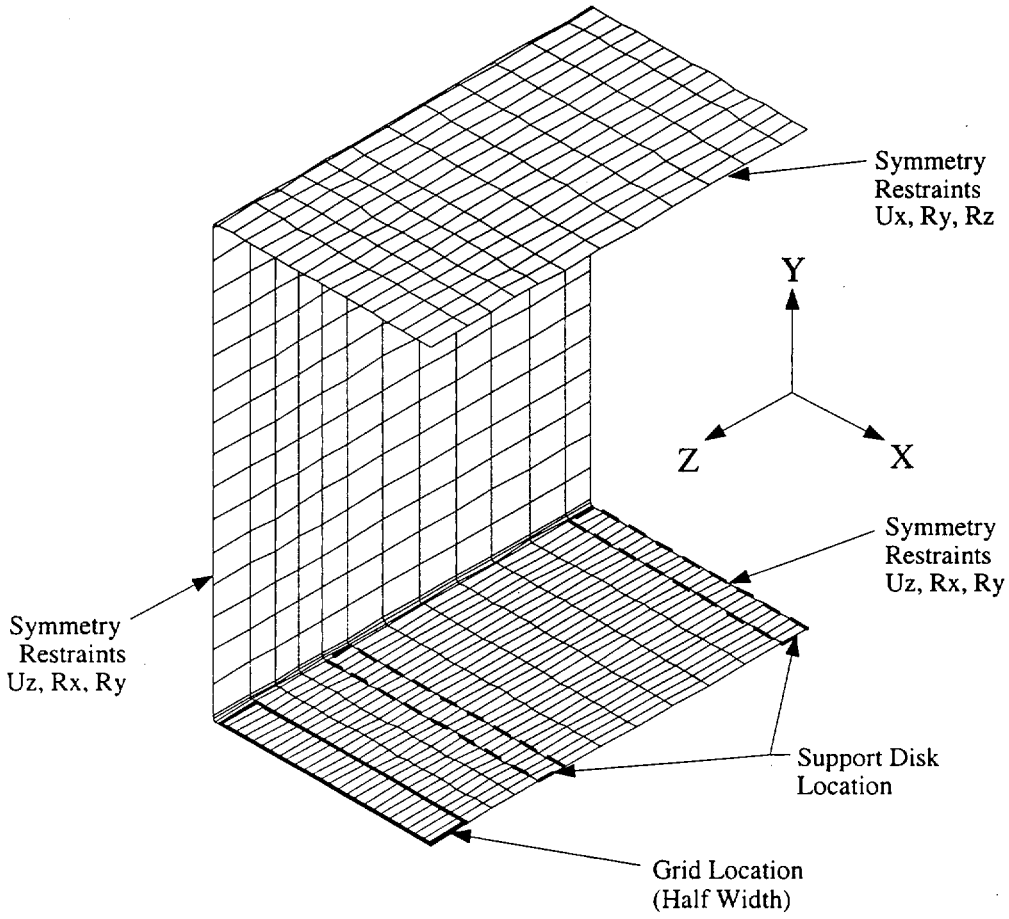

The finite element analysis results show that the maximum stress in the tube is 38.4 ksi, which is local to the corner of the tube at the grid spacer location of the model close to the side wall of the tube. At 750°F the ultimate strength for Type 304 stainless steel is 63.1 ksi. The margin of safety is

$$MS = \frac{63.1}{38.4} - 1 = +0.64$$

The analysis shows that the maximum total strain is 0.11 inch/inch. Defining the acceptable elastic-plastic response of the stainless steel as one half of the material failure strain of 0.40 in./in. at 750°F [42], the resulting margin of safety is:

$$MS = \frac{0.40/2}{0.11} - 1 = 0.82$$

Similarly, the margin of safety for elastic-plastic stress becomes

$$MS = \frac{63.1 - 17.3}{38.4 - 17.3} - 1 = 1.17$$

where the yield strength of Type 304 stainless steel is 17.3 ksi at 750°F.

Both the maximum total strain and the elastic-plastic stress analyses indicate that the tube position within the support basket is maintained.

Assurance that the BORAL remains attached to the fuel tube is evaluated by considering that loads produced by the BORAL plate and stainless steel attachment plate, assuming a 60g load, are carried by the attachment plate weld. Total load and resultant stress on the weld are calculated as:

$F_{b/ss} = (g)(\rho)(t)(w)(l)$ Load exerted by BORAL/Stainless Steel Attachment Plate

where:

- g = acceleration (g)
- ρ = density of material (lb/in^3) (The density of aluminum (0.098 lb/in^3) is conservatively used for the BORAL.
- t = thickness of material (in.)
- w = width of material (in.)
- l = length of material section (in.)

The forces on the weld due to a 12-inch section of BORAL (F_b) and a 12-inch section of stainless steel plate (F_{ss}) are:

F_b = (60g)(0.098 lb/in^3)(0.075 in.)(8.2 in.)(12 in.)
= 43.4 lbs

F_{ss} = (60g)(0.291 lb/in^3)(0.018 in.)(8.7 in.)(12 in.)
= 32.8 lbs

The total load (F_t) on a 1-inch attachment weld for a 12-inch section is:

$$F_t = 43.4 \text{ lbs} + 32.8 \text{ lbs} = 76.2 \text{ lbs}$$

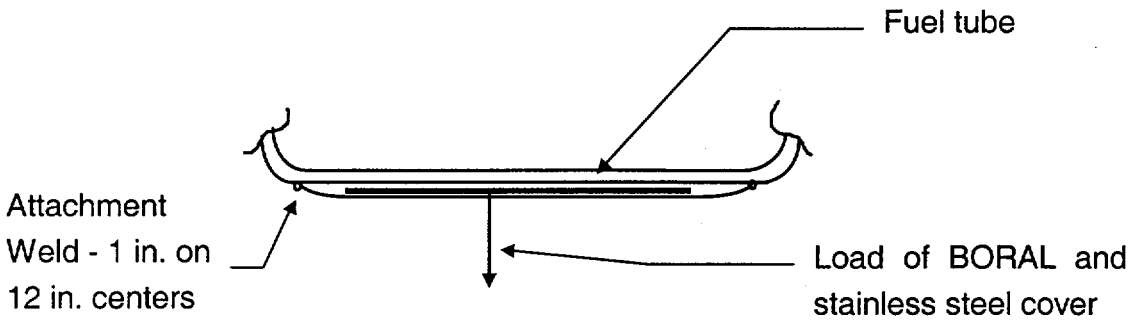

The resulting weld stress is: $\sigma = P/A = (76.2 \text{ lb}/2) / (1 \text{ in.}) (0.018 \text{ in.}) = 2{,}117 \text{ psi}$

Since the weld material is Type 304 stainless steel, the margin of safety (at 750°F) is:

$$MS = \frac{17{,}300}{2{,}117} - 1 = +7.2$$

Therefore, the BORAL remains enclosed on each outer surface of the fuel tube wall.

Figure 11.2.12.4.1-1 Standard PWR Basket Drop Orientations Analyzed for Tip-Over Conditions

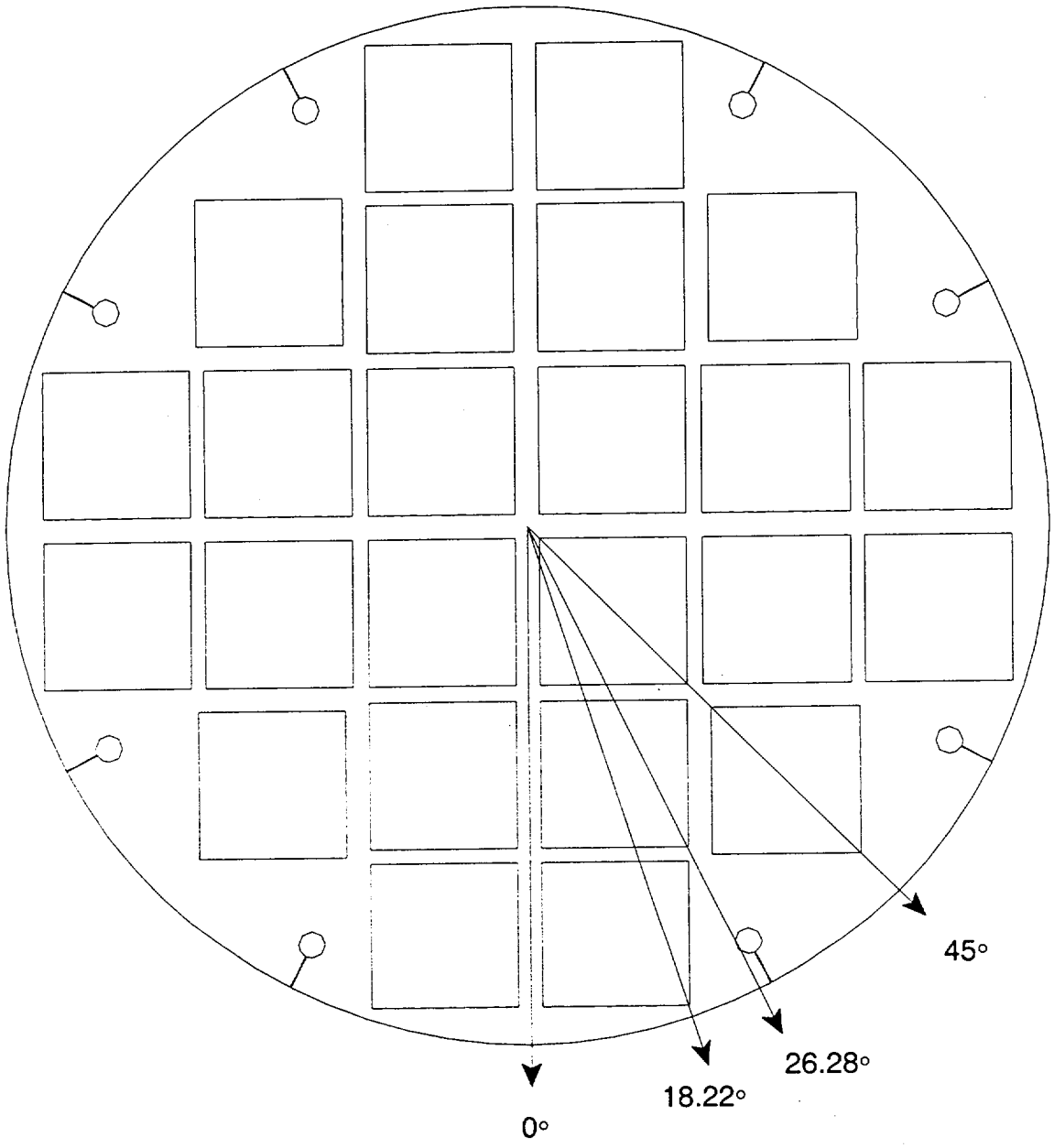

Figure 11.2.12.4.1-2 Standard PWR Fuel Basket/Canister Finite Element Model

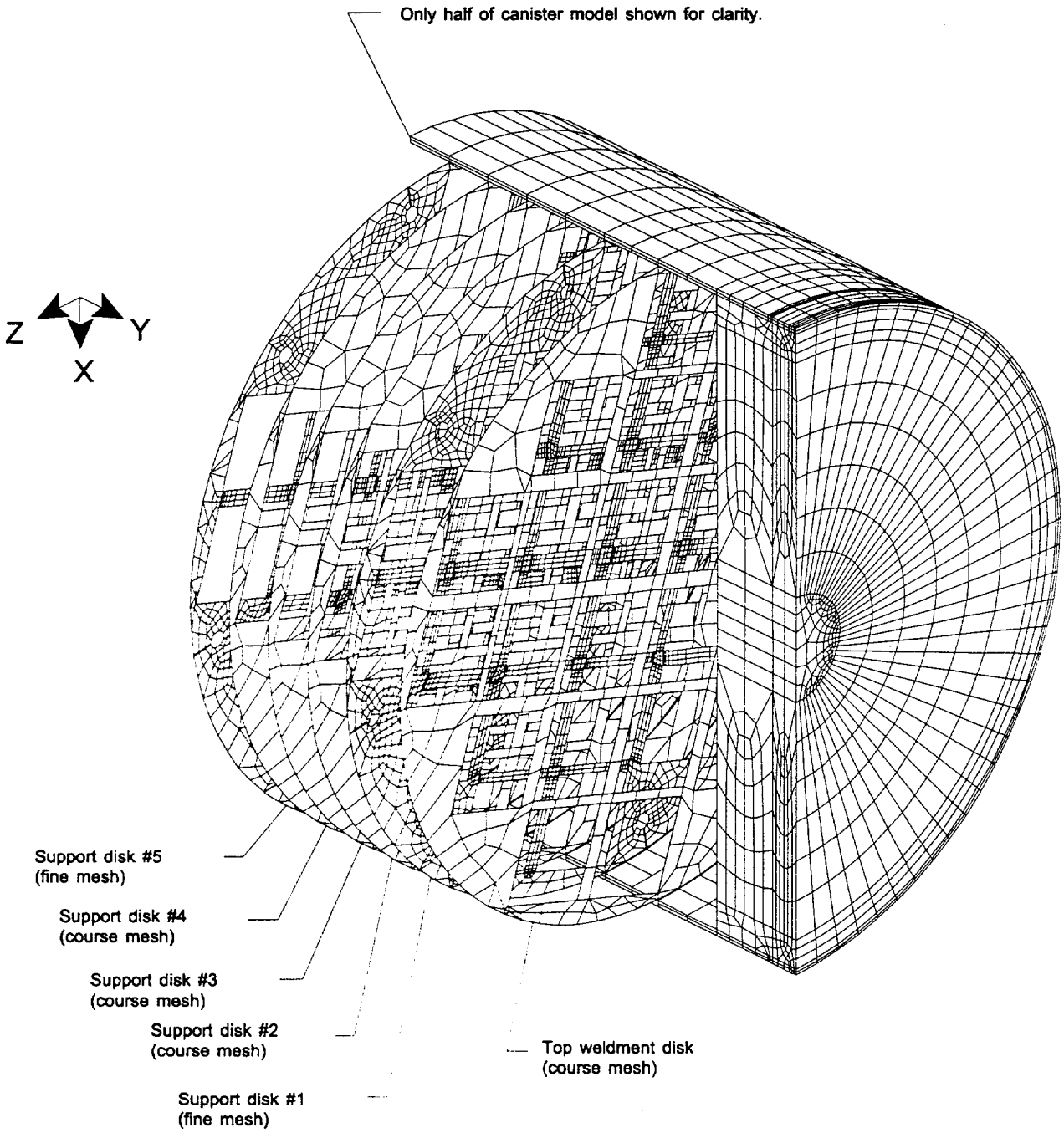

18.22° Basket Drop Orientation

Figure 11.2.12.4.1-3 Standard Fuel Basket/Canister Finite Element Model - Canister

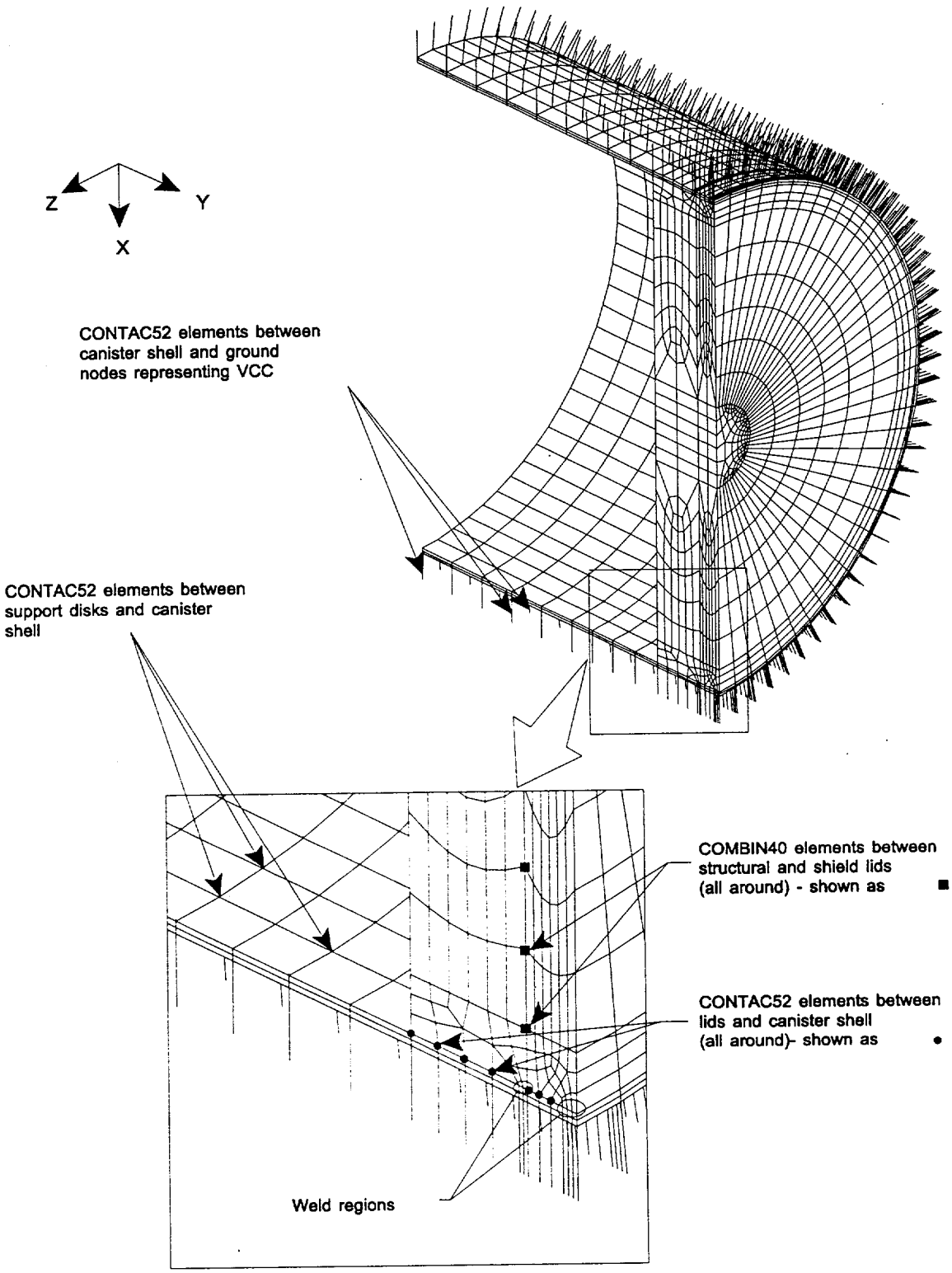

Only Half of Canister Shown for Clarity

Figure 11.2.12.4.1-4 Standard PWR Fuel Basket/Canister Finite Element Model - Support Disk

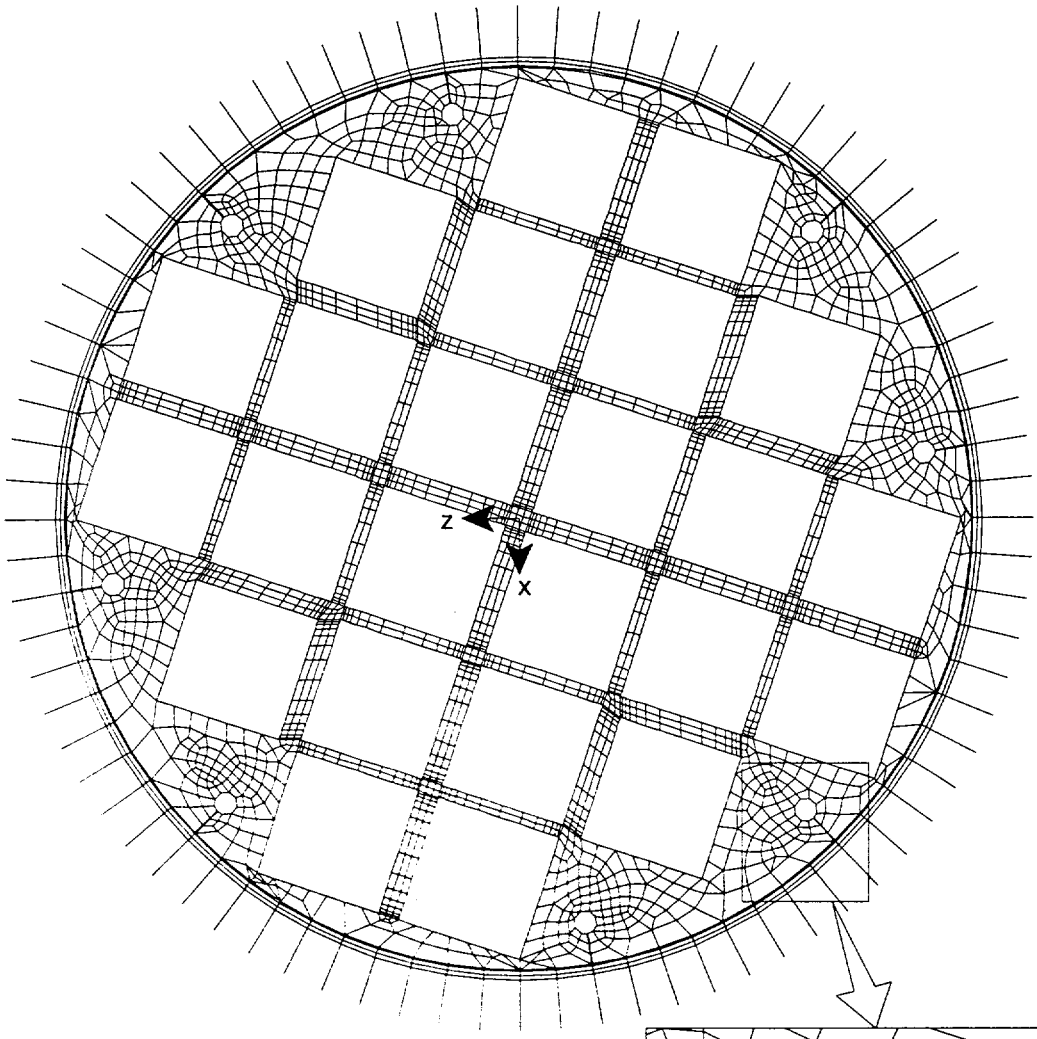

18.22° Basket Drop Orientation

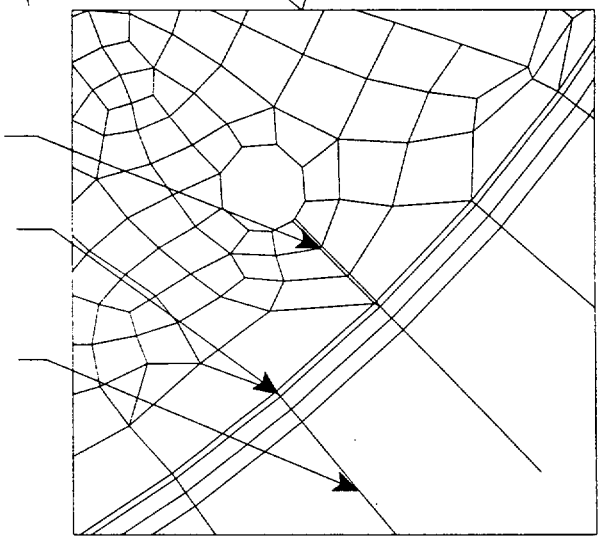

Figure 11.2.12.4.1-5 Standard PWR Fuel Basket/Canister Finite Element Model - Support Disk Loading

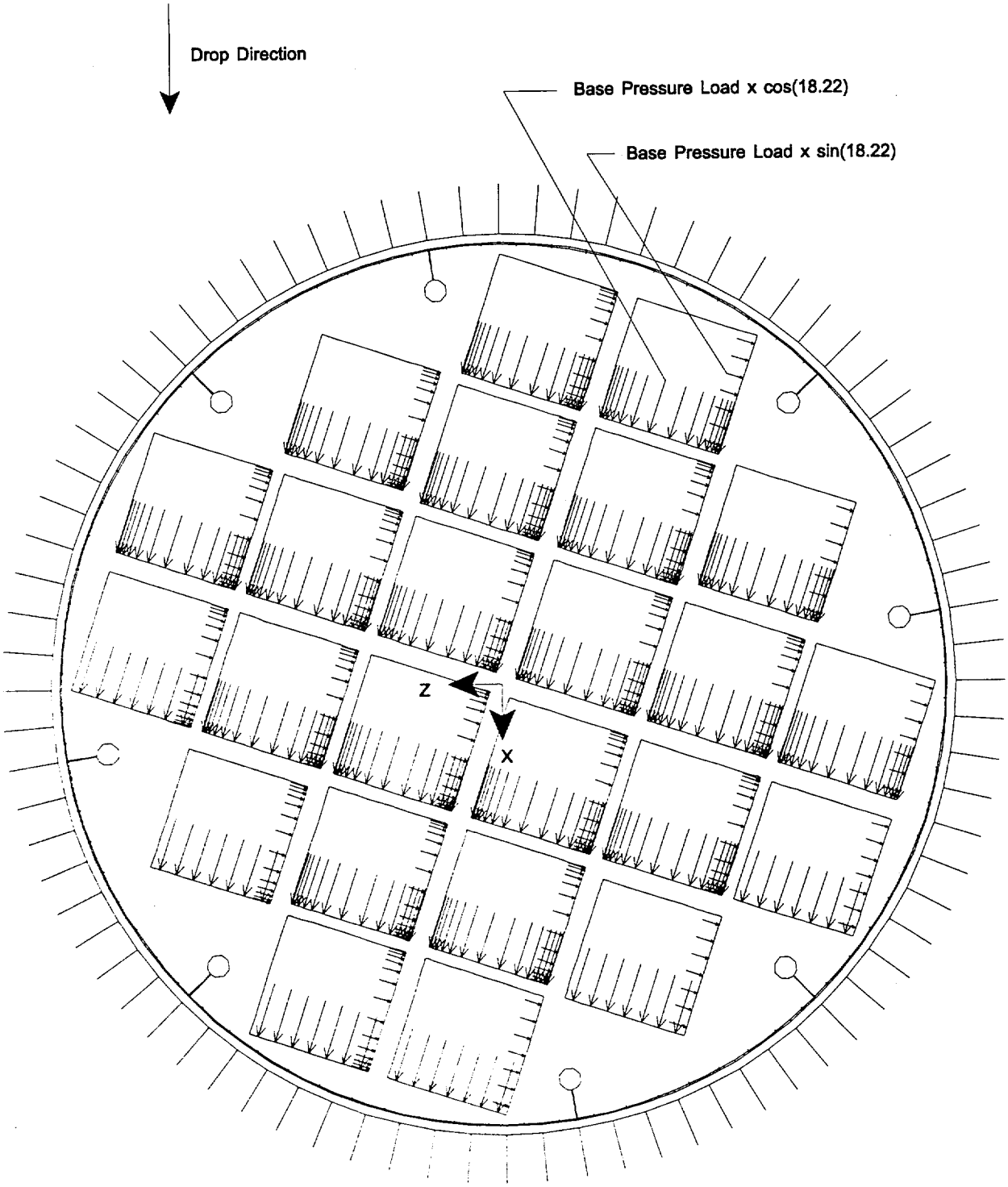

18.22° Basket Drop Orientation

Note: Finite Element Mesh Not Shown

Figure 11.2.12.4.1-6 Standard Canister Section Stress Locations

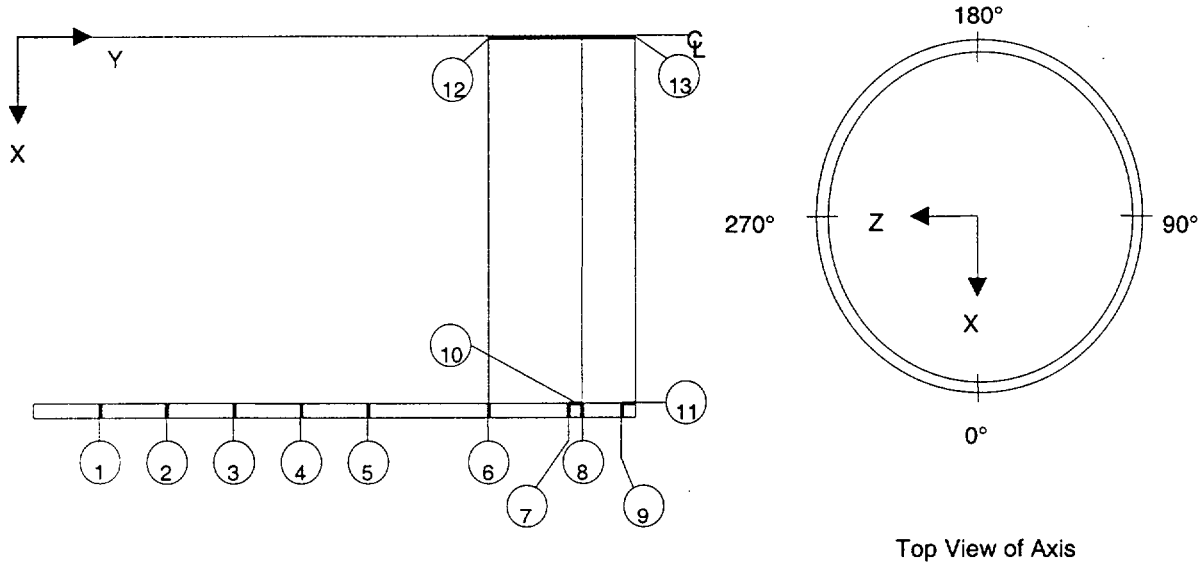

PWR 1
Section Coordinates at Z = 0 and X > 0

	Point 1		Point 2	
Location	X	Y	X	Y
1	32.905	131.42	33.53	131.42
2	32.905	136.34	33.53	136.34
3	32.905	141.26	33.53	141.26
4	32.905	146.18	33.53	146.18
5	32.905	151.10	33.53	151.10
6	32.905	165.25	33.53	165.25
7	32.905	171.75	33.53	171.75
8	32.905	172.25	33.53	172.25
9	32.905	174.37	33.53	174.37
10	32.905	171.75	32.905	172.25
11	32.905	174.37	32.905	175.25
12	0.1	165.25	0.1	172.23
13	0.1	172.27	0.1	175.25

BWR 4
Section Coordinates at Z = 0 and X > 0

	Point 1		Point 2	
Location	X	Y	X	Y
1	32.905	144.32	33.53	144.32
2	32.905	148.15	33.53	148.15
3	32.905	151.98	33.53	151.98
4	32.905	155.81	33.53	155.81
5	32.905	159.64	33.53	159.64
6	32.905	175.25	33.53	175.25
7	32.905	182.25	33.53	182.25
8	32.905	182.75	33.53	182.75
9	32.905	184.87	33.53	184.87
10	32.905	182.25	32.905	182.75
11	32.905	184.87	32.905	185.75
12	0.1	175.75	0.1	182.73
13	0.1	182.77	0.1	185.75

General Notes:

1) Impact from the tipover condition is at 0° (in the circumferential direction).

2) For the full 360° models, there are 80 sections at each location for a total of 1040 sections. For the half 180° models, there are 41 sections at each location for a total of 533 sections.

3) Location 10 is through the length of the shield lid weld. Locations 8 and 7 are through the canister shell at top and bottom of the shield lid weld, respectively.

4) Location 13 is through the length of the structural lid weld. Location 9 is through the canister shell at the bottom of the structural lid weld.

Figure 11.2.12.4.1-7 Standard PWR Basket Support Disk Section Stress Locations – Full Model

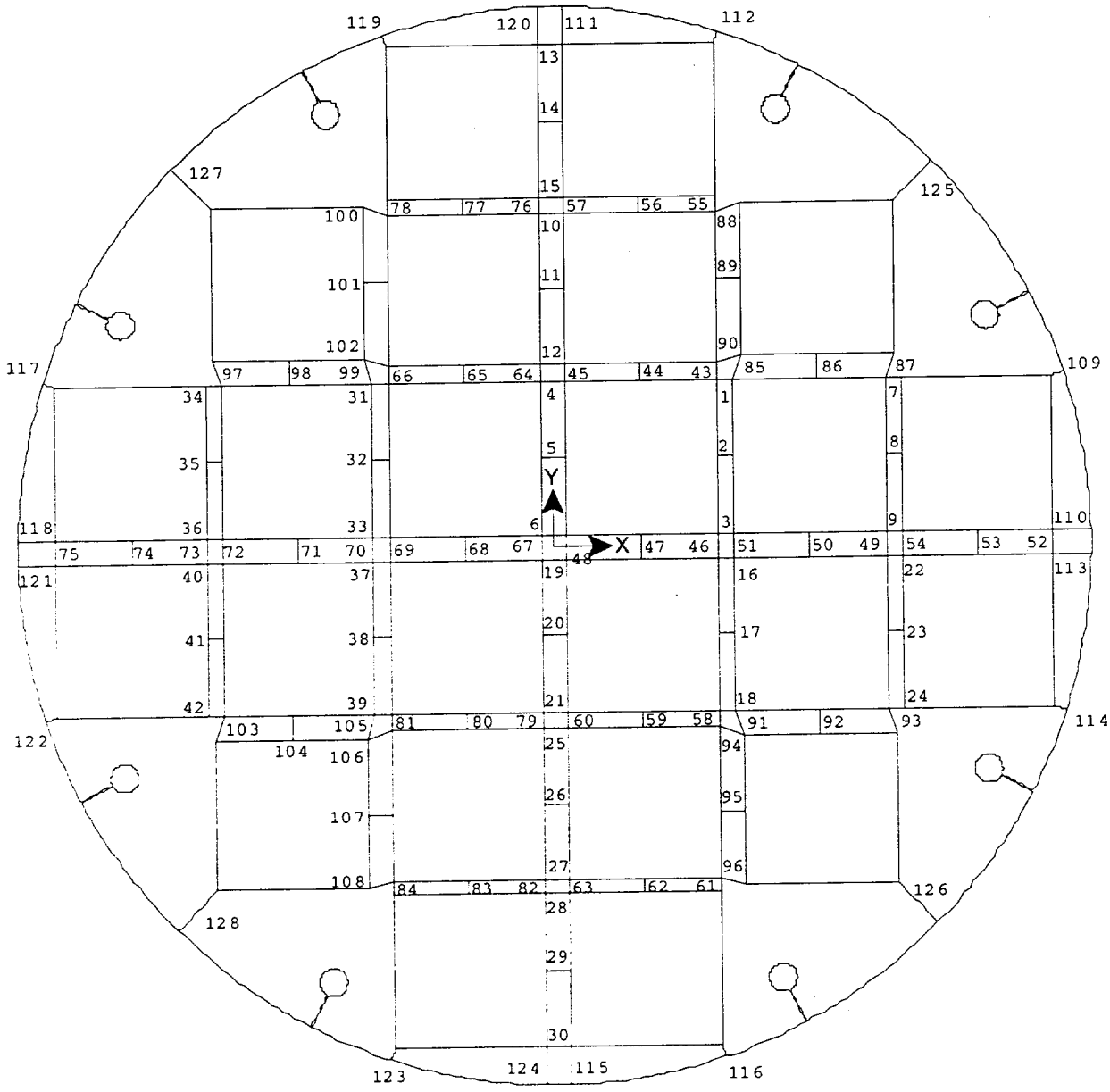

Figure 11.2.12.4.1-8 Standard PWR Support Disk- 109.7 Hz Mode Shape

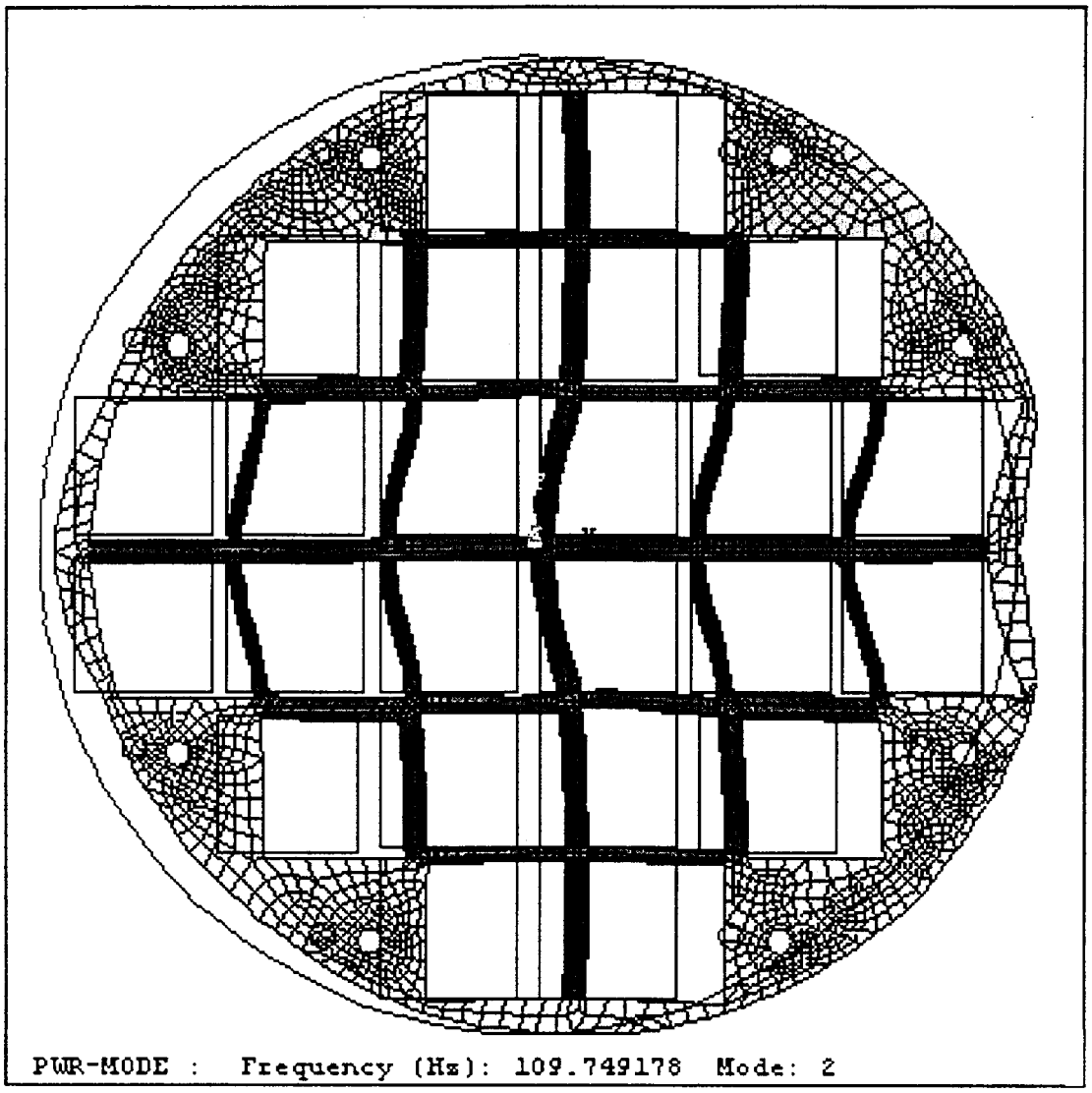

Note: Displacements are greatly exaggerated by the ANSYS program to illustrate the mode shapes.

Figure 11.2.12.4.1-9 Standard PWR Support Disk – 370.1 Hz Mode Shape

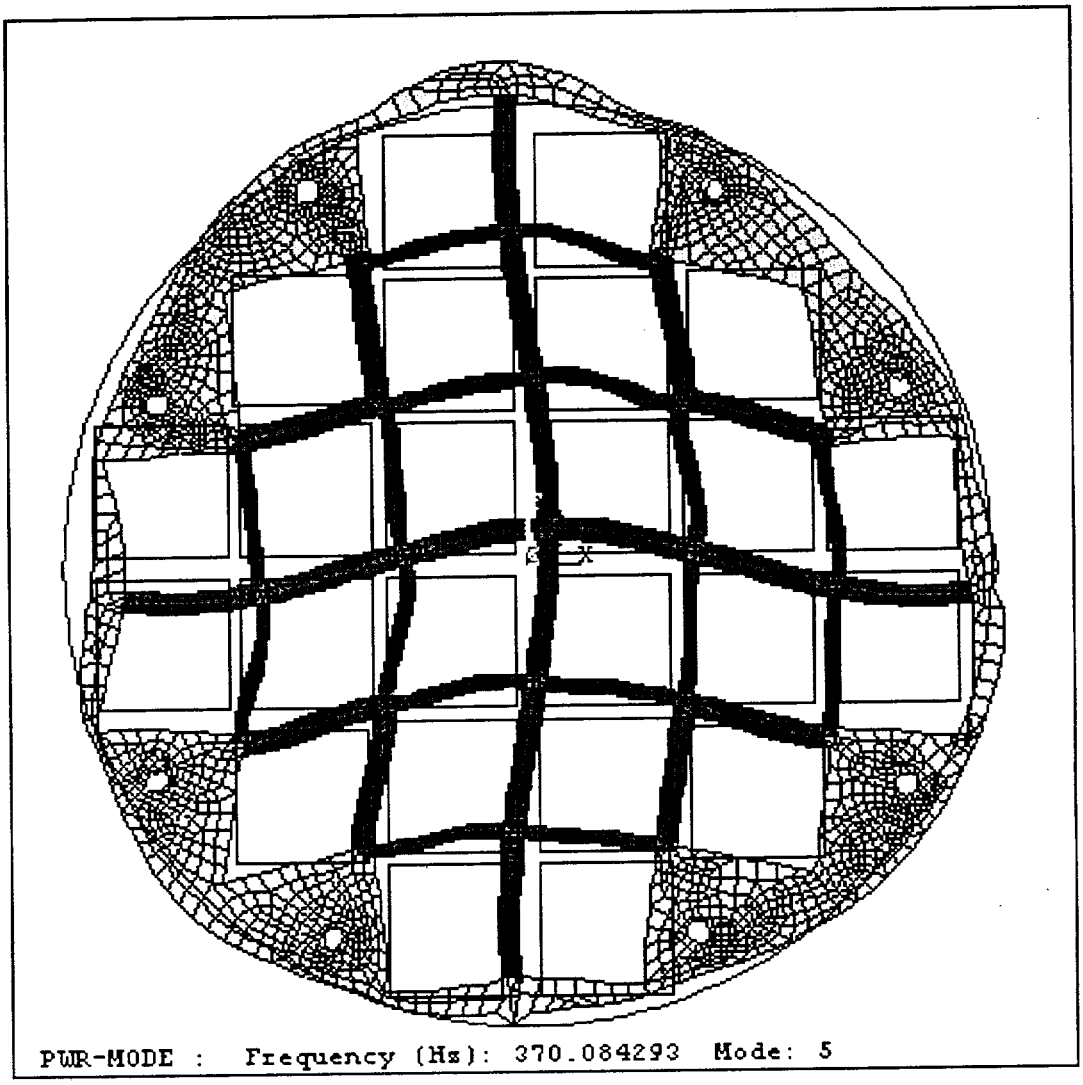

Note: Displacements are greatly exaggerated by the ANSYS program to illustrate the mode shapes.

Figure 11.2.12.4.1-10 Standard PWR Support Disk – 371.1 Hz Mode Shape

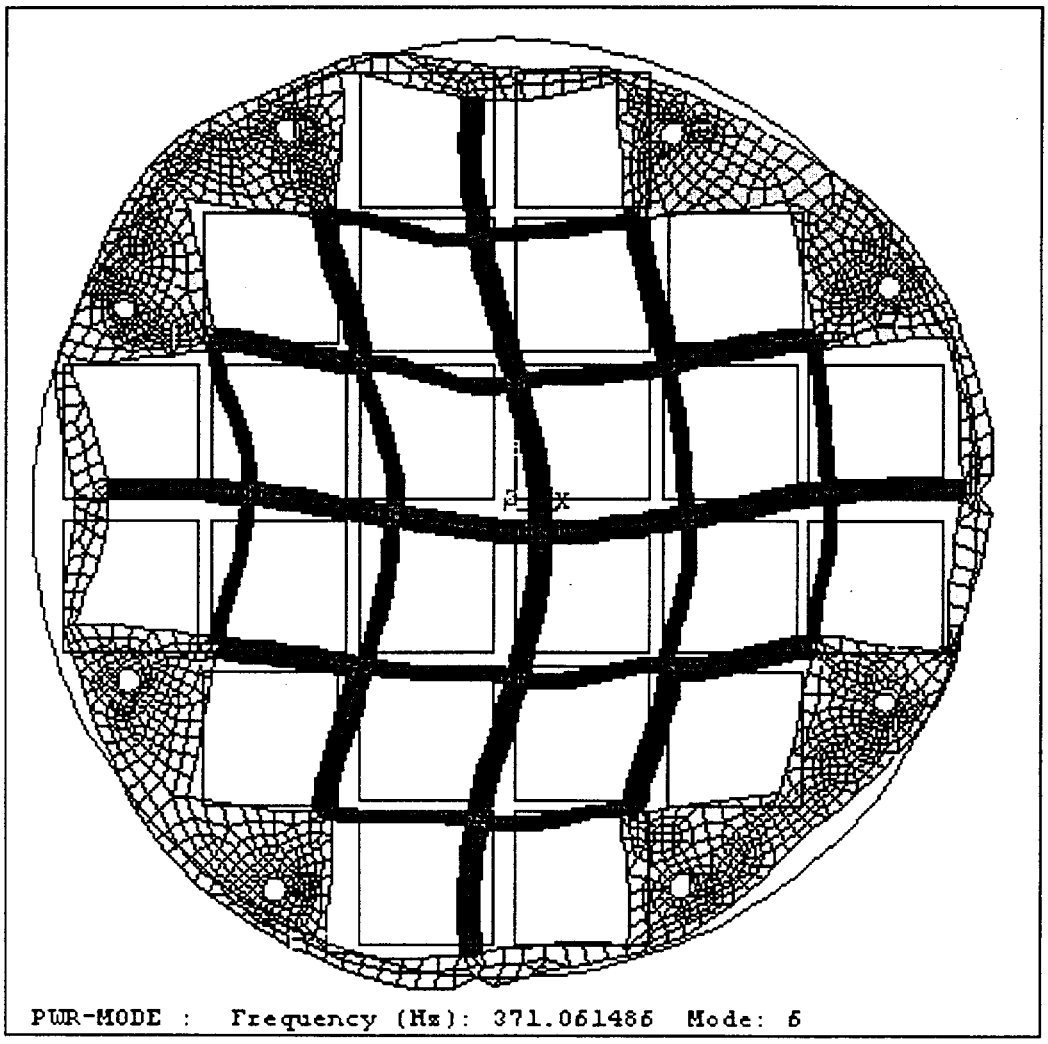

Note: Displacements are greatly exaggerated by the ANSYS program to illustrate the mode shapes.

Table 11.2.12.4.1-1 Standard PWR Canister Primary Membrane (P_m) Stresses for Tip-Over Conditions - 45° Basket Drop Orientation (ksi)

Section Location[1]	Section Angle (deg)	Sx	Sy	Sz	Sxy	Syz	Sxz	Stress Intensity	Allowable Stress	Margin of Safety
1	0	-1.5	6.5	1.4	-0.1	0.0	-0.2	8.06	35.52	3.41
2	0	-1.7	9.2	1.5	0.1	0.0	0.3	10.92	35.52	2.25
3	49.6	-0.2	9.4	6.3	-0.1	1.1	0.0	9.89	35.52	2.59
4	63.3	-0.3	8.9	5.1	0.1	3.4	0.5	11.24	35.52	2.16
5	90	0.1	2.8	-1.0	-0.3	6.0	0.1	12.67	35.52	1.80
6	85.6	0.0	0.3	0.1	-0.1	7.8	0.0	15.67	35.52	1.27
7[2]	8.7	1.1	0.9	7.4	2.5	-5.0	0.4	13.41	35.52	1.65
8[2]	8.7	5.3	-0.1	6.8	0.5	-3.1	-1.2	9.71	35.52	2.66
9[2]	8.7	6.6	-3.0	1.6	2.3	-3.8	-0.1	12.77	35.52	1.78
10	0	-45.3	-22.9	-40.0	0.6	-1.5	-15.0	35.45	40.08[3]	0.13
11[4]	0.0 – 8.0	-29.4	-14.4	-9.1	-4.6	-2.4	0.9	22.81	32.06[4]	0.41
12	0	-0.7	0.2	0.0	0.0	0.0	-0.1	0.93	35.52	37.09
13	0	-1.6	0.5	0.0	0.0	0.0	0.0	2.02	35.52	16.61

Stresses are presented in the cylindrical coordinate system, x = radial, y = circumferential and z = axial directions.

1. Section locations are shown in Figure 11.2.12.4.1-6.
2. Stresses are not presented for the sections with localized bearing stress. In accordance with ASME Section III, Appendix F, bearing stresses need not be evaluated for Level D service (accident) conditions.
3. Allowable stress at 300°F.
4. Stresses are determined by averaging the stresses over the impact region. A stress reduction factor of 0.8 is applied to the allowable stress at 250°F.

Table 11.2.12.4.1-2 Standard PWR Canister Primary Membrane + Primary Bending ($P_m + P_b$) Stresses for Tip-Over Conditions - 45° Basket Drop Orientation (ksi)

Section Location[1]	Section Angle (deg)	Sx	Sy	Sz	Sxy	Syz	Sxz	Stress Intensity	Allowable Stress	Margin of Safety
1	0	-2.0	19.3	4.3	-0.6	-0.1	-0.1	21.37	53.28	1.49
2	0	-1.9	22.3	3.0	-0.3	0.1	0.2	24.19	53.28	1.20
3	0	-2.6	22.2	6.2	0.2	0.0	-0.1	24.84	53.28	1.14
4	0	-1.8	21.0	3.8	-0.8	-0.1	-0.3	22.82	53.28	1.33
5	72.5	-0.7	20.6	12.5	0.1	3.9	-0.9	22.97	53.28	1.32
6	0	0.6	-29.7	-8.0	2.3	-1.1	-0.9	30.85	53.28	0.73
7[2]	8.7	0.7	9.4	24.5	0.2	-3.5	1.0	24.63	53.28	1.16
8[2]	8.7	4.7	8.2	21.9	-0.8	-4.9	-2.9	20.3	53.28	1.62
9[2]	8.7	8.7	-5.1	5.4	4.3	-4.6	-0.4	18.43	53.28	1.89
10	0	-46.3	-21.9	-38.2	1.1	-0.	-24.1	49.07	60.12[3]	0.23
11[4]	0.0 – 8.0	-24.4	-10.7	-2.0	-5.0	-0.4	3.2	25.03	48.09[4]	0.92
12	0	-0.9	0.1	0.0	0.0	0.0	-0.1	0.96	53.28	54.71
13	0	-0.8	1.5	0.0	0.1	0.0	0.0	2.33	53.28	21.83

Stresses are presented in the cylindrical coordinate system, x = radial, y = circumferential and z = axial directions.

1. Section locations are shown in Figure 11.2.12.4.1-6.
2. Stresses are not presented for the sections with localized bearing stress. In accordance with ASME Code Section III, Appendix F, bearing stresses need not be evaluated for Level D service (accident) conditions.
3. Allowable stress at 300°F.
4. Stresses are determined by averaging the stresses over the impact region. A stress reduction factor of 0.8 is applied to the allowable stress at 250°F.

Table 11.2.12.4.1-3 Standard PWR Support Disk Section Location for Stress Evaluation - Full Model

Sec. No.	Point 1		Point 2		Sec. No.	Point 1		Point 2	
	X	Y	X	Y		X	Y	X	Y
1	10.02	10.02	11.02	10.02	45	0.75	10.02	0.75	11.02
2	10.02	5.39	11.02	5.39	46	10.02	0.75	10.02	-0.75
3	10.02	0.75	11.02	0.75	47	5.39	0.75	5.39	-0.75
4	0.75	10.02	-0.75	10.02	48	0.75	0.75	0.75	-0.75
5	0.75	5.39	-0.75	5.39	49	20.29	0.75	20.29	-0.75
6	0.75	0.75	-0.75	0.75	50	15.66	0.75	15.66	-0.75
7	20.29	10.02	21.17	10.02	51	11.02	0.75	11.02	-0.75
8	20.29	5.39	21.17	5.39	52	30.44	0.75	30.44	-0.75
9	20.29	0.75	21.17	0.75	53	25.81	0.75	25.81	-0.75
10	0.75	20.29	-0.75	20.29	54	21.17	0.75	21.17	-0.75
11	0.75	15.66	-0.75	15.66	55	10.02	20.29	10.02	21.17
12	0.75	11.02	-0.75	11.02	56	5.39	20.29	5.39	21.17
13	0.75	30.44	-0.75	30.44	57	0.75	20.29	0.75	21.17
14	0.75	25.81	-0.75	25.81	58	10.02	-10.02	10.02	-11.02
15	0.75	21.17	-0.75	21.17	59	5.39	-10.02	5.39	-11.02
16	10.02	-0.75	11.02	-0.75	60	0.75	-10.02	0.75	-11.02
17	10.02	-5.39	11.02	-5.39	61	10.02	-20.29	10.02	-21.17
18	10.02	-10.02	11.02	-10.02	62	5.39	-20.29	5.39	-21.17
19	0.75	-0.75	-0.75	-0.75	63	0.75	-20.29	0.75	-21.17
20	0.75	-5.39	-0.75	-5.39	64	-0.75	10.02	-0.75	11.02
21	0.75	-10.02	-0.75	-10.02	65	-5.39	10.02	-5.39	11.02
22	20.29	-0.75	21.17	-0.75	66	-10.02	10.02	-10.02	11.02
23	20.29	-5.39	21.17	-5.39	67	-0.75	0.75	-0.75	-0.75
24	20.29	-10.02	21.17	-10.02	68	-5.39	0.75	-5.39	-0.75
25	0.75	-11.02	-0.75	-11.02	69	-10.02	0.75	-10.02	-0.75
26	0.75	-15.66	-0.75	-15.66	70	-11.02	0.75	-11.02	-0.75
27	0.75	-20.29	-0.75	-20.29	71	-15.66	0.75	-15.66	-0.75
28	0.75	-21.17	-0.75	-21.17	72	-20.29	0.75	-20.29	-0.75
29	0.75	-25.81	-0.75	-25.81	73	-21.17	0.75	-21.17	-0.75
30	0.75	-30.44	-0.75	-30.44	74	-25.81	0.75	-25.81	-0.75
31	-10.02	10.02	-11.02	10.02	75	-30.44	0.75	-30.44	-0.75
32	-10.02	5.39	-11.02	5.39	76	-0.75	20.29	-0.75	21.17
33	-10.02	0.75	-11.02	0.75	77	-5.39	20.29	-5.39	21.17
34	-20.29	10.02	-21.17	10.02	78	-10.02	20.29	-10.02	21.17
35	-20.29	5.39	-21.17	5.39	79	-0.75	-10.02	-0.75	-11.02
36	-20.29	0.75	-21.17	0.75	80	-5.39	-10.02	-5.39	-11.02
37	-10.02	-0.75	-11.02	-0.75	81	-10.02	-10.02	-10.02	-11.02
38	-10.02	-5.39	-11.02	-5.39	82	-0.75	-20.29	-0.75	-21.17
39	-10.02	-10.02	-11.02	-10.02	83	-5.39	-20.29	-5.39	-21.17
40	-20.29	-0.75	-21.17	-0.75	84	-10.02	-20.29	-10.02	-21.17
41	-20.29	-5.39	-21.17	-5.39	85	11.02	10.02	11.52	11.52
42	-20.29	-10.02	-21.17	-10.02	86	16.16	11.52	16.16	10.02
43	10.02	10.02	10.02	11.02	87	20.29	10.02	20.79	11.52
44	5.39	10.02	5.39	11.02	88	10.02	20.29	11.52	20.79

Note: See Figure 11.2.12.4.1-7 for section location.

Table 11.2.12.4.1-4 Summary of Maximum Stresses for Standard PWR Support Disk for Tip-Over Condition

Drop Orientation	P_m			$P_m + P_b$		
	Stress Intensity (ksi)	Allowable Stress (ksi)	Margin of Safety	Stress Intensity (ksi)	Allowable Stress (ksi)	Margin of Safety
0°	58.2	90.8	+0.56	81.9	129.8	+0.58
18.22°	47.5	90.4	+0.91	111.6	130.8	+0.17
26.28°	46.0	90.4	+0.97	124.6	130.8	+0.05
45°	34.4	91.5	+1.66	101.4	129.1	+0.27

Note: See Figure 11.2.12.4.1-1 for Drop Orientation.

Table 11.2.12.4.1-5 Summary of Buckling Evaluation of Standard PWR Support Disk for Tip-Over Condition

Drop Orientation	MS1	MS2
0°	+0.98	+0.96
18.22°	+0.31	+0.36
26.28°	+0.10	+0.15
45°	+0.31	+0.34

Note: See Figure 11.2.12.4.1-1 for Drop Orientation.

Table 11.2.12.4.1-6 Standard PWR Support Disk Primary Membrane (P_m) Stresses for Tip-Over Condition - Disk No. 5 - 26.28° Drop Orientation (ksi)

Section Number	Sx	Sy	Sxy	Stress Intensity	Allowable Stress	Margin of Safety
18	19.5	-26.1	3.1	46.0	90.4	0.97
3	27.1	-14.8	2.7	42.2	89.3	1.12
16	-38.3	-25.9	1	38.4	89.3	1.32
1	-33.5	-14.7	0.5	33.5	90.4	1.70
94	-28.3	-21.4	2.9	29.4	90.5	2.08
17	-0.1	-26	2	26.2	89.8	2.42
96	6.1	-16.4	-3.1	23.3	91.5	2.92
95	-0.1	-22.4	1.7	22.6	91.1	3.04
88	-18.4	-7	-7	21.7	91.5	3.21
84	-17.1	-20.7	-0.8	20.9	91.5	3.38
61	-17.8	-9.7	5.1	20.3	91.5	3.51
90	15	-5	0.6	20.1	90.5	3.51
60	-11.3	-18.4	1.1	18.6	89.3	3.80
30	-18	-10.1	3	19.0	91.9	3.83
82	-17.2	-7	4.1	18.7	90.8	3.87
62	-17.8	-0.2	2.6	18.4	91.2	3.97
58	-11.4	-13.8	5.4	18.2	90.4	3.97
91	-8.2	-17.5	-1.4	17.7	90.5	4.11
63	-17.8	-12.3	0.2	17.8	90.8	4.11
83	-17.2	-0.2	1.7	17.3	91.2	4.26
7	-16.5	-12.6	-0.8	16.7	91.5	4.49
24	-1.2	-15.8	2	16.1	91.5	4.69
28	-15.4	-10	1.6	15.8	90.9	4.74
23	-0.1	-15.8	0.8	15.8	91.2	4.78
22	-9.1	-15.7	-0.5	15.7	90.8	4.78
51	-3.6	-15.1	-2	15.4	89.4	4.79
37	11.1	-4.3	0.6	15.4	89.3	4.80
79	-6	6.5	4.5	15.4	89.3	4.82
2	-0.1	-14.7	1.6	15.0	89.8	5.00
85	-4.6	-11.2	-6.4	15.1	90.5	5.00

Note: See Figure 11.2.12.4.1-2 for disk location and Figure 11.2.12.4.1-6 for section locations.

Table 11.2.12.4.1-7 Standard PWR Support Disk Primary Membrane + Primary Bending ($P_m + P_b$) Stresses for Tip-Over Condition - Disk No. 5 - 26.28° Drop Orientation (ksi)

Section Number	Sx	Sy	Sxy	Stress Intensity	Allowable Stress	Margin of Safety
61	-123.4	-34.3	10.4	124.6	130.8	0.05
58	-115.3	-47.4	9.6	116.6	129.1	0.11
43	-95.4	-34.6	6.8	96.1	129.1	0.34
82	-92.1	-27.8	7.2	92.9	129.8	0.40
79	-86.9	-19.9	2.3	87.0	127.6	0.47
16	-54.3	-76.8	15.6	84.8	127.6	0.50
60	-82.9	-41	7.8	84.3	127.6	0.51
18	-4.1	-84.9	-2.5	85.0	129.1	0.52
46	-79.1	-52.5	10.4	82.7	127.6	0.54
55	-84.2	-31.4	5	84.7	130.8	0.54
3	9.1	-71.1	-5.7	81.0	127.6	0.57
64	-79.8	-32.4	7.2	80.9	127.6	0.58
30	-40.2	-74.7	11.7	78.3	131.3	0.68
63	-75.2	-27.9	4.9	75.7	129.8	0.71
76	72.6	21.9	5.2	73.1	129.8	0.77
48	-66.5	-43.2	3.9	67.1	125.7	0.87
19	-39.5	-66.4	2.9	66.7	125.7	0.88
6	-43.6	-63.2	5.2	64.5	125.7	0.95
94	-59.5	-44.7	11.1	65.5	129.3	0.97
21	-48.3	-59.4	5.2	61.5	127.6	1.08
45	-61.2	-14.4	-0.6	61.2	127.6	1.09
67	-56.6	-43.3	5.4	58.6	125.7	1.15
1	-49.4	-43.6	13.2	60.0	129.1	1.15
51	26.3	-30.4	4.7	57.5	127.7	1.22
33	-29.3	-54.9	7.1	56.7	127.6	1.25
39	-29.2	-52.9	6.2	54.5	129.1	1.37
24	-8.5	-52.1	4.1	52.5	130.8	1.49
81	-49.2	-30.8	5.5	50.7	129.1	1.55
4	-43.3	-43.7	5.8	49.3	127.6	1.59
28	-46.3	-28.1	9.2	50.1	129.9	1.59

Note: See Figure 11.2.12.4.1-2 for disk location and Figure 11.2.12.4.1-6 for section locations.

Table 11.2.12.4.1-8 Summary of Standard PWR Support Disk Buckling Evaluation for Tip-Over Condition - Disk No. 5 - 26.28° Drop Orientation

Section Number	P (kip)	Pcr (kip)	Py (kip)	M (in-kip)	Mp (in-kip)	Mm (in-kip)	MS1	MS2
61	7.80	44.18	38.91	6.74	8.51	8.18	0.10	0.15
58	5.69	51.79	43.78	8.66	10.94	10.67	0.23	0.25
82	7.52	43.76	38.54	4.78	8.43	8.10	0.44	0.48
18	13.04	51.79	43.78	4.90	10.94	10.67	0.51	0.48
43	1.95	51.79	43.78	7.62	10.94	10.67	0.54	0.58
16	12.97	50.82	42.93	4.24	10.73	10.47	0.62	0.57
79	3.00	50.82	42.93	6.74	10.73	10.47	0.63	0.66
60	5.66	50.82	42.93	5.96	10.73	10.47	0.65	0.66
63	7.78	43.76	38.54	3.66	8.43	8.10	0.73	0.75
55	0.92	44.18	38.91	5.24	8.51	8.18	0.76	0.83
64	2.18	50.82	42.93	6.29	10.73	10.47	0.79	0.83
3	7.40	50.82	42.93	4.69	10.73	10.47	0.86	0.84
46	1.85	83.64	64.39	14.37	24.15	24.15	0.89	0.88
30	7.60	87.05	67.05	12.10	25.14	25.14	1.00	0.92
19	3.78	81.50	62.70	11.51	23.51	23.51	1.15	1.10
48	1.80	81.50	62.70	12.01	23.51	23.51	1.19	1.17
6	2.46	81.50	62.70	11.23	23.51	23.51	1.29	1.25
45	1.91	50.82	42.93	4.78	10.73	10.47	1.34	1.37
21	3.89	83.64	64.39	10.16	24.15	24.15	1.47	1.40
24	6.92	44.18	38.91	2.31	8.51	8.18	1.46	1.45
67	1.00	81.50	62.70	10.37	23.51	23.51	1.58	1.57
33	1.95	50.82	42.93	4.25	10.73	10.47	1.59	1.63
84	7.49	44.18	38.91	1.82	8.51	8.18	1.73	1.67
39	2.19	51.79	43.78	4.04	10.94	10.67	1.72	1.75
17	13.00	51.32	43.37	0.79	10.84	10.58	2.13	1.77
1	7.33	51.79	43.78	2.41	10.94	10.67	1.95	1.82
81	2.97	51.79	43.78	3.61	10.94	10.67	1.88	1.88
37	2.13	50.82	42.93	3.24	10.73	10.47	2.26	2.27
4	2.35	83.64	64.39	7.60	24.15	24.15	2.37	2.30
66	2.15	51.79	43.78	3.25	10.94	10.67	2.31	2.33

Note: See Figure 11.2.12.4.1-2 for disk location and Figure 11.2.12.4.1-6 for section locations.

11.2.12.4.2 Analysis of the Standard Canister and Basket for BWR Configurations

Five three-dimensional models of the Standard BWR canister and fuel basket are evaluated for the cask tip-over event. Each model corresponds to a different fuel basket drop orientation. For the BWR fuel configuration, fuel basket drop orientations of 0°, 31.82°, 49.46°, 77.92°, and 90° are evaluated, as shown in Figure 11.2.12.4.2-1. Three-dimensional half-symmetry models are used for the basket drop orientations of 0° and 90°. Three-dimensional full-models are used for the basket orientations of 31.82°, 49.46° and 77.92°.

Model Description of the BWR Standard Canister and Fuel Basket

The models used for the evaluation of the canister and basket for the Standard BWR configuration are similar to those used for the PWR (Section 11.2.12.4.1). The three-dimensional model used for the basket drop orientation of 31.82° is presented in Figure 11.2.12.4.2-2 and Figure 11.2.12.4.2-3.

The same modeling and analysis techniques described for the PWR model (see Section 11.2.12.4.1) are used for the BWR models.

For the inertial loads, a maximum acceleration of 30g is conservatively applied to the entire model. As shown in Section 11.2.12.3.2, the maximum acceleration of the concrete cask steel liner at the locations of the top support disk and the top of the canister structural lid during the tip-over event is determined to be 25.3g and 29.1g, respectively. Using the same method described in Section 11.2.12.4.1 for the PWR models, the DLF for the acceleration at the top support disk is computed to be 1.04. Applying the DLF to the 25.3g results in a peak acceleration of 26.4g for the top support disk.

The dominant resonance frequencies and corresponding modal mass participation factors from the finite element modal analyses of the Standard BWR support disk are:

Frequency (Hz)	% Modal Mass Participation Factor
79.3	38.4
80.2	54.9
210.9	3.4

The mode shapes for these frequencies are shown in Figures 11.2.12.4.2-5 through 11.2.12.4.2-7. The displacement depicted in these figures is highly exaggerated by the ANSYS program in order

to illustrate the modal shape. The stresses associated with the actual displacement are shown in Tables 11.2.12.4.2-4 through 11.2.12.4.2-8.

The DLFs for the canister lids are considered to be unity since the lids have significant in-plane stiffness and are considered to be rigid. Therefore, applying 30g to the entire canister/basket model is conservative.

A uniform temperature of 75°F is applied to the model to determine material properties during solution. During post processing for the support disk, temperature distribution with a maximum temperature of 700°F (at the center) and a minimum temperature of 400°F (at the outer edge) are conservatively used to determine the allowable stresses. A constant temperature of 500° is used for the canister to determine the allowable stresses. These temperatures are the bounding temperatures for the normal, off-normal and accident conditions of storage.

Analysis Results for the Standard BWR Canister

The sectional stresses at 13 axial locations of the canister are obtained for each angular division of the model (a total of 80 angular locations for the full-models and a total of 41 angular locations for the half-symmetry models). The locations for the stress sections are shown in Figure 11.2.12.4.1-6.

The same stress allowables used in the evaluation of the PWR canister (see Section 11.2.12.4.1) are used in evaluating the BWR canister.

The primary membrane and primary membrane plus bending stresses for the BWR configuration for a 49.46° basket drop orientation are summarized in Table 11.2.12.4.2-1 and Table 11.2.12.4.2-2, respectively. The stress results of the canister are similar for all five models. Only the 49.46° basket drop orientation results are presented for the canister because this drop orientation generates the minimum margin of safety in the canister. The stress evaluation results for tip-over accident conditions show that the minimum margin of safety in the canister for BWR configurations is +0.35 for P_m (Section 10) and +0.46 for P_m+P_b (Section 10).

Analysis Results for the Standard BWR Basket Support Disks

To evaluate the most critical regions of the support disk, a series of cross sections are considered. To aid in the identification of these sections, Figure 11.2.12.4.2-4 shows the locations on a support disk for the full-models. Table 11.2.12.4.2-3 lists the cross-sections with their end point locations (Point 1 and Point 2), which spans the cross section of the ligament in the plane of the support disk.

Note that a local coordinate system (x and y parallel to the support disk ligaments) is used for the stress evaluation.

The stress evaluation for the support disk is performed according to ASME Code, Section III, Subsection NG. The allowable stresses for each section are determined based on the temperature of the support disk at the section location. The temperature distribution of the disk is determined by a thermal conduction solution for a single disk with a temperature of 700°F specified at the center of the disk and a temperature of 400°F specified at the outer edge of the disk as boundary conditions. These temperatures are bounding temperatures for the normal, off-normal and accident conditions of storage.

The highest stress occurs at the 5th support disk. The stress evaluation results for the 5th support disk are summarized in Table 11.2.12.4.2-4 for the five basket drop orientations evaluated. As shown in Table 11.2.12.4.2-4, the 77.92° drop orientation case generates the minimum margin of safety in the support disk; therefore, the P_m and $P_m + P_b$ stress intensities for the 77.92° basket drop orientation case are presented in Table 11.2.12.4.2-6 and Table 11.2.12.4.2-7, respectively. These tables list the stresses with the 30 lowest margins of safety for the 5th support disk. The highest P_m stress occurs at Section 202, with a margin of safety of +0.33 (See Table 11.2.12.4.2-6 for stresses and Figure 11.2.12.4.2-4 for section locations). The highest P_m+P_b stress occurs at Section 169, with a margin of safety of +0.04 (see Table 11.2.12.4.2-7 for stresses and Figure 11.2.12.4.2-4 for section locations).

Standard BWR Basket Support Disk Buckling Evaluation

The support disk buckling evaluation for the BWR support disks is performed using the same method as that presented for the PWR support disks (see Section 11.2.12.4.1). The support disk buckling evaluation results for the 5th support disk (the 5th support disk experiences the highest stresses) for the tip-over impact condition are summarized in Table 11.2.12.4.2-5 for the five basket drop orientations evaluated. As shown in Table 11.2.12.4.2-5, the 77.92° drop orientation case generates the minimum margin of safety for buckling; therefore, the results of the buckling analysis for the 77.92° basket drop orientation case are presented in Table 11.2.12.4.2-8. This table presents the results for 30 minimum margins of safety for this drop orientation. As the tables demonstrate, the support disks meet the requirements of NUREG/CR-6322.

Standard BWR Fuel Tube Analysis

The fuel tube provides structural support and a mounting location for BORAL neutron poison plates. The fuel tube does not provide structural support for the fuel assembly. To ensure that the fuel tube remains functional during a tip-over accident, a structural evaluation of the tube is performed for a side impact assuming a deceleration of 60g. This g-load bounds the maximum g-load (30g) calculated to occur for the BWR basket in a vertical concrete cask tipover event.

In the tipover event, the stainless steel support disks in the fuel basket support the fuel tube. The fuel basket support disks, which support the full length of the fuel tube, are spaced 3.205-inches apart (which is slightly more than one half of the fuel tube width of 5.9 inch). Considering the fuel tube subjected to a maximum BWR fuel assembly weight of 700 pounds with a 60g load factor and the 40 support locations provided by the basket support disks, the fuel tube shear stress is calculated as:

Shear load = (60g)(700)/40 = 1,050 lbs
Area = (0.048)(5.9)(2) = 0.566 in^2
Shear Stress = 1,050/0.566 = 1,855 psi

The yield strength of the tube material, Type 304 stainless steel, is 17,300 psi at 750°F. Conservatively using the allowable shear stress as one- half the yield strength of the tube material (8,650 psi) results in a large positive margin of safety. Conservative evaluation of the tube loading resulting from its own mass during a side impact shows that the tube structure maintains position and function.

The load transfer of the fuel assembly to the weight of the fuel basket support disk in the side impact is through direct bearing and compression of the distributed load of the fuel assembly through the fuel tube to the support disk web. Two load conditions are considered in the fuel tube evaluation. The first considers the fuel assembly load as a distributed pressure on the inside surface of the fuel tube. The second postulates that the fuel assembly grid is located at the center of the span between the support disks and produces a localized distributed load over the effective area of the grid.

Two different ANSYS finite element models of the tube are developed for these two load conditions since the fuel assembly structural performance for either load is nonlinear. The model conservatively considers the fuel tube wall thickness of 0.048 inch as the only material subjected to

a distributed pressure load representative of the fuel assembly deceleration of 60g. Fuel assembly stiffness is not considered in the development of the imposed pressure load on the fuel tube.

The first model represents a fuel tube section with a length of three spans, i.e., the model is support at four locations by support disks, as shown:

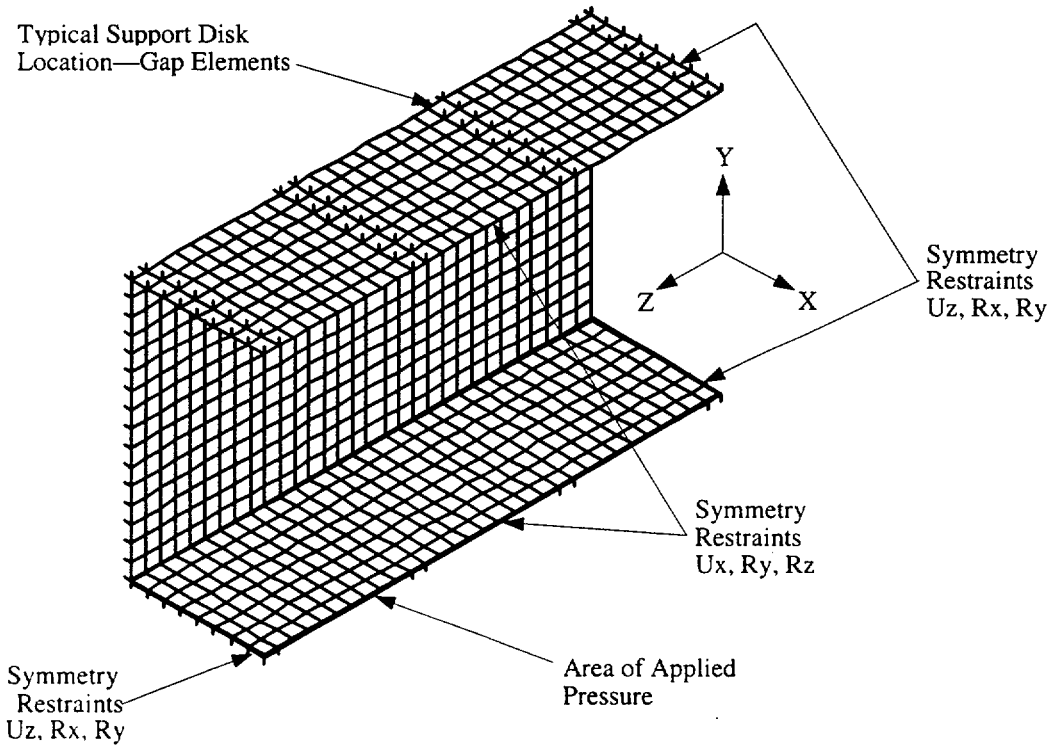

The fuel tube is modeled with the ANSYS plastic, quadrilateral shell element (SHELL43). The support disks are represented as rigid gap elements (CONTAC52). The outer nodes of the gap elements are fully restrained in all three translational directions. Edge restraints were applied to the model to represent symmetry boundary conditions. The effective load on the fuel tube due to the 60g deceleration of the assembly is applied as a pressure to the inside area of the fuel tube.

The finite element analysis results show that the maximum stress in the tube is 19.5 ksi, which is local to the sections of the tube resting on the support disks. At 750°F the ultimate strength for Type 304 stainless steel is 63.1 ksi. The margin of safety is:

$$MS = \frac{63.1}{19.5} - 1 = +2.24$$

The analysis shows that the maximum total strain is 0.0078 inch/inch. Defining the acceptable elastic-plastic response of the stainless steel as one half of the material failure strain of 0.40 in./in. at 750°F [42], the resulting margin of safety is:

$$MS = \frac{0.40/2}{0.0078} - 1 = +\text{Large}$$

Similarly, the margin of safety for elastic-plastic stress becomes

$$MS = \frac{63.1 - 17.3}{19.5 - 17.3} - 1 = +\text{Large}$$

where the yield strength of Type 304 stainless steel is 17.3 ksi at 750°F.

The second finite element model is used to evaluate the load condition with the fuel assembly grid located at the center of the span between two support disks. The fuel tube is subjected to a localized distributed load over the effective area of the grid. The model is a quarter-symmetry periodic section of the fuel tube, as shown:

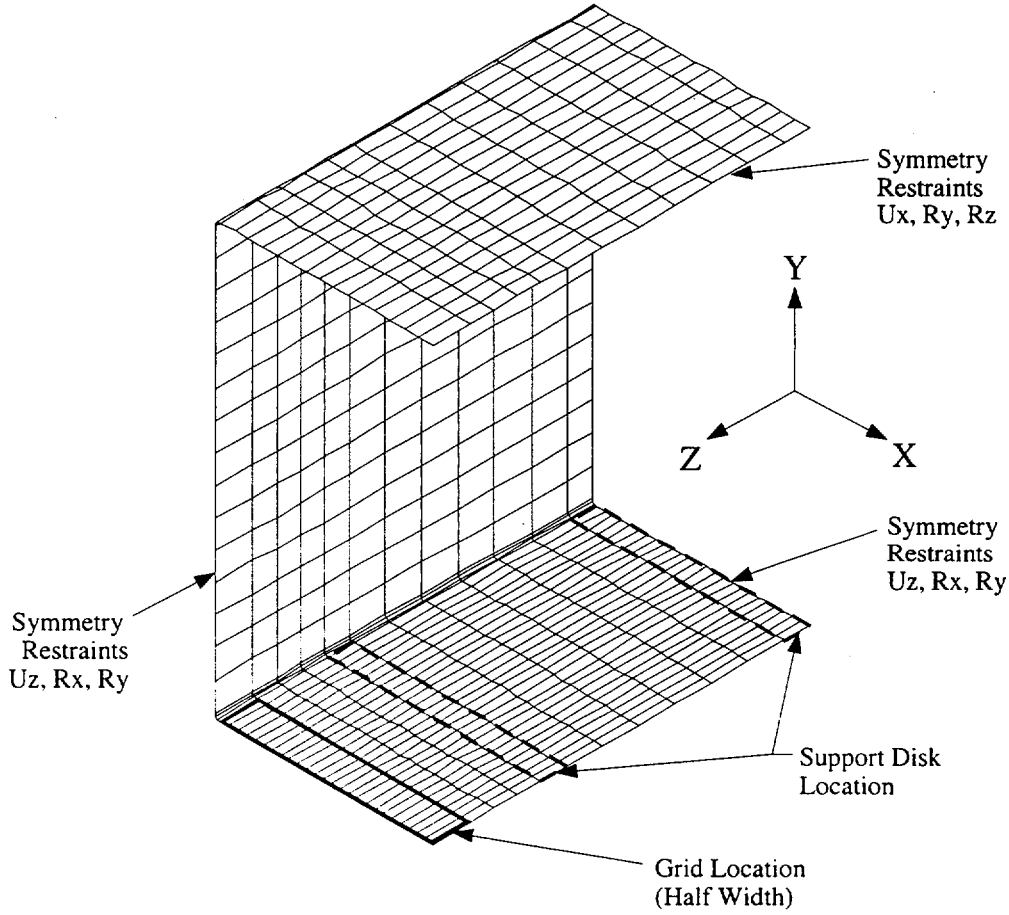

As in the finite element model used for the distributed pressure case, this model conservatively considers a fuel tube wall thickness of 0.048 inch. The BORAL plate (0.135 inch) and stainless steel cover plate (0.015 inch) are conservatively not included in the model. The tube wall is modeled with ANSYS SHELL43 elements. The support disks are modeled with CONTAC52 elements. A uniform pressure corresponding to the fuel assembly weight with the 60g load is applied to the elements at the grid location of the model. The displacement of the Y-direction for the nodes at the grid location of the model are coupled to represent the structural rigidity of the spacer grid. The finite element analysis results show that the maximum stress in the tube is 38.1 ksi. At 750°F the ultimate strength for Type 304 stainless steel is 63.1 ksi.

The margin of safety is:

$$MS = \frac{63.1}{38.1} - 1 = +0.66$$

The analysis shows that the maximum total strain is 0.10 inch/inch. Defining the acceptable elastic-plastic response of the stainless steel as one half of the material failure strain of 0.40 in./in. at 750°F [42], the resulting margin of safety is:

$$MS = \frac{0.40/2}{0.10} - 1 = +1.0$$

Similarly, the margin of safety for elastic-plastic stress becomes

$$MS = \frac{63.1 - 17.3}{38.1 - 17.3} - 1 = +1.2$$

where the yield strength of Type 304 stainless steel is 17.3 ksi at 750°F.

Both the maximum total strain and the elastic-plastic stress analyses indicate that the tube position within the support basket is maintained.

Assurance that the BORAL remains attached to the fuel tube is evaluated by considering that loads produced by the BORAL plate and stainless steel attachment plate, assuming a 60g load, are carried by the attachment plate weld. Total load and resultant stress on the weld are calculated as:

$F_{b/ss} = (g)(\rho)(t)(w)(l)$ Load exerted by BORAL/Stainless Steel Attachment Plate

where:

g = acceleration (g)
ρ = density of material (lb/in^3) (The density of aluminum (0.098 lb/in^3) is conservatively used for the BORAL.
t = thickness of material (in.)
w = width of material (in.)
l = length of material section (in.)

The forces on the weld due to a 12-inch section of BORAL (F_b) and a 12-inch section of stainless steel plate (F_{ss}) are:

$$F_b = (60g)(0.098\ lb/in^3)(0.135\ in)(5.45\ in)(12\ in)$$
$$= 51.9\ lbs$$

$$F_{ss} = (60g)(0.291\ lb/in^3)(0.018\ in)(5.79\ in)(12\ in)$$
$$= 21.8\ lbs$$

The total load (F_t) on a 1-inch attachment for a 12-inch section is:

$$F_t = 57.9\ lbs + 21.8\ lbs = 73.7\ lbs$$

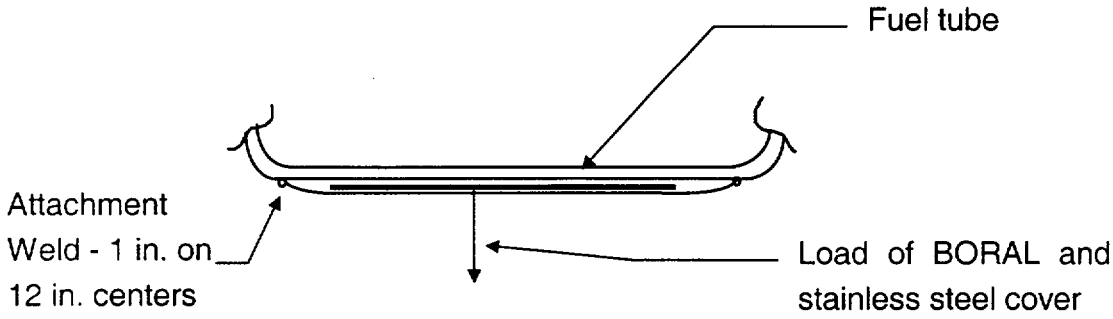

The resulting weld stress is: $\sigma = P/A = (73.7\ lbs/2) / (1\ in)(0.018\ in) = 2{,}074\ psi$

Since the weld material is Type 304 stainless steel, the margin of safety (at 750°F) is:

$$MS = \frac{17{,}300}{2{,}047} - 1 = +7.5$$

Therefore, the BORAL remains enclosed on each outer surface of the fuel tube wall.

Figure 11.2.12.4.2-1 Standard BWR Fuel Basket Drop Orientations Analyzed for Tip-Over Condition

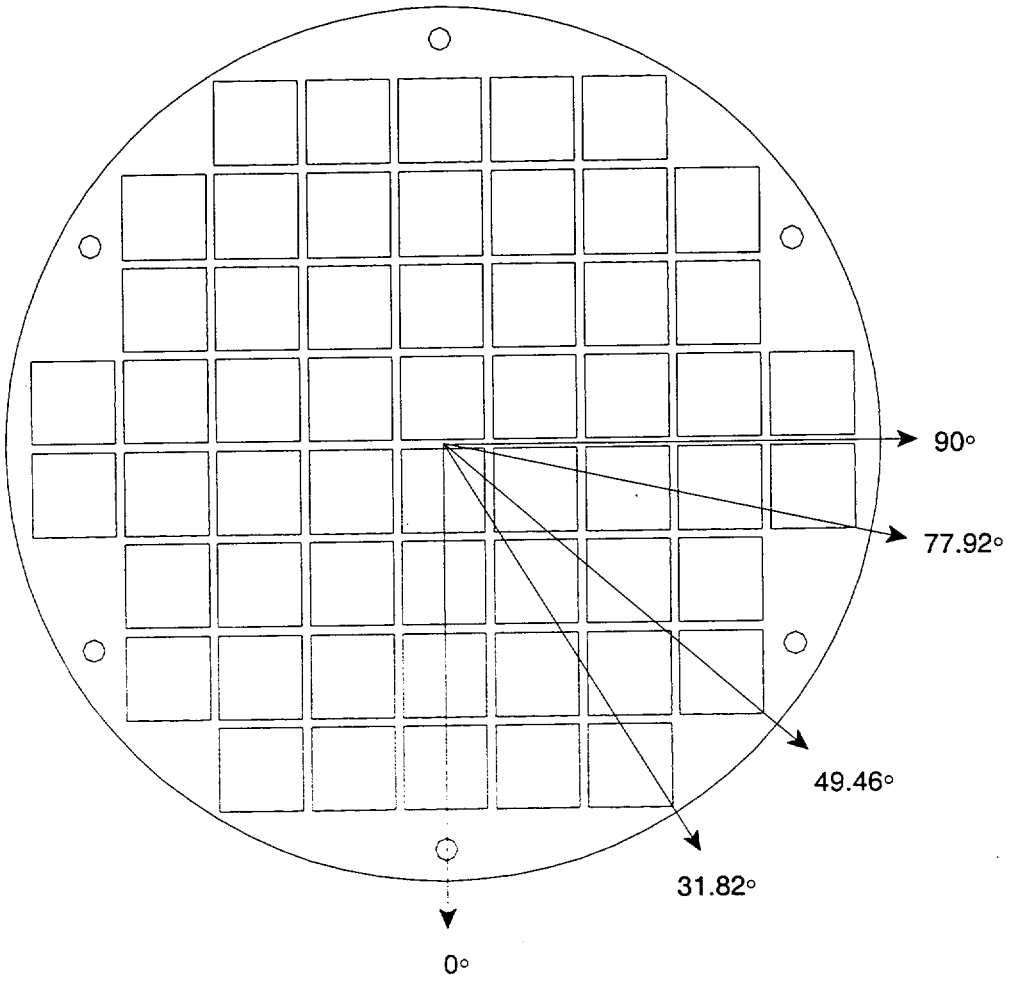

Figure 11.2.12.4.2-2 Standard BWR Fuel Basket/Canister Finite Element Model

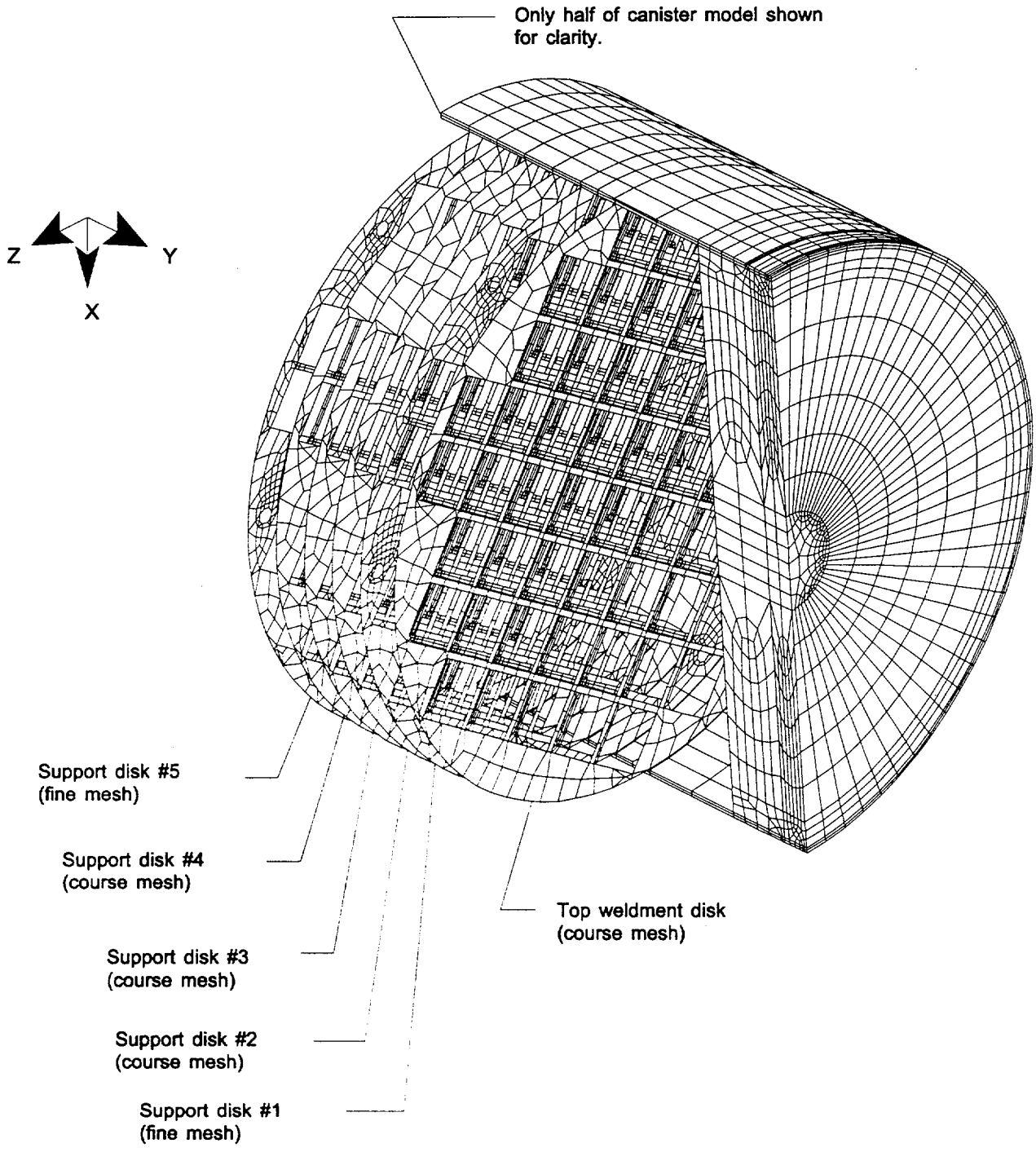

31.82° Basket Drop Orientation

Figure 11.2.12.4.2-3 Standard BWR Fuel Basket/Canister Finite Element Model - Support Disk

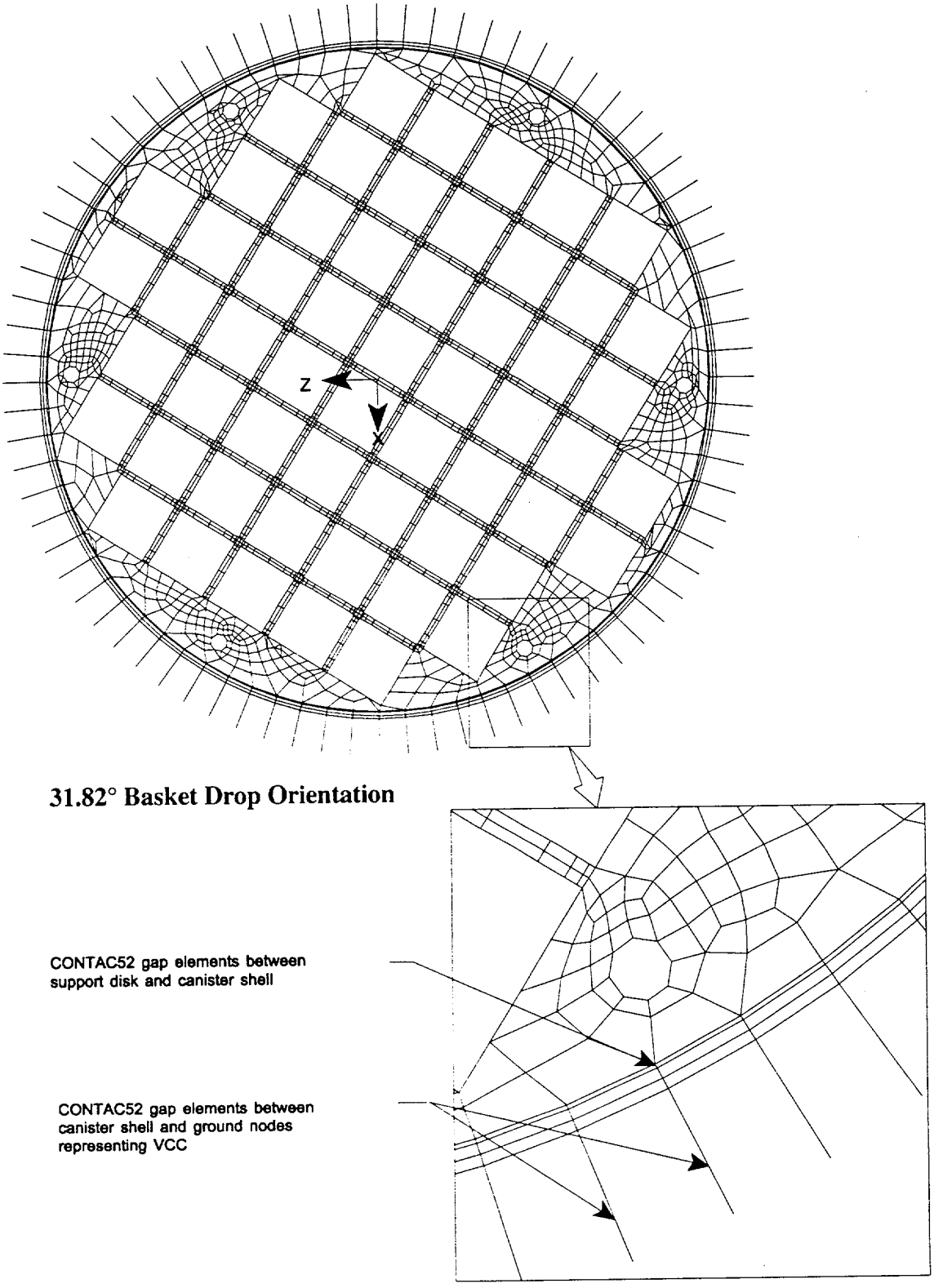

Figure 11.2.12.4.2-4 Standard BWR Support Disk Section Stress Locations - Full Model

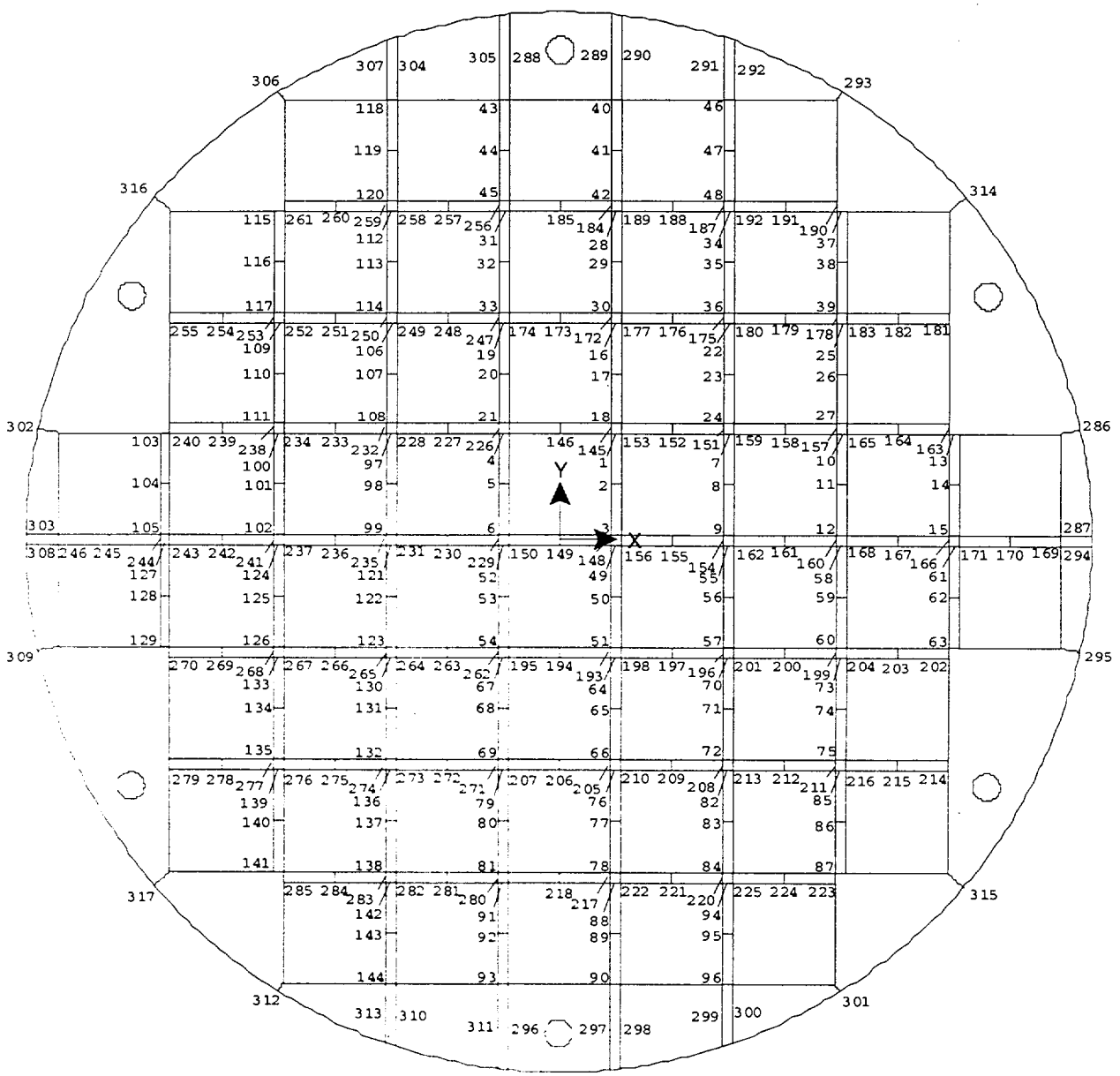

Figure 11.2.12.4.2-5 Standard BWR Support Disk – 79.3 Hz Mode Shape

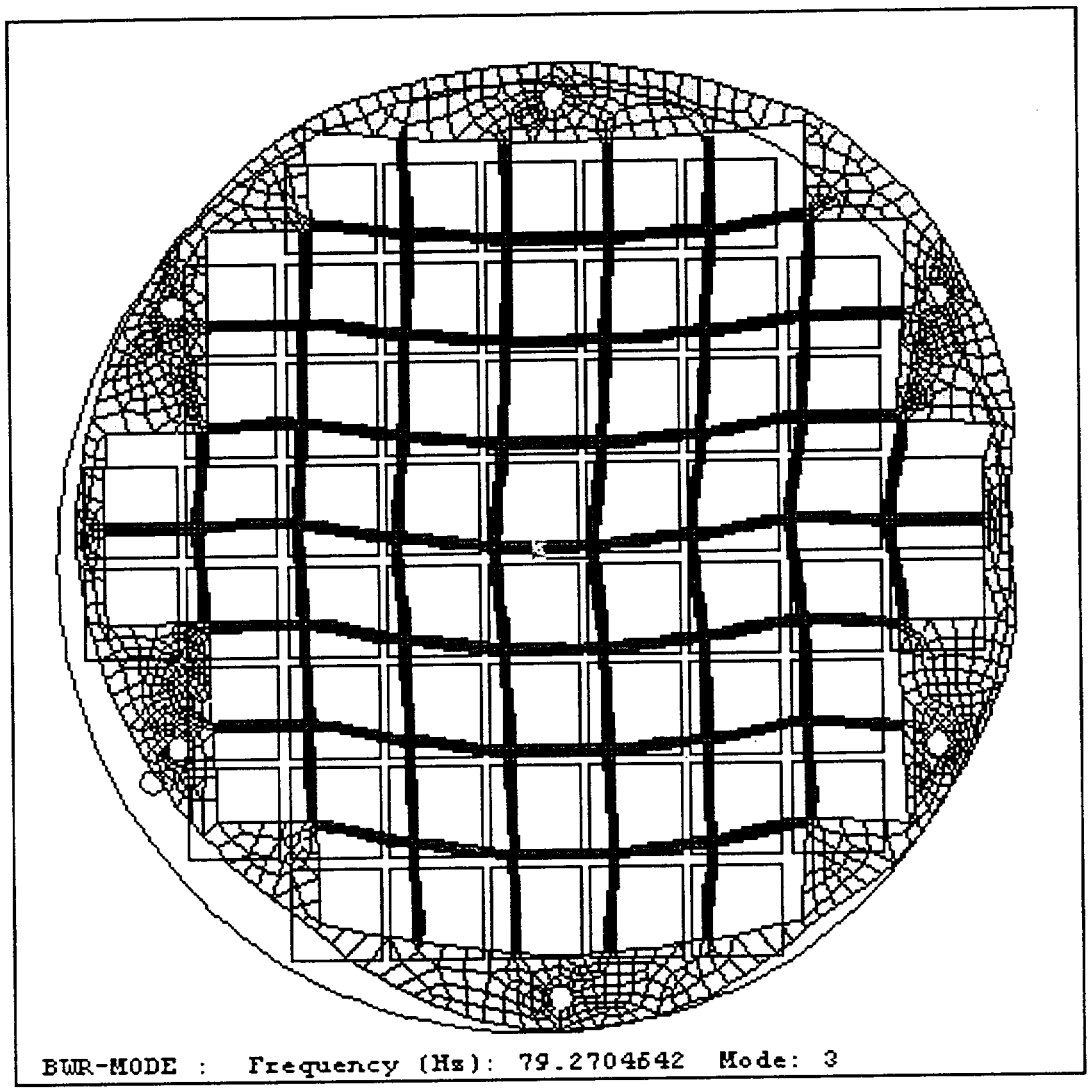

Note: Displacements are greatly exaggerated by the ANSYS program to illustrate the mode shapes.

Figure 11.2.12.4.2-6 Standard BWR Support Disk – 80.2 Hz Mode Shape

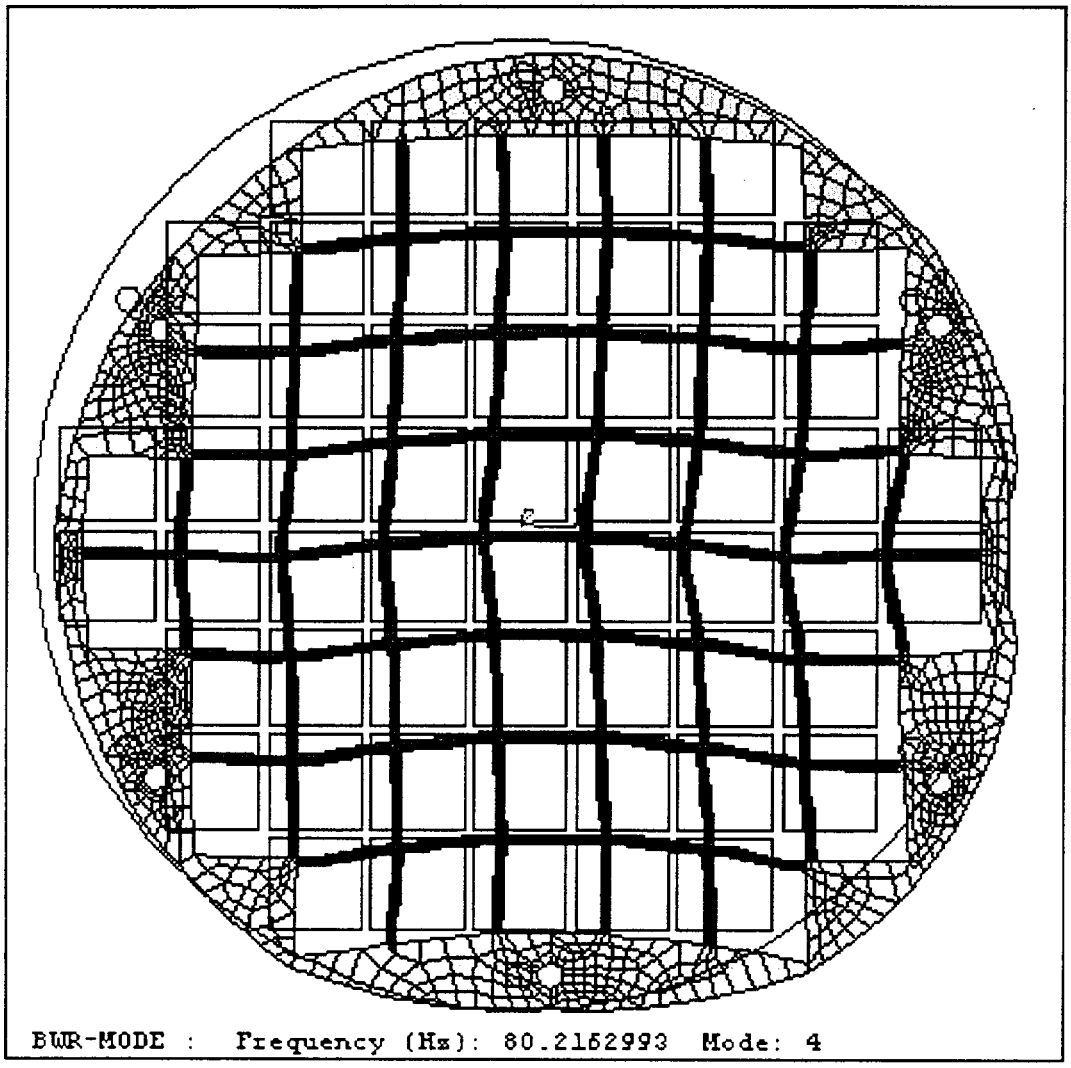

Note: Displacements are greatly exaggerated by the ANSYS program to illustrate the mode shapes.

Figure 11.2.12.4.2-7 Standard BWR Support Disk – 210.9 Hz Mode Shape

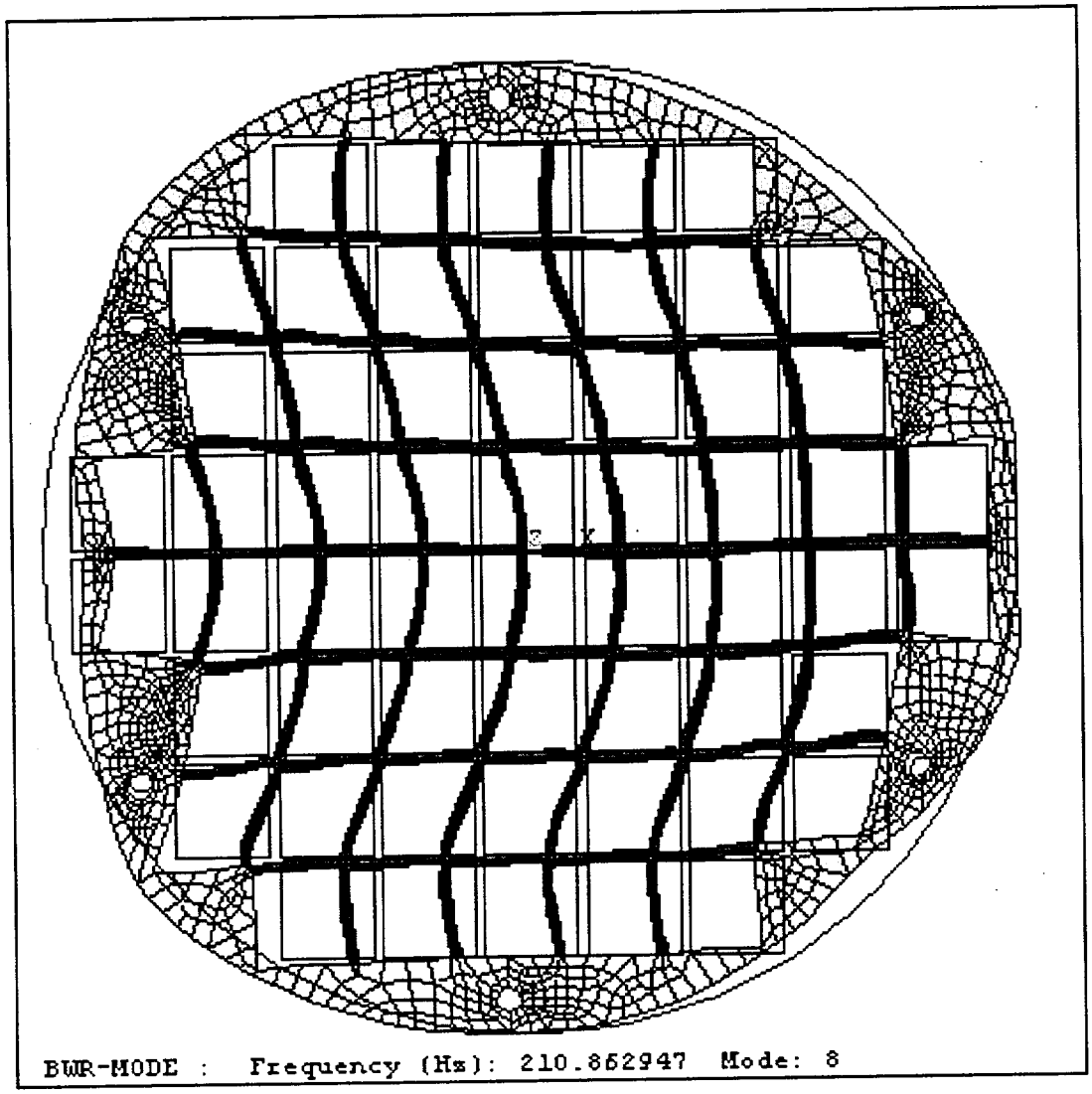

Note: Displacements are greatly exaggerated by the ANSYS program to illustrate the mode shapes.

Table 11.2.12.4.2-1 Standard BWR Canister Primary Membrane (P_m) Stresses for Tip-Over Conditions - 49.46° Basket Drop Orientation (ksi)

Section Location[1]	Section Angle (deg)	Sx	Sy	Sz	Sxy	Syz	Sxz	Stress Intensity	Allowable Stress	Margin of Safety
1	0	-1.2	6.2	1.4	-0.1	-0.1	0.0	7.46	35.52	3.76
2	0	-1.6	8.2	1.4	0.0	-0.2	0.1	9.77	35.52	2.63
3	0	-1.5	7.9	1.4	0.0	-0.2	-0.1	9.41	35.52	2.78
4	90	-0.1	3.0	-2.1	-0.2	3.7	0.1	8.92	35.52	2.98
5	85.5	0.0	2.8	-1.0	-0.2	4.8	-0.1	10.29	35.52	2.45
6	76.5	0.0	0.3	-0.4	0.0	6.0	0.0	12.09	35.52	1.94
7[2]	9.0	0.6	0.3	4.8	1.6	-3.8	-0.2	9.60	35.52	2.70
8[2]	351.0	4.5	0.1	5.2	-0.1	2.3	-0.6	7.06	35.52	4.03
9[2]	351.0	4.5	-1.0	1.5	-1.6	2.8	-0.2	8.17	35.52	3.35
10	0	-38.6	-16.2	-30.4	0.5	0.0	-10.7	29.74	40.08[3]	0.35
11[4]	351.9 – 8.2	-22.1	-9.9	-6.7	-0.1	0.0	1.1	15.51	32.06[4]	1.07
12	0	-0.6	0.2	0.0	0.0	0.0	-0.3	0.92	35.52	37.66
13	0	-1.0	0.3	0.0	0.0	0.0	-0.4	1.46	35.52	23.31

Stresses are presented in the cylindrical coordinate system, x = radial, y = circumferential and z = axial directions.

1. Section locations are shown in Figure 11.2.12.4.1-6.
2. Stresses are not presented for the sections with localized bearing stress. In accordance with ASME Section III, Appendix F, bearing stresses need not be evaluated for Level D service (accident) conditions.
3. Allowable stress at 300°F.
4. Stresses are determined by averaging the stresses over the impact region. A stress reduction factor of 0.8 is applied to the allowable stress at 250°F.

Table 11.2.12.4.2-2 Standard BWR Canister Primary Membrane + Primary Bending ($P_m + P_b$) Stresses for Tip-Over Conditions - 49.46° Basket Drop Orientation (ksi)

Section Location[1]	Section Angle (deg)	Sx	Sy	Sz	Sxy	Syz	Sxz	Stress Intensity	Allowable Stress	Margin of Safety
1	0.0	-1.6	18.5	4.6	-0.2	-0.4	0.1	20.13	53.28	1.65
2	0.0	-1.8	20.2	2.7	0.0	-0.4	0.1	22.01	53.28	1.42
3	0.0	-2.3	20.6	4.8	-0.1	-0.3	-0.1	22.92	53.28	1.32
4	0.0	-1.8	20.2	3.9	-0.2	-0.4	-0.1	22.00	53.28	1.42
5	0.0	-2.2	19.7	6.4	-0.1	-0.6	0.1	21.94	53.28	1.43
6	0.0	0.0	-21.0	-3.8	0.0	-0.7	-0.7	21.21	53.28	1.51
7[2]	351.0	0.1	6.4	17.2	0.2	2.3	0.2	17.50	53.28	2.04
8[2]	351.0	3.3	5.2	13.5	0.7	3.6	-2.1	13.02	53.28	3.09
9[2]	351.0	5.9	-3.0	3.6	-3.0	3.2	-0.6	12.44	53.28	3.28
10	0.0	-42.9	-15.8	-27.8	0.4	0.3	-19.1	41.17	60.12[3]	0.46
11[4]	351.9 – 8.1	-18.8	-7.2	-1.7	-0.1	0.0	2.6	17.86	48.09[4]	1.69
12	0.0	-0.9	0.1	-0.1	0.0	0.0	-0.5	1.37	53.28	37.81
13	0.0	-1.1	0.4	0.0	0.0	0.0	-0.1	1.56	53.28	33.07

Stresses are presented in the cylindrical coordinate system, x = radial, y = circumferential and z = axial directions.

1. Section locations are shown in Figure 11.2.12.4.1-6.
2. Stresses are not presented for the sections with localized bearing stress. In accordance with ASME Section III, Appendix F, bearing stresses need not be evaluated for Level D service (accident) conditions.
3. Allowable stress at 300°F.
4. Stresses are determined by averaging the stresses over the impact region. A stress reduction factor of 0.8 is applied to the allowable stress at 250°F.

Table 11.2.12.4.2-3 Standard BWR Support Disk Section Locations for Stress Evaluation - Full Model

Section[1]	Point 1		Point 2		Section[1]	Point 1		Point 2	
	X	Y	X	Y		X	Y	X	Y
1	3.14	6.6	3.79	6.6	44	-3.14	24.25	-3.79	24.25
2	3.14	3.46	3.79	3.46	45	-3.14	21.11	-3.79	21.11
3	3.14	0.33	3.79	0.33	46	10.07	27.39	10.72	27.39
4	-3.14	6.6	-3.79	6.6	47	10.07	24.25	10.72	24.25
5	-3.14	3.46	-3.79	3.46	48	10.07	21.11	10.72	21.11
6	-3.14	0.33	-3.79	0.33	49	3.14	-0.33	3.79	-0.33
7	10.07	6.6	10.72	6.6	50	3.14	-3.46	3.79	-3.46
8	10.07	3.46	10.72	3.46	51	3.14	-6.6	3.79	-6.6
9	10.07	0.33	10.72	0.33	52	-3.14	-0.33	-3.79	-0.33
10	17	6.6	17.65	6.6	53	-3.14	-3.46	-3.79	-3.46
11	17	3.46	17.65	3.46	54	-3.14	-6.6	-3.79	-6.6
12	17	0.33	17.65	0.33	55	10.07	-0.33	10.72	-0.33
13	23.92	6.6	24.57	6.6	56	10.07	-3.46	10.72	-3.46
14	23.92	3.46	24.57	3.46	57	10.07	-6.6	10.72	-6.6
15	23.92	0.33	24.57	0.33	58	17	-0.33	17.65	-0.33
16	3.14	13.53	3.79	13.53	59	17	-3.46	17.65	-3.46
17	3.14	10.39	3.79	10.39	60	17	-6.6	17.65	-6.6
18	3.14	7.25	3.79	7.25	61	23.92	-0.33	24.57	-0.33
19	-3.14	13.53	-3.79	13.53	62	23.92	-3.46	24.57	-3.46
20	-3.14	10.39	-3.79	10.39	63	23.92	-6.6	24.57	-6.6
21	-3.14	7.25	-3.79	7.25	64	3.14	-7.25	3.79	-7.25
22	10.07	13.53	10.72	13.53	65	3.14	-10.39	3.79	-10.39
23	10.07	10.39	10.72	10.39	66	3.14	-13.53	3.79	-13.53
24	10.07	7.25	10.72	7.25	67	-3.14	-7.25	-3.79	-7.25
25	17	13.53	17.65	13.53	68	-3.14	-10.39	-3.79	-10.39
26	17	10.39	17.65	10.39	69	-3.14	-13.53	-3.79	-13.53
27	17	7.25	17.65	7.25	70	10.07	-7.25	10.72	-7.25
28	3.14	20.46	3.79	20.46	71	10.07	-10.39	10.72	-10.39
29	3.14	17.32	3.79	17.32	72	10.07	-13.53	10.72	-13.53
30	3.14	14.18	3.79	14.18	73	17	-7.25	17.65	-7.25
31	-3.14	20.46	-3.79	20.46	74	17	-10.39	17.65	-10.39
32	-3.14	17.32	-3.79	17.32	75	17	-13.53	17.65	-13.53
33	-3.14	14.18	-3.79	14.18	76	3.14	-14.18	3.79	-14.18
34	10.07	20.46	10.72	20.46	77	3.14	-17.32	3.79	-17.32
35	10.07	17.32	10.72	17.32	78	3.14	-20.46	3.79	-20.46
36	10.07	14.18	10.72	14.18	79	-3.14	-14.18	-3.79	-14.18
37	17	20.46	17.65	20.46	80	-3.14	-17.32	-3.79	-17.32
38	17	17.32	17.65	17.32	81	-3.14	-20.46	-3.79	-20.46
39	17	14.18	17.65	14.18	82	10.07	-14.18	10.72	-14.18
40	3.14	27.39	3.79	27.39	83	10.07	-17.32	10.72	-17.32
41	3.14	24.25	3.79	24.25	84	10.07	-20.46	10.72	-20.46
42	3.14	21.11	3.79	21.11	85	17	-14.18	17.65	-14.18
43	-3.14	27.39	-3.79	27.39	86	17	-17.32	17.65	-17.32

1. See Figure 11.2.12.4.2-4 for section locations.

Table 11.2.12.4.2-3 Standard BWR Support Disk Section Locations for Stress Evaluation - Full Model (Continued)

Section[1]	Point 1		Point 2		Section[1]	Point 1		Point 2	
	X	Y	X	Y		X	Y	X	Y
87	17	-20.46	17.65	-20.46	130	-10.07	-7.25	-10.72	-7.25
88	3.14	-21.11	3.79	-21.11	131	-10.07	-10.39	-10.72	-10.39
89	3.14	-24.25	3.79	-24.25	132	-10.07	-13.53	-10.72	-13.53
90	3.14	-27.39	3.79	-27.39	133	-17	-7.25	-17.65	-7.25
91	-3.14	-21.11	-3.79	-21.11	134	-17	-10.39	-17.65	-10.39
92	-3.14	-24.25	-3.79	-24.25	135	-17	-13.53	-17.65	-13.53
93	-3.14	-27.39	-3.79	-27.39	136	-10.07	-14.18	-10.72	-14.18
94	10.07	-21.11	10.72	-21.11	137	-10.07	-17.32	-10.72	-17.32
95	10.07	-24.25	10.72	-24.25	138	-10.07	-20.46	-10.72	-20.46
96	10.07	-27.39	10.72	-27.39	139	-17	-14.18	-17.65	-14.18
97	-10.07	6.6	-10.72	6.6	140	-17	-17.32	-17.65	-17.32
98	-10.07	3.46	-10.72	3.46	141	-17	-20.46	-17.65	-20.46
99	-10.07	0.33	-10.72	0.33	142	-10.07	-21.11	-10.72	-21.11
100	-17	6.6	-17.65	6.6	143	-10.07	-24.25	-10.72	-24.25
101	-17	3.46	-17.65	3.46	144	-10.07	-27.39	-10.72	-27.39
102	-17	0.33	-17.65	0.33	145	3.14	6.6	3.14	7.25
103	-23.92	6.6	-24.57	6.6	146	0	6.6	0	7.25
104	-23.92	3.46	-24.57	3.46	147	-3.14	6.6	-3.14	7.25
105	-23.92	0.33	-24.57	0.33	148	3.14	0.33	3.14	-0.33
106	-10.07	13.53	-10.72	13.53	149	0	0.33	0	-0.33
107	-10.07	10.39	-10.72	10.39	150	-3.14	0.33	-3.14	-0.33
108	-10.07	7.25	-10.72	7.25	151	10.07	6.6	10.07	7.25
109	-17	13.53	-17.65	13.53	152	6.93	6.6	6.93	7.25
110	-17	10.39	-17.65	10.39	153	3.79	6.6	3.79	7.25
111	-17	7.25	-17.65	7.25	154	10.07	0.33	10.07	-0.33
112	-10.07	20.46	-10.72	20.46	155	6.93	0.33	6.93	-0.33
113	-10.07	17.32	-10.72	17.32	156	3.79	0.33	3.79	-0.33
114	-10.07	14.18	-10.72	14.18	157	17	6.6	17	7.25
115	-17	20.46	-17.65	20.46	158	13.86	6.6	13.86	7.25
116	-17	17.32	-17.65	17.32	159	10.72	6.6	10.72	7.25
117	-17	14.18	-17.65	14.18	160	17	0.33	17	-0.33
118	-10.07	27.39	-10.72	27.39	161	13.86	0.33	13.86	-0.33
119	-10.07	24.25	-10.72	24.25	162	10.72	0.33	10.72	-0.33
120	-10.07	21.11	-10.72	21.11	163	23.92	6.6	23.92	7.25
121	-10.07	-0.33	-10.72	-0.33	164	20.78	6.6	20.78	7.25
122	-10.07	-3.46	-10.72	-3.46	165	17.65	6.6	17.65	7.25
123	-10.07	-6.6	-10.72	-6.6	166	23.92	0.33	23.92	-0.33
124	-17	-0.33	-17.65	-0.33	167	20.78	0.33	20.78	-0.33
125	-17	-3.46	-17.65	-3.46	168	17.65	0.33	17.65	-0.33
126	-17	-6.6	-17.65	-6.6	169	30.85	0.33	30.85	-0.33
127	-23.92	-0.33	-24.57	-0.33	170	27.71	0.33	27.71	-0.33
128	-23.92	-3.46	-24.57	-3.46	171	24.57	0.33	24.57	-0.33
129	-23.92	-6.6	-24.57	-6.6	172	3.14	13.53	3.14	14.18

1. See Figure 11.2.12.4.2-4 for section locations.

Table 11.2.12.4.2-3 Standard BWR Support Disk Section Locations for Stress Evaluation - Full Model (Continued)

Section[1]	Point 1		Point 2		Section[1]	Point 1		Point 2	
	X	Y	X	Y		X	Y	X	Y
173	0	13.53	0	14.18	216	17.65	-13.53	17.65	-14.18
174	-3.14	13.53	-3.14	14.18	217	3.14	-20.46	3.14	-21.11
175	10.07	13.53	10.07	14.18	218	0	-20.46	0	-21.11
176	6.93	13.53	6.93	14.18	219	-3.14	-20.46	-3.14	-21.11
177	3.79	13.53	3.79	14.18	220	10.07	-20.46	10.07	-21.11
178	17	13.53	17	14.18	221	6.93	-20.46	6.93	-21.11
179	13.86	13.53	13.86	14.18	222	3.79	-20.46	3.79	-21.11
180	10.72	13.53	10.72	14.18	223	17	-20.46	17	-21.11
181	23.92	13.53	23.92	14.18	224	13.86	-20.46	13.86	-21.11
182	20.78	13.53	20.78	14.18	225	10.72	-20.46	10.72	-21.11
183	17.65	13.53	17.65	14.18	226	-3.79	6.6	-3.79	7.25
184	3.14	20.46	3.14	21.11	227	-6.93	6.6	-6.93	7.25
185	0	20.46	0	21.11	228	-10.07	6.6	-10.07	7.25
186	-3.14	20.46	-3.14	21.11	229	-3.79	0.33	-3.79	-0.33
187	10.07	20.46	10.07	21.11	230	-6.93	0.33	-6.93	-0.33
188	6.93	20.46	6.93	21.11	231	-10.07	0.33	-10.07	-0.33
189	3.79	20.46	3.79	21.11	232	-10.72	6.6	-10.72	7.25
190	17	20.46	17	21.11	233	-13.86	6.6	-13.86	7.25
191	13.86	20.46	13.86	21.11	234	-17	6.6	-17	7.25
192	10.72	20.46	10.72	21.11	235	-10.72	0.33	-10.72	-0.33
193	3.14	-6.6	3.14	-7.25	236	-13.86	0.33	-13.86	-0.33
194	0	-6.6	0	-7.25	237	-17	0.33	-17	-0.33
195	-3.14	-6.6	-3.14	-7.25	238	-17.65	6.6	-17.65	7.25
196	10.07	-6.6	10.07	-7.25	239	-20.78	6.6	-20.78	7.25
197	6.93	-6.6	6.93	-7.25	240	-23.92	6.6	-23.92	7.25
198	3.79	-6.6	3.79	-7.25	241	-17.65	0.33	-17.65	-0.33
199	17	-6.6	17	-7.25	242	-20.78	0.33	-20.78	-0.33
200	13.86	-6.6	13.86	-7.25	243	-23.92	0.33	-23.92	-0.33
201	10.72	-6.6	10.72	-7.25	244	-24.57	0.33	-24.57	-0.33
202	23.92	-6.6	23.92	-7.25	245	-27.71	0.33	-27.71	-0.33
203	20.78	-6.6	20.78	-7.25	246	-30.85	0.33	-30.85	-0.33
204	17.65	-6.6	17.65	-7.25	247	-3.79	13.53	-3.79	14.18
205	3.14	-13.53	3.14	-14.18	248	-6.93	13.53	-6.93	14.18
206	0	-13.53	0	-14.18	249	-10.07	13.53	-10.07	14.18
207	-3.14	-13.53	-3.14	-14.18	250	-10.72	13.53	-10.72	14.18
208	10.07	-13.53	10.07	-14.18	251	-13.86	13.53	-13.86	14.18
209	6.93	-13.53	6.93	-14.18	252	-17	13.53	-17	14.18
210	3.79	-13.53	3.79	-14.18	253	-17.65	13.53	-17.65	14.18
211	17	-13.53	17	-14.18	254	-20.78	13.53	-20.78	14.18
212	13.86	-13.53	13.86	-14.18	255	-23.92	13.53	-23.92	14.18
213	10.72	-13.53	10.72	-14.18	256	-3.79	20.46	-3.79	21.11
214	23.92	-13.53	23.92	-14.18	257	-6.93	20.46	-6.93	21.11
215	20.78	-13.53	20.78	-14.18	258	-10.07	20.46	-10.07	21.11

1. See Figure 11.2.12.4.2-4 for section locations.

Table 11.12.12.4.2-3 Standard BWR Support Disk Section Locations for Stress Evaluation - Full Model (Continued)

Section[1]	Point 1		Point 2		Section[1]	Point 1		Point 2	
	X	Y	X	Y		X	Y	X	Y
259	-10.72	20.46	-10.72	21.11	289	3.14	27.39	3.14	32.63
260	-13.86	20.46	-13.86	21.11	290	3.79	27.39	3.79	32.56
261	-17	20.46	-17	21.11	291	10.07	27.39	10.07	31.2
262	-3.79	-6.6	-3.79	-7.25	292	10.72	27.39	10.72	30.98
263	-6.93	-6.6	-6.93	-7.25	293	17	27.39	17.29	27.86
264	-10.07	-6.6	-10.07	-7.25	294	30.85	-0.33	32.78	-0.33
265	-10.72	-6.6	-10.72	-7.25	295	30.85	-6.6	32.06	-6.86
266	-13.86	-6.6	-13.86	-7.25	296	-3.14	-27.39	-3.14	-32.63
267	-17	-6.6	-17	-7.25	297	3.14	-27.39	3.14	-32.63
268	-17.65	-6.6	-17.65	-7.25	298	3.79	-27.39	3.79	-32.56
269	-20.78	-6.6	-20.78	-7.25	299	10.07	-27.39	10.07	-31.2
270	-23.92	-6.6	-23.92	-7.25	300	10.72	-27.39	10.72	-30.98
271	-3.79	-13.53	-3.79	-14.18	301	17	-27.39	17.29	-27.86
272	-6.93	-13.53	-6.93	-14.18	302	-30.85	6.6	-32.06	6.86
273	-10.07	-13.53	-10.07	-14.18	303	-30.85	0.33	-32.78	0.33
274	-10.72	-13.53	-10.72	-14.18	304	-10.07	27.39	-10.07	31.2
275	-13.86	-13.53	-13.86	-14.18	305	-3.79	27.39	-3.79	32.56
276	-17	-13.53	-17	-14.18	306	-17	27.39	-17.29	27.86
277	-17.65	-13.53	-17.65	-14.18	307	-10.72	27.39	-10.72	30.98
278	-20.78	-13.53	-20.78	-14.18	308	-30.85	-0.33	-32.78	-0.33
279	-23.92	-13.53	-23.92	-14.18	309	-30.85	-6.6	-32.06	-6.86
280	-3.79	-20.46	-3.79	-21.11	310	-10.07	-27.39	-10.07	-31.2
281	-6.93	-20.46	-6.93	-21.11	311	-3.79	-27.39	-3.79	-32.56
282	-10.07	-20.46	-10.07	-21.11	312	-17	-27.39	-17.29	-27.86
283	-10.72	-20.46	-10.72	-21.11	313	-10.72	-27.39	-10.72	-30.98
284	-13.86	-20.46	-13.86	-21.11	314	23.92	20.46	24.92	21.31
285	-17	-20.46	-17	-21.11	315	23.92	-20.46	24.92	-21.31
286	30.85	6.6	32.06	6.86	316	-23.92	20.46	-24.92	21.31
287	30.85	0.33	32.78	0.33	317	-23.92	-20.46	-24.92	-21.31
288	-3.14	27.39	-3.14	32.63					

1. See Figure 11.2.12.4.2-4 for section locations.

Table 11.2.12.4.2-4 Summary of Maximum Stresses for Standard BWR Support Disk for Tip-Over Condition

Drop Orientation	P_m			$P_m + P_b$		
	Stress Intensity (ksi)	Allowable Stress (ksi)	Margin of Safety	Stress Intensity (ksi)	Allowable Stress (ksi)	Margin of Safety
0°	35.1	63.0	+0.80	46.1	90.0	+0.95
31.82°	25.8	63.0	+1.44	65.7	90.0	+0.37
49.46°	23.7	63.0	+1.65	55.5	90.0	+0.62
77.92°	47.5	63.0	+0.33	86.6	90.0	+0.04
90°	58.4	63.0	+0.08	69.6	90.0	+0.29

Note: See Figure 11.2.12.4.2-1 for Drop Orientation.

Table 11.2.12.4.2-5 Summary of Buckling Evaluation of Standard BWR Support Disk for Tip-Over Condition

Drop orientation	MS1	MS2
0°	1.17	1.03
31.82°	0.56	0.53
49.46°	0.86	0.81
77.92°	0.18	0.16
90°	0.38	0.58

Table 11.2.12.4.2-6 Standard BWR Support Disk Primary Membrane (P_m) Stresses for Tip-Over Condition – Disk No. 5 - 77.92° Drop Orientation (ksi)

Section Number	Sx	Sy	Sxy	Stress Intensity	Allowable Stress	Margin of Safety
202	-24.9	22.5	1	47.5	63.0	0.33
199	-21.8	14.8	1.3	36.6	63.0	0.72
196	-18.8	12.5	1.3	31.4	63.0	1.01
193	-16	11.2	1.3	27.2	62.8	1.30
63	-18.3	8.5	2.4	27.2	63.0	1.32
203	-24.9	-0.1	0.8	24.9	63.0	1.53
204	-24.8	-16.1	0.7	24.9	63.0	1.53
262	-13.2	10.3	1.3	23.7	62.8	1.65
201	-21.7	-16	1	21.9	63.0	1.88
200	-21.7	0	1.1	21.8	63.0	1.89
73	-18.6	2.1	-0.6	20.8	63.0	2.03
265	-10.6	9.8	1.2	20.6	63.0	2.06
166	-12.3	7.9	1.6	20.4	63.0	2.09
169	-13.9	-19.2	2.3	20.0	63.0	2.15
198	-18.7	-15.1	1	19.0	62.8	2.31
197	-18.8	0	1.1	18.9	63.0	2.34
295	-6	-15.6	-6.3	18.7	63.0	2.37
15	-9.1	8.2	2.5	18.0	63.0	2.50
268	-8.1	9.7	0.9	17.8	63.0	2.53
195	-15.9	-14.2	1	16.3	62.8	2.85
194	-15.9	0	1.1	16.1	62.8	2.91
211	-12.2	3.6	0.6	15.8	63.0	2.98
60	-12.3	2.7	2.5	15.8	63.0	2.99
61	-6.8	8.5	1	15.5	63.0	3.06
160	-10.7	4.2	1.9	15.4	63.0	3.10
171	-13.8	0.8	2	15.2	63.0	3.15
70	-14.6	0.2	-0.3	14.9	63.0	3.24
170	-13.9	0	2.1	14.5	63.0	3.34
264	-13.2	-13.2	1	14.1	63.0	3.46
13	-5.7	8.2	1	14.1	63.0	3.48

See Figure 11.2.12.4.2-4 for section locations.

Table 11.2.12.4.2-7 Standard BWR Support Disk Primary Membrane + Primary Bending (P_m+P_b) Stresses for Tip-Over Condition - Disk No. 5 - 77.92° Drop Orientation (ksi)

Section Number	Sx	Sy	Sxy	Stress Intensity	Allowable Stress	Margin of Safety
169	-85.6	-34.9	7.1	86.6	90.0	0.04
202	-50.9	15.4	-2.3	66.5	90.0	0.35
63	1.2	63.9	-1.5	63.9	90.0	0.41
160	-61.6	-14.9	1.5	61.7	90.0	0.46
171	-60	-17.6	3	60.2	90.0	0.49
60	3.8	59.5	0.4	59.5	90.0	0.51
57	4.8	59.1	0.1	59.1	90.0	0.52
15	10.2	58.9	1.1	59.0	90.0	0.53
51	-28.2	-57	4.7	57.7	89.5	0.55
154	-57.6	-16.5	1.6	57.7	89.8	0.56
199	-54.3	3	-1.4	57.3	90.0	0.57
162	-56.8	-22.8	3.4	57.1	89.9	0.57
54	-26	-55.3	4.3	55.9	89.5	0.60
156	-54.4	-22.8	3.3	54.8	87.8	0.60
148	-54.3	-16.2	1.5	54.4	87.6	0.61
9	14.6	54.1	1.5	54.1	89.8	0.66
166	-54.1	-9.7	0.5	54.1	90.0	0.66
3	-25.2	-52.1	3.5	52.6	87.6	0.67
13	3.7	53.7	1.1	53.7	90.0	0.68
12	15.2	53.5	2.1	53.6	90.0	0.68
123	-23.9	-52.9	3.9	53.4	90.0	0.69
150	-51.3	-22.4	3.2	51.7	87.6	0.69
6	-23.6	-51.1	3.3	51.5	87.6	0.70
229	-51.1	-15.6	1.3	51.2	87.8	0.71
201	-50.2	-27.9	6.7	52.0	90.0	0.73
196	-51.2	-0.2	-1	51.3	90.0	0.76
168	-50.4	-19.2	2.9	50.7	90.0	0.78
198	-48.4	-27.4	6.3	50.1	89.5	0.79
99	-22.1	-49.4	3.1	49.7	89.8	0.81
231	-48.5	-21.6	3	48.8	89.8	0.84

See Figure 11.2.12.4.2-4 for section locations.

Table 11.2.12.4.2-8 Summary of Standard BWR Support Disk Buckling Evaluation for Tip-Over Condition - Disk No. 5 - 77.92° Drop Orientation

Section Number	P (kip)	Pcr (kip)	Py (kip)	M (in-kip)	Mp (in-kip)	Mm (in-kip)	MS1	MS2
169	5.65	31.59	25.67	3.15	4.17	4.11	0.18	0.16
199	8.84	31.4	25.52	1.43	4.15	4.09	0.69	0.57
171	5.62	31.52	25.62	2.03	4.16	4.1	0.64	0.58
160	4.34	31.35	25.48	2.24	4.14	4.08	0.63	0.59
202	10.12	31.55	25.64	1.14	4.17	4.11	0.76	0.59
201	8.82	31.23	25.38	1.25	4.12	4.07	0.80	0.65
196	7.63	31.22	25.37	1.43	4.12	4.07	0.81	0.68
162	4.32	31.1	25.28	2.03	4.11	4.05	0.74	0.70
154	3.7	31.07	25.26	2.14	4.1	4.05	0.74	0.70
204	10.09	31.41	25.53	0.88	4.15	4.09	0.95	0.74
198	7.61	30.97	25.18	1.31	4.09	4.04	0.89	0.75
156	3.67	30.35	24.73	2	4.02	3.97	0.80	0.75
166	4.98	31.51	25.61	1.84	4.16	4.1	0.82	0.76
148	3.05	30.27	24.67	2.06	4.01	3.96	0.82	0.79
193	6.48	30.96	25.18	1.41	4.09	4.04	0.94	0.82
168	4.96	31.36	25.49	1.68	4.14	4.08	0.94	0.86
150	3.02	30.27	24.67	1.93	4.01	3.96	0.92	0.88
51	0.11	30.96	25.18	2.5	4.09	4.04	0.89	0.92
195	6.46	30.96	25.18	1.3	4.09	4.04	1.04	0.90
229	2.39	30.35	24.73	1.99	4.02	3.97	0.96	0.94
54	0.26	30.96	25.18	2.4	4.09	4.04	0.94	0.97
262	5.37	30.97	25.18	1.39	4.09	4.04	1.11	0.99
123	0.25	31.22	25.37	2.3	4.12	4.07	1.04	1.07
6	0.14	30.27	24.67	2.24	4.01	3.96	1.06	1.09
231	2.36	31.07	25.26	1.88	4.1	4.05	1.11	1.08
264	5.35	31.22	25.37	1.29	4.12	4.07	1.23	1.10
99	0.15	31.07	25.26	2.16	4.1	4.05	1.18	1.22
235	1.73	31.1	25.28	1.87	4.11	4.05	1.21	1.20
265	4.31	31.23	25.38	1.32	4.12	4.07	1.38	1.27
237	1.7	31.35	25.48	1.82	4.14	4.08	1.29	1.28

See Figure 11.2.12.4.2-4 for section locations.

11.2.12.5 Analysis of Advanced Concrete Cask Tip-Over

For a tip-over event to occur, the center of gravity of the Advanced concrete cask and loaded canister must be displaced beyond its outer radius, i.e., the point of rotation. When the center of gravity passes beyond the point of rotation, the potential energy of the cask and canister is converted to kinetic energy as the cask and canister rotate toward a horizontal orientation on the concrete pad. The subsequent motion of the cask is governed by the structural characteristics of the concrete cask, the concrete pad and the underlying soil. The parameters of the concrete pad and foundation for the Advanced configurations are:

Concrete thickness (inches)	36 (maximum)
Pad subsoil thickness (feet)	10 (minimum)
Specified concrete compressive strength (psi)	$\leq$ 5,000 at 28 days
Concrete dry density (ρ) (lbs/ft^3)	$125 \leq \rho \leq 160$
Soil in place density (ρ) (lbs/ft^3)	$100 \leq \rho \leq 160$
Soil Modulus of Elasticity (psi)	$\leq$ 60,000 (PWR)

The objective of the evaluation is to determine the maximum acceleration to be used in the structural evaluation of the loaded Advanced configuration canister and basket. However, the Advanced basket is a tabbed and slotted plate design that holds more fuel assemblies than the fuel tube and disk design of the Standard basket. The canister and Advanced basket together constitute the Advanced canister. The methodology to determine the concrete cask response follows the methodology contained in NUREG/CR-6608, "Summary and Evaluation of Low-Velocity Impact Tests of Solid Steel Billet Onto Concrete Pads" [38]. The LS-DYNA program is used in the evaluation. The validation of the analysis methodology is provided in Section 11.2.12.7.

11.2.12.5.1 Analysis of the Advanced Cask Tip-Over for PWR Configurations

The concrete pad in the model corresponds to a pad 30-feet by 30-feet square and 3-feet thick, supporting one concrete cask in the center of the pad. The soil under the concrete pad is considered to be 35-feet by 35-feet square and 10-feet thick. Only one-half of the concrete cask, pad and soil configuration is modeled due to symmetry, as shown:

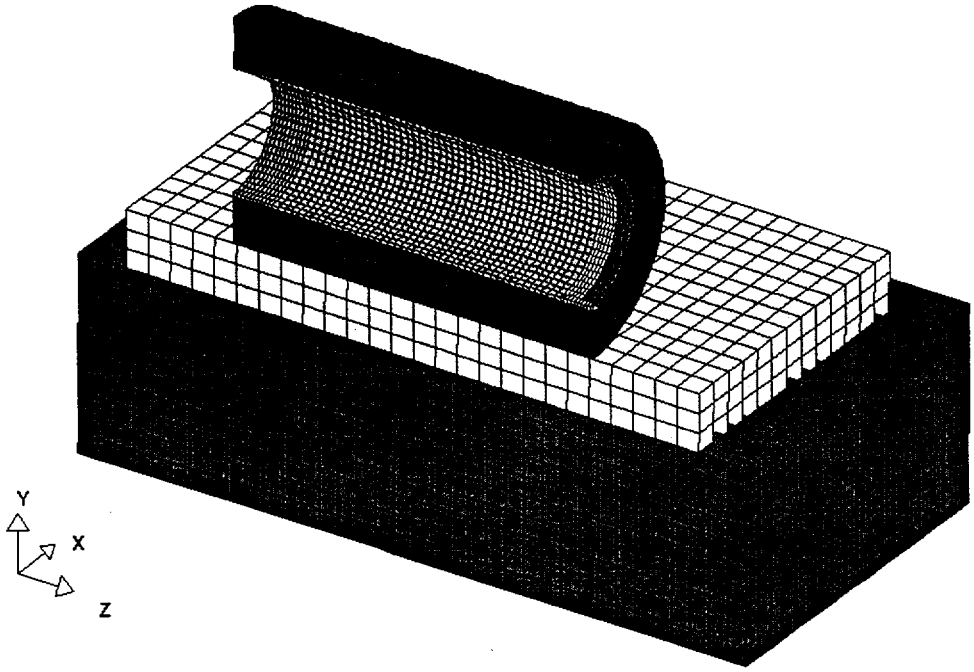

The concrete is represented as a homogeneous isotropic material. The values for concrete pad and soil properties provided below are typical for the input to the LS-DYNA model. The material properties used in the model for the concrete concrete pad are:

Compressive Strength ($f_c^{'}$)	= 5,000 psi	
Density (ρ_c)	= 125 pcf through 160 pcf	
Poisson's Ratio (ν_c)	= 0.22	(NUREG/CR-6608 [38])
Modulus of Elasticity (E_c)	$= 33\rho_c^{1.5}\sqrt{f_c^{'}}$ = 3.261E6 psi	(ACI 318-95)
Shear Modulus (G_c)	$= \frac{E_c}{2(1+\nu_c)}$ = 1.337E6 psi	(Blevins [19])
Bulk Modulus (K_c)	$= \frac{E_c}{3(1-2\nu_c)}$ = 1.941E6 psi	
Volumetric Strain (ε_v)	$= \frac{f_c^{'}}{K_c}$ = 0.002576	

The material properties used in the model for the soil below the concrete pad are:

Density	= 100 pcf and 160 pcf	
Poisson's Ratio (ν_s)	= 0.45	(NUREG/CR-6608)
Modulus of Elasticity	= 60,000 psi	

The Advanced concrete cask steel liner has the properties:

Density	= 0.284 lbs/in^3
Poisson's ratio	= 0.31
Modulus of elasticity	= 2.9E7 psi

To account for the weight of the shield plug, the loaded canister, and the concrete cask pedestal, effective densities are used for the elements in the first row of the steel liner in the model adjacent to the impact plane of symmetry. These densities represent the regions (6° in the circumferential direction) of the steel liner subjected to the weight of the shield plug, the loaded canister and the pedestal, during the side impact (tip-over) condition. The contact angle (6°) is determined based on the canister/basket analysis for the tip-over condition (Section 11.2.12.6).

Boundary Conditions and Initial Conditions for the Advanced Concrete Cask

A friction coefficient of 0.25 is used at the interface between the steel liner and the concrete shell, between the concrete cask and the pad, and between the pad and the soil. For all the embedded faces (three side surfaces and the bottom surface) of the soil in the model, the displacements in the direction normal to the surface are restrained. The symmetry boundary conditions are applied for all nodes at the plane of symmetry.

The initial condition corresponds to the concrete cask in a horizontal position with an initial vertical velocity into the concrete pad. The pad and soil are initially at rest.

The distribution of initial velocity of the concrete cask is simulated by applying an angular velocity (ω) to the entire cask. The point of rotation is taken to be the lower edge of the base of the concrete cask. The angular velocity value is computed by considering energy conservation at the cask "center of gravity over corner" tip condition versus the side impact condition.

From energy conservation:

$$mgh = \frac{I\omega^2}{2}$$

where:

mg = conservative, bounding weight of the loaded concrete cask
= 313,000 lbs (PWR Class 1)
= 324,000 lbs (PWR Class 2)
= 329,000 lbs (PWR Class 3)

h = height change of the concrete cask center of gravity (L_{CG}) = $\sqrt{R^2 + \left(\frac{L_{CG}}{2}\right)^2} - R$

= 61.32 inches (PWR Class 1)
= 65.60 inches (PWR Class 2)
= 69.93 inches (PWR Class 3)

where:

L_{CG} = location of the center of gravity above the pad for the concrete cask
= 111.0 inches (PWR Class 1)
= 115.0 inches (PWR Class 2)
= 119.0 inches (PWR Class 3)

R = radius of the concrete cask = 68 inch

I = total mass moment of inertia of the cask about the point of rotation
= 8,284,344 lbs-sec^2-inch (PWR Class 1)
= 9,165,994 lbs-sec^2-inch (PWR Class 2)
= 9,853,583 lbs-sec^2-inch (PWR Class 3)

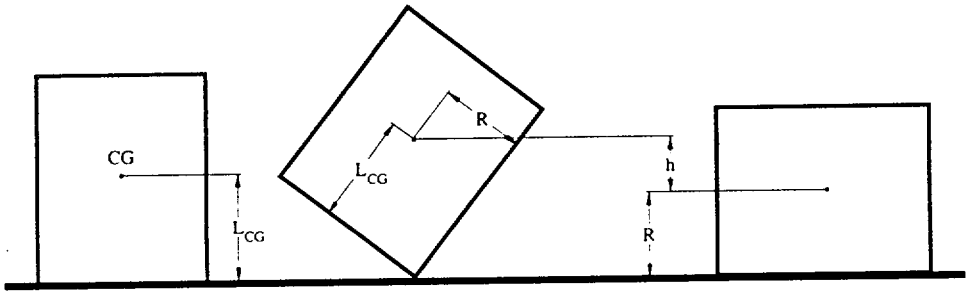

The mass moment of inertia for the concrete shell and the steel liner is calculated using the formula for a hollow right circular cylinder (Blevins).

$$I=\frac{m}{12}(3R_1^2+3R_2^2+4L^2)+md^2$$

where:

m = mass (lbs-sec^2/in)
R_1 and R_2 = the outer and inner radius of the cylinder (inch)
L = height of the cylinder (inch)
d = distance between the center of gravity and the point of rotation (inch)

For the mass of the shield plug, loaded canister and the pedestal, the formula for the moment of inertia for a solid cylinder is used:

$$I=\frac{m}{12}(3R^2+4L^2)+md^2$$

where:

m = mass of the cylinder (lbs-sec^2/in)
R = radius of the cylinder (inch)
L = height of the cylinder (inch)
d = distance between the two pivot axes (inch)

The angular velocity is given by $\omega=\sqrt{\frac{2mgh}{I}}$

= 1.528 radians/sec (PWR Class 1)
= 1.530 radians/sec (PWR Class 2)
= 1.535 radians/sec (PWR Class 3)

Filter Frequency for the Advanced Concrete Cask

The accelerations are evaluated at the inner surface of the cask liner, which physically corresponds to the interface of the liner and the loaded canister nearest the plane of impact. Following the methodology contained in NUREG/CR-6608, the Butterworth filter is applied to the nodal accelerations. The filter frequency is based on the fundamental mode of the cask.

The fundamental natural frequency of a beam in transverse vibration due to flexure only is given by Blevins as:

$$f = \frac{\lambda^2}{2\pi}\sqrt{\frac{EI}{\rho A L^4}}$$

where:

$\lambda = 3.92660231$ for a pin-free beam

The frequencies of the concrete (f_c) and the steel liner (f_s) are computed as:

Area of concrete cask = $\pi \{(68)^2 - (39.75)^2\} = 9562.8 \text{ in}^2$

Moment of inertia of concrete cask = $\frac{\pi}{4}\{(68)^4 - (39.75)^4\} = 14{,}832{,}070 \text{ in}^4$

$$f_c = 811{,}872 \frac{\lambda^2}{L^2}$$

= 286 Hz (PWR Class 1)
= 263 Hz (PWR Class 2)
= 245 Hz (PWR Class 3)

Area of steel liner = $\pi \{(39.75)^2 - (37.25)^2\} = 604.8 \text{ in}^2$

Moment of inertia of steel liner = $\frac{\pi}{4}\{(39.75)^4 - (37.25)^4\} = 448{,}673 \text{ in}^4$

$$f_s = 861068 \frac{\lambda^2}{L^2}$$

= 303 Hz (PWR Class 1)
= 279 Hz (PWR Class 2)
= 260 Hz (PWR Class 3)

Since the concrete cask is short compared to its diameter, the contribution of the flexibility due to shear is also incorporated. This is accomplished by using Dunkerley's formula (Blevins). The system frequency is:

$$\frac{1}{f^2} = \frac{1}{f_c^2} + \frac{1}{f_s^2}$$

Thus, the system frequencies are 208 Hz (PWR Class 1), 191 Hz (PWR Class 2), and 178 Hz (PWR Class 3). A cut-off frequency of 210 Hz (PWR Class 1), 190 Hz (PWR Class 2), and 180 Hz (PWR Class 3) is applied to filter the analysis results and measure the peak accelerations.

Results of the Transient Analysis for the Advanced Concrete Cask

The maximum accelerations at key locations of the concrete cask liner, which are required in the evaluation of the loaded canister/basket model (Section 11.2.12.4), are:

Location on Component	Position Measured from the Bottom of the Concrete Cask (inches)			Acceleration (g)		
	PWR Class 1	PWR Class 2	PWR Class 3	PWR Class 1	PWR Class 2	PWR Class 3
Top of Basket	188.75	197.85	205.45	28.0	31.1	32.0
Top of Canister	199.45	208.55	216.15	29.3	32.5	33.3

Note: Critical condition is concrete density of 160 pcf and a soil density of 100 pcf.

Advanced Concrete Cask Cooling Channel/Liner Attachment:

Side-load tangential to concrete cask liner due to impact is:

$$P_s = \frac{3600000}{2}\sin(\frac{15.0}{2}) \approx 235000 \text{ lbs}$$

Channel weldments are held in place on the concrete cask inner liner with 0.25 inch fillet welds on either side of the channel. Using an allowable stress of 0.42Su, the required weld length on each channel side is:

$$\tau = \frac{P}{A} = \frac{P}{L \times W_t}$$

$$0.42(58000) = \frac{(235000/2)}{L(0.25 \times 0.7071)}$$

$$L = 27.3 \text{ inches}$$

where:

τ = weld shear allowable (0.42Su)
L = Length of weld required on each side of the channel
W_t = weld throat area
Su = 58.0 ksi at 350°F for A36 carbon steel

The required length of 0.25 inch fillet weld on either side of the cooling channel for attachment to the concrete cask liner is 27.3 inches.

11.2.12.6 Analysis of Advanced Canister and Basket for the Cask Tip-Over Event

The Advanced canister and basket structural evaluations are performed for the canister and fuel basket for tip-over accident conditions for the PWR fuel configuration. ANSYS finite element models are used to evaluate this side impact loading condition. The Advanced basket consists of a series of interlocking plates that form square fuel loading positions within the canister. The canister is generally identical to that used in the Standard configuration, but has a 2" thick bottom plate and is referred to as the Advanced canister.

Comparison of maximum stress results to the allowable stress intensities shows that the canister and interlocking plates are structurally adequate for the concrete cask tip-over condition and satisfies the stress criteria in accordance with the ASME Code, Section III, Division I, Subsection NB and NG, respectively.

The structural response of the Advanced PWR canister and fuel basket to the tip-over condition is evaluated using ANSYS three-dimensional finite element models. During a tip-over event, the concrete cask, canister and fuel basket are subjected to side impact accelerations that vary along the length of the canister – with the fuel basket experiencing increasingly higher impact accelerations going from the bottom to the top of the basket. The structural analyses consist of static analyses of the finite element model with boundary conditions simulating the side impact of the loaded canister. A tapered side impact acceleration is conservatively applied to the ANSYS model for each of the fuel basket orientations analyzed.

11.2.12.6.1 Analysis of the Advanced Canister and Basket for PWR Configurations

The tapered side impact acceleration is designed to provide a bounding 40g acceleration at the top of the top weldment. It is only necessary to model the top portion of the basket and canister to

determine the maximum stress in the basket and canister. Five basket orientations, 0°, 33°, 45°, 56°, and 90° are used in the evaluation of the PWR configuration (Figure 11.2.12.6.1-8).

Post-processing of Advanced basket and canister model results is performed using the ANSYS finite element code. To obtain the minimum margin of safety for the basket and canister, numerous section cuts (using the PRSECT command) are taken throughout the basket and canister to determine the membrane and membrane plus bending stresses. These stresses are then compared to the appropriate material allowable to calculate a margin of safety.

Advanced Canister Model Description

A three-dimensional finite model of the canister and fuel basket is used to evaluate side-loading conditions that conservatively simulate a tip-over event. One model is constructed. However, a three-dimensional half-symmetry model, from the full model, is used for the 0° and 90° basket orientations based on symmetry. The full model is used to evaluate the 33°, 45°, and 56° basket orientations. Figure 11.2.12.6.1-1 provides a cut-away view of the canister and basket finite element model.

The canister shell, shield lid, and structural lid are constructed of SOLID45 elements, which have three degrees of freedom (Ux, Uy, and Uz) at each node (Figures 11.2.12.6.1-2 and 11.2.12.6.1-3). The center section of the shield and structural lid is filled with solid elements to prevent a small hole that can cause a stress concentration or a series of degenerate solid elements that can produce a region of excessive stiffness. The welds connecting the structural lid and shield lid to the canister shell are modeled using coincident nodes for the elements in these regions. The interactions of the shield lid and structural lid with the canister shell (below the lid weld regions) are modeled using CONTAC52 gap elements with the gap size based on nominal dimensions. The interaction of the shield lid and structural lid is modeled using CONTAC52 gap elements with gap size of 0.03 inches. All gap elements in the canister have a stiffness (K) of 1.0E6 lb/in. The canister shell and structural lid is constructed from SA304L stainless steel. The shield lid is constructed from SA304 stainless steel.

The inner surface of the concrete cask is modeled as a series of "ground" nodes. The ground nodes represent the inner surface of the channel weldments on the liner inner surface and are fixed in all six degrees of freedom. The gap is modeled using CONTAC52 gap elements with a stiffness of 1.0E6 lb/in. Weak beam elements (BEAM4) are also modeled across the canister/concrete cask gap (1.50 inches) to help stabilize the solution process.

The Advanced fuel basket is comprised of two primary components: the basket sidewall modeled with SOLID45 elements and basket ligament plates modeled with SHELL63 elements (Figure 11.2.12.6.1-4). The upper 32.99 inches of the basket is modeled for this analysis. The basket is held together by a top and bottom weldment region, which maintain basket continuity with the bottom weldment not modeled. The weldment regions are comprised of the basket sidewalls (which are continuous over the entire axial length of the basket) and stiffener plates that run across the width of the basket. The internal ligament plates define the fuel slots of the basket. The basket ligaments are plates that are connected together by a tab and slot design. This tab and slot design, which maintains the slot geometry, allows the transfer of in-plane loads without transferring bending loads. The integrity of the basket fuel cells is maintained by ensuring that the tabs do not disconnect from the slots during all operational or accident conditions. The tab and slots and ligament plate interaction is modeled using CONTAC52 and COMBIN40 elements. CONTAC52 elements (gap = 0.02 inch, K = 1.0E6 lb/in) are used to model the gap between perpendicular ligament plates. COMBIN40 elements (gap = 0.03 inch, K = 1.0E6 lb/in) are used to model the tab/slot gap (side-to-side in the plane of the slot). The ligament plates are connected to the basket sidewall using the tab/slot design and are also welded in certain locations. The welded locations maintain the structural and geometric integrity of the basket. Where the SHELL63 are connected to the SOLID45 elements, stiff BEAM4 elements are used to transfer the rotational degrees of freedom across the common node. The slits in the basket sidewall are modeled using CONTAC49 elements (K = 1.0E5 lb/in). The maximum gap in the basket sidewall is 0.12 inch. The weight of aluminum cooling inserts and cooling shunts, located in the outer regions of the basket, are modeled by increasing the density of the basket sidewalls to represent the weight of the heat shunts and basket sidewall. The basket is constructed from SA537 Class 2 carbon steel.

Boundary Conditions for the Advanced Canister Finite Element Model

The finite element model loading consists of canister internal pressure, fuel loads, and inertia loads. A 30 psi canister internal pressure is applied to canister sidewall and shield lid. The pressure load applied to the basket ligaments represents the weight of the PWR fuel and neutron absorber sheets (Figure 11.2.12.6.1-5). The weight of the fuel and neutron absorber sheets is evenly distributed over the fuel loading positions. A tapered acceleration load is used for the tip-over accident event. The tapered g-load is applied based on a bounding 40g loading at the top of the basket. The taper is calculated with a slope that provides 0g at the base of the basket. The tapered g-load is applied with angular accelerations that result in a tapered inertia loading of the basket and canister. The point of rotation for the angular acceleration is the tip-over point at the base.

The pressure load (1g) applied to fuel cells is

$$P_s = \frac{(1567 \times 32 + 950.0)/32}{153.3 \times 8.8} = 1.18 \text{ psi, Class 1}$$

$$P_s = \frac{(1602 \times 32 + 950.0)/32}{160.3 \times 8.8} = 1.16 \text{ psi, Class 2}$$

$$P_s = \frac{(1480 \times 32 + 950.0)/32}{171.5 \times 8.8} = 1.00 \text{ psi, Class 3}$$

where:

fuel weight =	1,567 lbs, Class 1
	1,602 lbs, Class 2;
	1,480 lbs, Class 3
neutron absorber sheets (bounding) =	950.0 lbs
basket length excluding weldment regions =	153.3 in., Class 1;
	160.3 in, Class 2;
	171.5 in, Class 3
fuel cell width =	8.80 in

Since the ligament plates are modeled at the centerline of the plate, the pressure load is adjusted to the modeled cell width to maintain the correct fuel loading for each standard size fuel cell.

The angular acceleration is:

$$\alpha = \frac{g - load}{r} = \frac{40 \times 386.4}{\sqrt{68.0^2 + 189.00^2}} = 76.9 \text{ rad/sec}^2, \text{ Class 1}$$

$$\alpha = \frac{g - load}{r} = \frac{40 \times 386.4}{\sqrt{68.0^2 + 198.10^2}} = 73.8 \text{ rad/sec}^2, \text{ Class 2}$$

$$\alpha = \frac{g - load}{r} = \frac{40 \times 386.4}{\sqrt{68.0^2 + 205.70^2}} = 71.3 \text{ rad/sec}^2, \text{ Class 3}$$

where:

40g	applied g-load at top of fuel basket (top of top weldment)
68.0 in.	concrete cask radius
189.00 in.	location of top of top weldment from the concrete cask base, Class 1
198.10 in.	location of top of top weldment from the concrete cask base, Class 2
205.70 in.	location of top of top weldment from the concrete cask base, Class 3
386.4 in/sec^2	acceleration constant

To stabilize the model, nodal constraints are applied. At the bottom of the model, all nodes are restrained in the Uz direction. As stated earlier, the concrete cask inner shell is represented by constrained nodes. For the 0° and 90° analysis runs, the model is restrained along the y-axis and x-axis, respectively, to represent symmetry conditions. The weak beams are constrained in the three rotational degrees (ROTx, ROTy, and ROTz) of freedom where they come in contact with SOLID45 elements. The Class 1 configuration is the bounding configuration for an Advanced PWR concrete cask tip-over event.

Advanced Canister Modal and DLF Analysis

The periodic finite element model used in the modal analysis is shown in Figure 11.2.12.6.1-8. The finite element model is constructed to facilitate the modal analyses only. SHELL63 and SOLID45 elements are used in the construction of the basket model. SHELL63 elements are used for the interior ligament plates. SOLID45 elements are used for the outer basket shell. The thickness (in the global Z-direction) of the representative periodic model is 7.84 inches. Nodal coupled degrees of freedom are used to represent the various basket plate joints. There are five impact configurations about the global Z-axis to be studied. The five impact angles are 0°, 33°, 45°, 56°, and 90°, as shown in Figure 11.2.12.6.1-8.

The Advanced fuel basket is enclosed in the canister. The canister is enclosed by the concrete cask. It was found from a static analysis that, under a 40g static lateral loading, the fuel basket would move towards the canister liner closing the gaps between the fuel basket, the canister and the concrete cask. Taking into account all interactions between the basket wall, canister and concrete cask, the angle of contact was found to be 58° in that study. When deformed under this static loading, the fuel basket exterior wall conforms to the canister contour thus effectively making the portion of the fuel basket exterior wall included in the angle of contact (58°) as a composite part of the canister wall thickness.. The combined thickness of this composite material is one inch, and it is supported by the rigid concrete cask liner. Therefore, in the modal analysis, the portion of the fuel basket wall that is included within the angle of contact (58°) is treated as rigid.

The purpose of the modal analyses is to find the fundamental mode along the impact direction. In a three-dimensional structure, the fundamental modes may not align with the impact direction since the impact angle is arbitrary, but the fundamental modes of the structure are orthogonal to the principal axes. In the DLF calculation, the DLF is a vector quantity applied only to the direction of impact. The dynamic response of a structural system is the summation of the modal response multiplied by the modal participation factor. The modal participation factor for a particular global axis derives from the projection (direction component) of modal displacements along the global direction. Therefore, in order to maximize the modal participation factor for the fundamental mode, the finite element model under a particular impact angle is rotated so that the impact angle aligns with one of the global axis. In this calculation, the model is rotated so that the impact angle aligns with the global Y-axis. Since the modal participation factor derives from the vector quantity aligned with the Y-axis only, all other modal displacements in the orthogonal directions (x and z) are insignificant. The nodal DLFs of the model in the global X and Z directions are therefore fixed to maximize the modal participation factor in Y-direction.

The fundamental mode frequencies for each of the 5 impact angles are listed in table below. The mode shapes are presented in Figures 11.2.12.6.1-9 through 11.2.12.6.1-13.

Impact angle (degrees)	Modal frequency (Hz)
0	155.4
33	203.7
45	204.5
56	204.9
90	136.7

Using the acceleration time history of the concrete cask steel liner at the top basket location (Section 11.2.12.5), the maximum DLF is computed to be 1.17. Applying the DLF to the 32g acceleration results in a peak acceleration of 37.4g for the top of the basket. The DLFs for the canister lids are considered to be unity since the lids have significant in-plane stiffness and are considered to be rigid. Therefore, applying a 40g acceleration to the top of the basket is conservative.

Analysis Results for the Advanced Canister

The critical cross sections are determined by sorting the maximum nodal stress intensities of the canister shell. After the nodal stresses are sorted, section cuts are taken (PRSECT command) at the most critical locations. The location of the section cuts and section cut stresses with margin of safety for the critical canister/basket orientations are presented in Tables 11.2.12.6.1-1 through 11.2.12.6.1-5.

The inertial load of the shield lid and structural lids also results in localized bending stresses at the canister shell (at the shield lid and structural lid welds). This stress state is identified as the case of a cylindrical shell at the junction with a vessel head, as shown in Table NB-3217-1 of the ASME Code, Section III, Subsection NB. The localized bending stress at the structural discontinuity is classified as secondary (Q) stress. In accordance with ASME Section III, Appendix F, secondary stresses are not considered for the stress evaluation for Level D (accident) conditions. Therefore, the $P_m + P_b$ stresses are not presented for the region local to the impact of the shield lid and structural lid and the canister.

In accordance with ISG-4, a 0.8 reduction factor is applied to the stress allowable for the structural lid/canister shell weld. This reduction factor is applicable for this analysis because the tensile strength of the weld is greater than the canister material. The weld structural evaluations (shield lid and structural lid) are performed by averaging the sectional stress components of the radial compressive stress region of the weld. Conservatively, this compressive stress region is assumed to be from ±6.0° from the point of impact, circumferentially. Section cuts for the weld regions only include elements from the shield lid or structural lid. Only the averaged stress components of the compressive radial region are reported in the result summary for the shield and structural lids.

Stresses are reported for membrane and membrane plus bending for the canister shell and the shield and structural lid welds. Other than the lid welds, no other stress results are reported for the shield lid and structural lid weld because the stresses are small. The stress evaluation is performed in accordance with ASME Code, Section III, Subsection NB. For accident conditions (Level D), the allowable stress is based on the following criteria:

Stress	Allowable Stress for Accident (Level D)
P_m	Lesser of $0.7S_u$ and $2.4S_m$
$P_m + P_b$	Lesser of $1.0S_u$ and $3.6S_m$

For the canister, stress allowables are taken at the following bounding temperatures,

Component	Temperature (°F)	Material
Canister Shell	325 - 375	SA240 304L Stainless Steel
Shield Lid	325	SA240 304 Stainless Steel
Structural Lid	325	SA240 304L Stainless Steel

The stress evaluation results for the tip-over accident condition show that the minimum margin of safety for the canister is + 0.25 for P_m Stresses and + 0.20 for $P_m + P_b$ stresses. A summary of the margins of safety for the five-drop orientations is presented in Table 11.2.12.6.1-1. The gap closure angle between the canister and concrete cask inner shell is 18°.

Analysis Results for the Advanced PWR Basket

The stress evaluation for the support disk is performed according to the ASME Code Section III Subsection NG. According to this subsection, linearized section stresses are to be compared against the allowable stresses for membrane and membrane plus bending for accident condition (Level D).

For the PWR fuel basket, stress allowables are taken at the following bounding temperatures.

Component	Temperature (°F)	Material
Basket Ligaments	700	537 Class 2 Carbon Steel
Basket Sidewall	700	537 Class 2 Carbon Steel
Top Weldment Ligaments	500	537 Class 2 Carbon Steel
Top Weldment Sidewall	500	537 Class 2 Carbon Steel

The stress evaluation results for the tip-over accident condition show that the minimum margin of safety for the basket is + 0.64 for P_m Stresses and + 0.25 for P_m+P_b stresses. A summary of the margins of safety for the five-drop orientations is presented in Table 11.2.12.6.1-6.

As shown in Table 11.2.12.6.1-6, the 56° drop orientation case generates the minimum margin of safety in the basket. Therefore, the P_m and the P_m+P_b stress intensities for the 56° basket drop orientation case are presented in Tables 11.2.12.6.1-9 and 11.2.12.6.1-10, respectively. These tables identify the section number as well as the basket component corresponding to the section number. These tables show the critical stress margin in each basket component as well as an overall distribution of the stresses in each of the four components; top weldment ligament, top weldment side wall basket region ligament plate, and basket region side wall (see Figure 11.2.12.6.1-4). These two summary tables contain the lowest thirty margins, which were selected from the lowest ten margins for each component. The location for the sections as well as the definition of the points defining the section for the stress summary tables are contained in Tables 11.2.12.6.1-7 and 11.2.12.6.1-8.

Advanced Basket Tab/Slot Gap Status

The key to the fuel baskets structural integrity is the ability of the tabs to stay inside the slots during all operational and accident conditions. The tab/slot configuration is designed to act as a simply supported beam; no bending loads are transmitted from the tabbed ligament to the slotted ligament plate. The tabs are 0.05 inches shorter than the nominal thickness of the plate they are inserted into; an additional 0.05 inches for each tab is subtracted to account for manufacturing tolerances. Since each ligament plate is supported by two sets of tabs the allowable gap movement is defined as:

$$\text{Gap allowable} = t_{plate} - 0.05 - 0.05 = t_{plate} - 0.10$$

where:

t_{plate} = the nominal thickness of the slotted plate

$$\text{Engagement} = \text{Gap}_{allow} - \text{Gap} \quad \text{(Tab length engaged in slot)}$$

where:

Gap = gap opening value

The results of the Tab/Slot Gap Status check are presented in the following table. Also, only the tabs in the upper portions of the basket are measurably affected. Tabs throughout the rest of the basket assure that the tabbed plates remain in place.

Basket Orientation	T_{plate} = 0.3125 in		T_{plate} = 0.3125 in [1]		T_{plate} = 0.438 in	
	Gap_{allow} = 0.213 in		Gap_{allow} = 0.313 in		Gap_{allow} = 0.338 in	
	Gap	Engagement[2]	Gap	Engagement[2]	Gap	Engagement[2]
0°	0.148	0.065	0.237	0.076	0.063	0.275
33°	0.142	0.071	0.257	0.056	0.063	0.275
45°	0.152	0.061	0.221	0.092	0.063	0.275
56°	0.140	0.073	0.212	0.101	0.063	0.275
90°	0.041	0.172	0.062	0.251	0.061	0.277

1. The allowable gap accounts for the tab extending 0.10 inches beyond the thickness of the slotted plate.
2. Engagement – Tab length engaged in slot during a tip-over event with manufacturing tolerance taken into account.

Therefore, the tabs, when considering the minimal manufacturing engagement, do not separate from the slotted plates during a tip-over event.

Ligament Plate/Tab Structural Evaluation for the Advanced Basket

The evaluation of the tab/slot design showed that the tabs remain engaged with the slots during the postulated concrete cask tip-over event. A further structural evaluation of the tabs is performed to evaluate the structural adequacy of the tabs during a 40g tip-over event.

The tab is evaluated using a simply supported beam of length 8.80 inches and width of 15.68 inches (center to center distance of the tabs).

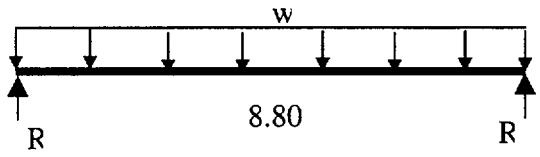

where:

$w = 1.18\ \text{psi} \times 15.68\ \text{in} \times 60\text{g} = 1{,}110\ \text{lbs/in}$ (use 1,200 lbs/in)

1.18 psi = pressure load of fuel assembly and neutron absorber sheets

15.68 in = center to center spacing of ligament plate tabs

60g = bounding acceleration (30 ft. side-drop)

The reaction load for the beam is:

$$R = \frac{1{,}200 \times 8.80}{2} = 5{,}280\ \text{lbs}$$

The maximum shear stress on the tab is:

$$S_{shear} = \frac{5{,}280}{3.28 \times 0.3125} = 5{,}151\ \text{psi}$$

where:

3.28 in = length of tab

0.3125 in = minimum ligament plate thickness

The margin of safety is:

$$MS = \frac{0.42Su}{S_{shear}} - 1 = \frac{0.42 \times 77{,}800}{5{,}151} - 1 = +5.34$$

The maximum bending load at the tab/ligament plate interface is conservatively (assuming tab locks up in the slot during side drop):

$$M = 5280 \times (0.3125 + 0.06) = 1{,}967 \text{ in - lbs} \quad (\text{use } 2{,}000 \text{ in - lbs})$$

where 0.3125 inch is the ligament plate thickness and 0.06 inch is for tolerances.

The maximum bending stress in the tab is:

$$S_b = \frac{6M}{bt^2} = \frac{6 \times 2{,}000}{3.28 \times 0.3125^2}$$

$$S_b = 37{,}463 \text{ psi}$$

The margin of safety is:

$$MS = \frac{Su}{S_b} - 1 = \frac{77{,}800}{37{,}463} - 1 = +1.08$$

Therefore, under tipover events, the tabs are freely restored to their pre-tipover position following the accident loading.

Advanced PWR Basket METAMIC Plate Analysis

The neutron absorber sheets are held in place using tabs and slots similar to the ligament plates. The structural evaluation of the neutron absorber sheets demonstrates that they are structurally adequate to meet all of the storage conditions. For normal conditions, the minimum margin of safety is 0.53. For accident conditions, the minimum margin of safety is 0.02. For primary plus secondary loads, the minimum margin of safety is 0.46.

Advanced PWR Basket End and Side Drop Analysis for METAMIC

The bottom end-drop analysis for the Advanced PWR basket is presented in Section 11.2.4. This analysis presents the evaluation and results of the side drop.

ANSYS models are used to calculate the stresses of the METAMIC sheet under various g-loads for the lateral loadings. The finite element models are constructed using SHELL63 elements. There are three different poison plates in the PWR basket with three possible lengths, depending on fuel class. Therefore, nine models are generated for the deflection analysis. For this analysis material properties are taken at 700°F. The models are constrained in the y-direction at the bottom of the sheet and in the z-direction at the interface between the sheet and the sheet perpendicular to it

at the slot locations. The models are restrained in the x-direction along the vertical centerline of the sheet. Gap elements are used to allow for the tabs to rotate within the slot and come in contact with the structural carbon. Figures 11.2.12.6.1-15 and 11.2.12.6.1-16 show the basic models used in this analysis.

To bound all possible fuel and sheet loading scenarios, three cases are evaluated.

Case 1 Maximum gap between neutron absorber sheets and fuel assemblies.
Case 2 Minimum gap between neutron absorber sheets and fuel assemblies.
Case 3 No fuel in the basket fuel loading positions.

Thermal stresses are evaluated by adding temperature boundary conditions of 450°F at the top of the sheet, 400°F at the bottom of the sheet, and 700°F at the center of the sheet.

Membrane and membrane plus bending stresses are evaluated using the PRSECT command. Section cuts are taken at various locations of the plate to determine the maximum stresses. Figures 11.2.12.6.1-17 and 11.2.12.6.1-18 provide schematics for the section cut locations.

To bound storage conditions, 60g is used for accident conditions. For membrane plus bending stresses, stress allowables are taken at 700°F. Membrane stresses are not reported because there is no membrane stress developed during a side drop due to the pure bending of the sheets. Results are summarized in Tables 11.2.12.6.1-11 through 11.2.12.6.1-13, which are compared against an allowable stress of S_u. The sheets at the center of the basket are bounding because of the higher temperatures; therefore, only these sheets are analyzed.

The allowable yield stress is 14.8 ksi at 500°F and 8.9 ksi at 700°F. From $P_m + P_b$ stresses for 60g, the maximum sectional stress is 10.85 ksi at 500°F and 5.61 ksi at 700°F. The margins of safety against yield are 0.36 and 0.59 for 500°F and 700°F, respectively. Because the stresses are below the yield stress allowable for METAMIC, there is no permanent deformation of the plates. Therefore, under 60g loading conditions, the METAMIC tabs are freely restored to their pre-loading position following the accident loading.

Fuel Bearing on Neutron Absorber Sheets

During a tip-over event, the fuel will bear on the neutron absorber sheets at the fuel assembly. Using the smallest fuel assembly width (7.76 in.), spacer plate height of 1.50 in, maximum fuel assembly weight (1602 lbs), and the minimum number of spacer plates (6), the maximum bearing

stress on the neutron absorber sheets, assuming the fuel assembly is supported by the fuel support grids only, is:

$$S_{brg} = \frac{1602 \times 60}{6 \times (7.76 \times 1.50)} \times 2.00 = 2753 \text{ psi @ 60g}$$

Note:

1. 2.00 is a conservatism factor for miss-location or missing fuel assembly support grids.
2. 60g bounding acceleration of side-drops and tip-over events

At 900°F (conservative), Sy = 3.2 ksi

The margin of safety against the neutron absorber sheet yielding is

$$MS = \frac{3200}{2753} - 1 = 0.16$$

Therefore, the poison sheet will not yield, through the thickness of the plate, during a 60g side-drop.

Advanced Basket Tab Analysis

The neutron absorber sheets are supported by the baskets tab/slot configuration during a side drop. From the deflection analysis of neutron absorber sheets results, the maximum deflection of the tab in the slot is 0.0002 in. at 1g; therefore, for 60g, the maximum tab deflection is 0.012 in. The slot in the neutron absorber sheets is 0.070 ±0.003 in. in height. The neutron absorber sheets have a thickness of 0.050 ±0.003 in. The minimum clearance between in the slot is 0.014 in. (0.067 – 0.053); therefore, the tab will not come in contact with the opposing side of the slot (clearance of 0.002 in).

The tab/slot geometry has neutron absorber sheets and carbon plate in the same slot. For the neutron absorber sheet to generate a bending moment in the tab, the tab needs to come in contact with the carbon plate. The deflection of the carbon plate tip is:

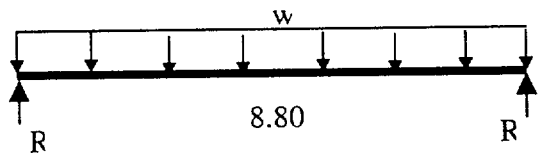

where:

$$w = 1.18\,\text{psi} \times 15.68\,\text{in} \times 60g = 1110\#/\text{in};\ \text{use}\ 1200\#/\text{in}$$

1.18 psi = pressure load of standard fuel assembly and neutron absorber sheets (Class #4)

15.68 in = center to center spacing of ligament plate tabs – carbon plates

60g = bounding side-drop acceleration (30 ft. side-drop)

From Roark's (Table 3, 2e), the rotation at the reaction point is:

$$\theta = \frac{\omega l^3}{24EI} = \frac{1200 \times 8.8^3}{24 \times 29E6 \times \frac{15.68 \times 0.3125^3}{12}} = 0.03\,\text{rad. or}\,1.69\,\text{deg.} \qquad \text{(Ref. 7.7)}$$

The tip deflection of the carbon plate is:

$$\Delta = (0.3125 - 0.05) \times \tan(1.69) = 0.008\,\text{in.}$$

Therefore the total clearance for the neutron absorber sheet tip is:

$$D_{tab} = 0.014 + 0.008 = 0.022\,\text{in.}$$

For a poison sheet tip deflection of 0.012 in., the clearance is 0.01 in. The factor of safety is

$$FS = \frac{0.022}{0.012} = 1.83$$

Therefore, the tabs on the METAMIC neutron absorber sheet will only carry shear loads.

Side Drop Shear on Tabs:

The shear load is (tab spacing = 7.84 in center to center):

$$P_{shear} = \frac{0.095 \times 7.84 \times 0.050 \times 8.8}{2} \times 1.5 = 0.25\,\text{lbs for 1g}$$

60g: $P_{shear} = 15.0$ lbs

Where 1.5 is a conservative DLF for this analysis.

The tab shear stress is:

$$\tau = \frac{15}{0.50 \times 0.050} = 600 \text{ psi}$$

$$MS = \frac{0.42Su}{\tau} - 1 = \frac{0.42 \times 11100}{600} - 1 = 6.77 \text{ @ } 700F$$

The minimum tab length in the Advanced PWR basket is 0.50 inch.

Advanced Basket Neutron Absorber Sheet Thermal Expansion

The maximum average temperature of the neutron absorber sheets is 600°F; therefore, the amount of thermal expansion for a poison sheet and carbon plate at the extreme tab locations is:

$$TE_{\text{neutron absorber sheets}} = 173.5 \times 5.51e-6 \times 530 = 0.51 \text{ in.}$$
$$TE_{\text{carbon plate}} = 173.5 \times 7.16e-6 \times 530 = 0.66 \text{ in.}$$

The carbon plates will grow 0.15 inches (0.66 – 0.51 = 0.15) more than the neutron absorber sheets. A review of the PWR basket drawings show that there is sufficient clearance in the tabs and slots to prevent the plates from binding; therefore, no further evaluation of thermal expansion is required.

Advanced Concrete Cask T-Shaped Channel Weldment Analysis

During a hypothetical Advanced concrete cask tip-over (Figure 11.2.12.6.1-18), the maximum load on one channel weldment is:

$$P = 40 \times 90{,}000 = 3{,}600{,}000 \text{ lbs}$$

where:

Tip-over g-loading = 40g
Loaded canister bounding weight = 90,000 lbs

The minimum channel weldment length is 166.3 inches; therefore, the load per unit length is conservatively calculated as:

$$W = \frac{3600000}{166.3} \approx 22000 \text{ lbs/in}$$

Using the Euler equation for buckling, the critical buckling load per unit length is:

$$W_{cr} = \frac{K_c EI}{L} = \frac{2.47 \times 28e6 \times \frac{1 \times 0.25^3}{12}}{2.22} = 40{,}560 \text{ lbs/in (Ref 7.14, pg. 85)}$$

where:

$K_c = 2.47$ for clamped-free column
$E = 28e6$ lbs/in^2 at 350°F
$t = 0.25$ inch, flange and web thickness of the weldment

The margin of safety against channel weldment buckling is:

$$MS = \frac{40560}{22000} - 1 = +0.84$$

Advanced PWR Basket Buckling Evaluation

For the tip-over accident, the basket plates will experience in-plane compression loads due to the deceleration of the fuel assemblies. To evaluate the buckling of the plates, a conservative approach is used with respect to plate loading. The centermost plate is assumed to carry the weight of 6 fuel assemblies (1/2 of the 12 assemblies located on both sides of the centermost plate). In addition, the weight of ½ of the basket is considered to be reacted thru this plate. This is considered to be very conservative since the basket has other plates that will also be in the load path during the tip-over condition. Additionally any reaction by the end weldments are neglected. The accumulative loading only occurs at the slot nearest the plane of impact (the outer most slot of the basket). The total load the plate is

$[1{,}602 \times 6 + ½ \times 17{,}806 \text{ lb (basket weight)}] \, 40g = 740{,}600 \text{ lbs.}$

Where

1,602 = maximum fuel assembly weight (lb)
17,806 = maximum basket weight (lb) (PWR Class 3)

Conservatively using the active length of the fuel of 144 inches, the load per inch is:

740,600 lb./ 144 inches = 5,143 lb/in.

The critical buckling load for a one-inch strip of the plate is given by:

$$P_{cr} = \pi^2 E I / L^2$$

Where L is the length of plate (8.8 inches), E is the modulus of elasticity at 500°F (at the outer basket slot location) , and I is the moment of inertia given by:

$$I = (1/12)\, b\, h^3 = 1/12\ (1\ \text{inch})\ (5/16\ \text{inch})^3 = 0.00254\ \text{in}^4$$

The critical load is then:

$$P_{cr} = \pi^2\ (27E6\ \text{lb/in}^2 \times 0.00254\ \text{in}^4)/\ 8.8^2\ \text{in}^2 = 8{,}740\ \text{lbs.}$$

The factor of safety against buckling is M.S. = 8,740/5,143 = 1.70. This confirms that the basket will maintain its configuration during the tip-over event.

Figure 11.2.12.6.1-1 Advanced PWR Canister and Fuel Basket ANSYS Model

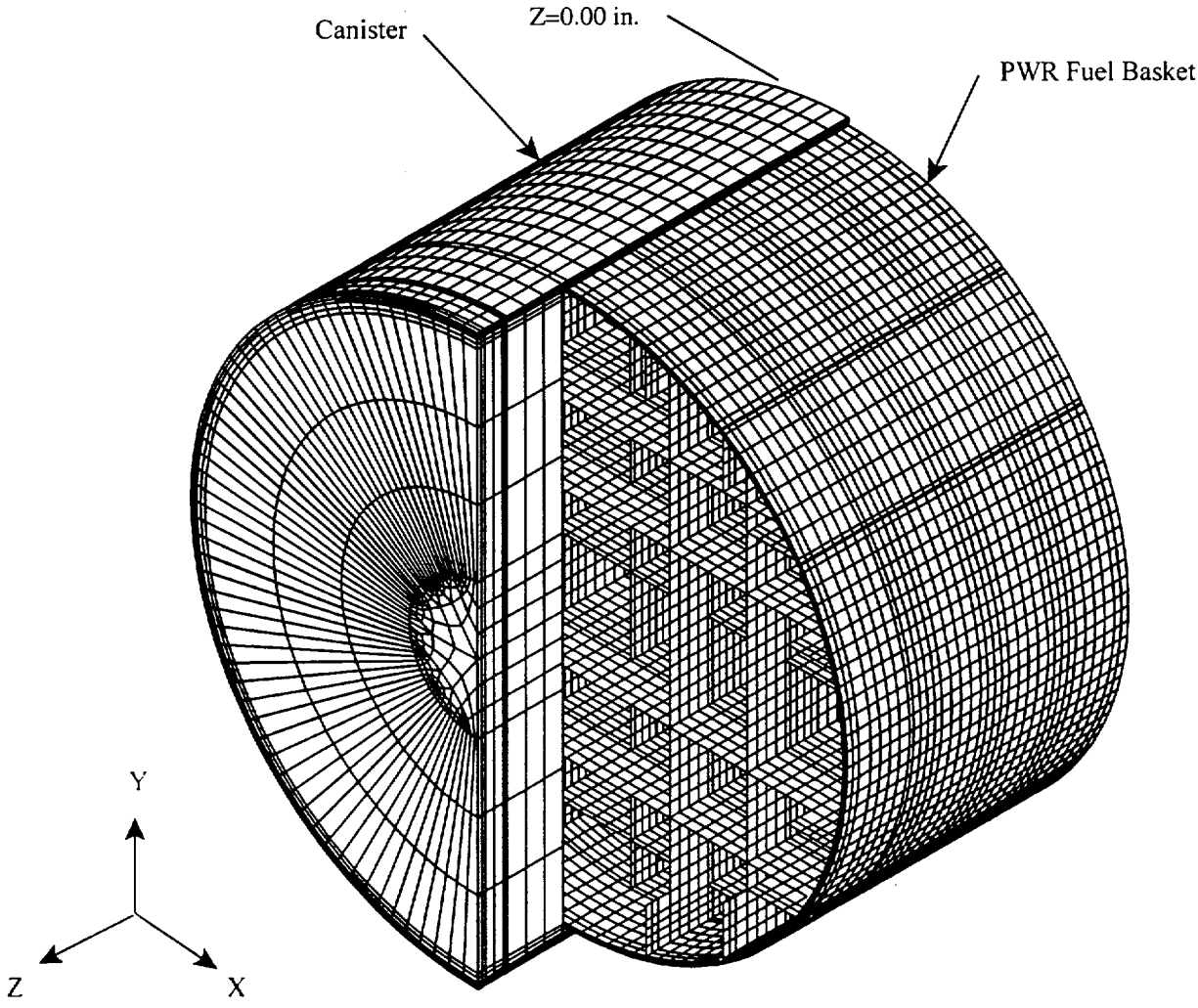

For cylindrical coordinate, the angular position is measured from:

(1) One-half of canister and gap elements omitted for clarity.

(2) +X-axis, ccw.

Figure 11.2.12.6.1-2 Advanced PWR Canister Model

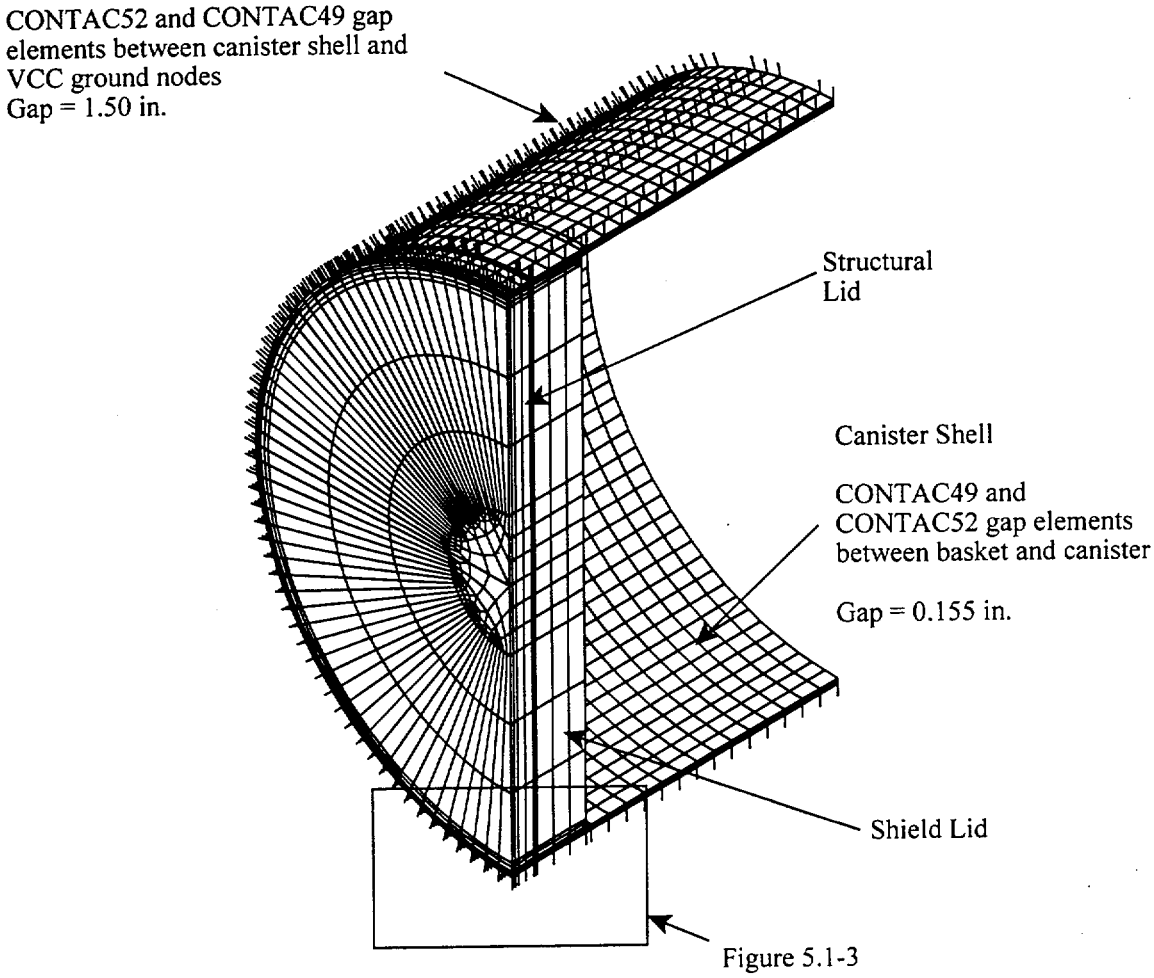

Figure 11.2.12.6.1-3 Canister Shield Lid and Structural Lid Weld Detail

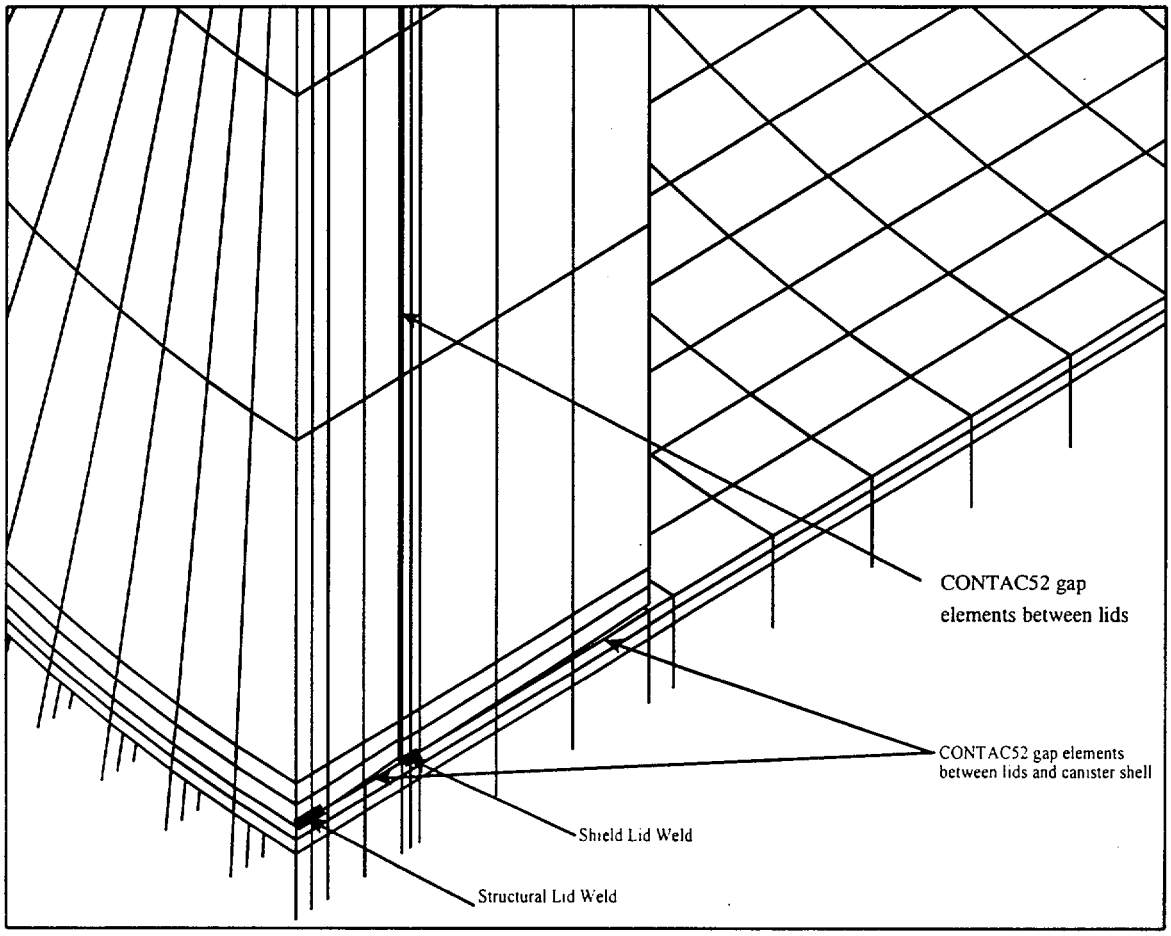

Figure 11.2.12.6.1-4 Advanced PWR Fuel Basket Model – Isometric View

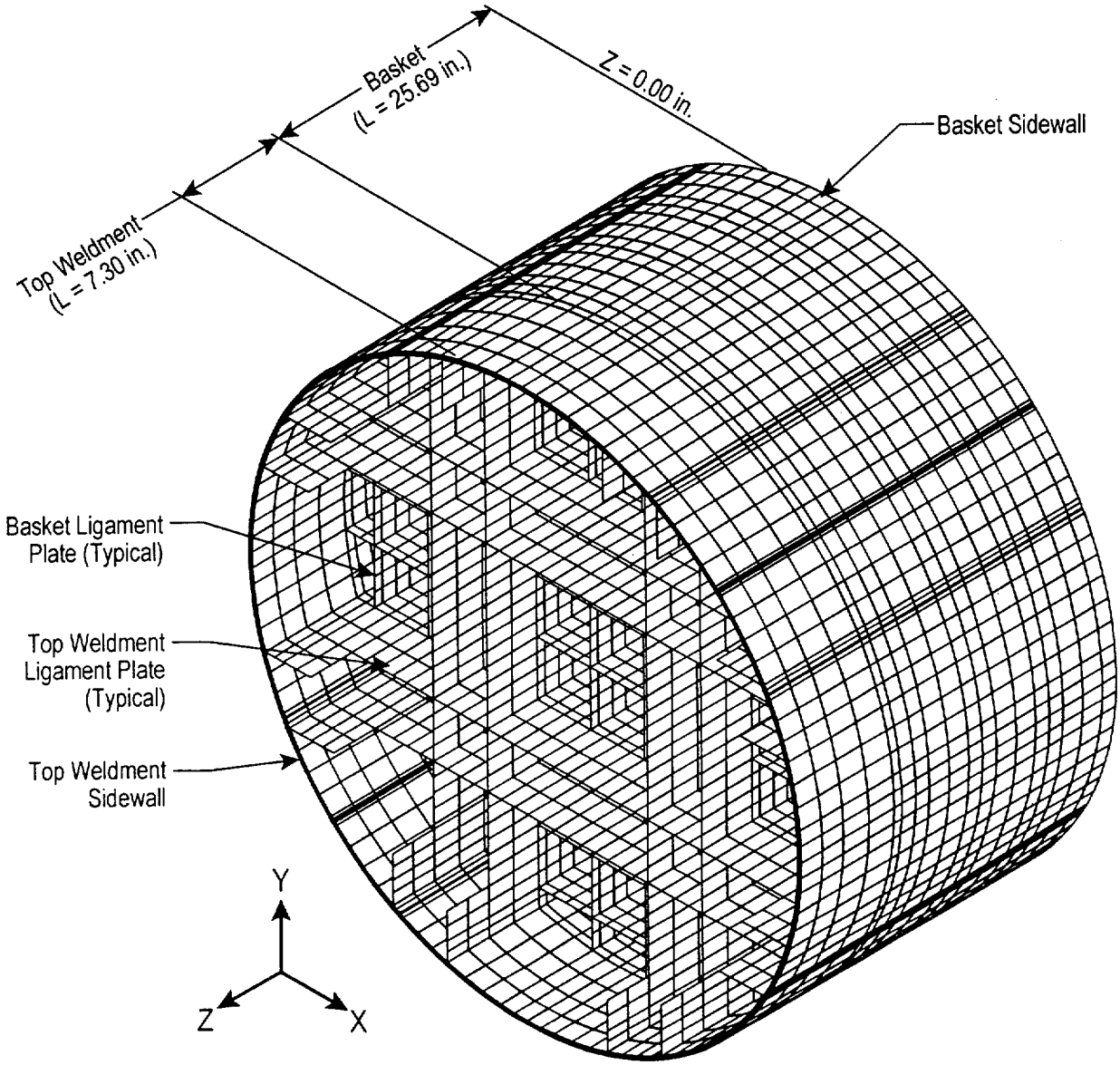

Figure 11.2.12.6.1-5 Typical Loading of Advanced PWR Basket – 45° Basket Orientation

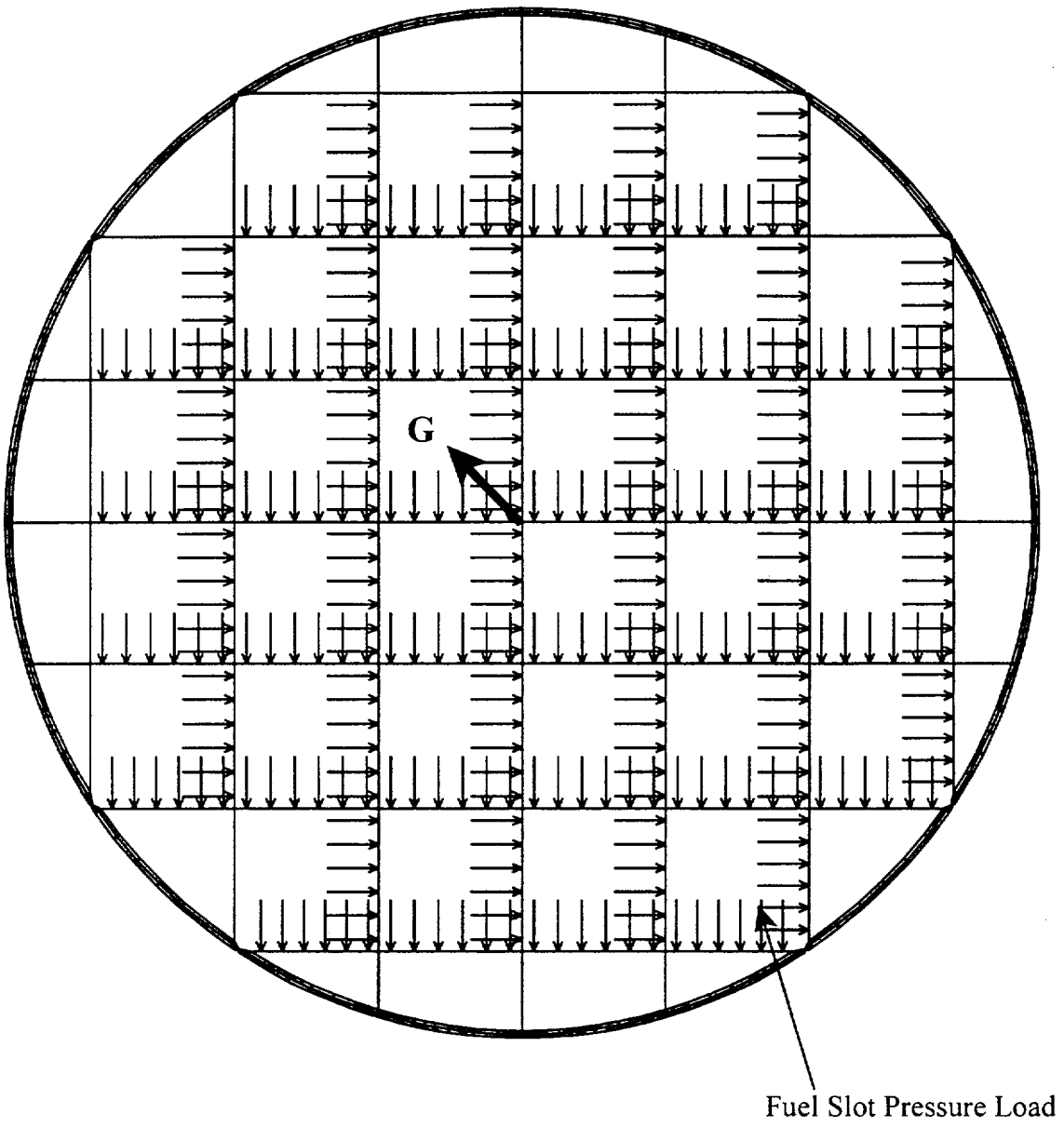

Figure 11.2.12.6.1-6 Advanced PWR Fuel Basket Top Weldment Region

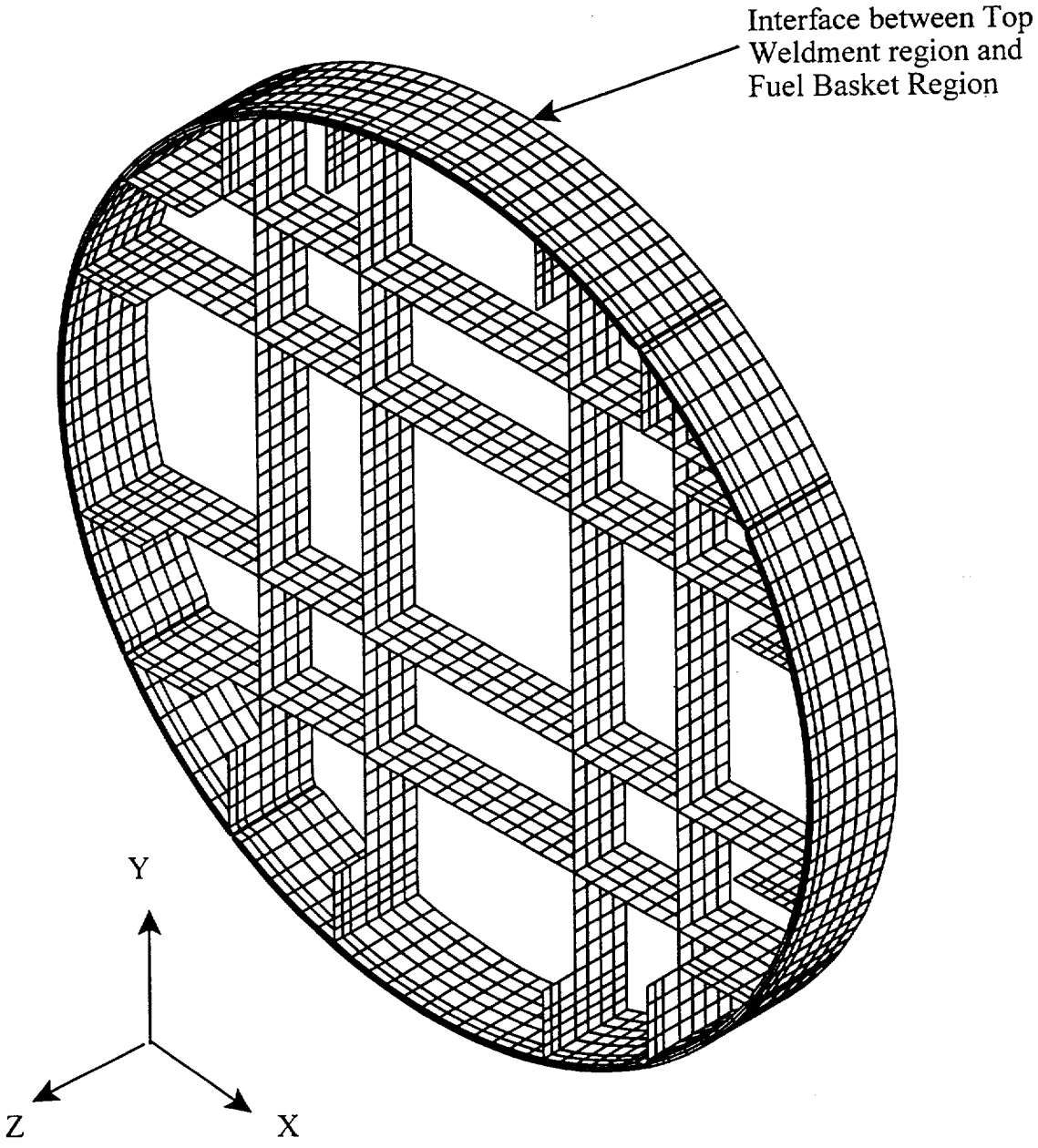

Figure 11.2.12.6.1-7 Location of Section Cuts in the Advanced PWR Fuel Basket for Basket Tip-Over Conditions

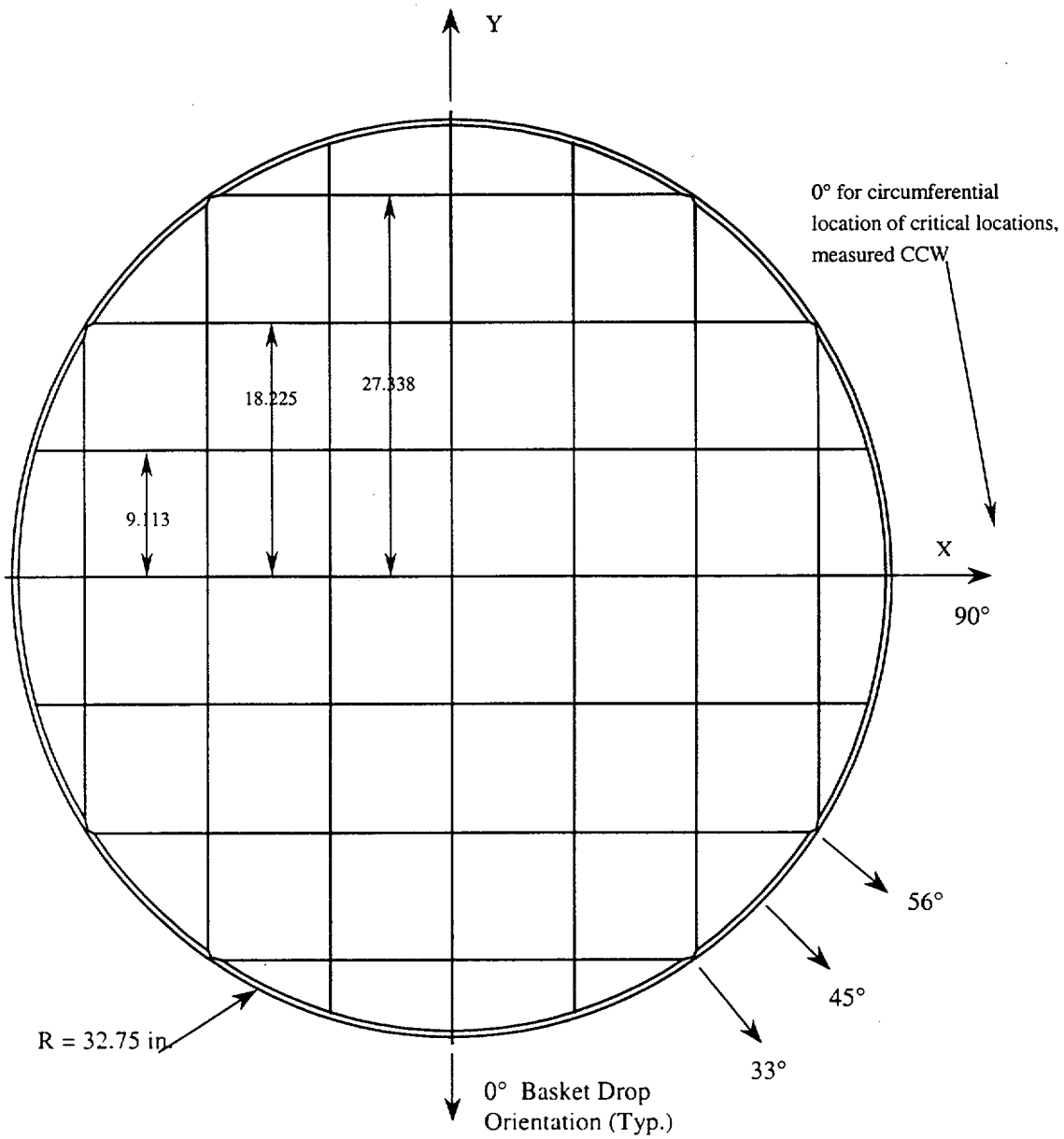

Note: All dimensions are in inches. Dimensions are symmetric in X and Y directions.

Figure 11.2.12.6.1-8 Advanced PWR Basket Periodic Model, Modal Analysis

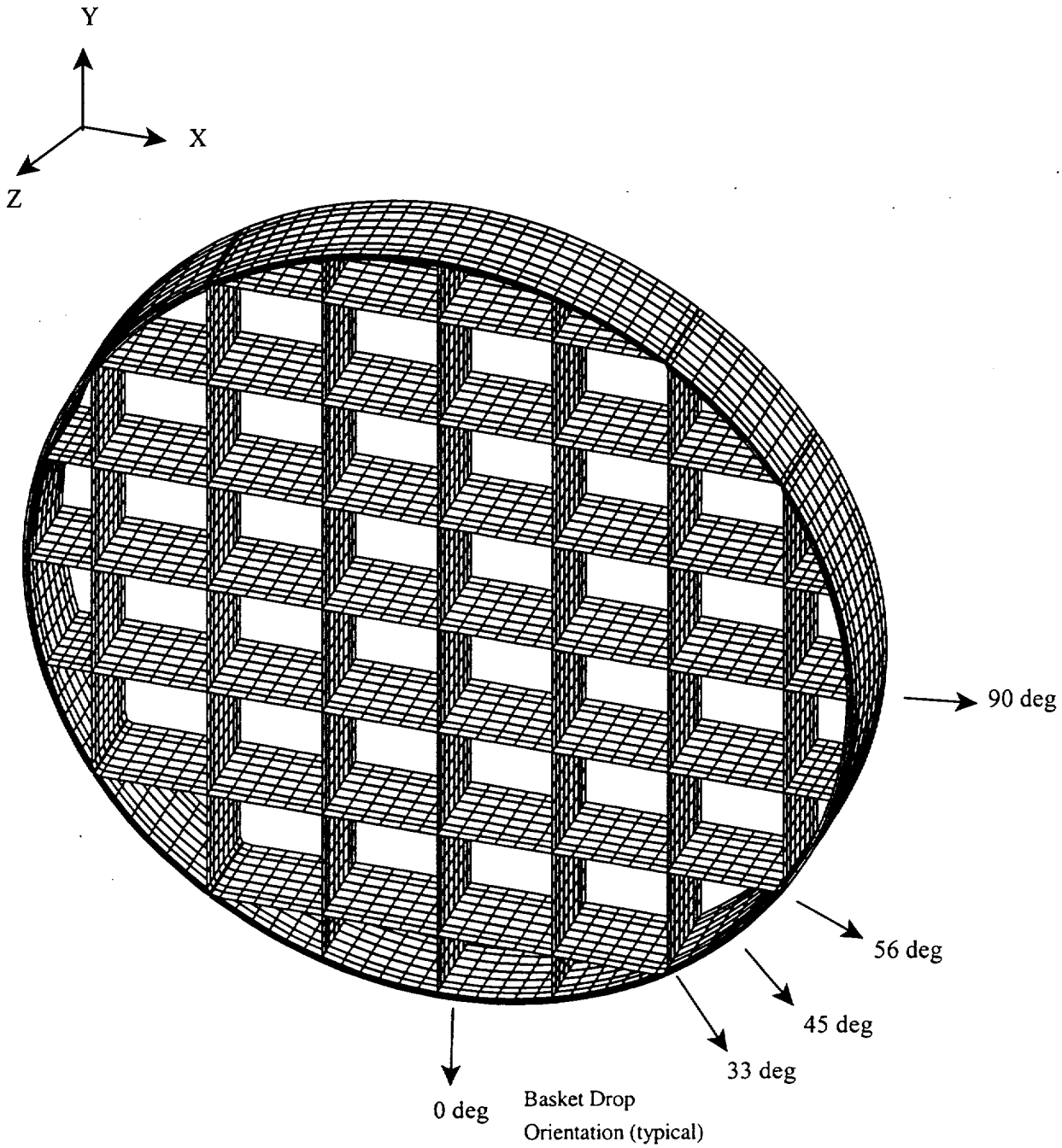

Figure 11.2.12.6.1-9 Advanced PWR Basket Modal Shape for 0-Degree Impact Angle

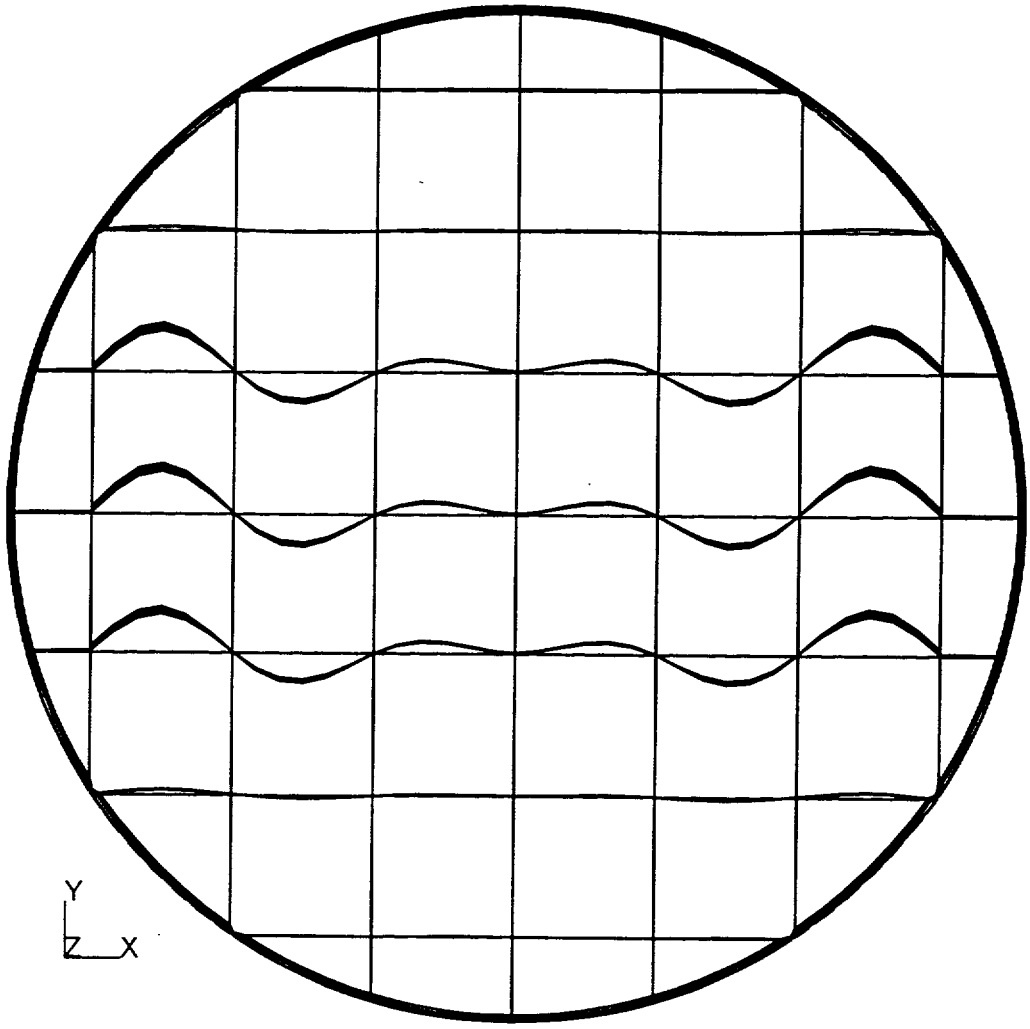

A-UMS_0 : Frequency (Hz): 155.412795 Mode: 6

Figure 11.2.12.6.1-10 Advanced PWR Basket Modal Shape for 33-Degree Impact Angle

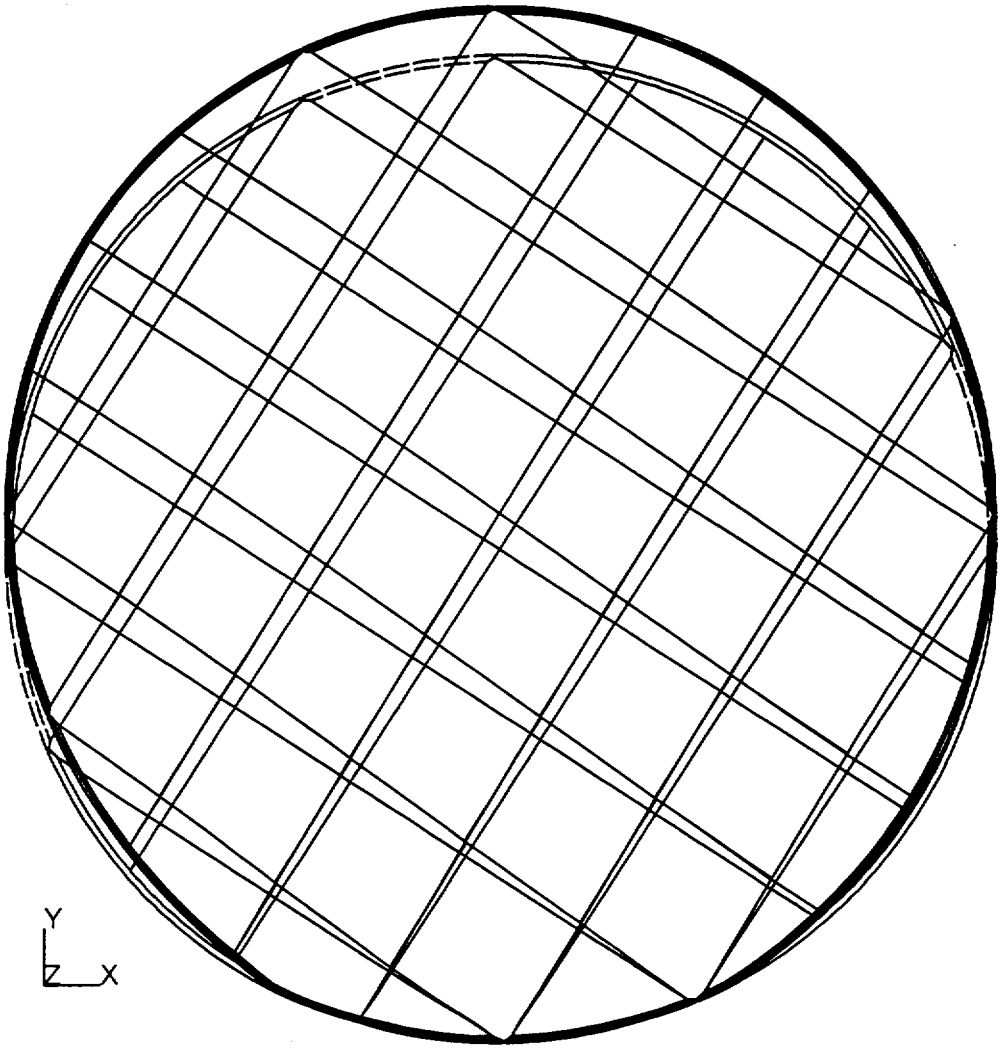

A-UMS_33 : Frequency (Hz): 203.729507 Mode: 1

Figure 11.2.12.6.1-11 Advanced PWR Basket Modal Shape for 45-Degree Impact Angle

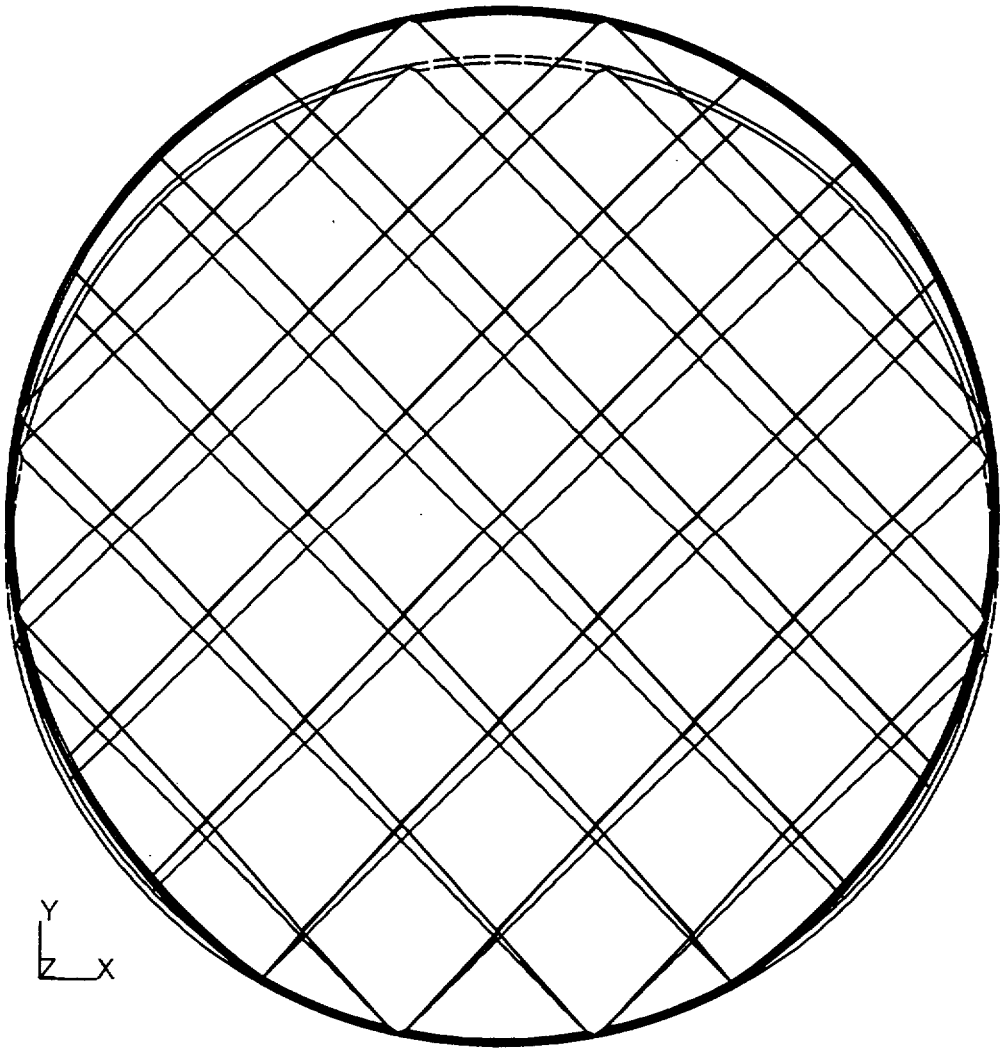

A-UMS_45 : Frequency (Hz): 204.541522 Mode: 1

Figure 11.2.12.6.1-12 Advanced PWR Basket Modal Shape for 56-Degree Impact Angle

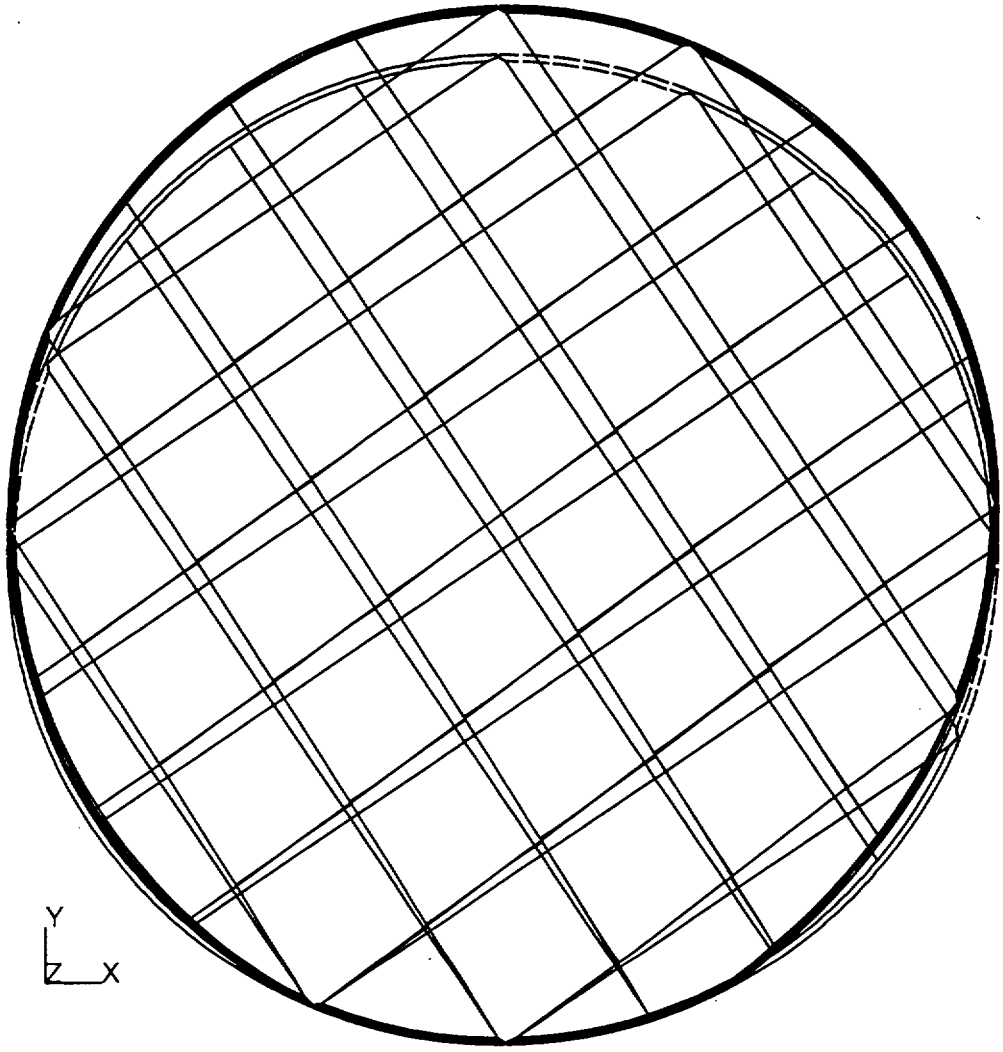

A-UMS_56 : Frequency (Hz): 204.928389 Mode: 1

Figure 11.2.12.6.1-13 Advanced PWR Basket Modal Shape for 90-Degree Impact Angle

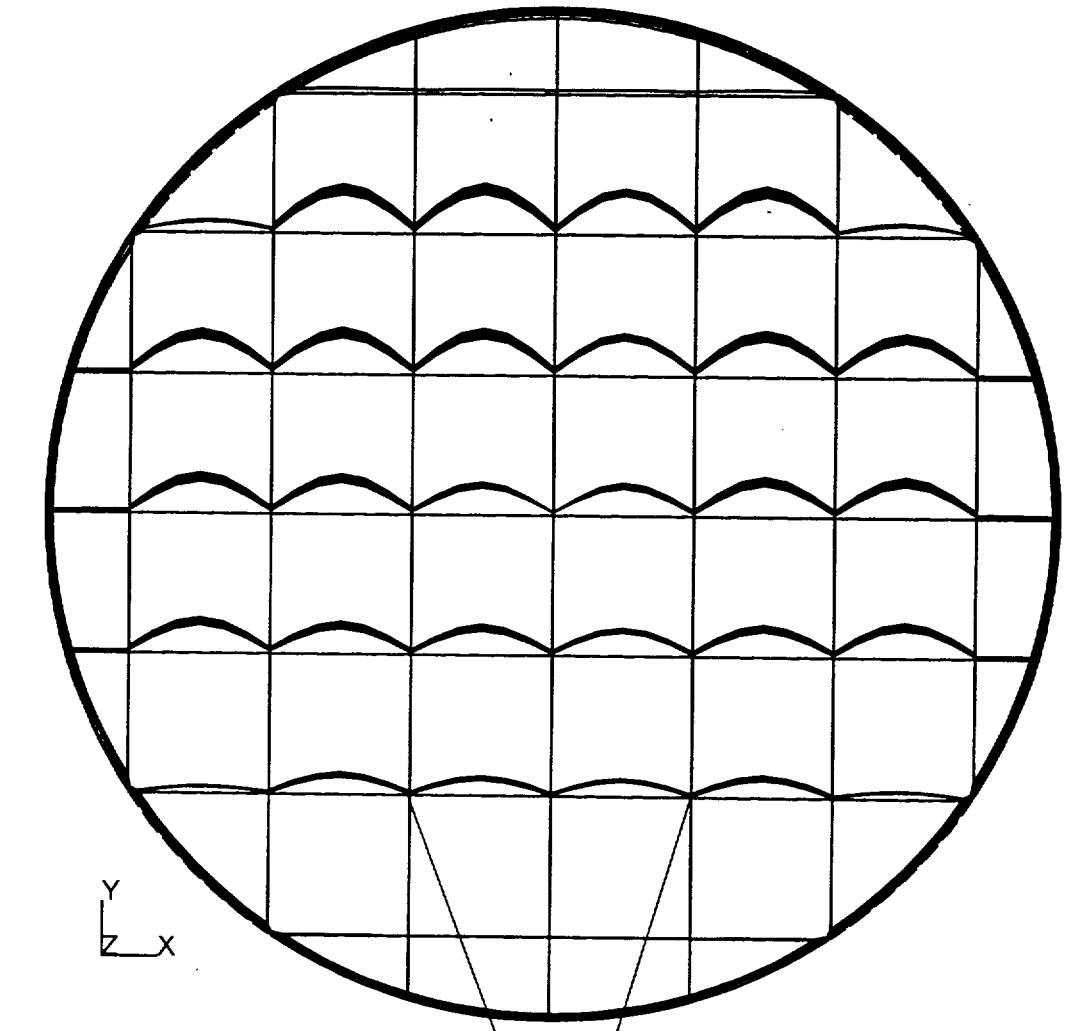

Figure 11.2.12.6.1-14 Advanced PWR Basket Neutron Absorber Sheet Finite Element Model

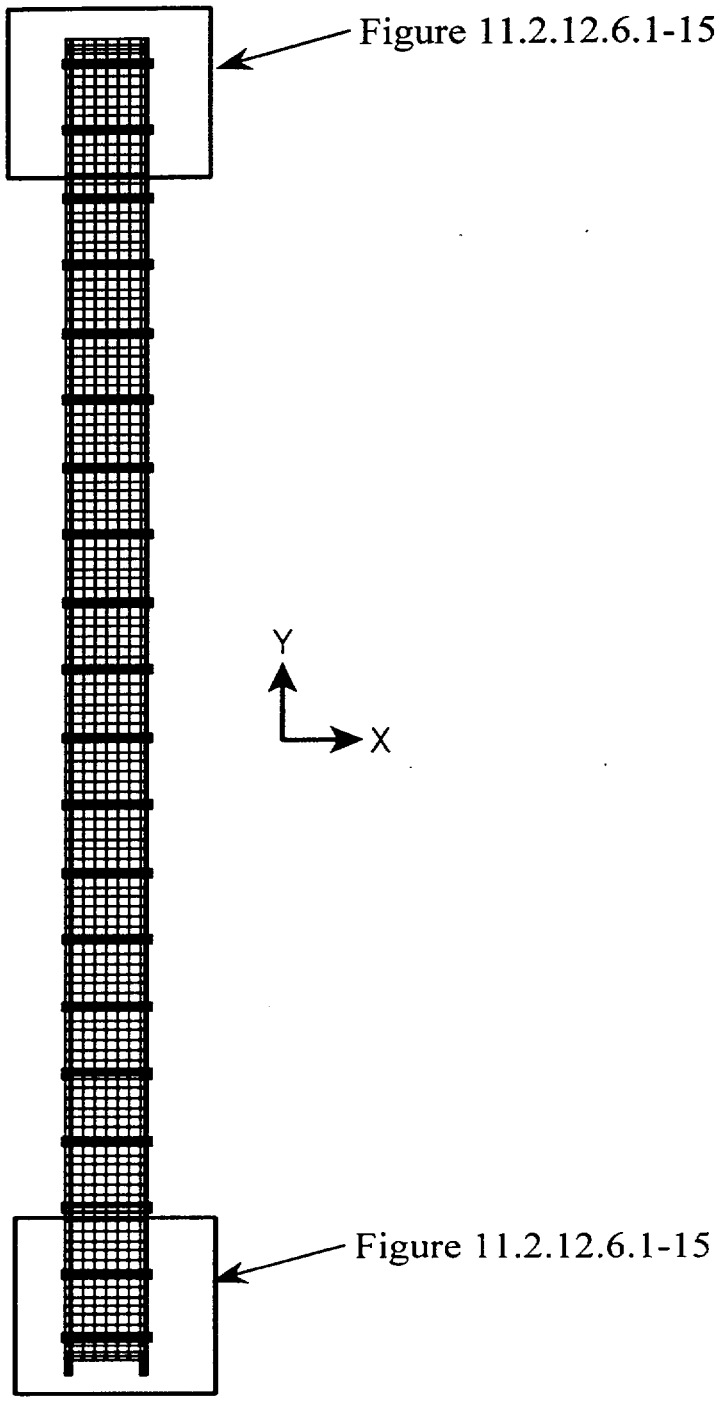

Figure 11.2.12.6.1-15 Advanced PWR Neutron Absorber Model Detail

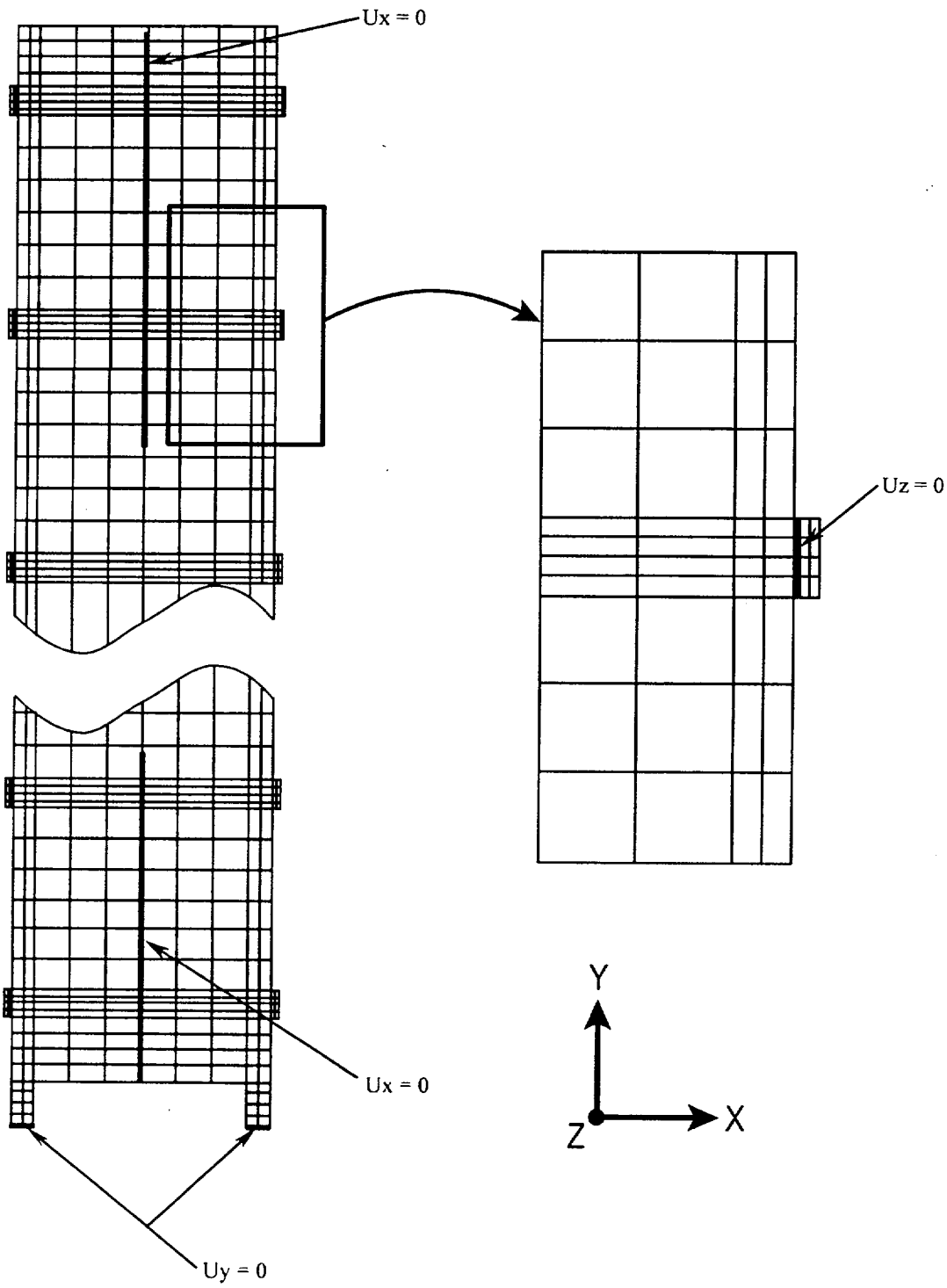

Figure 11.2.12.6.1-16 Section Cut Schematic - #1 – Typical Advanced PWR Neutron Absorber Sheet Details

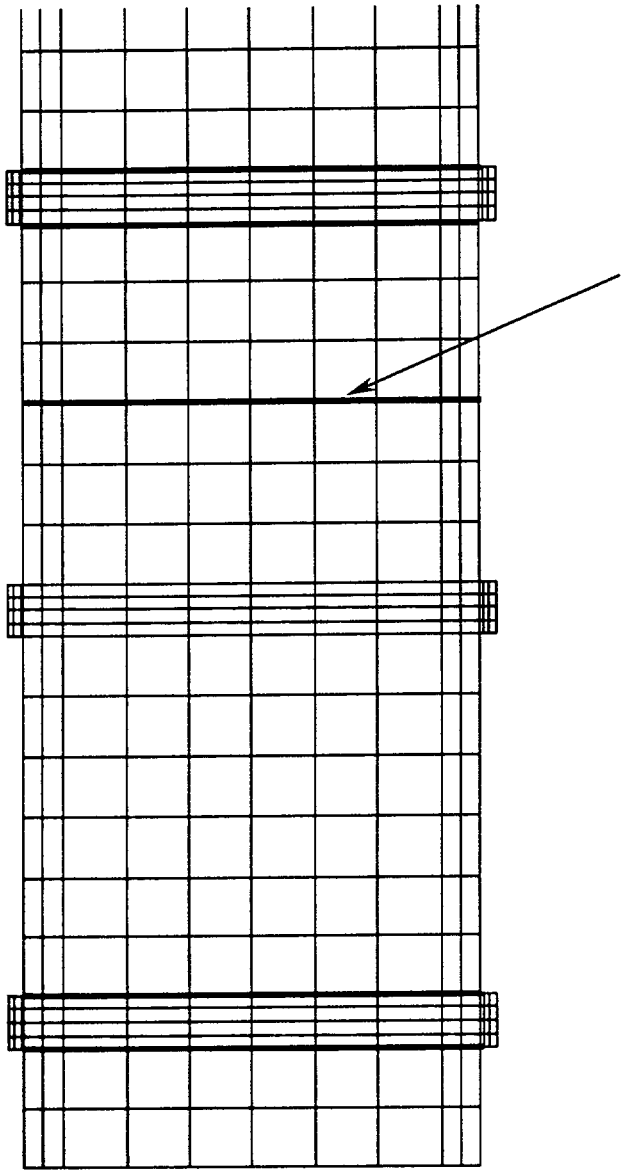

Notes:

Plate Cuts : Section cuts through the main body of the sheet are taken at the mid-span between tabs and at the top and bottom of the tabs. The elements that make up the tabs are not selected for the section cuts.

Figure 11.2.12.6.1-17 Section Cut Schematic - #2 – Typical Advanced PWR Neutron Absorber Sheet Details

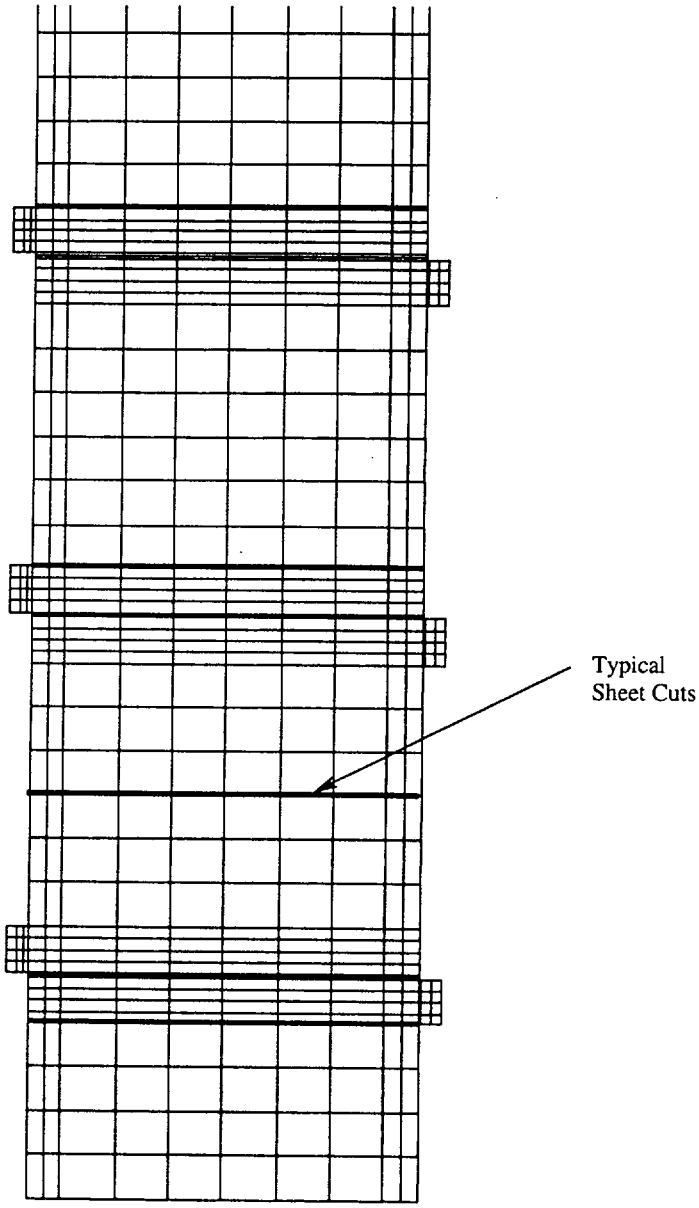

Notes:

Plate Cuts: Section cuts through the main body of the sheet are taken at the mid-span between tabs and at the top and bottom of the tabs. The elements that make up the tabs are not selected for the section cuts.

Figure 11.2.12.6.1-18 Advanced Canister in Impact Position with T-Shaped Channel Weldments

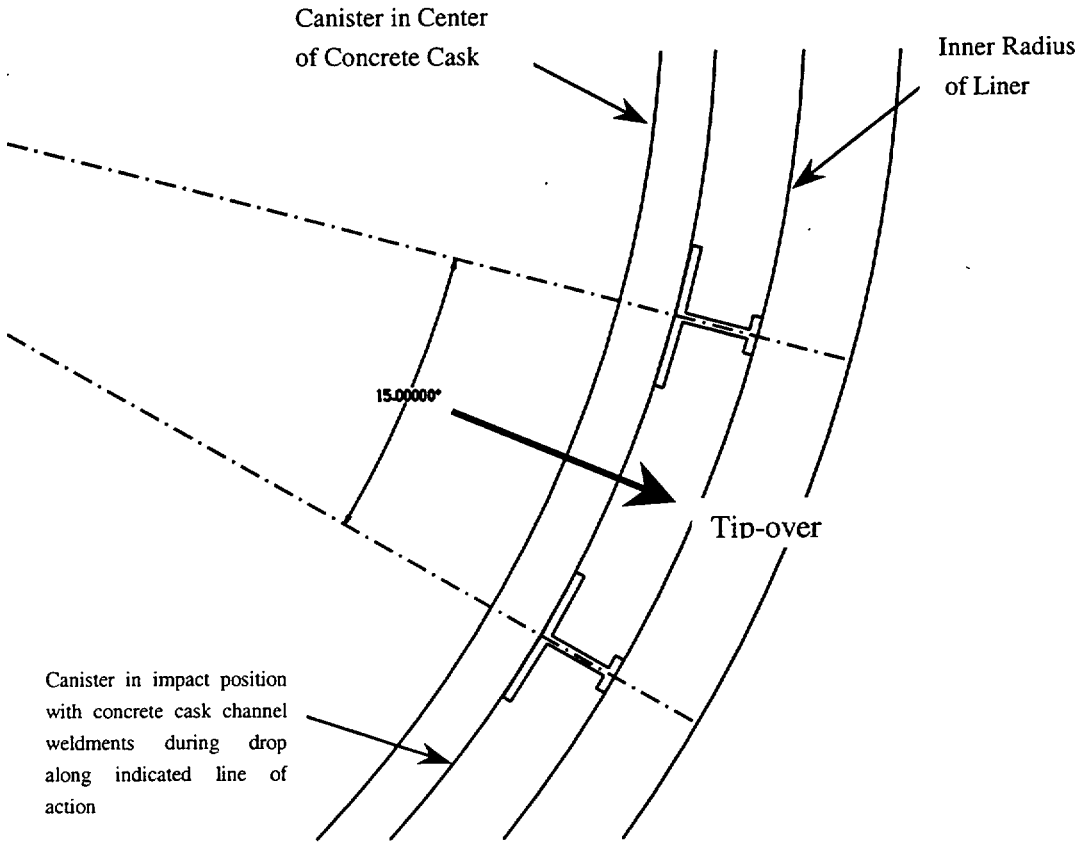

Table 11.2.12.6.1-1 Summary of Maximum Stresses for Advanced PWR Canister for Tip-over Conditions

Basket Angle[1]	Stress	Canister Shell		Shield Lid Weld		Structural Lid Weld[2]	
		$S_{int.}$, ksi	MS	$S_{int.}$, ksi	MS	$S_{int.}$, ksi	MS[1]
0°	P_m	21.75	0.82	18.42	1.15	22.97	0.38
	$P_m + P_b$	34.48	0.72	25.07	1.37	25.26	0.88
33°	P_m	29.77	0.33	17.02	1.32	23.39	0.35
	$P_m + P_b$	39.22	0.51	25.67	1.31	24.87	0.91
45°	P_m	26.34	0.50	15.41	1.57	23.83	0.33
	$P_m + P_b$	35.82	0.66	25.53	1.32	24.95	0.90
56°	P_m	31.68	0.25	16.23	1.44	23.25	0.36
	$P_m + P_b$	49.53	0.20	24.86	1.39	25.23	0.88
90°	P_m	22.83	0.73	18.38	1.15	23.04	0.37
	$P_m + P_b$	39.53	0.50	24.97	1.38	25.22	0.88

1. See Figure 11.2.12.6.1-8 for basket orientation angles for the tip-over condition.
2. A stress reduction factor of 0.8 is applied to the allowable stress.

Table 11.2.12.6.1-2 Canister Section Locations for Advanced PWR Canister Shell – 56° Basket Drop Orientation

Section	Node 1				Node 2			
	Node	R (in)	θ (deg)	Z (in)	Node	R (in)	θ (deg)	Z (in)
1	9747	32.905	33.000	23.564	9227	33.530	33.000	23.564
2	9748	32.905	33.000	25.921	9228	33.530	33.000	25.921
3	9016	32.905	42.000	32.990	8984	33.530	42.000	32.990
4	10318	32.905	42.000	33.690	10286	33.530	42.000	33.690
5	9746	32.905	33.000	21.208	9226	33.530	33.000	21.208
6	9017	32.905	45.000	32.990	8985	33.530	45.000	32.990
7	9711	32.905	42.000	30.634	9269	33.530	42.000	30.634
8	9698	32.905	45.000	30.634	9282	33.530	45.000	30.634
9	10317	32.905	39.000	33.690	10285	33.530	39.000	33.690
10	9015	32.905	39.000	32.990	8983	33.530	39.000	32.990
11	10319	32.905	45.000	33.690	10287	33.530	45.000	33.690
12	9018	32.905	48.000	32.990	8986	33.530	48.000	32.990
14	9685	32.905	48.000	30.634	9295	33.530	48.000	30.634
16	10320	32.905	48.000	33.690	10288	33.530	48.000	33.690
26	9019	32.905	51.000	32.990	8987	33.530	51.000	32.990
32	10321	32.905	51.000	33.690	10289	33.530	51.000	33.690

See Figure 11.2.12.6.1-1 for definition position.

Table 11.2.12.6.1-3 Advanced PWR Canister Shell Primary Membrane (P_m) Stress for Tip-Over – 56°, Basket Drop Orientation (ksi)

Section[1]	Sx	Sy	Sz	Sxy	Syz	Sxz	S_{int}	S_{allow}	MS
6	0.06	4.26	1.49	-0.12	15.78	0.05	31.68	39.54	0.25
11	0.00	3.89	1.41	0.09	15.77	0.01	31.63	39.54	0.25
16	0.07	4.39	2.00	0.08	15.70	-0.02	31.50	39.54	0.26
12	-0.16	4.32	1.68	0.35	15.67	0.02	31.46	39.54	0.26
3	-0.07	4.42	1.22	-0.32	15.51	-0.03	31.19	39.54	0.27
4	-0.01	3.66	0.85	-0.06	15.49	-0.05	31.12	39.54	0.27
8	-0.03	6.12	1.44	-0.08	15.32	0.13	30.99	39.54	0.28
14	0.06	5.81	1.26	-0.08	15.16	0.13	30.65	39.54	0.29
32	0.07	5.15	2.55	0.20	15.25	-0.04	30.61	39.54	0.29
26	-0.06	5.10	1.97	0.53	15.18	0.06	30.54	39.54	0.29

1. See Table 11.2.12.6.1-2 for section cut locations.
2. Stresses are presented in cylindrical coordinate system.

Table 11.2.12.6.1-4 Advanced PWR Canister Shell Primary Membrane + Primary Bending ($P_m + P_b$) Stress for Tip-Over – 56°, Basket Drop Orientation (ksi)

Section[1]	Sx	Sy	Sz	Sxy	Syz	Sxz	S_{int}	S_{allow}	MS
1	-1.32	46.00	24.06	0.08	7.32	-0.07	49.53	59.31	0.20
2	-1.25	44.29	22.82	-0.05	8.30	-0.10	48.37	59.31	0.23
3	-0.16	7.66	1.80	-0.35	22.01	-0.02	44.42	59.31	0.34
5	-0.75	41.76	19.38	-0.03	6.37	0.08	44.19	59.31	0.34
4	-0.05	6.71	2.23	-0.07	21.91	-0.06	44.05	59.31	0.35
6	-0.01	9.98	2.59	-0.18	21.45	0.07	43.54	59.31	0.36
7	-0.17	10.39	2.08	-0.41	21.28	0.13	43.37	59.31	0.37
8	-0.10	13.86	3.45	-0.09	20.96	0.13	43.19	59.31	0.37
9	-0.19	1.50	0.41	-0.12	21.51	-0.20	43.04	59.31	0.38
10	-0.03	2.06	-0.38	-0.77	21.38	-0.13	42.85	59.31	0.38

1. See Table 11.2.12.6.1-2 for section cut locations.
2. Stresses are presented in cylindrical coordinate system.

Table 11.2.12.6.1-5 Advanced PWR Canister Shell/Shield Lid and Structural Lid Weld, Maximum Stresses (ksi)

		Angle	Sx	Sy	Sz	Sxy	Syz	Sxz	S_{int}	S_{allow}	MS
Shield Lid	M	0°	-26.02	-17.65	-20.43	6.10	-0.58	-5.54	18.42	39.54	1.15
	M+B	33°	-44.26	-26.54	-33.54	-2.57	-0.44	-10.82	25.67	59.31	1.31
Structural Lid	M	45°	-32.75	-18.60	-8.98	-0.03	0.00	-0.76	23.83	31.63	0.33
	M+B	0°	-31.74	-16.40	-9.10	5.93	-1.45	-0.59	25.26	47.45	0.88

1. Stress results presented in cylindrical coordinate system.
2. A stress reduction factor of 0.8 is applied to the stress allowable for the structural lid weld.

Table 11.2.12.6.1-6 Summary of Maximum Stresses for Advanced PWR Basket for Tip-Over Conditions

Drop Orientation	P_m			$P_m + P_b$		
	Stress Intensity (ksi)	Allowable Stress (ksi)	Margin of Safety	Stress Intensity (ksi)	Allowable Stress (ksi)	Margin of Safety
0°	20.30	55.51	+1.73	40.85	77.80	+0.90
33°	33.87	55.51	+0.64	61.48	79.30	+0.29
45°	28.94	55.51	+0.92	56.85	79.30	+0.39
56°	33.14	55.51	+0.68	63.37	79.30	+0.25
90°	28.19	55.51	+0.97	40.95	77.80	+0.90

Note: See Figure 11.2.12.6.1-8 for Drop Orientation.

Table 11.2.12.6.1-7 Advanced PWR Basket Locations for Stress Evaluation - Section Cut Locations, Advanced PWR Basket Ligament Plates for Primary Membrane (P_m) Stresses for Tip-Over Condition

Section[1]	Coordinate System[2]	Node 1				Node 2			
		Node	X (in)	Y (in)	Z (in)	Node	X (in)	Y (in)	Z (in)
1	Cylindrical	6890	32.31	32.22	25.69	6887	32.75	32.22	25.69
2	Cylindrical	6944	32.31	55.67	25.69	6941	32.75	55.67	25.69
3	Cylindrical	32687	32.31	-55.67	25.69	32684	32.75	-55.67	25.69
4	Cylindrical	44622	32.31	-122.22	25.69	44620	32.75	-122.22	25.69
5	Cylindrical	6954	32.31	34.34	25.69	6952	32.75	34.34	25.69
6	Cylindrical	44684	32.31	-124.34	25.69	44681	32.75	-124.34	25.69
7	Cylindrical	7008	32.31	29.58	25.69	7007	32.75	29.58	25.69
8	Cylindrical	7940	32.31	8.19	32.99	7924	32.75	8.19	32.99
9	Cylindrical	32639	32.31	-32.22	25.69	32636	32.75	-32.22	25.69
10	Cylindrical	7936	32.31	13.65	32.99	7928	32.75	13.65	32.99
11	Cylindrical	4700	32.31	55.67	23.52	4697	32.75	55.67	23.52
12	Cartesian	2543	27.34	17.23	15.68	4673	27.34	17.23	23.52
13	Cylindrical	4979	32.31	32.22	16.50	4976	32.75	32.22	16.50
14	Cylindrical	42894	32.31	-122.22	23.52	42893	32.75	-122.22	23.52
15	Cylindrical	4728	32.31	29.58	23.52	4723	32.75	29.58	23.52
16	Cartesian	27971	27.34	-9.11	0.00	28048	27.34	-9.11	7.84
17	Cylindrical	86	32.31	32.22	0.00	83	32.75	32.22	0.00
18	Cartesian	1576	27.34	0.00	0.00	1662	27.34	0.00	7.84
19	Cylindrical	4729	32.31	26.94	23.52	4724	32.75	26.94	23.52
20	Cartesian	26535	27.34	-17.23	0.00	27264	27.34	-17.23	7.84
21	Cartesian	28048	27.34	-9.11	7.84	30007	27.34	-9.11	15.68
22	Cartesian	27264	27.34	-17.23	7.84	28740	27.34	-17.23	15.68
23	Cylindrical	4730	32.31	24.30	23.52	4725	32.75	24.30	23.52
24	Cartesian	1662	27.34	0.00	7.84	3858	27.34	0.00	15.68
25	Cylindrical	39309	32.31	-122.22	0.00	39308	32.75	-122.22	0.00
26	Cylindrical	5313	32.31	16.38	20.74	5292	32.75	16.38	20.74
27	Cartesian	28740	27.34	-17.23	15.68	30646	27.34	-17.23	23.52
28	Cylindrical	5505	32.31	19.02	20.74	5478	32.75	19.02	20.74
29	Cartesian	8600	16.71	18.23	25.71	8297	16.71	18.23	30.19
30	Cartesian	836	27.34	17.23	7.84	2543	27.34	17.23	15.68

1. See Figure 11.2.12.6.1-8 for coordinate system definition.
2. For a cylindrical coordinate system, x,y, are interpreted as the radial and angular coordinate for the nodes defining the cross-section.

Table 11.2.12.6.1-8 Advanced PWR Basket Locations for Stress Evaluation for Primary Membrane + Primary Bending Stress ($P_m + P_b$) for Tip-Over Condition

Section[1]	Coordinate System[2]	Node 1				Node 2			
		Node	X (in)	Y (in)	Z (in)	Node	X (in)	Y (in)	Z (in)
1	Cylindrical	6890	32.31	32.22	25.69	6887	32.75	32.22	25.69
2	Cartesian	27264	27.34	-17.23	7.84	28740	27.34	-17.23	15.68
3	Cartesian	26535	27.34	-17.23	0.00	27264	27.34	-17.23	7.84
4	Cartesian	2543	27.34	17.23	15.68	4673	27.34	17.23	23.52
5	Cylindrical	5313	32.31	16.38	20.74	5292	32.75	16.38	20.74
6	Cartesian	28740	27.34	-17.23	15.68	30646	27.34	-17.23	23.52
7	Cartesian	836	27.34	17.23	7.84	2543	27.34	17.23	15.68
8	Cartesian	86	27.34	17.23	0.00	836	27.34	17.23	7.84
9	Cylindrical	6944	32.31	55.67	25.69	6941	32.75	55.67	25.69
10	Cylindrical	5319	32.31	0.00	20.74	5295	32.75	0.00	20.74
11	Cylindrical	2606	32.31	16.38	14.86	2599	32.75	16.38	14.86
12	Cylindrical	44622	32.31	-122.22	25.69	44620	32.75	-122.22	25.69
13	Cylindrical	6954	32.31	34.34	25.69	6952	32.75	34.34	25.69
14	Cylindrical	6920	32.31	16.38	25.69	6913	32.75	16.38	25.69
15	Cartesian	2624	18.23	26.68	15.68	4700	18.23	26.68	23.52
16	Cylindrical	107	32.31	16.38	0.00	101	32.75	16.38	0.00
17	Cartesian	27312	18.23	-26.68	7.84	28812	18.23	-26.68	15.68
18	Cylindrical	2608	32.31	0.00	14.86	2600	32.75	0.00	14.86
19	Cartesian	26607	18.23	-26.68	0.00	27312	18.23	-26.68	7.84
20	Cartesian	42049	-9.11	-22.78	15.68	42994	-9.11	-22.78	23.52
21	Cylindrical	109	32.31	0.00	0.00	100	32.75	0.00	0.00
22	Cylindrical	8072	32.31	19.02	32.99	8054	32.75	19.02	32.99
23	Cylindrical	7008	32.31	29.58	25.69	7007	32.75	29.58	25.69
24	Cylindrical	43335	32.31	-106.38	20.74	43317	32.75	-106.38	20.74
25	Cylindrical	6876	32.31	57.78	25.69	6874	32.75	57.78	25.69
26	Cylindrical	5505	32.31	19.02	20.74	5478	32.75	19.02	20.74
27	Cylindrical	32687	32.31	-55.67	25.69	32684	32.75	-55.67	25.69
28	Cylindrical	19811	32.31	106.38	25.69	19805	32.75	106.38	25.69
29	Cartesian	32687	18.22	-26.68	25.69	33625	18.22	-26.68	32.99
30	Cylindrical	4730	32.31	24.30	23.52	4725	32.75	24.30	23.52

1. See Figure 11.2.12.6.1-8 for coordinate system definition.
2. For a cylindrical coordinate system, x,y, are interpreted as the radial and angular coordinate for the nodes defining the cross-section.

Table 11.2.12.6.1-9 Advanced UMS Basket Primary Membrane (P_m) Stresses for 56° Drop Orientation (ksi)

Component[1]	Section[2]	Coordinate System[3]	S_x	S_y	S_z	S_{xy}	S_{yz}	S_{xz}	S_{int}	S_{allow}	MS
Top Weldment Sidewall	1	Cylindrical	-2.45	7.06	-13.94	-1.65	1.76	-14.32	33.14	55.51	0.68
Top Weldment Sidewall	2	Cylindrical	0.35	3.36	0.43	13.75	-1.41	1.74	28.06	55.51	0.98
Top Weldment Sidewall	3	Cylindrical	-1.15	2.63	0.32	-9.84	0.02	-0.56	20.07	55.51	1.77
Top Weldment Sidewall	4	Cylindrical	-1.66	2.91	-9.50	-1.17	-1.44	-7.71	17.75	55.51	2.13
Top Weldment Sidewall	5	Cylindrical	-0.56	6.07	-2.27	1.26	0.11	-7.56	16.11	55.51	2.45
Top Weldment Sidewall	6	Cylindrical	0.25	2.81	-0.68	-5.98	-0.05	-3.09	13.88	55.51	3.00
Top Weldment Sidewall	7	Cylindrical	0.60	6.02	-0.75	1.53	1.93	4.59	12.56	55.51	3.42
Top Weldment Sidewall	8	Cylindrical	-0.06	-12.21	0.09	-0.19	0.00	0.08	12.33	55.51	3.50
Top Weldment Sidewall	9	Cylindrical	-0.32	4.32	-4.37	1.20	-0.55	-4.52	12.33	55.51	3.50
Top Weldment Sidewall	10	Cylindrical	0.25	-10.93	0.45	1.63	0.33	-0.72	12.32	55.51	3.51
Basket Sidewall	11	Cylindrical	-2.30	1.11	-8.60	2.66	0.03	-0.73	11.27	54.46	3.83
Basket Ligament Plates	12	Cartesian	-0.02	-6.09	-7.97	0.00	-2.86	0.00	10.02	54.46	4.44
Basket Sidewall	13	Cylindrical	-0.38	5.00	-3.97	1.89	0.71	-0.37	9.73	54.46	4.59
Basket Sidewall	14	Cylindrical	-1.04	2.34	-4.95	-1.65	-2.33	-1.46	9.67	54.46	4.63
Basket Sidewall	15	Cylindrical	0.00	4.44	-1.46	0.85	3.55	0.91	9.51	54.46	4.72
Basket Ligament Plates	16	Cartesian	-0.02	-8.95	-1.87	0.00	0.16	0.00	8.94	54.46	5.09
Basket Sidewall	17	Cylindrical	0.58	6.32	-1.31	2.52	-0.69	0.35	8.91	54.46	5.11
Basket Ligament Plates	18	Cartesian	-0.02	-8.71	-0.85	0.00	-0.17	0.00	8.70	54.46	5.26
Basket Sidewall	19	Cylindrical	-0.23	4.46	0.08	0.76	3.55	-0.08	8.50	54.46	5.40
Basket Ligament Plates	20	Cartesian	-0.02	-8.48	-4.65	0.00	0.23	0.00	8.47	54.46	5.43
Basket Ligament Plates	21	Cartesian	-0.02	-8.36	-1.40	0.00	0.62	0.00	8.40	54.46	5.48
Basket Ligament Plates	22	Cartesian	-0.02	-7.93	-4.67	0.00	1.22	0.00	8.32	54.46	5.55
Basket Sidewall	23	Cylindrical	-0.65	4.53	0.84	0.04	3.30	-0.90	8.20	54.46	5.64
Basket Ligament Plates	24	Cartesian	-0.02	-8.15	-0.42	0.00	-0.33	0.00	8.14	54.46	5.69
Basket Sidewall	25	Cylindrical	-0.28	3.98	-2.26	-2.64	0.73	0.65	8.15	54.46	5.69
Basket Sidewall	26	Cylindrical	-0.78	6.54	3.02	0.36	1.57	-0.40	8.01	54.46	5.80
Basket Ligament Plates	27	Cartesian	-0.02	-6.83	-4.54	0.00	2.03	0.00	8.00	54.46	5.81
Basket Sidewall	28	Cylindrical	0.31	6.87	3.02	-1.22	1.85	0.25	7.80	54.46	5.98
Top Weldment Ligament Plates	29	Cartesian	-7.49	0.00	0.06	0.00	0.00	-0.81	7.72	55.51	6.19
Basket Ligament Plates	30	Cartesian	-0.02	-6.56	-5.39	0.00	-1.46	0.00	7.53	54.46	6.23

1. Figure 11.2.12.6.1-4 contains the identification of the basket components.
2. Section locations are identified in Table 11.2.12.6.1-7.
3. Identifies whether the stresses are measured in an X,Y,Z Cartesian or R,θ,Z polar coordinate system.

Table 11.2.12.6.1-10 Advanced UMS Basket Primary Membrane plus Bending (P_m+P_b) Stresses for 56° Drop Orientation (ksi)

Component[1]	Section[2]	Coordinate System[3]	S_x	S_y	S_z	S_{xy}	S_{yz}	S_{xz}	S_{int}	S_{allow}	MS
Top Weldment Sidewall	1	Cylindrical	-4.97	8.61	-45.70	-4.89	-4.92	-17.99	63.37	79.30	0.25
Basket Ligament Plates	2	Cartesian	0.00	-44.15	-15.87	0.00	1.11	0.00	44.19	77.80	0.76
Basket Ligament Plates	3	Cartesian	0.00	-44.16	-15.65	0.00	0.15	0.00	44.16	77.80	0.76
Basket Ligament Plates	4	Cartesian	0.00	-43.68	-18.86	0.00	-3.45	0.00	44.15	77.80	0.76
Basket Sidewall	5	Cylindrical	-2.11	40.60	20.53	0.26	1.86	-0.38	42.90	77.80	0.81
Basket Ligament Plates	6	Cartesian	0.00	-42.53	-15.57	0.00	1.72	0.00	42.64	77.80	0.82
Basket Ligament Plates	7	Cartesian	0.00	-42.08	-16.24	0.00	-1.57	0.00	42.17	77.80	0.84
Basket Ligament Plates	8	Cartesian	0.00	-40.22	-14.69	0.00	-0.44	0.00	40.22	77.80	0.93
Top Weldment Sidewall	9	Cylindrical	3.51	17.63	10.06	14.96	-12.02	-0.86	40.50	79.30	0.96
Basket Sidewall	10	Cylindrical	-2.10	34.60	18.19	-0.11	0.32	-0.40	36.71	77.80	1.12
Basket Sidewall	11	Cylindrical	-1.97	33.59	12.35	0.25	0.08	0.07	35.56	77.80	1.19
Top Weldment Sidewall	12	Cylindrical	-3.83	0.93	-29.54	0.27	-0.82	-9.51	33.78	79.30	1.35
Top Weldment Sidewall	13	Cylindrical	-0.88	16.02	-9.31	3.33	3.64	-9.69	33.20	79.30	1.39
Top Weldment Sidewall	14	Cylindrical	-4.86	27.11	1.90	-0.86	3.65	1.92	33.11	79.30	1.40
Basket Ligament Plates	15	Cartesian	0.00	-32.01	-15.80	0.00	0.23	0.00	32.02	77.80	1.43
Basket Sidewall	16	Cylindrical	-1.69	30.08	12.16	0.20	0.04	-0.85	31.83	77.80	1.44
Basket Ligament Plates	17	Cartesian	0.00	-31.23	-11.17	0.00	-0.31	0.00	31.24	77.80	1.49
Basket Sidewall	18	Cylindrical	-2.14	29.05	11.28	-0.10	0.53	0.09	31.21	77.80	1.49
Basket Ligament Plates	19	Cartesian	0.00	-31.06	-11.32	0.00	-0.08	0.00	31.06	77.80	1.50
Basket Ligament Plates	20	Cartesian	-0.04	-30.68	-7.91	0.00	0.51	0.00	30.65	77.80	1.54
Basket Sidewall	21	Cylindrical	-2.86	25.88	10.98	-0.13	-0.01	-0.79	28.78	77.80	1.70
Top Weldment Sidewall	22	Cylindrical	1.64	-26.78	-0.84	-1.51	-2.47	-1.14	29.19	79.30	1.72
Top Weldment Sidewall	23	Cylindrical	2.79	16.55	-8.29	2.79	-3.76	6.02	29.05	79.30	1.73
Basket Sidewall	24	Cylindrical	-1.18	26.62	14.73	0.18	-1.39	-0.26	27.97	77.80	1.78
Top Weldment Sidewall	25	Cylindrical	-0.39	9.22	-14.37	2.70	5.96	-5.28	28.55	79.30	1.78
Basket Sidewall	26	Cylindrical	-0.27	27.06	14.67	-0.90	2.16	0.25	27.76	77.80	1.80
Top Weldment Sidewall	27	Cylindrical	1.00	17.33	9.10	-10.94	2.89	-1.15	27.97	79.30	1.84
Top Weldment Sidewall	28	Cylindrical	-2.38	25.03	16.04	-1.39	-0.38	-2.37	27.86	79.30	1.85
Top Weldment Ligament Plates	29	Cartesian	0.00	-19.30	-5.50	0.00	-11.94	0.00	27.59	79.30	1.87
Basket Sidewall	30	Cylindrical	-0.76	24.38	7.27	-0.17	3.50	-0.82	25.92	77.80	2.00

1. Figure 11.2.12.6.1-4 contains the identification of the basket components.
2. Section locations are identified in Table 11.2.12.6.1-8.
3. Identifies whether the stresses are measured in an X,Y,Z Cartesian or R,θ,Z cylindrical coordinate system.

Table 11.2.12.6.1-11 Case #1: Plate Membrane plus Bending Stress Summary for Tip-over Conditions – Advanced (ksi)

792-600 Plate Id[1]	S_x	S_y	S_z	S_{xy}	S_{yz}	S_{xz}	S_{int}	S_{allow}	MS
1	-5.12	3.53	0.00	0.00	0.00	0.00	8.66	11.1	0.28
2	-4.87	0.51	0.00	0.00	0.00	0.00	5.37	11.1	1.07
3	-4.95	2.46	0.00	0.00	0.00	0.00	7.41	11.1	0.50
4	-5.39	5.46	0.00	0.00	0.00	0.00	10.85	11.1	0.02
5	-4.86	0.46	0.00	0.00	0.00	0.00	5.32	11.1	1.09
6	-5.36	5.40	0.00	0.00	0.00	0.00	10.76	11.1	0.03
7	-4.60	0.35	0.00	0.32	0.00	0.00	4.99	11.1	1.22
8	-4.38	1.74	0.00	0.92	0.00	0.00	6.39	11.1	0.74
9	-4.53	0.48	0.00	0.19	0.00	0.00	5.02	11.1	1.21

1. Plate Id corresponds to the Item Number on Drawing 792-600.

Table 11.2.12.6.1-12 Case #2: Plate Membrane plus Bending Stress Summary for Tip-over Conditions – Advanced (ksi)

792-600 Plate Id[1]	S_x	S_y	S_z	S_{xy}	S_{yz}	S_{xz}	S_{int}	S_{allow}	MS
1	-5.12	3.53	0.00	0.00	0.00	0.00	8.66	11.1	0.28
2	-1.91	0.49	0.00	0.00	0.00	0.00	2.40	11.1	3.63
3	-5.23	0.97	0.00	0.00	0.00	0.00	6.20	11.1	0.79
4	-4.81	5.52	0.00	0.00	0.00	0.00	10.33	11.1	0.07
5	-2.06	0.31	0.00	0.00	0.00	0.00	2.38	11.1	3.66
6	-4.54	2.12	0.00	0.00	0.00	0.00	6.67	11.1	0.66
7	-4.60	0.35	0.00	0.32	0.00	0.00	4.99	11.1	1.22
8	-1.78	0.16	0.00	0.31	0.00	0.00	2.03	11.1	4.46
9	-4.53	0.48	0.00	0.19	0.00	0.00	5.02	11.1	1.21

1. Plate Id corresponds to the Item Number on Drawing 792-600.

Table 11.2.12.6.1-13 Case #3: Plate Membrane plus Bending Stress Summary for Tip-over Conditions – Advanced (ksi)

792-600 Plate Id[1]	S_x	S_y	S_z	S_{xy}	S_{yz}	S_{xz}	S_{int}	S_{allow}	MS
1	-5.12	3.53	0.00	0.00	0.00	0.00	8.66	11.1	0.28
2	-4.87	0.51	0.00	0.00	0.00	0.00	5.37	11.1	1.07
3	-4.95	2.46	0.00	0.00	0.00	0.00	7.41	11.1	0.50
4	-5.39	5.46	0.00	0.00	0.00	0.00	10.85	11.1	0.02
5	-4.87	0.51	0.00	0.00	0.00	0.00	5.37	11.1	1.07
6	-5.36	5.40	0.00	0.00	0.00	0.00	10.76	11.1	0.03
7	-4.60	0.35	0.00	0.32	0.00	0.00	4.99	11.1	1.22
8	-4.38	1.74	0.00	0.92	0.00	0.00	6.39	11.1	0.74
9	-4.53	0.48	0.00	0.19	0.00	0.00	5.02	11.1	1.21

1. Plate Id corresponds to the Item Number on Drawing 792-600.

11.2.12.7 Validation of the LS-DYNA Program

The LS-DYNA program is used in the evaluation of the response of the concrete cask in the tip-over event to determ ine the maximum acceleration to be used in the structural evaluation of the loaded canister and basket. The methodology to determine the concrete cask response follows the methodology contained in NUREG/CR-6608, "Summary and Evaluation of Low-Velocity Impact Tests of Solid Steel Billet Onto Concrete Pads" [38].

Tip-over tests of a steel billet onto a concrete pad were conducted and reported in NUREG/CR-6608. The purpose of the tests was to provide data, against which, analysis methodology could be validated. Using the geometry described in the benchmark along with the modeling methodology, these analyses were re-performed using the LS-DYNA program to validate the LS-DYNA results.

Using the filter frequency reported in the NUREG/CR-6608 benchmark, LS-DYNA program was validated as shown by the following results:

Nodes / Gauge Location	Maximum Experiment (g)	NAC Analysis (g)
16115 / A1	237.5	237.1
17265 / A5	231.5	229.4

11.2.12.8 Corrective Actions

The most important recovery action required following a concrete cask tip-over is the uprighting of the cask to minimize the dose rate from the exposed bottom end. The uprighting operation will require a heavy lift capability and rigging expertise. The concrete cask must be returned to the vertical position by rotation around a convenient bottom edge, and by using a method and rigging that controls the rotation to the vertical position.

Surface and top and bottom edges of the concrete cask are expected to exhibit cracking and possibly loss of concrete down to the layer of reinforcing bar. If only minor damage occurs, the concrete may be repairable by using grout. Otherwise, it may be necessary to remove the canister for installation in a new concrete cask. If the canister remains in the cask, it should be returned to its centered storage position within the cask.

The storage pad must be repaired to preclude the intrusion of water that could cause further deterioration of the pad in freeze-thaw cycles.

11.2.12.9 Radiological Impact

There is an adverse radiological consequence in the hypothetical tip-over of either the Standard or Advanced concrete casks, since the bottom ends of the concrete cask and the canister have significantly less shielding than the sides and tops of these same components. The dose rate at 1 meter is calculated, using a 1–D analysis, to be approximately 34 rem/hour, and the dose at 4 meters is estimated to be approximately 4 rem/hour. Consequently, following a tip-over event, supplemental shielding should be used until the concrete cask can be uprighted. Stringent access controls must be applied to ensure that personnel do not enter the area of radiation shine from the exposed bottom of the tipped-over concrete cask. The tip-over event is hypothetical since, as shown in Section 11.2.12, there are no design basis events that result in cask tip-over.

Damage to the edges or surface of the concrete cask may occur following a tip-over, which could result in marginally higher dose rates at the bottom edge or at surface cracks in the concrete. This increased dose rate is not expected to be significant, and would be dependent on the specific damage incurred.

11.2.13 Full Blockage of Vertical Concrete Cask Air Inlets and Outlets

This section evaluates the Standard and Advanced Vertical Concrete Casks for the steady state effects of full blockage of the air inlets and outlets at the normal ambient temperature (76°F). It estimates the duration of the event that results in the fuel cladding, the fuel basket and the concrete reaching their design basis limiting temperatures (See Table 4.1-3 for the allowable temperatures for short term conditions).

The evaluation demonstrates that there are no adverse consequences due to this accident, provided that debris is cleared within 24 hours.

11.2.13.1 Cause of Full Blockage

The likely cause of complete cask air inlet and outlet blockage is the covering of the cask with earth in a catastrophic event that is significantly greater than the design basis earthquake or a landslide. This event is a bounding condition accident and is not credible.

11.2.13.2 Detection of Full Blockage

Blockage of the cask air inlets and outlets will be visually detected during the general site inspection following an earthquake, landslide, or other event with a potential for such blockage.

11.2.13.3 Analysis of Full Blockage

The accident temperature conditions are evaluated using the thermal models described in Section 4.4.1.1.1 for the Standard configuration and in Section 4.4.1.2.1 for the Advanced configuration. The analysis for both configurations assumes initial normal storage conditions, with the sudden loss of convective cooling of the canister. The loss of convective cooling results in the fairly rapid and sustained heat-up of the canister and the concrete cask.

11.2.13.3.1 Analysis of the Standard Concrete Cask with Full Blockage

With the loss of convective cooling, heat is rejected from the Standard canister to the Standard concrete cask liner by radiation and conduction. To account for the loss of convective cooling in the ANSYS air flow model (Section 4.4.1.1.1), the elements in the model are replaced with thermal conduction elements. This model is used to evaluate the thermal transient resulting from the

postulated boundary conditions. The analysis indicates that the maximum basket temperature (support disk and heat transfer disk) remain less than the allowable temperature for 24 hours after the initiation of the event. The maximum fuel cladding temperature and the maximum concrete bulk temperature remain less than the allowable temperatures for about 6 days (150 hours) after the initiation of the event. The heat up of the fuel cladding, canister shell and concrete (bulk temperature) are shown in Figures 11.2.13-1 and 11.2.13-2, for the Standard PWR and BWR configurations, respectively.

11.2.13.3.2 Analysis of the Advanced Concrete Cask with Full Blockage

Similar to the Standard configuration analysis, with the loss of convective cooling, heat is rejected from the Advanced canister to the Advanced concrete cask liner by radiation and conduction. The Advanced configuration full blockage condition is evaluated using the thermal model described in Section 4.4.1.2.1. Zero heat flux boundary condition (adiabatic condition) is applied to all external surfaces of the computational fluid dynamics model, including the air inlet and outlet. The velocity field is set to zero, and only heat transfer by conduction and radiation is solved. The analysis indicates that the maximum temperature of the fuel cladding, the basket and the concrete remains less than the allowable temperature for 24 hours after the initiation of the event. The heat up of canister shell and concrete (bulk temperature) are shown in Figures 11.2.13-3 and 11.2.13-4, for the Advanced PWR configuration.

11.2.13.4 Corrective Actions

The obstruction blocking the are inlets must be manually removed. The nature of the obstruction may indicate that other actions are required to prevent recurrence of the blockage.

11.2.13.5 Radiological Impact

There are no significant radiological consequences for this event, as the Vertical Concrete Cask retains its shielding performance. Dose is incurred as a consequence of uncovering the concrete cask and vent system. Since the dose rates at the air inlets and outlets are higher than the nominal rate (35 mrem/hr) at the cask wall, personnel will be subject to an estimated maximum dose rate of <50 mrem/hr when clearing the inlets and 300 mrem/hr when clearing the outlets of the Advanced concrete cask. The dose rate for the Standard concrete cask is less. If it is assumed that a worker kneeling with his hands on the inlets or outlets requires 15 minutes to clear each inlet or outlet, the estimated extremity dose is 400 mrem for the 8 openings. The whole body dose will be slightly less. In addition, some dose is incurred clearing debris away from the cask body. This dose is estimated at 50 mrem, assuming 2 hours is spent near the cask exterior surface.

Figure 11.2.13-1 Standard PWR Configuration Temperature History—All Vents Blocked

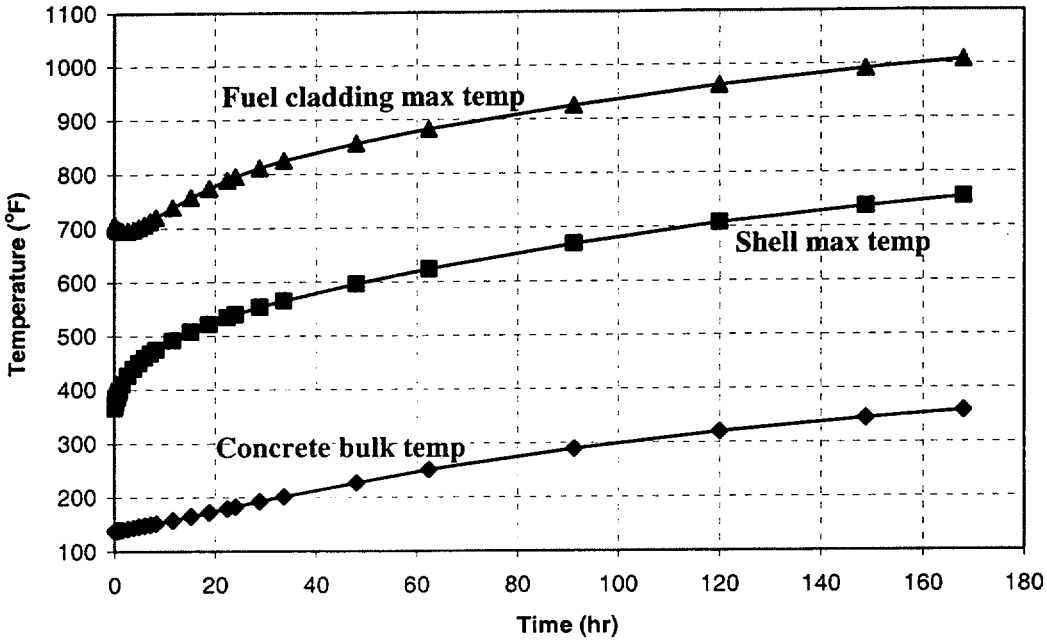

Figure 11.2.13-2 Standard BWR Configuration Temperature History—All Vents Blocked

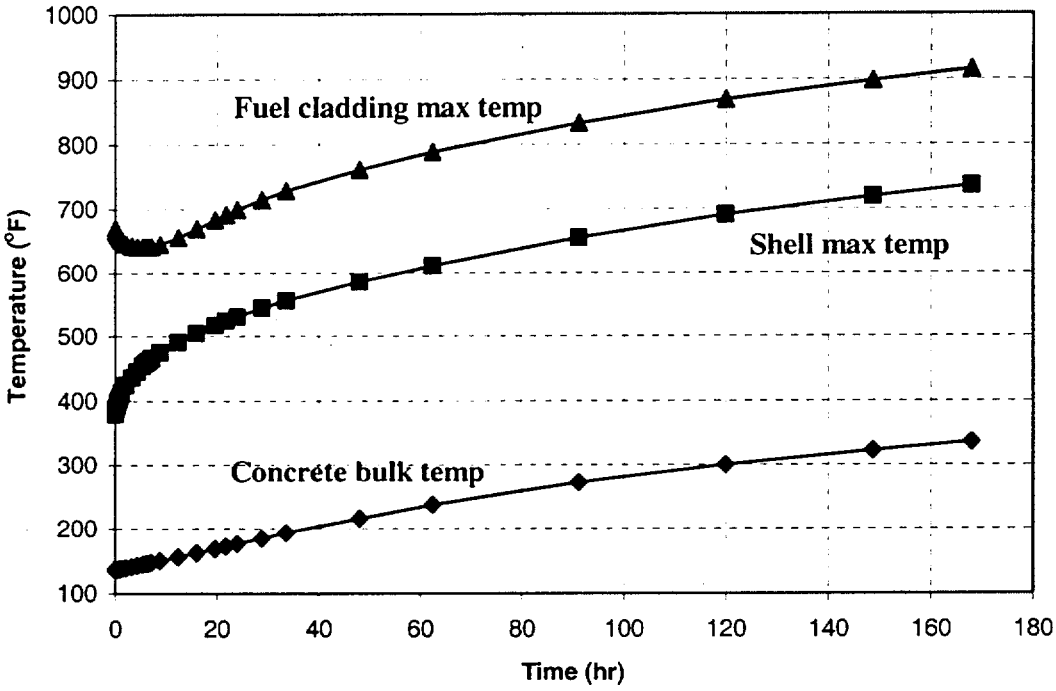

Figure 11.2.13-3 Advanced Configuration Bulk (Volume Average) Concrete Temperature History — Adiabatic Boundary Conditions on all External Surfaces and No Air Flow

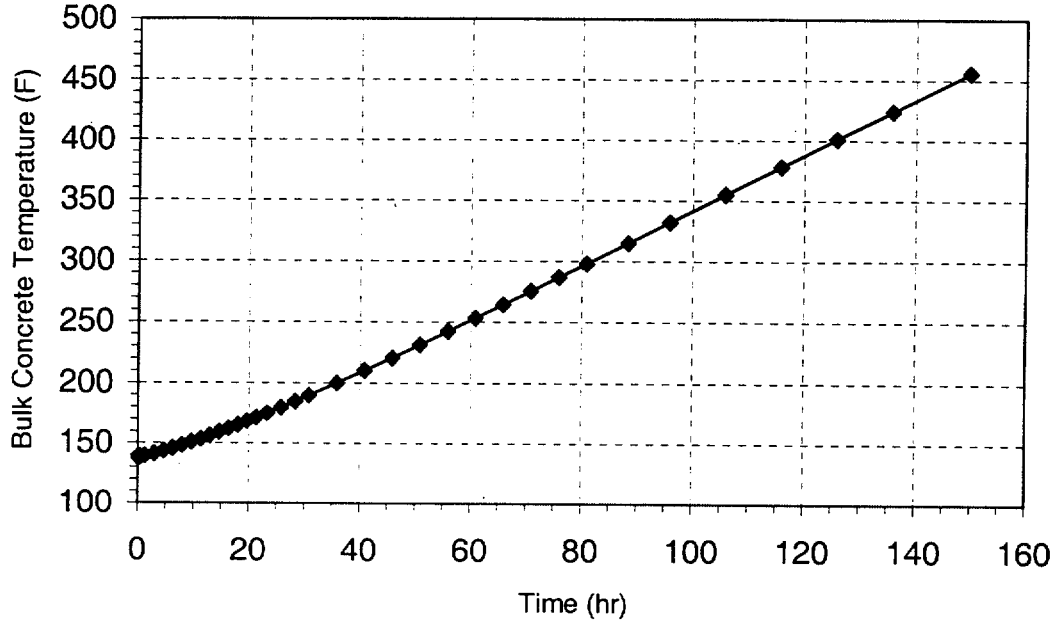

Figure 11.2.13-4 Advanced Configuration Maximum Shell Temperature History — Adiabatic Boundary Conditions on all External Surfaces and No Air Flow

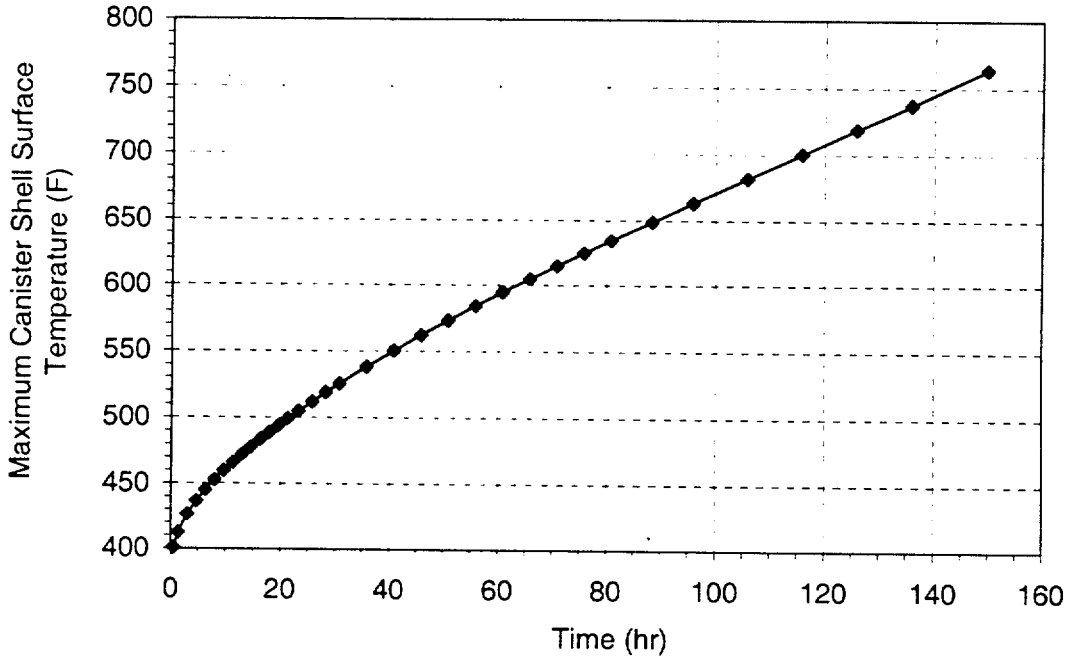

11.2.14 Canister Closure Weld Evaluation

The closure weld for the Standard and Advanced canister configurations is a groove weld with a thickness of 0.9 inches. The evaluation of this weld, in accordance with NRC guidance, is to incorporate a 0.8 stress reduction factor. Applying a factor of 0.8 to the weld stress allowable incorporates the stress reduction factor.

The closure weld for the canister is comprised of multiple weld passes using a compatible weld material for Type 304L stainless steel. An allowable (critical) flaw evaluation has been performed to determine the critical flaw size in the weld region. The result of the flaw evaluation is used to define the minimum flaw size, which must be identifiable in the nondestructive examination of the weld. Due to the inherent toughness associated with Type 304L stainless steel, a limit load analysis is used in conjunction with a J-integral/tearing modulus approach. The safety margins used in this evaluation correspond to the stress limits contained in Section XI of the ASME Code.

One of the stress components used in the evaluation for the critical flaw size is the radial stress component in the weld region of the structural lid. For an accident (Level D) event, in accordance with ASME Code Section XI, a safety factor of $\sqrt{2}$ is required.

11.2.14.1 Closure Weld Evaluation for the Standard Canister

The stresses for the canister are evaluated using sectional stresses as permitted by Subsection NB of the ASME Code. Canister stresses resulting from the concrete cask tip-over accident (Section 11.2.12) are used for evaluation. The location of the section for the canister weld evaluation is shown in Figure 11.2.12.4.1-6 and corresponds to Section 11. The governing P_m and $P_m + P_b$ stress intensities for Section 11 and the associated allowables are listed in Tables 11.2.12.4.1-1 and Table 11.2.12.4.1-2, respectively. The factored allowables, incorporating a 0.8 stress reduction factor, and the resulting controlling Margins of Safety are:

Stress Category	Analysis Stress (ksi)	0.8 × Allowable Stress (ksi)	Margin of Safety
P_m	22.81	32.06	0.41
$P_m + P_b$	25.03	48.09	0.92

This confirms that the canister closure weld is acceptable for accident conditions.

For the purpose of identifying the stress for the flaw evaluation, the weld region corresponds to Section 11 in Figure 11.2.12.4.1-6 is considered.

The maximum tensile radial stress at Section 11 is 6.9 ksi, based on the analysis results of the tip-over accident (Section 11.2.12.4). To perform the flaw evaluation, a 10 ksi stress is conservatively used, resulting in a significantly larger safety factor than the required safety factor of $\sqrt{2}$. Using 10 ksi as the basis for the evaluation, the minimum detectable flaw size is 0.52 inch for a flaw that extends 360 degrees around the circumference of the canister. Stress components for the circumferential and axial directions are also reported in the concrete cask tip-over analysis, which would be associated with flaws oriented in the radial or horizontal directions respectively. The maximum stress for these components is 2.5 ksi, which is also enveloped by the value of 10 ksi used in the critical flaw evaluation for stresses in the radial direction. The 360-degree flaw employed for the circumferential direction is considered to be bounding with respect to any partial flaw in the weld, which could occur in the radial and horizontal directions. Therefore, using a minimum detectable flaw size of 0.375 inch is acceptable, since it is less than the very conservatively determined 0.52-inch critical flaw size.

11.2.14.2 Closure Weld Evaluation for the Advanced Canister

The stresses for the canister are evaluated using sectional stresses as permitted by Subsection NB of the ASME Code. Canister stresses resulting from the concrete cask tip-over accident (Section 11.2.12) are used for evaluation. The governing P_m and $P_m + P_b$ stress intensities for and the associated allowables are listed in Table 11.2.12.6.1-5. The factored allowables, incorporating a 0.8 stress reduction factor, and the resulting controlling Margins of Safety are:

Stress Category	Analysis Stress (ksi)	0.8 × Allowable Stress (ksi)	Margin of Safety
P_m	23.83	31.63	0.33
$P_m + P_b$	25.26	47.45	0.88

This confirms that the canister closure weld is acceptable for accident conditions.

The maximum tensile radial stress is 5.54 ksi, based on the analysis results of the tip-over accident for the 56° orientation (Section 11.2.12.6). To perform the flaw evaluation, a 10 ksi stress is conservatively used, resulting in a significantly larger safety factor than the required safety factor of

$\sqrt{2}$. Using 10 ksi as the basis for the evaluation, the minimum detectable flaw size is 0.52 inch for a flaw that extends 360 degrees around the circumference of the canister. Stress components for the circumferential and axial directions are also reported in Section 11.2.12.6, which would be associated with flaws oriented in the radial or horizontal directions respectively. The maximum stress for these components is 5.59 ksi, which is also enveloped by the value of 10 ksi used in the critical flaw evaluation for stresses in the radial direction. The 360-degree flaw employed for the circumferential direction is considered to be bounding with respect to any partial flaw in the weld, which could occur in the radial and horizontal directions. Therefore, using a minimum detectable flaw size of 0.375 inch is acceptable, since it is less than the very conservatively determined 0.52-inch critical flaw size.

THIS PAGE INTENTIONALLY LEFT BLANK

11.2.15 Accident and Natural Phenomena Events Evaluation for Site Specific Spent Fuel

This section presents the accident and natural phenomena events evaluation of spent fuel assemblies or configurations, which are unique to specific reactor sites. These site specific fuel configurations result from conditions that occurred during reactor operations, participation in research and development programs, and from testing programs intended to improve reactor operations. Site specific fuel includes fuel assemblies that are uniquely designed to accommodate reactor physics, such as axial fuel blankets and variable enrichment assemblies, fuel with burnup that exceeds the design basis, and fuel that is classified as damaged. Damaged fuel includes fuel rods with cladding that exhibits defects greater than pinhole leaks or hairline cracks.

Site specific fuel assembly configurations are either shown to be bounded by the analysis of the standard design basis fuel assembly of the same type (PWR or BWR), or are shown to be acceptable contents, by specific evaluation of the configuration.

Specific reactor sites may use either the Standard or Advanced configurations of the Universal Storage System.

11.2.15.1 Accident and Natural Phenomena Events Evaluation for Maine Yankee Site Specific Fuel

Maine Yankee site specific fuels are described in Section 1.3.2.1 and are only loaded in the Standard configuration of the Universal Storage System. A thermal evaluation has been performed for Maine Yankee site specific fuels that exceed the design basis burnup, as shown in Section 4.5.1.2. As shown in that section, loading of fuel with a burnup between 45,000 and 50,000 MWD/MTU is subject to preferential loading in designated basket positions in the Transportable Storage Canister, and certain high burnup fuel may require loading in the Maine Yankee fuel can.

With preferential loading, the design basis total heat load of the canister is not changed. Consequently, the thermal performance for the Maine Yankee site specific fuels is bounded by the design basis PWR fuels. Therefore, no further evaluation is required for the thermal accident events, as presented in Sections 11.2.6, 11.2.7, and 11.2.13.

As shown in Section 3.6.1.1, the total weight of the contents of the Standard Transportable Storage Canister for Maine Yankee fuels is bounded by the total weight for the PWR design basis fuels. However, some design parameters for the Maine Yankee site ISFSI pad are different from those for

the design basis ISFSI pad. Therefore, the hypothetical accident (non-mechanistic) tip-over event is evaluated to ensure that the maximum tip-over g-load remains below the bounding g-load (40g) used in the evaluation of the PWR canister and basket in Section 11.2.12.4. The evaluation of the Standard Vertical Concrete Cask tip-over event on the Maine Yankee site ISFSI pad is presented in Section 11.2.15.1.1. The methodology used is similar to that used in Section 11.2.12.3.1.

Although the total weight, and the maximum g-load, for the Maine Yankee fuel is bounded by the PWR design basis fuels, the maximum weight of the consolidated fuel lattices (2,100 lbs) is larger than that of a single PWR Class 1 design basis fuel assembly (1,567 lbs). This additional weight need only be considered in the support disk evaluation for a side impact condition, similar to the analysis presented in Section 11.2.12.4.1. A parametric study is presented in Section 11.2.15.1.2 to demonstrate that the maximum stress in the support disk due to the consolidated fuel lattice remains bounded by the maximum stress for the support disk for the PWR design basis fuels for a side impact condition.

Section 11.2.15.1.3 provides the structural evaluation for the Maine Yankee fuel can for the 24-inch drop (Section 11.2.4) and the tip-over (Section 11.2.12) accident events.

A Maine Yankee site earthquake evaluation is presented in Section 11.2.15.1.4 to demonstrate the stability of the Standard Vertical Concrete Cask on the Maine Yankee site ISFSI pad.

11.2.15.1.1 Maine Yankee Vertical Concrete Cask Tip-Over Analysis

This section evaluates the maximum acceleration of the Transportable Storage Canister and basket during the Vertical Concrete Cask tip-over event on the Maine Yankee site ISFSI pad. This evaluation applies the methodology of Section 11.2.12 for the design basis cask tip-over evaluation.

A finite element model is generated using the LS-DYNA program to determine the acceleration of the vertical concrete cask during the tip-over event.

The concrete pad in the model corresponds to a pad 31-feet by 31-feet square and 3-feet thick, supporting one concrete cask in the center of the pad. The soil under the concrete pad is considered to be 40-feet by 40-feet square and made up of two layers: a 4.5-foot thick upper layer and a 10-foot thick lower layer. Only one-half of the concrete cask, pad and soil configuration is modeled due to symmetry. Both the Class 1 and Class 2 Standard configurations are evaluated.

The model includes a half section of the concrete cask, the concrete ISFSI pad and soil subgrade, as shown:

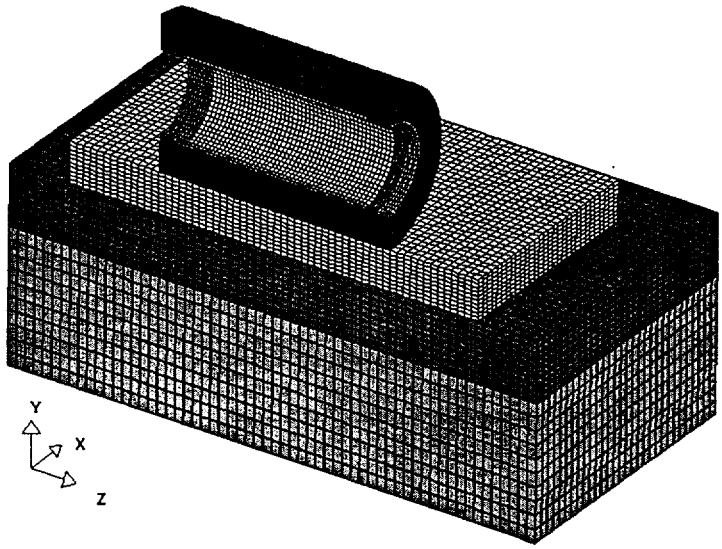

Concrete Pad Properties

Vertical concrete cask tip-over analyses are performed for ISFSI pad concrete compressive strengths of 3,000 and 4,000 psi. The Poisson's Ratio (ν_c) is 0.22. The concrete dry density is considered to be between 135 pcf and 145 pcf. To account for the weight of reinforcing bar in the pad, three values of Density (ρ) are used in the model:

ρ (lbs/ft^3)	E_c (psi)	K_c (psi)
140	2.994×10^6	1.782×10^6
145	3.156×10^6	1.879×10^6
152	3.387×10^6	2.016×10^6

The corresponding values of Modulus of Elasticity (E_c) and Bulk Modulus (K_c) are also provided, where:

$$\text{Modulus of Elasticity } (E_c) = 33\rho_c^{1.5}\sqrt{f_c'} \quad \text{(ACI 318-95)}$$

$$\text{Bulk Modulus } (K_c) = \frac{E_c}{3(1-2\nu_c)} \quad \text{(Blevins [19])}$$

Soil Properties

The soil properties used in the model are based on three soil sets. The vertical concrete cask tip-over analyses are performed for three different combinations of soil densities: (1) 4.5-foot thick upper layer density of 135 pcf (Modulus of Elasticity, E = 162,070 psi), with a 10-foot thick lower layer density of 127 pcf (E = 31,900 psi); (2) 4.5-foot thick upper layer density of 130 pcf, with a 10-foot thick lower layer density of 127 pcf; and (3) 15-foot depth with density of 145 pcf ($E \leq$ 60,000 psi). The Poisson's Ratio (ν_s) of the soil is 0.45.

Summary of Design Basis ISFSI Pad Parameters

The ISFSI pads and foundation shall include the following characteristics as applicable to the end drop and tip-over analyses:

Concrete thickness	36 inches maximum
Pad subsoil thickness	15 feet minimum
Specified concrete compressive strength	$\leq$ 4,000 psi at 28 days
Soil in place density (ρ)	$\rho \leq 145$ lbs/ft^3 (upper layer)
Concrete dry density (ρ)	$135 \leq \rho \leq 145$ lbs/ft^3
Soil Modulus of Elasticity	$\leq$ 60,000 psi

The concrete pad maximum thickness excludes the ISFSI pad footer. The compressive strength of the concrete is determined in accordance with Section 5.6 of ACI-318 with concrete acceptance in accordance with the same section. Steel reinforcement is used in the pad and footer. The soil modulus of elasticity is determined according to the test method described in ASTM D4719.

Vertical Concrete Cask Properties

The material properties used in the model for the Vertical Concrete Cask are the same as the properties used in the PWR models in Section 11.2.12.3. The tip-over impact is simulated by applying an initial angular velocity of 1.485 rad/sec (PWR Class 1) and 1.483 rad/sec (PWR Class 2), respectively, to the entire cask. The angular velocity values are determined by the method used in Section 11.2.12 based on the weight of the loaded concrete cask with Maine Yankee fuel (285,513 pounds and 297,509 pounds for PWR Class 1 and PWR Class 2, respectively).

A cut-off frequency of 210 Hz (PWR Class 1) and 190 Hz (PWR Class 2) is applied to filter the analysis results from the LS-DYNA models and determine the peak accelerations. The resulting calculated accelerations on the canister at the location of the top support disk and of the top of the structural lid are tabulated for all of the analysis cases that were run. The maximum accelerations at the two key locations on the canister for the PWR Class 1 and Class 2 configurations are:

Component Location	Position Measured from the Bottom of the Concrete Cask (inches)		Acceleration (g)	
	Class 1	Class 2	Class 1	Class 2
Top Support Disk	176.7	185.2	32.3	34.2
Top of the Canister Structural Lid	197.9	207.0	35.3	37.6

The impact accelerations for the vertical concrete cask tip-over on the Maine Yankee ISFSI pad site are observed to be slightly higher than those reported in Section 11.2.12.3.1 for the design-basis ISFSI pad. Therefore, peak accelerations are calculated for the top support disk and are evaluated with respect to the analysis presented in Section 11.2.12.4.1.

To determine the effect of the rapid application of the inertia loading for the support disk, a dynamic load factor (DLF) is computed using the method presented in Section 11.2.12.4. The DLF is computed to be 1.07 and 1.02 for PWR Class 1 and Class 2, respectively. Applying the DLFs to the 32.3g and 35.4g results in peak accelerations of 34.6g and 36.1g for the top support disk PWR Class 1 and Class 2, respectively. The DLFs for the canister lids are considered to be unity since the lids have significant in-plane stiffness and are considered to be rigid. Additional sensitivity evaluations considering varying values of the ISFSI concrete pad density have been performed. The results of those evaluations demonstrate that the maximum acceleration for the canister and basket are below 40g. Therefore, the maximum acceleration for the canister and basket for the cask tipover accident on the Maine Yankee site ISFSI pad is bounded by the 40g used in Section 11.2.12.4.1 (analysis of canister and basket for PWR configurations for tip-over event).

11.2.15.1.2 Parametric Study of Support Disk Evaluation for Maine Yankee Consolidated Fuel

A parametric study is performed to show that the PWR basket loaded with a Maine Yankee consolidated fuel lattice is bounded by the PWR basket design basis loading for a side impact condition. Only one consolidated fuel lattice, in a Maine Yankee Fuel Can, will be loaded in any single Transportable Storage Canister. However, Maine Yankee Fuel Cans holding other intact or damaged fuel can be loaded in the other three corner positions of the basket. (Maine Yankee Fuel

Cans may be loaded only in the four corner positions of the basket. See Figure 11.2.15.1.2-2 for corner positions. Therefore, the bounding case for Maine Yankee is the basket configuration with twenty (20) Maine Yankee fuel assemblies, three (3) fuel cans containing spent fuel, and one (1) fuel can containing consolidated fuel.

A two-dimensional ANSYS model is employed for the parametric study as shown in Figure 11.2.15.1.2-1. The load from a PWR fuel assembly is modeled as a pressure load at the inner surface of each support disk slot opening. The design basis fuel pressure loading (1g) is 12.26 psi. Based on the same design parameters (slot size = 9.272 in., disk thickness = 0.5 inch, and the number of disks = 30), the pressure load corresponding to a Maine Yankee standard CE 14 × 14 fuel assembly is 10.3 psi. The pressure load is 11.3 psi for a Maine Yankee fuel can holding an intact or damaged fuel assembly. For a Maine Yankee fuel can holding consolidated fuel the pressure load is 17.0 psi.

This study considers a 60g side impact condition for four different basket orientations: 0°, 18.22°, 26.28° and 45°, as shown in Figure 11.2.15.1.2-2. The 60g bounds the g-load for the PWR support disks (40g) due to the Vertical Concrete Cask tip-over accident as shown in Section 11.2.12.

A total of five cases are considered in the study. Inertial loads are applied to the support disk in all cases. The base case considers that all 24 fuel positions hold design basis PWR fuel assemblies. The other four cases (Cases 1 through 4) represent four possible load combinations for the placement of four Maine Yankee fuel cans in the corner positions, one of which holds consolidated fuel. The remaining twenty basket positions hold Maine Yankee standard 14 × 14 fuel assemblies. The basket loading positions are shown in Figure 11.2.15.1.2-2. The load combinations evaluated in the four Maine Yankee fuel can loading cases are:

Case	Basket Position 1	Basket Position 2	Basket Position 3	Basket Position 4
1	Consolidated	Damaged	Damaged	Damaged
2	Damaged	Consolidated	Damaged	Damaged
3	Damaged	Damaged	Damaged	Consolidated
4	Damaged	Damaged	Consolidated	Damaged

Table 11.2.15.1.2-1 provides a parametric comparison between the Base Case and the four cases evaluated, based on the maximum sectional stress in the support disk. As shown in the table, the maximum stress in the PWR basket support disk loaded with 20 standard fuel assemblies and four Maine Yankee fuel cans, including one holding consolidated fuel, is bounded by that for the support disk loaded with the design basis PWR fuel.

Additionally, a three-dimensional analysis was performed for Case 4 with a 26.28° drop orientation using the three-dimensional canister/basket model presented in Section 11.2.12.4.1. Results of the analysis for the top support disk, where maximum stress occurs, are presented in Tables 11.2.15.1.2-2 and 11.2.15.1.2-3. The minimum margin of safety is +1.12 and +0.11 for P_m stresses and $P_m + P_b$ stresses, respectively. The minimum margin of safety for the corresponding analysis for the design basis PWR configuration is +0.97 and +0.05 for P_m and $P_m + P_b$ stresses, respectively (see Table 11.2.12.4.1-4). Therefore, it is further demonstrated that the maximum stress in the PWR support disk loaded with Maine Yankee fuel with consolidated fuel is bounded by the stress for the PWR support disk loaded with the design basis PWR fuel.

Since no credit is taken for the structural integrity of the consolidated fuel or damaged fuel inside the fuel can, it is assumed that 100% of the fuel rods fail during an accident. For a Maine Yankee standard 14×14 fuel assembly, the volume of 176 fuel rods (100%) and 5 guide tubes will fill up the lower 103.6 inches (about at the elevation of the 21st support disk) assuming a 50% volume compaction factor. For the consolidated fuel, the volume of 283 rods (100%) and 4 connector rods will fill up the lower 109.6 inches (about at the elevation of the 22nd support disk) assuming a 75% compaction factor. The compaction factor of 75% for the consolidated fuel considers that the number of rods in the consolidated fuel is approximately 1.5 times of the number of rods in the standard Maine Yankee fuel and these rods are initially more closely spaced.

During a tip-over accident of the vertical concrete cask, the maximum total load on the support disk (top/30th disk) for the design basis PWR basket is 54.6 kips (12.26 psi × 9.272-inch × 0.5-inch × 24 × 40g), considering the design deceleration of 40g (Section 11.2.12.4). With the assumption of 100% rod failure for the damaged fuel and consolidated fuel in the Maine Yankee fuel can, the 21st disk is subjected to the maximum total load (including weight from 20 standard fuel assemblies, 3 damaged fuel assemblies and the consolidated fuel). The pressure load (1g) on the support disk corner slot corresponding to 100% failed damaged fuel is 15.3 psi (load distributed to 21 support disks) and the pressure load corresponding to the 100% failed consolidated fuel is 22.6 psi (load distributed on 22 support disks). In the tip-over accident, the g-load at the 21st disk is 30g, based on the design deceleration of 40g at the top (30th) disk. The total load (W_{21}) on the 21st support disk is:

$$W_{21} = (10.3\times20+15.3\times3+22.6\times1) \times 9.272 \times 0.5 \times 30 = 38{,}200 \text{ pounds} = 38.2 \text{ kips}$$

The support disk load is only 70% (38.2/54.6 = 0.7) of the maximum total load on the support disk due to the design basis PWR fuel load. Consequently, the maximum stress in the support disk, assuming 100% rod failure of the damaged and consolidated fuel in Maine Yankee fuel cans, is bounded by the maximum stress in the support disk calculated for the design basis fuel.

Figure 11.2.15.1.2-1 Two-Dimensional Support Disk Model

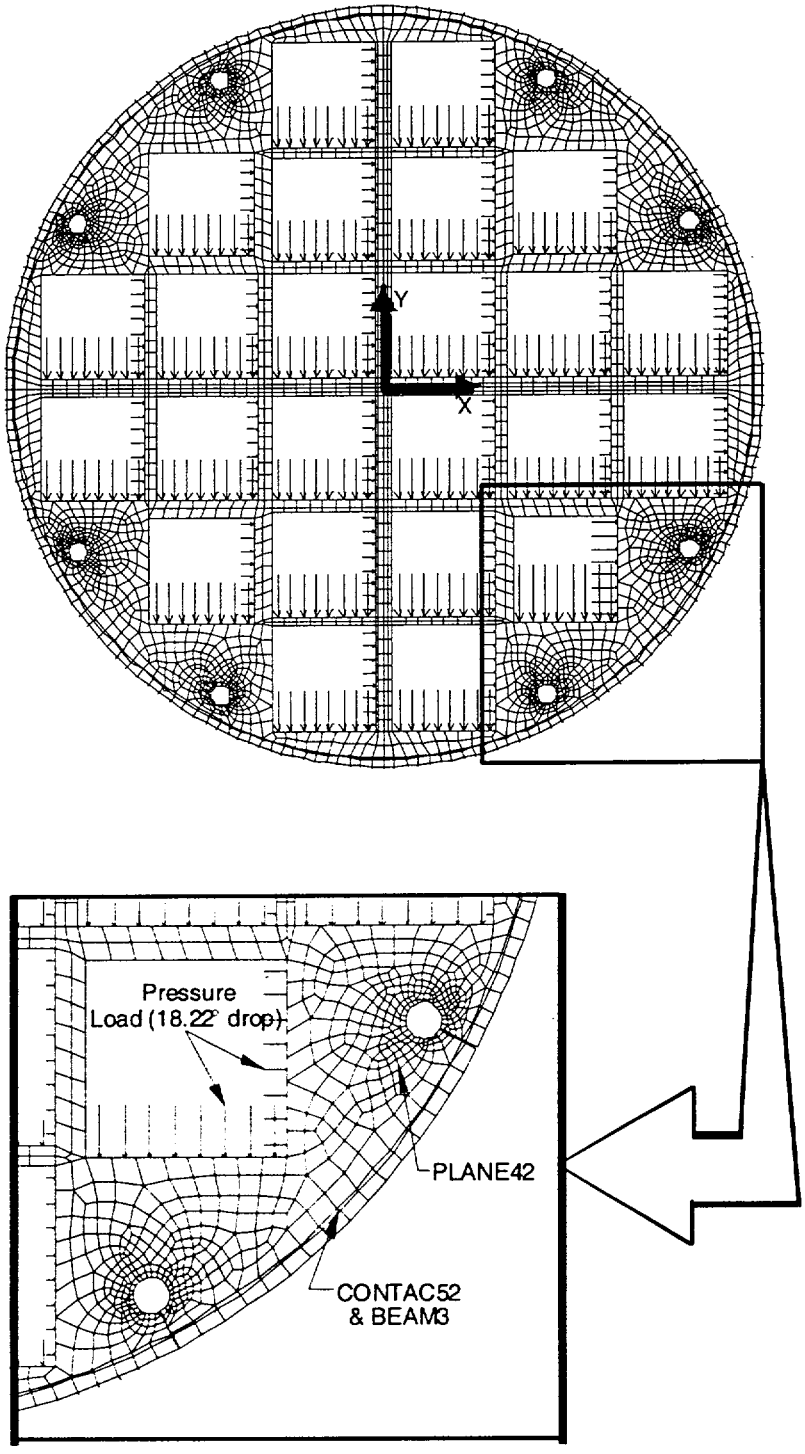

Figure 11.2.15.1.2-2 PWR Basket Impact Orientations and Case Study Loading Positions for Maine Yankee Consolidated Fuel

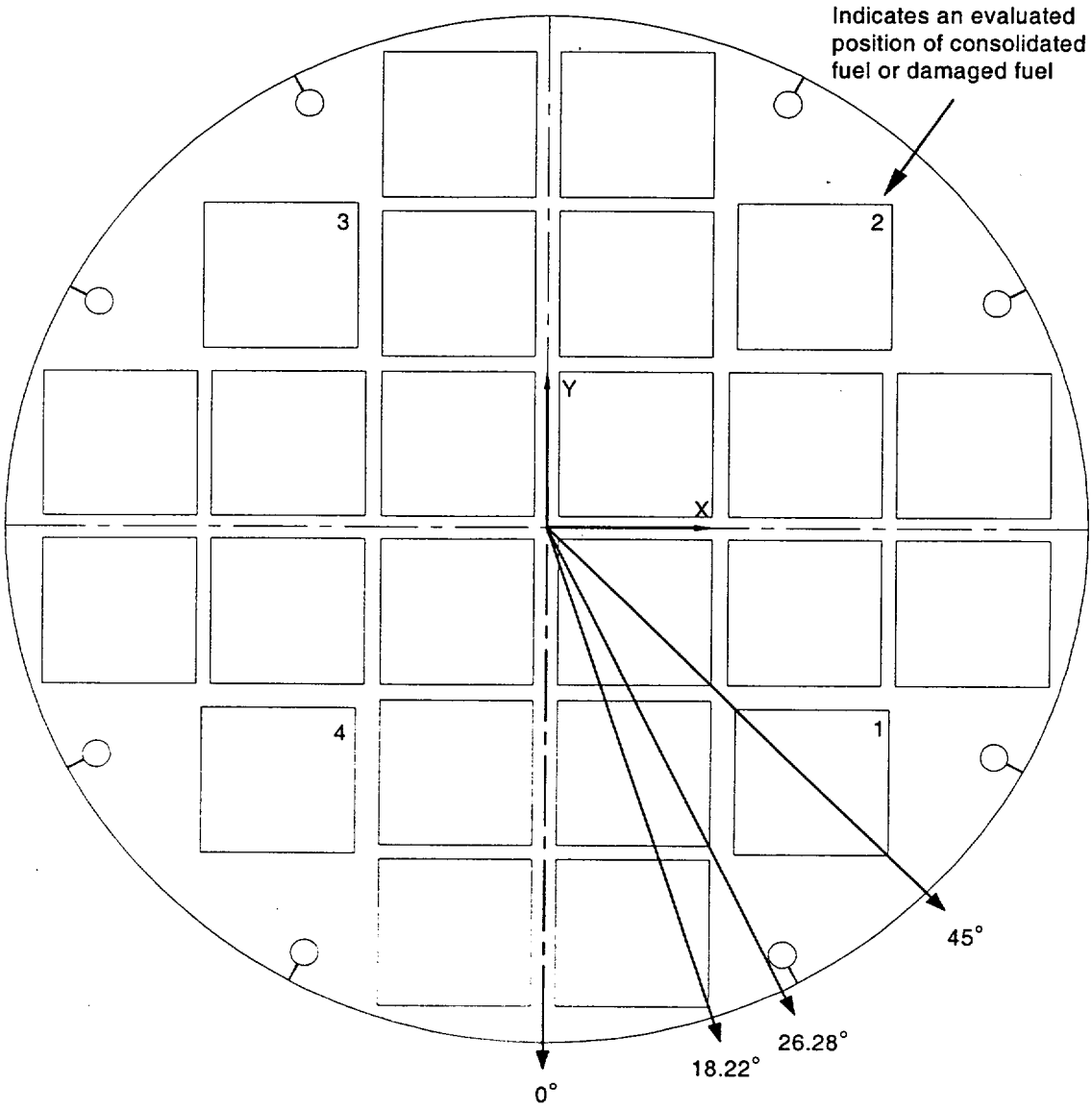

Table 11.2.15.1.2-1 Normalized Stress Ratios – PWR Basket Support Disk Maximum Stresses

Orientation[1]	Membrane Stress Ratio[2]				Membrane + Bending Stress Ratio[2]			
	0°	18.22°	26.28°	45°	0°	18.22°	26.28°	45°
Base Case	1.00	1.00	1.00	1.00	1.00	1.00	1.00	1.00
Case 1	0.91	0.94	0.94	0.94	0.96	0.94	0.94	0.94
Case 2	0.91	0.94	0.94	0.95	0.95	0.95	0.95	0.95
Case 3	0.91	0.95	0.95	0.95	0.96	0.95	0.95	0.95
Case 4	0.91	0.95	0.95	0.96	0.96	0.98	0.98	0.97

1. Orientations correspond to those shown in Figure 11.2.15.1.2-2.
2. Stress ratios are based on the maximum sectional stresses of the support disk.

Table 11.2.15.1.2-2 Support Disk Primary Membrane (P_m) Stresses for Case 4, 26.28° Drop Orientation (ksi)

Section Number	Sx	Sy	Sxy	Stress Intensity	Allowable Stress	Margin of Safety
18	19.3	-22.9	2.8	42.6	90.4	1.12
3	27.1	-12.2	2.4	39.6	89.3	1.26
16	37.1	-22.8	1	37.2	89.3	1.4
1	32.3	-12.1	0.6	32.3	90.4	1.8
94	26.8	-19	2.7	27.6	90.5	2.28
17	-0.1	-22.8	1.9	23.1	89.8	2.9
88	18.3	-5.6	-7.3	21.6	91.5	3.23
96	6.7	-13.8	-3.2	21.4	91.5	3.27
95	-0.1	-19.9	1.5	20	91.1	3.55
90	15.3	-3.5	0.8	18.9	90.5	3.8
84	15.6	-18.5	-0.4	18.6	91.5	3.93
61	15.7	-10.5	4.7	18.5	91.5	3.96
60	10.2	-17.5	1.3	17.7	89.3	4.03
82	15.7	-7.8	3.8	17.2	90.8	4.27
37	11.9	-4.3	0.6	16.3	89.3	4.49
58	10.3	-12.1	5	16.3	90.4	4.54
62	15.7	-0.2	2.6	16.3	91.2	4.59
83	15.7	-0.2	1.7	15.8	91.2	4.75
91	-7.4	-15.4	-1.5	15.7	90.5	4.78
63	15.6	-9.9	0.5	15.7	90.8	4.8
30	14.1	-9.3	3.1	15.6	91.9	4.89
33	14.6	-4.7	2.3	15.1	89.3	4.93
108	13.5	-5.6	-3.9	15.1	91.5	5.07
24	-2	-14.3	1.7	14.5	91.5	5.31
79	-5.3	6.3	4.1	14.2	89.3	5.31
23	-0.1	-14.2	0.7	14.2	91.2	5.41
22	-7.3	-14.1	-0.4	14.2	90.8	5.42
28	13.2	-9.1	1.8	13.9	90.9	5.56
7	13.6	-11.9	-0.7	13.8	91.5	5.62
46	-2.4	-10.8	5.1	13.2	89.3	5.74

Note: See Figure 11.2.12.4.1-7 for Section locations.

Table 11.2.15.1.2-3 Support Disk Primary Membrane + Primary Bending ($P_m + P_b$) Stresses for Case 4, 26.28° Drop Orientation (ksi)

Section Number	Sx	Sy	Sxy	Stress Intensity	Allowable Stress	Margin of Safety
61	-116.4	-39.3	10.1	117.7	130.8	0.11
58	-109.5	-43.9	8.7	110.6	129.1	0.17
43	-92.6	-32.4	6.2	93.2	129.1	0.39
82	-87.8	-27.9	7	88.6	129.8	0.46
60	-81.6	-39.9	7.7	83	127.6	0.54
79	-82	-18.9	2	82	127.6	0.56
55	-83.5	-29.3	4.6	83.9	130.8	0.56
16	-52.5	-71.9	15	80.1	127.6	0.59
46	-77.1	-49.3	9.5	80	127.6	0.59
64	-76.2	-31.8	7	77.2	127.6	0.65
30	-34.4	-75.2	13.1	79.1	131.3	0.66
18	-2.8	-77.6	-2.9	77.8	129.1	0.66
3	10.1	-65.4	-6	76.5	127.6	0.67
63	-75.4	-26	4.3	75.8	129.8	0.71
76	69	21	4.7	69.5	129.8	0.87
48	-66	-42.7	4	66.7	125.7	0.89
19	-38.2	-65.3	2.6	65.5	125.7	0.92
6	-43.2	-62	5.4	63.4	125.7	0.98
45	-63.2	-15.3	-0.2	63.2	127.6	1.02
94	-56.3	-40.8	10.4	61.5	129.3	1.1
21	-47.1	-57.5	5.3	59.7	127.6	1.14
67	-54.5	-42.3	5.3	56.5	125.7	1.22
1	-47.7	-40.7	12.7	57.3	129.1	1.25
33	-29.7	-52.9	7.4	55	127.6	1.32
51	26.7	-27.3	3.9	54.5	127.7	1.34
39	-29	-49.8	6.3	51.6	129.1	1.5
81	-49.9	-29.5	5.3	51.2	129.1	1.52
84	-48	-26.1	6.2	49.7	130.8	1.63
4	-41.7	-43.6	5.3	48	127.6	1.66
28	-44.6	-29.6	8.3	48.2	129.9	1.69

Note: See Figure 11.2.12.4.1-7 for Section locations.

11.2.15.1.3 Structural Evaluation for the Maine Yankee Fuel Can

Twenty-Four Inch Drop of the Vertical Concrete Cask

The 24-inch drop of the Vertical Concrete Cask onto an unyielding surface (Section 11.2.4) results in accelerations that are bounded by the 60g acceleration used in this structural evaluation for the Maine Yankee fuel can. The compressive load (P) on the tube is the combined weight of the lid, side plates and tube body.

The compressive load (P) is:

$$P = (17.89 + 6.57 + 78.77) \times 60 = 6{,}193.8 \text{ lbs, use } 8{,}500 \text{ lbs.}$$

The compressive stress (S_c) in the tube body is:

$$S_c = \frac{P}{A} = \frac{8{,}500}{1.714} = 4{,}959 \text{ psi}$$

The margin of safety (MS) is determined based on the accident condition allowable primary membrane stress (0.7 S_u) at a bounding temperature of 600°F for Type 304 stainless steel:

$$MS = \frac{0.7S_u}{S_c} - 1 = \frac{0.7(63{,}300)}{4{,}959} - 1 = +7.9$$

The potential buckling of the tube is evaluated, using the Euler formula, to determine the critical buckling load (P_{cr}):

$$P_{cr} = \frac{\pi^2 EI}{L_e^2} = \frac{\pi^2 (25.2 \times 10^6)(20.98)}{2(157.8)} = 16.5 \times 10^6 \text{ lbs}$$

where:

$E = 25.2 \times 10^6$ psi

$$I = \frac{8.62^4 - 8.52^4}{12} = 20.98 \text{ in.}^4$$

L_e = 2L (worst case condition)

L = tube body length (157.8 in.)

Because the maximum compressive load (8,500 lbs under the accident condition) is much less than the critical buckling load (16.5×10^6 psi) the tube has adequate resistance to buckling.

Tip–Over of the Vertical Concrete Cask

The majority of the fuel can tube body is contained within the fuel tube in the basket assembly. Because both the tube body of the fuel can and the fuel tube have square cross sections, they are effectively in full contact (for 153.0 in. longitudinally) during a side impact and no significant bending stress is introduced into the tube body. The last 4.8 inches of the tube body and the 5.0 inches length of the side plates are unsupported past the fuel tube flange in the side impact orientation.

The tube body is evaluated as a cantilevered beam with the combined weight (P) of the overhanging tube body and side plates and conservatively, concentrated at the top end of the side plates multiplied by a deceleration factor of 60g. Note that the maximum g-load for the PWR basket is 40g for the tip-over accident (Section 11.2.12).

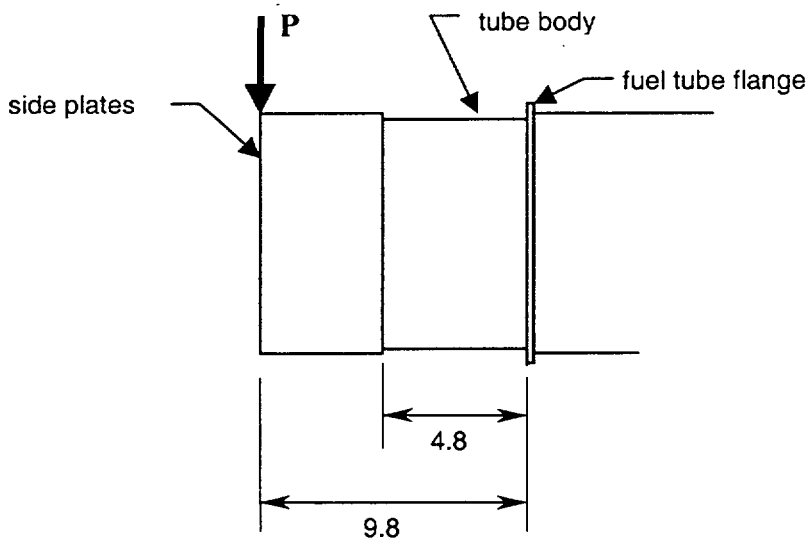

The maximum bending moment (M) is:

$$M = Pg \times L = 25(60)(9.8) = 14{,}700 \text{ lbs·in.}$$

where:

P = 25 lbs (weight of the overhung tube and side plates)

g = 60 (conservative g-load that bounds the tip over condition)

L = 9.8 in. (the total overhung length of the tube body and side plates)

The maximum bending stress, f_b, is:

$$f_b = \frac{Mc}{I} = \frac{14{,}700(4.31)}{20.98} = 3{,}020 \text{ psi}$$

where:

c = half of the outer dimension of the tube

I = the moment of inertia

The shear stress (τ) is:

$$\tau = \frac{Pg}{A} = \frac{25(60)}{1.714} = 875 \text{ psi}$$

where:

A = the cross-sectional area of the tube = 1.714 in^2

The principle stresses are calculated to be 3,255 psi and - 470 psi, and the corresponding stress intensity is determined to be 3,725 psi.

The margin of safety (MS) is calculated based on the allowable primary membrane plus bending stress (1.0 S_u) at a bounding temperature of 600°F for Type 304 stainless steel:

$$MS = \frac{1.0S_u}{\sigma_{max}} - 1 = \frac{63{,}300 \text{ psi}}{3{,}725 \text{ psi}} - 1 = +16$$

As discussed in Section 11.2.15.1.2, the Maine Yankee fuel can may hold a 100% failed damaged fuel lattice or consolidated fuel lattice. An evaluation is performed to demonstrate that the fuel can maintains its integrity during a tip-over accident for this condition. The fuel can is evaluated using the methodology presented in Section 11.2.12.4.1 for the PWR Fuel Tube Analysis for a 60-g side impact condition. This g-load bounds the maximum g-load (40g) for the PWR basket in the concrete cask tip-over event. Similar to the finite element model used for the PWR fuel tube analysis for the uniform pressure case (see Section 11.2.12.4.1), an ANSYS finite element model is generated to represent a section of the damage fuel can with a length of three spans, i.e. the model is supported at four locations by the support disks. The fuel tube, the BORAL plate, and its stainless steel cover plate are conservatively ignored in the model. A bounding uniform pressure is applied to the lower inside surface of the fuel can wall. The pressure is determined based on the weight of the 100% failed consolidated fuel (2,100 lbs × 60g) occupying a length of 109.6 inches (see Section 11.2.15.1.2) as shown below. The inside dimension of the fuel can is 8.52-inches.

$$P = \frac{2{,}100}{109.6(8.52)} \times 60 = 135 \text{ psi}$$

The finite element analysis results show that the maximum stress in the fuel can is 25.4 ksi, which is local to the sections of the tube resting on the support disks. At 750°F the ultimate strength for Type 304 stainless steel is 63.1 ksi. The Margin of Safety is:

$$MS = \frac{63.1}{25.4} - 1 = +1.48$$

The analysis shows that the maximum total strain is 0.05 inch/inch. Defining the acceptable elastic-plastic response of the stainless steel as one half of the material failure strain of 0.40 in./in. at 750°F, the resulting Margin of Safety is:

$$MS = \frac{0.40/2}{0.05} - 1 = +3.0$$

Similarly, the Margin of Safety for elastic-plastic stress is:

$$MS = \frac{63.1 - 17.3}{25.4 - 17.3} - 1 = +4.65$$

where the yield strength of Type 304 stainless steel is 17.3 ksi at 750°F.

Therefore the Maine Yankee fuel can maintains its integrity for the accident conditions.

11.2.15.1.4 Maine Yankee Site Specific Earthquake Evaluation of the Vertical Concrete Cask

This section provides an evaluation of the response of the vertical concrete cask to an earthquake imparting a horizontal acceleration of 0.38g at the top surface of the concrete pad. The evaluation shows that the loaded or empty vertical concrete cask does not tip over or slide in the earthquake event. The methodology used in this evaluation is identical to that presented in Section 11.2.8.

Tip-Over Evaluation of the Vertical Concrete Cask

To maintain the concrete cask in equilibrium, the restoring moment, M_R must be greater than, or equal to, the overturning moment, M_o (i.e. $M_R \geq M_o$). Based on this premise, the following derivation shows that a 0.38g acceleration of the design basis earthquake at the surface of the concrete pad is well below the acceleration required to tip-over the cask.

The combination of horizontal and vertical acceleration components is based on the 100-40-40 approach of ASCE 4-86 [36], which considers that when the maximum response from one component occurs, the response from the other two components are 40% of the maximum. The vertical component of acceleration is obtained by scaling the corresponding ordinates of the horizontal components by two-thirds.

Using this method, two cases are evaluated where:

$a_x = a_z = a$ = horizontal acceleration components
$a_y = (2/3)\ a$ = vertical acceleration component
G_h = Vector sum of two horizontal acceleration components
G_v = Vertical acceleration component

In the first case, the horizontal acceleration is at its maximum. In the second, one horizontal acceleration is at its maximum.

Case 1) The vertical acceleration, a_y, is at its peak: ($a_y = 2/3a$, $a_x = 0.4a$, $a_z = 0.4a$)

$$G_h = \sqrt{a_x^2 + a_z^2}$$

$$G_h = \sqrt{(0.4 \times a)^2 + (0.4 \times a)^2} = 0.566 \times a$$

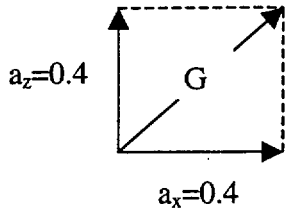

$$G_v = 1.0 \times a_y = 1.0 \times \left(a \times \frac{2}{3}\right) = 0.667 \times a$$

Case 2) One horizonal acceleration, a_x, is at its peak: ($a_y = 0.4 \times 2/3a$, $a_x = a$, $a_z = 0.4a$)

$$G_h = \sqrt{a_x^2 + a_z^2}$$

$$G_h = \sqrt{(1.0 \times a)^2 + (0.4 \times a)^2} = 1.077 \times a$$

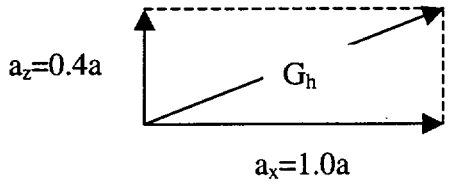

$$G_v = 0.4 \times a_y = 0.4 \times \left(a \times \frac{2}{3}\right) = 0.267 \times a$$

In order for the cask to resist overturning, the restoring moment, M_R, about the point of rotation, must be greater than the overturning moment, M_o, that:

$$M_R \geq M_o \text{, or}$$

$$F_r \times b \geq F_o \times d \Rightarrow (W \times 1 - W \times G_v) \times b \geq (W \times G_h) \times d$$

where:

- d = vertical distance measured from the base of the Vertical Concrete Cask to the center of gravity
- b = horizontal distance measured from the point of rotation to the C.G.
- W = the weight of the Vertical Concrete Cask
- F_o = overturning force
- F_r = restoring force

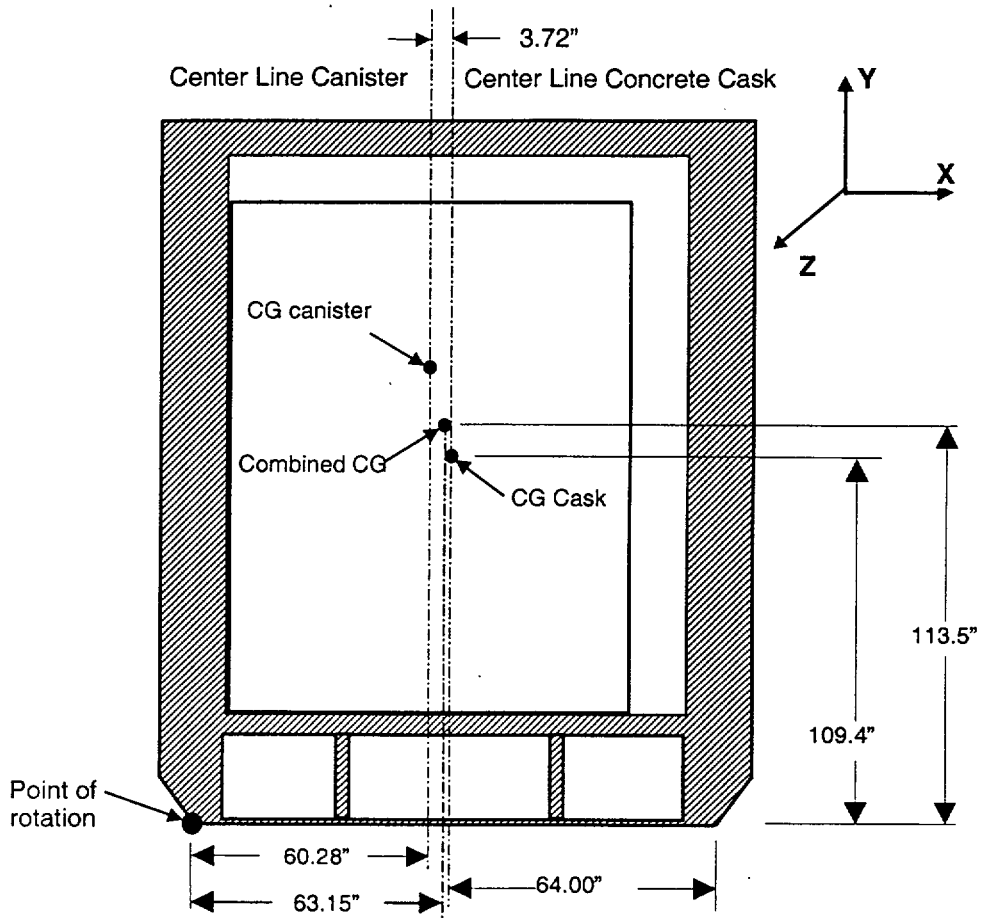

Substituting for G_h and G_v gives:

Case 1

$$(1 - 0.667a)\ \frac{b}{d} \geq 0.566 \times a$$

$$a \leq \frac{b/d}{0.566 + 0.667\ (b/d)}$$

Case 2

$$(1 - 0.267a)\frac{b}{d} \geq 1.077a$$

$$a \leq \frac{b/d}{1.077 + 0.267(b/d)}$$

Because the canister is not attached to the concrete cask, the combined center of gravity for the concrete cask, with the canister in its maximum off-center position, must be calculated. The point of rotation is established at the outside lower edge of the concrete cask.

The inside diameter of the concrete cask is 74.5 inches and the outside diameter of the canister is 67.06 inches; therefore, the maximum eccentricity between the two is:

$$e = \frac{74.50\,\text{in} - 67.06\,\text{in}}{2} = 3.72\,\text{in.}$$

The horizontal displacement, x, of the combined C.G. due to eccentric placement of the canister is

$$x = \frac{70{,}783(3.72)}{308{,}432} = 0.85\,\text{in}$$

Therefore,

$$b = 64 - 0.85 = 63.15\,\text{in.}$$

and

$$d = 113.5\,\text{in.}$$

The C.G. of the loaded Maine Yankee Vertical Concrete Cask is conservatively assumed to be 113.5 inches, which bounds all of the Maine Yankee UMS® Storage System configurations.

1) $a \le \frac{63.15/113.5}{0.566 + 0.667 \times (63.15/113.5)}$

$a \le 0.59g$

2) $a \le \frac{63.15/113.5}{1.077 + 0.267 \times (63.15/113.5)}$

$a \le 0.45g$

Therefore, the minimum ground acceleration that may cause a tip-over of a loaded concrete cask is 0.45g. Since the 0.38g design basis earthquake ground acceleration for the UMS® System at the Maine Yankee site is less than 0.45g, the storage cask will not tip-over.

The factor of safety is 0.45 / 0.38 = 1.18, which is greater than the required factor of safety of 1.1 in accordance with ANSI/ANS-57.9.

Since an empty vertical concrete cask has a lower C.G. as compared to a loaded concrete cask, the tip-over evaluation for the empty concrete cask is bounded by that for the loaded concrete cask.

Sliding Evaluation of the Vertical Concrete Cask

To keep the cask from sliding on the concrete pad, the force holding the cask (F_s) has to be greater than or equal to the force trying to move the cask.

Based on the equation for static friction:

$$F_s = \mu N \geq G_h W$$
$$\mu(1 - G_v)W \geq G_h W$$

Where:

μ = coefficient of friction
N = the normal force
W = the weight of the concrete cask
G_v = vertical acceleration component
G_h = resultant of horizontal acceleration component

Substituting G_h and G_v for the two cases:

Case 1) $\mu(1 - 0.667a) \geq 0.566\,a$

$$\mu \geq \frac{0.566a}{1 - 0.667a}$$

Case 2) $\mu(1 - 0.267a) \geq 1.077\,a$

$$\mu \geq \frac{1.077a}{1 - 0.267a}$$

For a = 0.38g

Case 1) $\mu \geq 0.29$

Case 2) $\mu \geq 0.45$

The analysis shows that the minimum coefficient of friction, μ, required to prevent sliding of the concrete cask is 0.45. The coefficient of friction between the steel bottom plate of the concrete cask and the concrete surface (broom finish) of the storage pad, 0.50, is greater than the coefficient of friction required to prevent sliding of the concrete cask [45,46]. Therefore, the concrete cask will not slide under design-basis earthquake conditions. The factor of safety is 0.50 / 0.45 =1.11 which is greater than the required factor of safety of 1.1 in accordance with ANSI/ANS-57.9 [1].

11.2.15.1.5 Buckling Evaluation for Maine Yankee High Burnup Fuel Rods

This section presents the buckling evaluation for Maine Yankee high burnup fuel (burnup between 45,000 and 50,000 MWD/MTU) having cladding oxide layers that are 80 and 120 microns thick. A similar evaluation is presented in Section 11.2.15.1.6 for Maine Yankee high burnup fuel with an oxide layer thickness of 80 microns that is also mechanically damaged. These analyses show that the high burnup fuel and the damaged high burnup fuel do not buckle in the design basis accident events. An end drop orientation is considered with an acceleration of 60 g, which subjects the fuel rod to axial loading. A reduced clad thickness is assumed, due to the cladding oxide layer.

In the end drop orientation, the fuel rods are laterally restrained by the grids and may come into contact with the fuel assembly base. The only vertical constraint for the fuel rod is the base of the assembly. The weight of the fuel pellets is included in this evaluation, as the pellets are considered to be vertically supported by the cladding. A two-dimensional model comprised of ANSYS BEAM3 elements, shown in Figure 11.2.15.1.5-1, is used for the evaluation. This evaluation is considered to be the bounding condition (as opposed to an evaluation, which considers the cladding only).

80 Micron Oxide Layer Thickness Evaluation

During the end drop, the fuel rod impacts the fuel assembly base. The fuel rod itself will respond as an elastic bar under a sudden compression load at its bottom end. The duration of this impact is bounded by the first extentional mode shape of the fuel rod. Contribution of higher frequency extentional modes of the rod would tend to shorten the duration of impact of the fuel rod with the fuel assembly base. The fuel rod, upon initiation of impact, corresponds to an undeformed state. In the process of the impact, the compression of the fuel rod will increase to a maximum and then return to a near uncompressed state, at which point the time of impact has been completed. This actually represents half of a cycle of the lowest frequency mode shape of the fuel rod. The shape of the time dependence of the deformation is sinusoidal. The single extentional mode shape can also be considered to be a single degree of freedom with a corresponding mass and stiffness. In viewing such an event as a spring mass system, the time variation of the deformation during the impact is expected to be sinusoidal.

The buckling mode for the fuel rod is governed by the boundary conditions. For this configuration, the grids provide a lateral support, but no vertical support. The only vertical restraint is considered to be at the point of contact of the fuel rod and the base of the assembly. The weight of the fuel rod

pellets and cladding is assumed to be uniformly distributed along the length of the fuel rod. In the end drop, this results in the maximum compressive load occurring at the base of the fuel rod. The first buckling mode shape corresponding to these conditions is computed as shown in Figure 11.2.15.1.5-2.

Typically eigenvalue buckling is applied for static environments. For dynamic loading, it is assumed that the duration of the loading is sufficiently long to allow the system to experience the complete load, even as the deformation associated with the buckling is commenced. For dynamic loading, the lateral motion, which would correspond to the buckled shape, will correspond to the lowest mode shape. This lowest frequency mode shape is shown in Figure 11.2.15.1.5-2 and corresponds to a frequency of 25.9 Hz. The similarity of the two shapes shown in Figure 11.2.15.1.5-2 is expected, since both have the same displacement boundary conditions, the same stiffness matrix, and the same governing finite element equations, i.e.,

$$[K]\{\phi_i\} = \lambda_i [A]\{\phi_i\}$$

where:

[K] = structure stiffness matrix
$\{\phi_i\}$ = eigenvector
λ_i = eigenvalue
[A] = mass matrix for the mode shape calculation or stress stiffening matrix for the buckling evaluation

Based on the time duration of the impact and the inherent inability of the fuel rod to rapidly displace in the lateral direction, the effect of the actual lateral motion of buckling can be computed with a dynamic load factor (DLF) [47]. The expression for the DLF for a half-sine loading for a single degree of freedom is given by

$$DLF = \frac{2\beta \cos(\pi/2\beta)}{1 - \beta^2}$$

where:

β = ratio of the first extentional mode frequency to the first lateral mode frequency

These values, computed in this section, are $\beta = 8.32$ and DLF = 0.244.

This DLF is applied to the end drop acceleration of 60g, which is the bounding load to potentially result in the buckling of the fuel rod. The product of 60g × DLF (= 14.6g) is well below the vertical acceleration corresponding to the first buckling mode shape, 37.9g as computed in this section. This indicates that the time duration of the impact of the fuel onto the fuel assembly base is of sufficiently short nature that buckling of the fuel rod cannot occur.

An effective cross-sectional property is used in the model to consider the properties of the fuel pellet and the fuel cladding. The modulus of elasticity (EX) for the fuel pellet has a nominal value of 26.0×10^6 psi [48]. To be conservative, only 50 percent of this value is used in the evaluation. The EX for the fuel pellet was, therefore, taken to be 13.0×10^6 psi. The value of EX (10.47×10^6 psi) was used for the irradiated Zircaloy cladding (ISG-12). Reference information shows that there is no additional reduction of the ductility of the cladding due to extended burnup into the 45,000 – 50,000 MWD/MTU range [49].

The bounding dimensions and physical data (minimum clad thickness, maximum rod length and minimum number of support grids) for the Maine Yankee fuel rod used in the model are:

Outer diameter of cladding (inches)	0.434
Cladding thickness (inches)	0.023
Cladding density (lb/in^3)	0.237
Fuel pellet density (lb/in^3)	0.396

The cladding is reduced from its nominal value of 0.026 inches by the assumed 80 micron oxidation layer (0.003 inches) to 0.023 inches. Similarly, the fuel rod outer diameter is reduced from the nominal value of 0.44 inches to 0.434 inches.

The elevation of the grids, measured from the bottom of the fuel assembly are: 2.3, 33.0, 51.85, 70.7, 89.6, 108.4, 127.3 and 144.9 (inches).

The effective cross-sectional properties (EI_{eff}) for the beam are computed by adding the value of EI for the cladding and the pellet, where:

E = modulus of elasticity (lb/in^2)
I = cross-sectional moment of inertia (in^4)

The lowest frequency for the extentional mode shape was computed to be 219.0 Hz. The first mode shape corresponds to a frequency of 25.9 Hz. Using the expression for the DLF previously discussed, the DLF is computed to be 0.240 (β = 8.44).

120 Micron Oxide Layer Thickness Evaluation

The buckling calculation used the same model employed for the mode shape calculation. The load that would potentially buckle the fuel rod in the end drop is due to the deceleration of the rod. This loading was implemented by applying a 1g acceleration in the direction that would result in compressive loading of the fuel rod. The acceleration required to buckle the fuel rod is computed to be 37.3g.

Using the same fuel rod model, the acceleration required to buckle the fuel rods is found to be 37.3g, which is much higher than the calculated effective g-load (14.3g) due to the 60g end drop. Therefore, the fuel rods with a 120 micron cladding oxide layer do not buckle in the 60g end drop event.

Figure 11.2.15.1.5-1 Two-Dimensional Beam Finite Element Model for Maine Yankee Fuel Rod

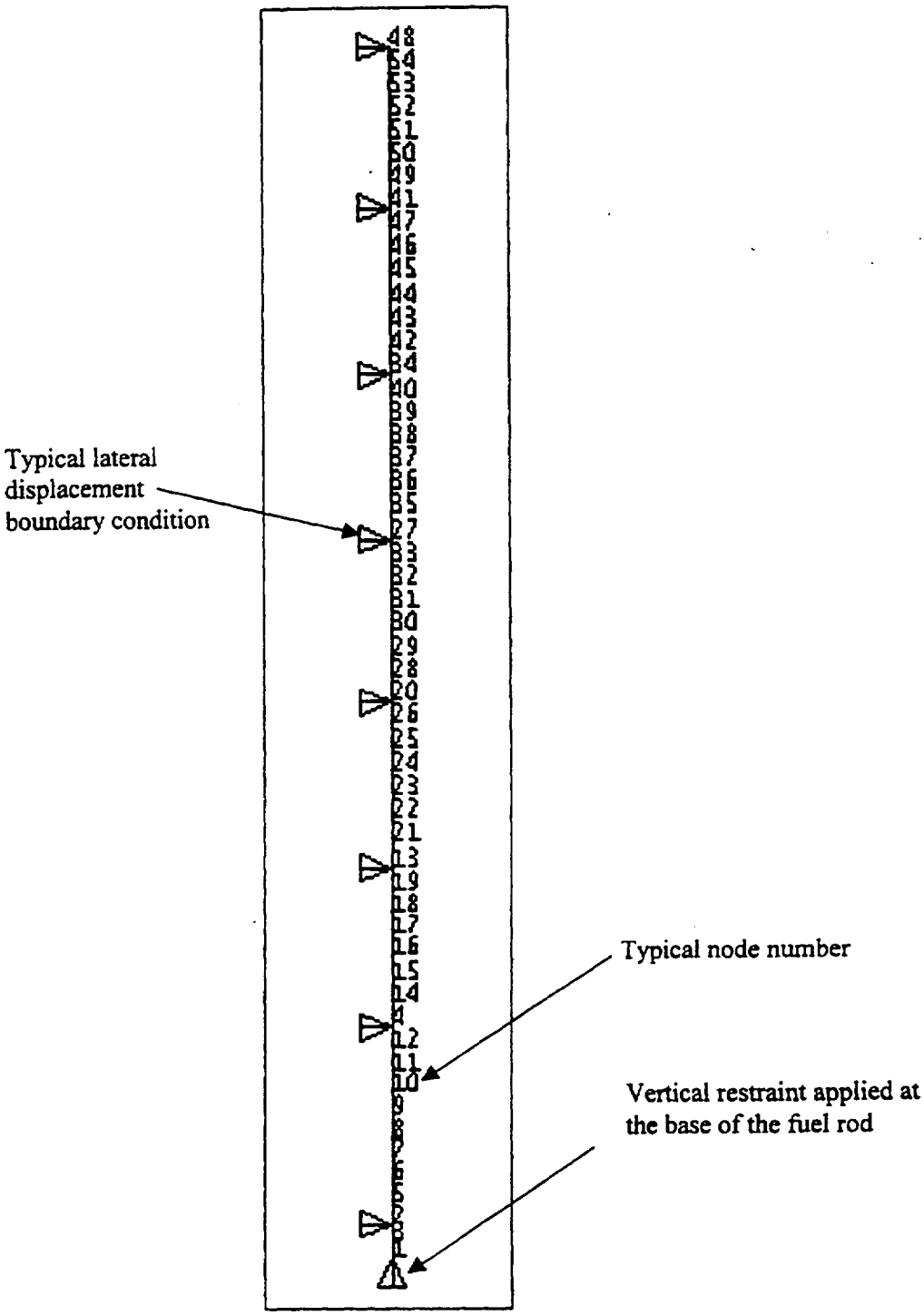

Figure 11.2.15.1.5-2 Mode Shape and First Buckling Shape for the Maine Yankee Fuel Rod

First Lateral Dynamic
Mode Shape at 25.9 Hz

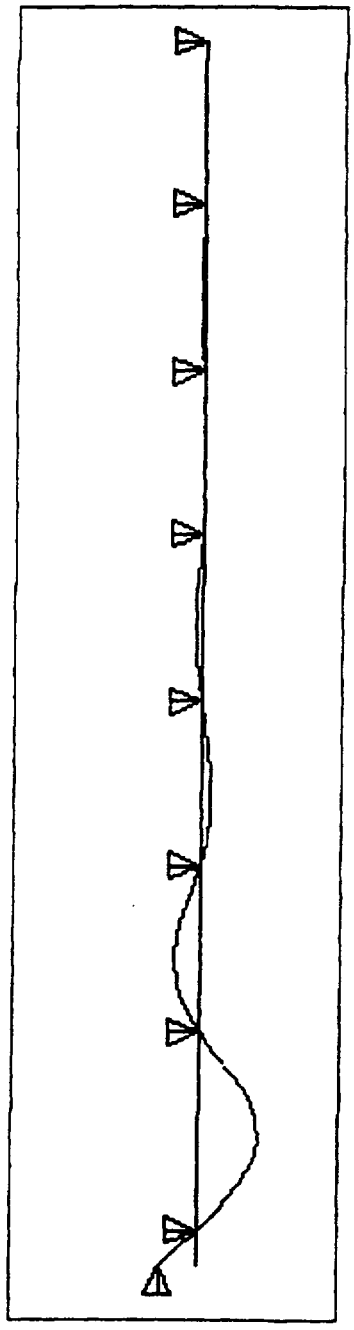

First Buckling
Shape at 37.9g

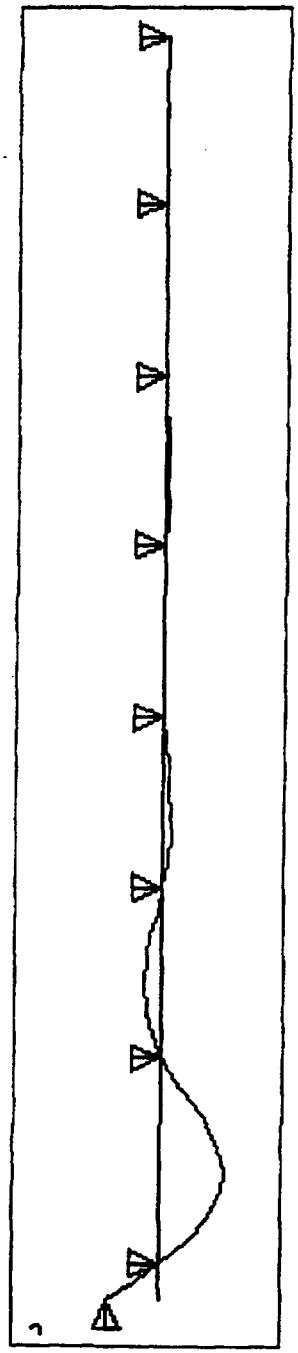

11.2.15.1.6 Buckling Evaluation for High Burnup Fuel with Mechanical Damage

This section presents the buckling evaluation for high burnup fuel having an 80 micron cladding oxide layer thickness and with mechanical damage consisting of one or more missing support grids up to an unsupported fuel rod length of 60 inches.

End Drop Evaluation

The buckling load is maximized at the bottom of the fuel assembly. The bounding evaluation is the removal of the grid strap that maximizes the spacing at the lowest vertical elevation. The elevations of the grids in the model, measured from the bottom of the fuel assembly are: 2.3, 51.85, 70.7, 89.6, 108.4, 127.3 and 144.9 inches (Figure 11.2.15.1.6-1). The grid at the 33.0-inch elevation is removed, resulting in a grid spacing of approximately 50.0 inches. The grid located at 51.85 inches is conservatively assumed to be located at 62.3 inches, resulting in an unsupported rod length of 60.0 inches.

The case of the missing grid is evaluated using the methodology presented in Section 11.2.15.1.5 for the fuel assembly with the grids being present. The dimensions and physical data for the Maine Yankee fuel rod used in the model are:

Outer diameter of cladding (inches)	0.434
Cladding thickness (inches)	0.023
Cladding density (lb/in^3)	0.237
Fuel pellet density (lb/in^3)	0.396
Fuel pellet Modulus of Elasticity (psi)	13.0×10^6
Zircaloy cladding Modulus of Elasticity (psi)	10.47×10^6

The cladding is reduced from its nominal value of 0.026 inches by the assumed 80 micron oxidation layer thickness (0.003 inches) to 0.023 inches. Similarly, the fuel rod outer diameter is reduced from the nominal value of 0.44 inches to 0.434 inches. The fuel pellet modulus of elasticity is conservatively reduced 50%. The modulus of elasticity of the Zircaloy cladding is taken from ISG-12 [50].

With the grid missing, the frequency of the fundamental lateral mode shape is 7.8 Hz. The natural frequency of the fundamental extensional mode was determined to be 218.9 Hz. The DLF is computed to be 0.072, resulting in an effective acceleration of $0.072 \times 60 = 4.3$ g. Using the same method to compute the acceleration at which buckling occurs, the lowest buckling acceleration is 14.4 g, which is significantly greater than 4.3 g. Therefore, the fuel rod does not buckle during an

end drop. Figures 11.2.15.1.6-1 and 11.2.15.1.6-2 show the finite element model and buckling results and mode shape.

Side Drop Evaluation

The Maine Yankee fuel rod is evaluated for a 60 g side drop with a missing support grid in the fuel assembly. Using the same assumptions as for the end drop evaluation, the span between support grids is assumed to be 60.0 inches.

For this analysis, the dimensions and physical data used are:

Fuel rod OD	0.434 in. (80 micron oxidation layer)
Clad ID	0.388 in.
E_{clad}	10.47E6 psi
E_{fuel}	13.0E6 psi
Clad density	0.237 lb/in^3
Fuel density	0.396 lb/in^3
A_{clad}	0.030 in^2 (cross-sectional area)
A_{fuel}	0.118 in^2 (cross-sectional area)

The mass of the fuel rod per unit length is:

$$m = \frac{0.396(0.122) + 0.237(0.030)}{386.4} = 0.000143\ \text{lb-s}^2/\text{in}^2$$

For the fuel rod, the product of the Modulus of Elasticity (E) and Moment of Inertia (I), is:

$$EI_{clad} = 10.47E6\frac{\pi\left(0.217^4 - 0.194^4\right)}{4} = 6{,}586\ \text{lb-in}^2$$

$$EI_{fuel} = 13.0E6\frac{\pi\left(0.194^4\right)}{4} = 14{,}462\ \text{lb-in}^2$$

$$EI = 6{,}586 + 14{,}462 = 21{,}048\ \text{lb-in}^2$$

During a side drop, the maximum deflection of a fuel rod is based on the fuel rod spacing of the fuel assembly. The pitch (center-to-center spacing) of fuel rods is 0.58 inches [51]. The maximum pitch is across the diagonal of the fuel assembly. The maximum pitch is:

$$dp = \frac{0.58}{\sin 45} = 0.82\,\text{in.}$$

The maximum deflection of a fuel rod is at the top of the fuel assembly and the minimum deflection is at the bottom of the fuel assembly.

Assuming a 17 × 17 array (which envelopes the Maine Yankee 14 × 14 array), the maximum fuel rod deflection is:

$$(17\text{-}1) \times (0.82\text{-}0.43) = 6.18 \text{ in.}$$

The deflection of a simply supported beam with a distributed load is given by the equation:

$$\Delta = \frac{5\omega l^4}{384EI} = \frac{5(g\omega)l^4}{384\,(EI_{total})} \qquad [52]$$

$$g = \frac{384\Delta(EI_{total})}{5\omega l^4}$$

The cladding bending stress is given by the equation:

$$S = \frac{Mc}{I} = \frac{\left(\left(g\omega l^2\right)/8\right)c}{I_{clad}}\left(\frac{EI_{clad}}{EI_{total}}\right)$$

Inserting the equation for 'g':

$$S = \frac{384\Delta c E_{clad}}{40 \times L^2}$$

where:

c = 0.217 inch distance from center of fuel rod to extreme outer fiber

L = 60 inches (the unsupported fuel rod length)

Δ = 6.18 inches (the maximum deflection)

The bending stress in the fuel rod is:

$$S = \frac{384 \times 6.18 \times 0.217 \times 10.47E6}{40(60)^2} = 37.4 \text{ ksi}$$

The maximum hoop stress due to the fuel rod internal pressure is determined to be 19.1 ksi (131.4 MPa per Tables 4.4.7-3 and 4.5.1.2-1). Therefore, the maximum axial stress is 9.6 ksi (one half of the hoop stress [53]).

The bearing stress between two fuel rods under a 60 g load is:

$$S_{brg} = 0.591\sqrt{\frac{\omega E}{K_D}} = 0.591\sqrt{\frac{(0.000143 \times 386.4) \times 60 \times 10.47E6}{0.22}} = 7.4 \text{ ksi} \quad [53]$$

where:

$$K_D = \frac{D_1 D_2}{D_1 + D_2} = \frac{0.434 \times 0.434}{0.434 + 0.434} = 0.22$$

The total stress is:

$$S = 37.4 + 9.6 + 7.4 = 54.4 \text{ ksi}$$

The ultimate strength allowable for irradiated Zircaloy–4 is 83.4 ksi (Figure 3-2 [54]). Therefore, the margin of safety for ultimate strength is:

$$MS = \frac{83.4}{54.4} - 1 = 0.53$$

The yield strength allowable for irradiated Zircaloy–4 is 78.3 ksi (Figure 3-2 [54]). Therefore, the margin of safety for yield strength is:

$$MS = \frac{78.3}{54.4} - 1 = 0.44$$

The maximum bearing stress occurs between the bottom fuel rod and the fuel tube. The bearing stress is:

$$S_{brg} = 0.591\sqrt{\frac{17\times0.000143\times386.4\times60\times10.47E6}{0.44}} = 21.6\,\text{ksi}$$

The bending stress is negligible because the maximum deflection is equal to the spacing of the fuel rods established by the grid. Therefore, the top fuel rod is bounding.

Consequently, the fuel rods are demonstrated to be structurally adequate for the 60g side drop loading condition.

Figure 11.2.15.1.6-1 Two-Dimensional Beam Finite Element Model for a Fuel Rod with a Missing Grid

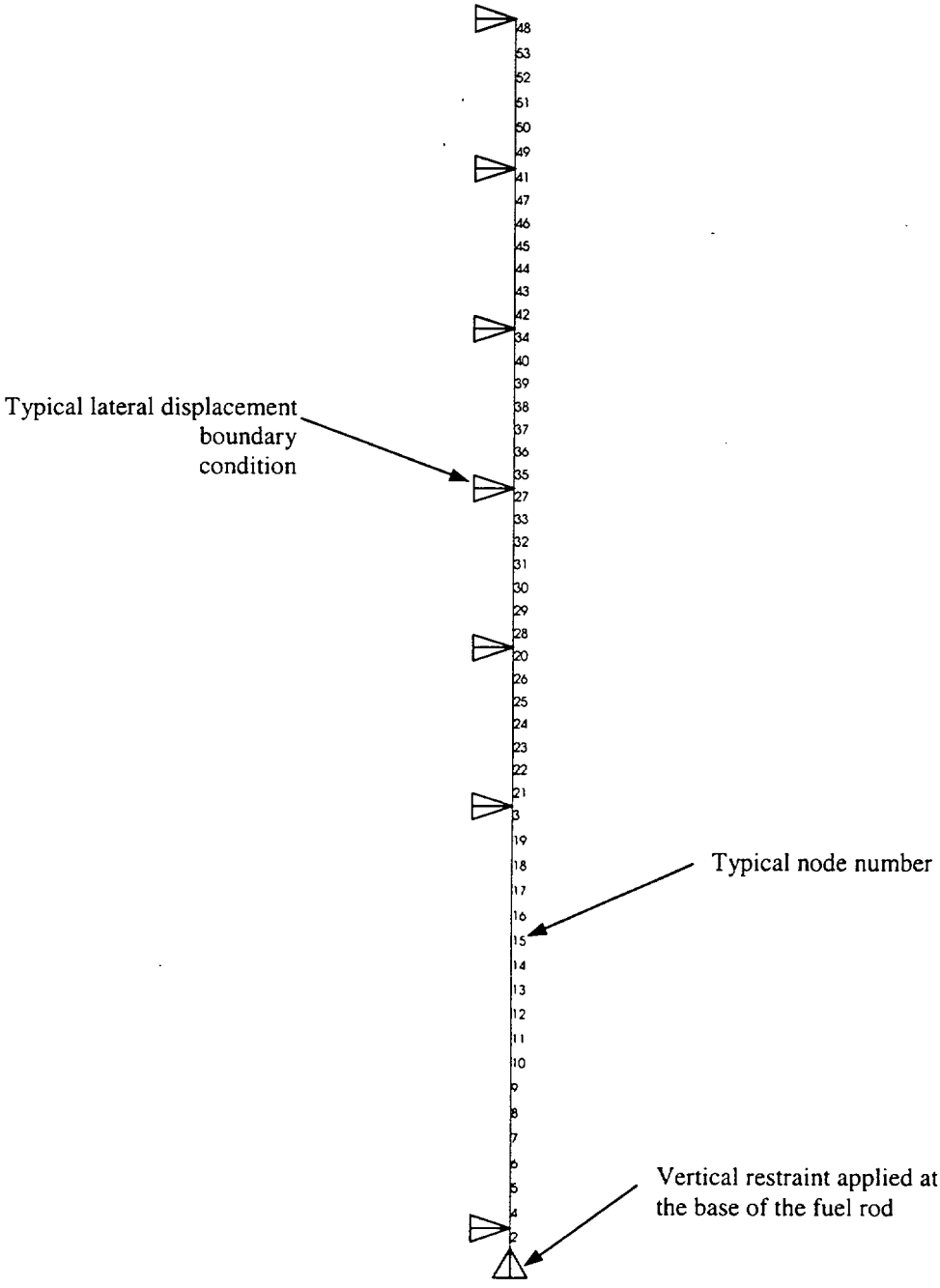

Figure 11.2.15.1.6-2 Modal Shape and First Buckling Mode Shape for a Fuel Rod with a Missing Grid

First Lateral Dynamic Mode Shape at 7.8 Hz

First Buckling Mode Shape at 14.4g

THIS PAGE INTENTIONALLY LEFT BLANK

11.2.16 100-Ton Transfer Cask Side Drop

During transfer conditions, the 100-ton transfer cask is postulated to roll off the transfer cradle. Because the properties affect the final impact acceleration of the 100-ton transfer cask, the bounding side drop is considered to occur on the ISFSI pad that was used to evaluate the vertical concrete cask during the tip-over accident in Section 11.2.12. The non-linear structural dynamic analysis program, LS-DYNA, is used to predict the acceleration response of the 100-ton transfer cask, during an on-site transfer side-drop accident. The analysis simulates the transfer cask's drop onto a horizontal concrete pad (30-ft × 30-ft × 3-ft) supported by a subsoil mat (35-ft × 35-ft × 10-ft). Two side drop impact analyses are performed on the 100-ton transfer cask, each corresponding to the soil properties associated with the ISFSI pads contained in Section 11.2.12.3.

11.2.16.1 Cause of 100-Ton Transfer Cask Side Drop

During transfer conditions, the 100-ton transfer cask is fastened in a horizontal position to a transfer cradle. The postulated accident scenario predicts that the transfer cask breaks away and rolls off the transfer cradle and drops onto the ISFSI pad.

11.2.16.2 Detection of Cask Tip-Over

The damaged configuration of the 100-Ton transfer cask will be obvious during inspection following the initiating event.

11.2.16.3 Analysis of the 100-Ton Transfer Cask Side Drop

The non-linear structural dynamic analysis program, LS-DYNA, is used to predict the acceleration response of the 100-ton transfer cask, during an on-site transfer side-drop accident. The assumed effective drop height of the 100-ton transfer cask is 53 inches, i.e., from the transfer cradle to the ground. Since the 53-inch drop represents the dynamic force input, the initial velocity is 202.38 in/sec, which is the vertical velocity of a rigid body after a free fall of 53-in under 1g gravitational force ($v = \sqrt{2gh}$).

The 100-ton transfer cask model consists of the fuel canister, inner shell, lead shell, divider shell, and outer shell (water jacket). The finite element model of the 100-ton transfer cask and canister is shown in Figures 11.2.16-1 and 11.2.16-2. The overall length of the transfer cask model is 189.25

inches. The outside diameter of the transfer cask model at the water jacket is 83.25 inches. A 8-inch diameter trunnion is located 9 inches from the top plate. The bottom plate of the 100-ton transfer cask provides the attachment for the shield door rails. The center of the transfer cask is open so that the fuel canister can be transferred in and out of the cask. The fuel canister does not share nodes with the transfer cask, i.e., it is not connected in the model with the transfer cask. The weight of the fuel is distributed along a rigid strip inside the canister model. Water in the water jacket is not modeled. The fuel canister in the transfer cask model is shown in Figure 11.2.16-3. The ISFSI concrete pad upon which the cask impacts has dimensions of 30-ft × 30-ft × 3-ft. The subsoil mat under the concrete pad has dimensions of 35-ft × 35-ft × 10-ft. The transfer cask, canister, concrete pad and soil are modeled using 8-node solid brick elements and 4-node shell elements. Figure 11.2.16-2 shows the complete loaded 100-ton transfer cask model on the concrete and subsoil model.

11.2.16.3.1 100-Ton Transfer Cask Side Drop for the Standard PWR Canister

The side drop of the 100-ton transfer cask with the loaded PWR Standard canister was evaluated using the finite model described above. The soil material properties and the concrete pad material properties in Section 11.2.12.3.1 were incorporated in the model for the side drop. The canister, basket and contents are included in the model as additional mass along the symmetry plane on the inner shell near the plane of impact. A bounding weight of 89,000 lbs is used to bound the weight of the canister and contents for the Standard PWR canister. To account for large deformation and buckling, the mechanical property of Type 304 stainless steel is represented by an elastic-plastic material formula with LS-DYNA material type 24 (Piecewise_Linear_Plasticity). The detailed stress-strain curve for Type 304 stainless steel at room temperature beyond yield [55] is presented in Figure 11.2.16-4 ("Impact Dynamics," J. A. Zukas, T. Nicholas, H. F. Swift, L. B. Greszczuk and D. R. Curran, John Wiley & Sons).

Boundary and Initial Condition

The assumed effective drop height of the 100-ton transfer cask is 53 inches. Since the 53-inch drop represents the dynamic force input, the initial velocity is 202.38 in/sec, i.e., the vertical velocity of a rigid body after a free fall of 53-in under 1g gravitational force ($v = \sqrt{2gh}$). The kinetic energy is checked to ensure that the total initial energy is correct.

The symmetry condition is at the XZ-plane (Y=0), at which all displacements in the Y-direction are constrained. The soil mat is constrained at the boundaries (X_{max}, X_{min}, Y_{max}, Z_{min}) with a roller

predicted accelerations are, therefore, obtained by filtering the LS-DYNA acceleration outputs using a filter frequency of 50 Hz.

100-Ton Transfer Cask Side Drop Analysis Results (Standard BWR Canister)

The analysis results are obtained by using the LS-DYNA postprocessor, LS-POST, to display the nodal acceleration time-histories. From the modal analysis, a filter frequency of 50 Hz is used in conjunction with the LS-POST Butterworth filter. For the BWR basket/canister, the maximum filtered acceleration of 20.7g occurs at the basket top support disk location of the canister.

11.2.16.3.3 100-Ton Transfer Cask Side Drop with Advanced PWR Canister

The side drop of the 100-ton transfer cask with the loaded Advanced PWR canister was evaluated using the finite model described above. The soil material model proprerties and the concrete pad material model in Section 11.2.12.5.1. The canister, basket and contents are included in the model as additional was along the asymmetry plane on the inner shell near the plane of impact. A bounding weight of 89,000 lbs is used to bound the weight of the canister and contents for the Advanced PWR canister. To account for large deformation and buckling, the mechanical property of Type 304 stainless steel is represented by an elastic-plastic material formula with LS-DYNA material type 24 (Piecewise_Linear_Plasticity). The detailed stress-strain curve for Type 304 stainless steel at room temperature beyond yield is presented in Figure 11.2.16-4 ("Impact Dynamics," J.A. Zukas, T. Nicholas, H.F. Swift, L.B. Greszczuk, and D.R. Curran, John Wiley & Sons). The boundary conditions and the filter frequency used for the evaluation of the Advanced PWR canister were the same conditions and filter frequency as used for the evaluation of the Standard PWR canister.

100-Ton Transfer Cask Side Drop Analysis Results for the PWR Canister

The analysis results are obtained by using the LS-DYNA postprocessor, LS-POST, to display the nodal acceleration time-histories. From the modal analysis, a filter frequency of 50 Hz is used in conjunction with the LS-POST Butterworth filter. For the PWR basket/canister, the maximum filtered acceleration of 24.9g occurs near the bottom of fuel canister.

11.2.16.3.4 Dynamic Load Factor

To determine the effect of the rapid application of the inertia loading during the side drop of the 100-ton transfer cask, a dynamic load factor (DLF) is computed using the mode shape of the

support disk, the most flexible component of the cask/canister/basket system. The mode shapes corresponding to the in-plane motions of the disk are extracted using ANSYS. Only the dominant modes with respect to the modal mass participation factor are used in computing the DLF.

Standard PWR Support Disk Modal Analysis

The primary modal frequencies calculated for the PWR support disk and corresponding modal mass participation factors are:

Mode	Frequency (Hz)	Percent Participation (%)
1	109.4	0.8%
2	109.7	85.8%
3	370.1	2.7%
4	371.1	7.2%
5	480.6	0.6%
6	482.0	1.8%
Total		98.9%

Standard BWR Support Disk Modal Analysis

The primary modal frequencies calculated for the BWR support disk and corresponding modal mass participation factors are:

Mode	Frequency (Hz)	Percent Participation (%)
1	79.3	38.4%
2	80.2	54.9%
3	202.9	0.0%
4	210.9	3.4%
5	282.3	0.3%
Total		97.0%

Advanced PWR Basket Modal Analysis

Using the basket finite element model developed in Section 11.2.12.6, the dominant modal frequencies for each basket drop angle are presented in the following table.

Mode	Frequency (Hz)	Basket Clocking Angle
1	155.4	0°
2	203.7	33°
3	204.5	45°
4	204.9	56°
5	136.7	90°

Response Spectrum Analysis Results

The DLFs for the Standard basket support disks subjected to an impulse are found by performing response spectrum analyses using the results of the modal analysis and the frequency response spectrum analyses. The following table summarizes the DLF and resulting acceleration for each case. The maximum filtered acceleration at the top support disk for the BWR and canister top for the PWR are obtained from the LS-DYNA analyses presented in the main body of this calculation. For the BWR and PWR support disks, the corresponding amplified acceleration is obtained from the response spectrum analysis using the SRSS method. When the SRSS calculated DLF is less than 1.0, the DLF is assumed to be 1.0.

Case	Filtered Acceleration (g)	DLF	Resulting Acceleration (g)
Standard PWR	24.9	1.00	24.9
Standard BWR	20.7	1.38	28.5
Advanced PWR	24.9	1.03	25.7

11.2.16.4 Analysis of Canister and Basket for 100-Ton Transfer Cask Side Drop

Because the accelerations calculated during the side drop of the 100-ton transfer cask are less than the accelerations calculated during the tip-over event presented in Section 11.2.12, the analyses presented in Section 11.2.12 for the canister, basket, and fuel tubes are bounding.

Figure 11.2.16-1 100-Ton Transfer Cask Side-Drop Model

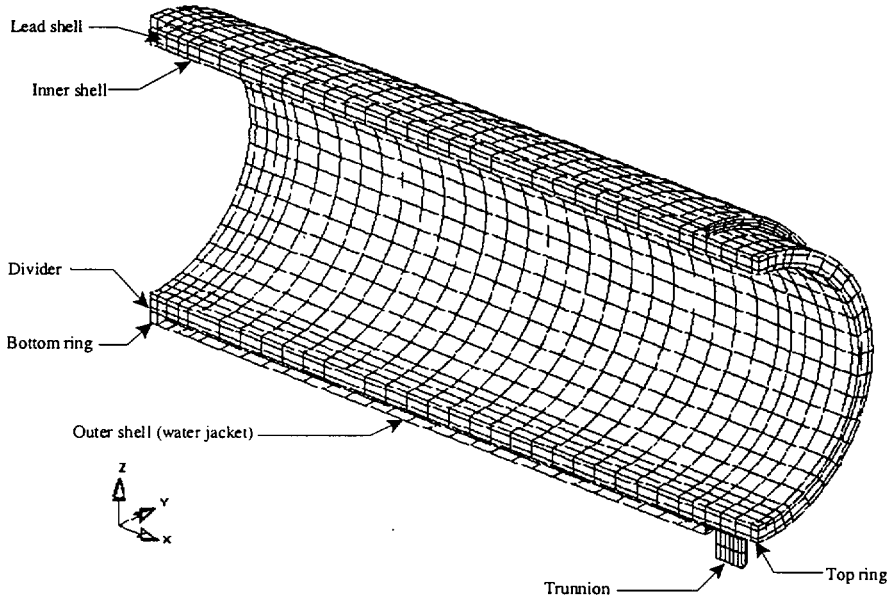

Figure 11.2.16-2 Finite Element Model of the 100-Ton Transfer Cask Side Impact Analysis

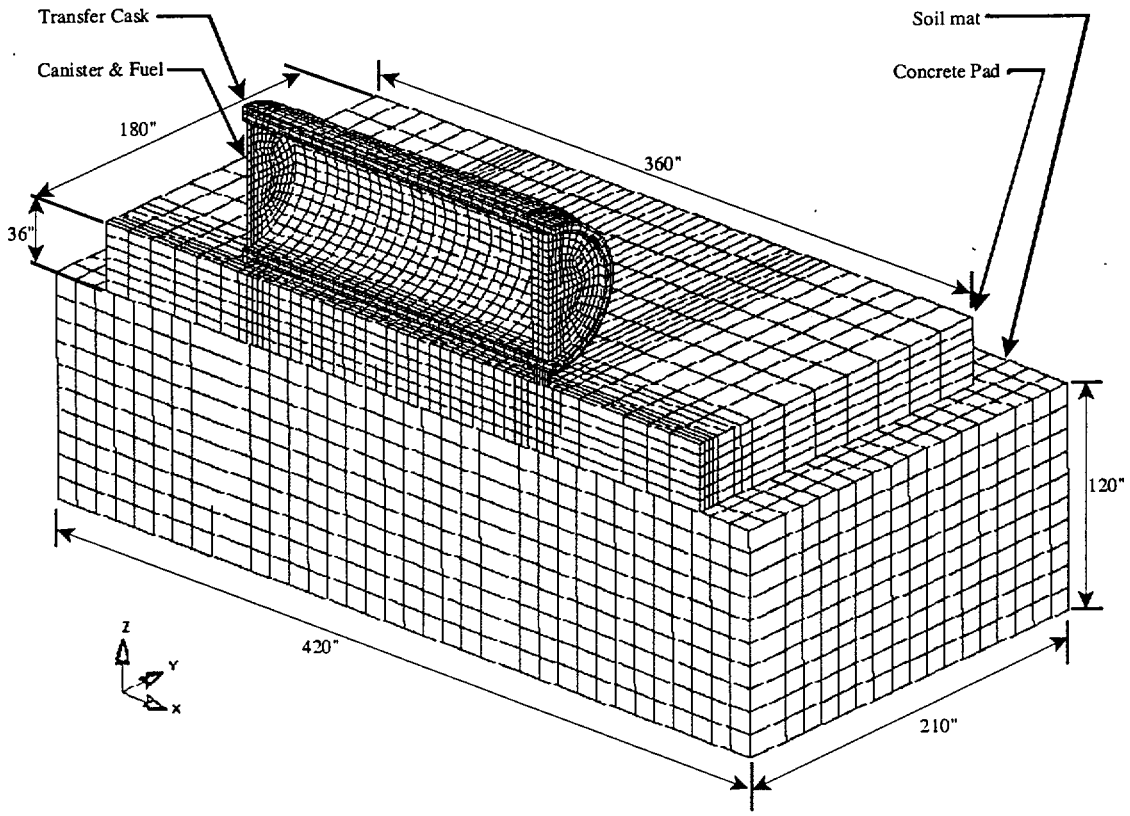

Figure 11.2.16-3 Fuel Canister in the Transfer Cask Model

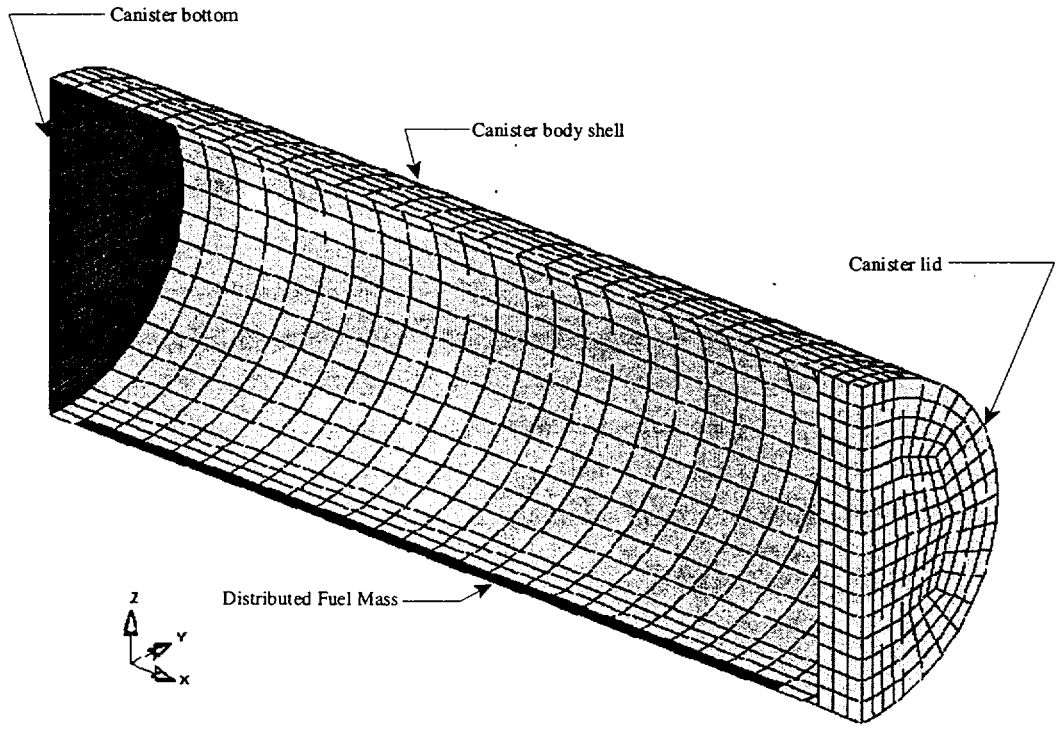

Figure 11.2.16-4 Strain-rate Dependent Stress-Strain Curves for Type 304 Stainless Steel

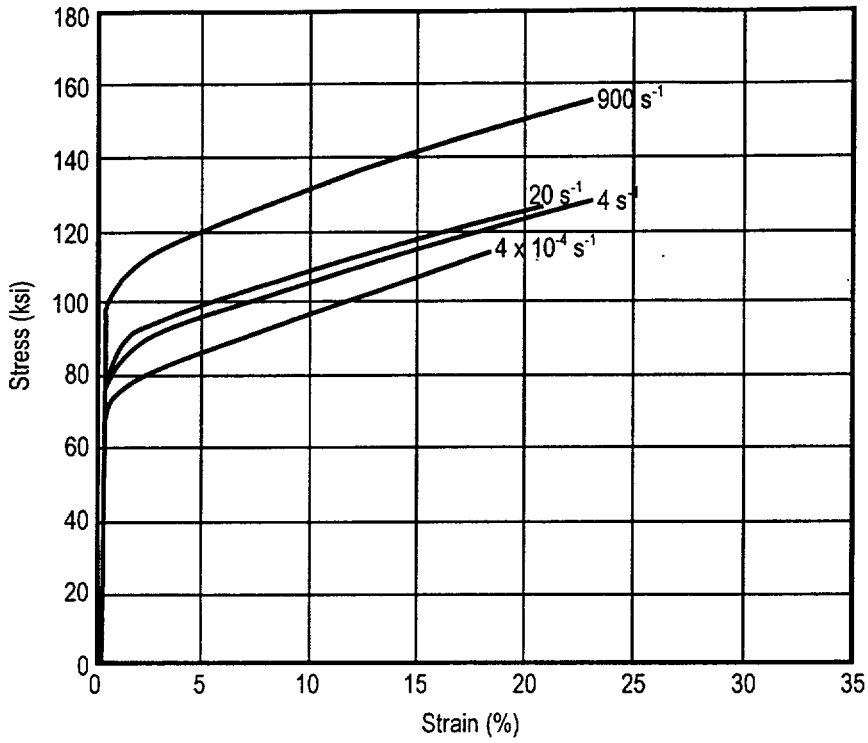

Figure 11.2.16-5 100-Ton Transfer Cask Modal Analysis Finite Element Model

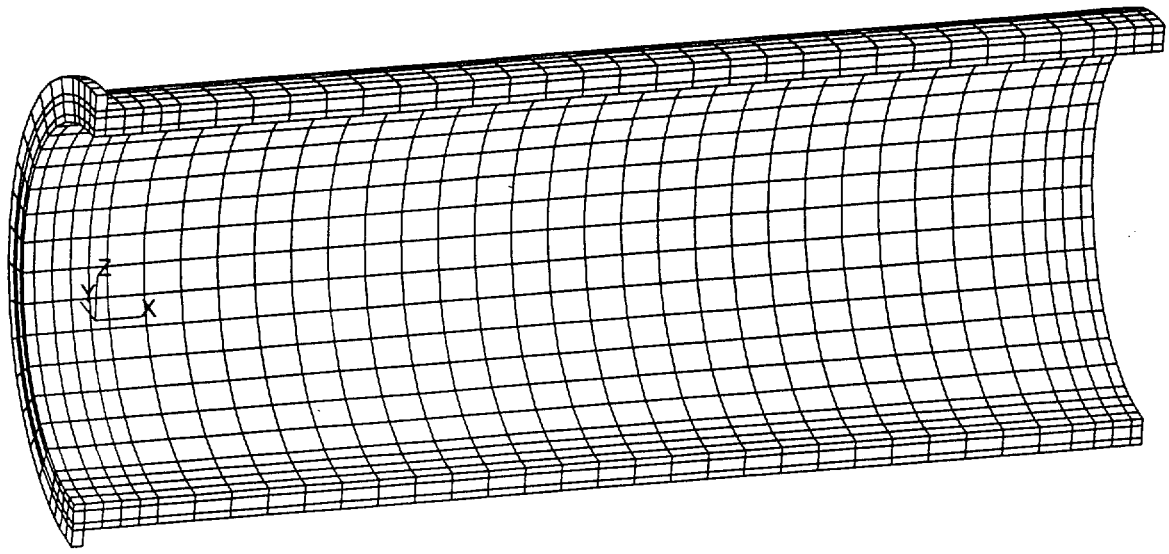

Figure 11.2.16-6 Mode Shape for Excitation in the Lateral (Z) Direction

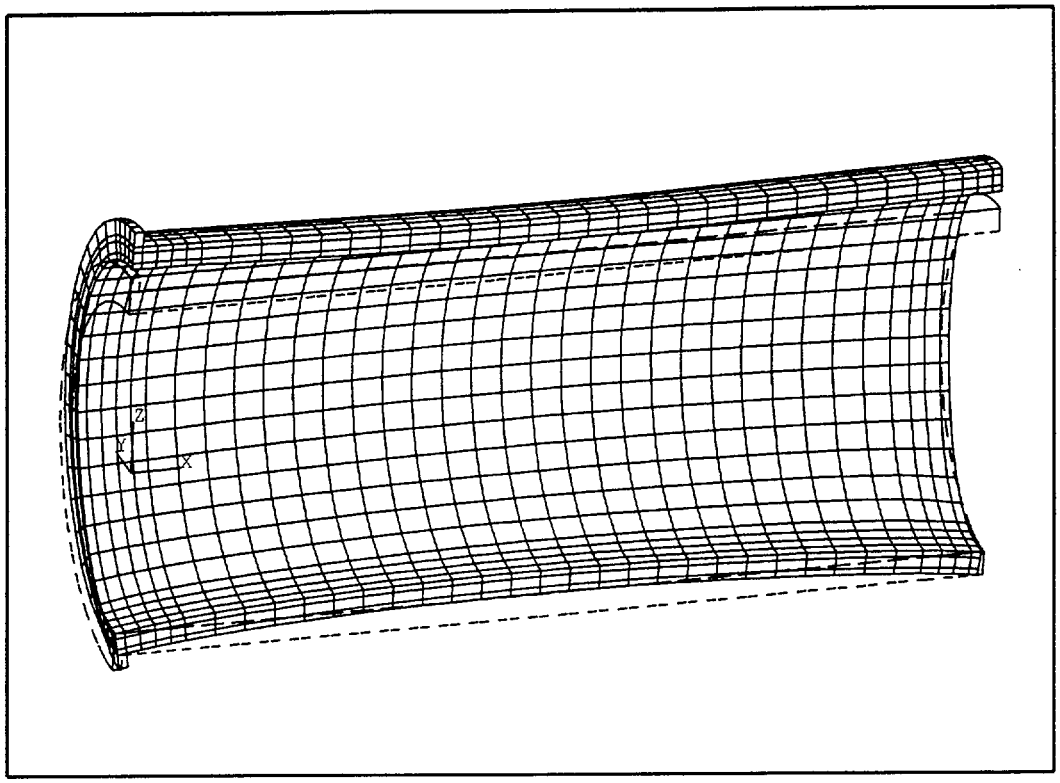

THIS PAGE INTENTIONALLY LEFT BLANK

11.3 References

1. ANSI/ANS-57.9-1992, "Design Criteria for an Independent Spent Fuel Storage Installation (Dry Type)," American Nuclear Society, May 1992.

2. Code of Federal Regulations, "Packaging and Transportation of Radioactive Materials," Part 71, Title 10, April 1996.

3. NAC Document No. EA790-SAR-001, "Safety Analysis Report for the UMS™ Universal Transport Cask," Docket No. 71-9270.

4. Code of Federal Regulations, "Licensing Requirements for the Independent Storage of Spent Nuclear Fuel and High-Level Radioactive Waste," Part 72, Title 10, January 1996.

5. Olander, D.R., "Fundamental Aspects of Nuclear Reactor Fuel Elements," U.S. Department of Energy Technical Information Center, 1985.

6. NRC, "Standard Review Plan for Dry Cask Storage Systems," NUREG–1536, Final Report, January 1997.

7. EPA Federal Guidance Report No.11, Limiting Values of Radionuclide Intake and Air Concentration and Dose Conversion Factors for Inhalation, Submersion and Ingestion, 1988.

8. EPA Federal Guidance Report No.12, External Exposure to Radionuclides in Air, Water and Soil, 1993.

9. NRC Regulatory Guide 1.109, Calculation of Annual Doses to Man from Routine Releases of Reactor Effluents for the Purpose of Evaluating Compliance with 10CFR50 Appendix I, 1977.

10. Code of Federal Regulations, Part 20, "Standards for Protection Against Radiation," 1993.

11. NRC Regulatory Guide 8.34, "Monitoring Criteria and Methods to Calculate Occupational Radiation Doses," 1992.

12. NRC Regulatory Guide 1.25, Assumptions Used for the Potential Radiological consequences of a Fuel Handling Accident and Storage Facility for Boiling and Pressurized Water Reactors, 1972.

13. Nuclear Regulatory Commission, "Atmospheric Dispersion Models for Potential Accident Consequence Assessments at Nuclear Power Plants," Regulatory Guide 1.145, September 1980.

14. SAND80-2124, "Transportation Accident Scenarios for Commercial Spent Fuel," Sandia National Laboratories, February 1981.

15. NRC, "Standard Review Plan for Dry Cask Storage Systems," Draft NUREG–1536, February 1996.

16. Kreith & Bohn, *Principles of Heat Transfer,* 5th Edition, West Publishing Company, St. Paul, Minnesota, 1993.

17. Regulatory Guide 1.60, "Design Response Spectra for Seismic Design of Nuclear Power Plants," Revision 1, December 1973.

18. ANSYS Revision 5.2, Computer Program, ANSYS, Inc., Houston, Pennsylvania.

19. Blevins, R.D., *Formulas for Natural Frequency and Mode Shape,* Krieger Publishing Co., Malabar, Florida, 1995.

20. "Topical Safety Analysis Report for the NAC Storable Transport Cask for use at an Independent Spent-Fuel Storage Installation," NAC-T-90002, Revision 3, NAC Services, Inc., Norcross, Georgia, July 1994.

21. Funk, R. "Shear Friction Transfer Mechanisms for Supports Attached to Concrete," American Concrete International Journal, Volume 11, No. 7, pp 53-58, July 1989.

22. NRC, "Three Components of Earthquake Motion," NUREG-0800, Revision 1, Section 3.7.2, Subsection II.6.

23. "Steel to Concrete Coefficient of Friction, Preliminary Tests," Report No. CEB 77-46, Tennessee Valley Authority, Knoxville, Tennessee, December 1977.

24. Roberson, J.A. and C.T. Crowe, "Engineering Fluid Mechanics," Houghton Mifflin Co., Boston, Massachusetts, 1975.

25. Cianos, N., and E.T. Pierce, "A Ground Lightning Environment for Engineering Usage," Technical Report No. 1, Stanford Research Institute, Menlo Park, California, Contract No. LS-2817-A3, SRI Project No. 1834, August 1972.

26. Summer, W.I., "American Electrician's Handbook," 10th Edition, McGraw-Hill, Inc., New York, 1981.

27. Fink, D.G., and Beaty, W. H., "Standard Handbook for Electrical Engineers," 13th Edition, McGraw-Hill, Inc., New York, 1993.

28. Black, W.Z. and J.G. Hartley, *Thermodynamics,* 2nd Edition, Harper Collins Publishers, 1991.

29. U.S. NRC Regulatory Guide 1.76, "Design Basis Tornado for Nuclear Power Plants," April 1974.

30. NUREG-0800, "Standard Review Plan," US NRC, June 1987. (Missile masses taken from Draft Revision 3, April 1996.)

31. "Minimum Design Loads for Building and Other Structures," ASCE 7-93, American Society of Civil Engineers, New York, May 12, 1994.

32. "A Review of Procedures for the Analysis and Design of Concrete Structures to Resist Missile Impact Effects," NSS 5-940.1, Nuclear and Systems Sciences Group, Holmes & Narver, Inc., Anaheim, California, September 1975.

33. Full-Scale Tornado-Missile Impact Tests," EPRI NP-440, Sandia Laboratories for the Electric Power Research Institute, Palo Alto, California, July 1977.

34. "Code Requirements for Nuclear Safety Related Concrete Structures (ACI-349-85) and Commentary-ACI 349R-85," American Concrete Institute, Detroit, Michigan, March 1986.

35. Topical Report, "Design of Structures for Missile Impact," BC-TOP-9A, Revision 2, Bechtel Power Corporation, San Francisco, California, September 1974.

36. "Seismic Analysis of Safety-related Nuclear Structures and Commentary on Standard for Seismic Analysis of Safety-related Nuclear Structures," ASCE 4-86, American Society of Civil Engineers, September 1986.

37. Cote, Arthur E., Fire Protection Handbook, 18th Edition, National Fire Protection Association, Quincy, Massachusetts.

38. NUREG/CR-6608, "Summary and Evaluation of Low-Velocity Impact Tests of Solid Steel Billet onto Concrete Pads," Lawrence Livermore National Laboratory, February 1998.

39. NUREG/CR-6322, "Buckling Analysis of Spent Fuel Basket," Lee, A.S., and Bumpas, S.E., Office of Nuclear Material and Safeguards, U.S. Nuclear Regulatory Commission, Washington, DC, May 1995.

40. EPRI TR-108760, "Validation of EPRI Methodology of Analysis of Spent-Fuel Cask Drop and Tipover Events," ANATECH Corp., San Diego, CA, August 1997.

41. Green, Robert E, "Machinery's Handbook 25th Edition," Industrial Press Inc., New York, 1996.

42. NUREG/CR-0481, SAND77-1872, "An assessment of Stress-Strain Data Suitable for Finite-Element Elastic-Plastic Analysis of Shipping Containers," Henry J. Rack & Gerald A. Knorosky, September 1978.

43. Biggs, J.M., Introduction to Structural Dynamics, McGraw-Hill, Inc., New York, 1964.

44. Boyer, H. E., Atlas of Stress-Strain Curves, ASM International, Metals Park, Ohio, 1987.

45. ACI 116R-90, "Cement and Concrete Technology," American Concrete Institute, 1990.

46. ACI 302.1R-89, "Guide for Concrete Floor and Slab Construction," American Concrete Institute, 1989.

47. Clough, R.W., and Joseph Penzien, "Dynamics of Structures," 2nd Edition, McGraw-Hill, Inc., New York, NY, 1993.

48. Rust, J. H., Nuclear Power Plant Engineering, Georgia Institute of Technology, 1979.

49. NUREG/CR-5009, "Assessment of the Use of Extended Burnup Fuel in Light Water Power Reactors," Battelle Pacific Northwest Labs, Richland, Washington, February 1988.

50. ISG-12, "Buckling of Irradiated Fuel Under Bottom End Drop Conditions," Interim Staff Guidance –12, Nuclear Regulatory Commission, June 1999.

51. "Maine Yankee Atomic Power Company Specification for Independent Spent Fuel Storage Installation and Transport Facility," NAC Document 12412-DI-01, NAC International, Atlanta, Georgia.

52. Blake, Alexander, "Practical Stress Analysis in Engineering Design," 2nd Edition, Marcell Dekker, Inc., New York, 1990.

53. Young, Warren C., "Roark's Formulas for Stress & Strain," 6th Edition, McGraw-Hill, 1989.

54. "Fuel-Assembly Behavior Under Dynamic Impact Loads Due to Dry-Storage Cask Mishandling," EPRI NP-7419, ABB Combustion Engineering, Inc., Windsor, Connecticut, July 1991.

55. "Impact Dynamics" J.A. Zukas, T. Nicholas, H.F. Swift, L.B. Greszczuk, and D.R. Curran, John Wiley & Sons, 1982.

56. ISG-4, Revision 1, "Cask Closure Weld Inspections," Interim Staff Guidance –4, Nuclear Regulatory Commission, May 1999.

57. Regulatory Guide 7.6, "Design Criteria for the Structural Analysis of Shipping Cask Containment Vessels," U.S. Nuclear Regulatory Commission, March 1978.

58. ASME Boiler and Pressure Vessel Code Cases, Nuclear Components, Case N-284-1, "Metal Containment Shell Buckling Design Methods," Approved March 1985.

59. American Concrete Institute, "Code Requirements for Nuclear Safety Related Concrete Structures (ACI-349-95) and Commentary (ACI 349R-85)," March 1986.

THIS PAGE INTENTIONALLY LEFT BLANK